CALCIFIC AORTIC VALVE DISEASE

Shedding light on its onset

Jesper Hjortnaes

Calcific Aortic Valve Disease – Shedding Light on its Onset

PhD thesis, Utrecht University, The Netherlands, with a summary in Dutch

ISBN: 978-94-6299-189-7
Author: Jesper Hjortnaes
Cover: design Laurens Hebly
Layout: Ridderprint BV - www.ridderprint.nl
Printed by: Ridderprint BV - www.ridderprint.nl

Calcific Aortic Valve Disease

Shedding light on its onset

Aortaklepverkalking

Ontrafelen van het onstaansproces

(met een samenvatting in het Nederlands)

Proefschrift

ter verkrijging van de graad van doctor aan de Universiteit Utrecht op gezag van de rector magnificus, prof.dr. G.J. van der Zwaan, ingevolge het besluit van het college voor promoties in het openbaar te verdedigen op donderdag 8 oktober 2015 des middags te 4.15 uur

door

Jesper Hjortnaes

geboren op *28 juli 1983*
te *Leiden*

Promotor: Prof. dr. L.A. Van Herwerden

Copromotoren: Dr. J. Kluin
Dr. E. Aikawa

Het verschijnen van dit proefschrift werd mede mogelijk gemaakt door de steun van de Nederlandse Hartstichting, de Nederlandse Organisatie voor Wetenschappelijk Onderzoek en de Hart & Long Stichting Utrecht. Daarnaast werd er financiële steun geleverd door St. Jude Medical, Maquet en ChipSoft.

TABLE OF CONTENTS

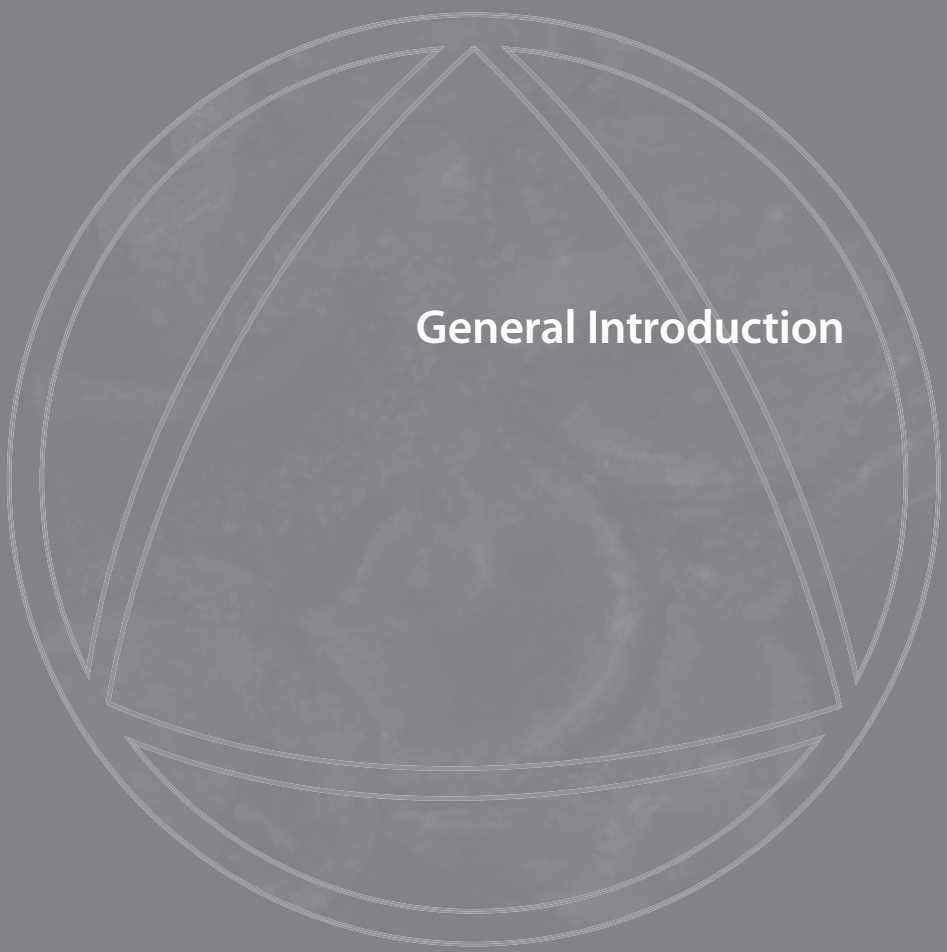

General Introduction

1

Calcific Aortic Valve Disease – Status Quo

based on

J. Hjortnaes[1,2] & E. Aikawa[2]

The Aortic Valve *Intech Open Access 2011*

[1]Department of Cardiothoracic Surgery, Division of Heart and Lungs, University Medical Center Utrecht, Utrecht, The Netherlands [2]Center of Excellence in Vascular Biology, Department of Medicine, Brigham and Women's Hospital, Harvard Medical School, Boston, USA

1. INTRODUCTION

Calcific aortic valve disease (CAVD) has become the most common heart valve disease in the Western population, affecting approximately 25% of adults over 65 years, of which 2-3% has clinically significant aortic stenosis.[1] Even mild CAVD is associated with adverse outcomes, with a 50% increased risk of cardiovascular death.[2] There are no known therapies that slow disease progression, and surgical valve replacement is the only effective treatment for aortic stenosis.[3] Over 275,000 aortic valve replacement surgeries are performed annually worldwide. This number is expected to triple by 2050.[4] These statistics emphasize the burden of aortic valve disease and the necessity of understanding its mechanisms.

CAVD is a progressive disease that starts with initial changes in the cell biology of the valve leaflets, which develop into atherosclerotic-like lesions and aortic sclerosis, and eventually lead to calcification of the valve, causing left ventricular outflow tract obstruction.[5, 6] In turn pressure overload leads to progressive left ventricular hypertrophy and eventual heart failure. Although CAVD progresses with age, it is not an inevitable consequence of aging. CAVD traditionally has been considered a degenerative phenomenon, in which years of mechanical stress on an otherwise normal valve, cause calcium to deposit on the surface of the aortic valve leaflets. The evolving concept, however, is that CAVD is an actively regulated process that cannot be characterized simply as "senile" or "degenerative". The progressive calcification process involves lipid accumulation, increasing angiotensin-converting enzyme activity, inflammation, neovascularization, and extracellular matrix degradation.

The risk factors for CAVD are similar to those for atherosclerosis: age, gender, hypercholesterolemia, diabetes, smoking, renal failure, and hypertension.[1] In addition, pathological studies of explanted human stenotic aortic valves have identified lesions similar to those in atherosclerotic plaques, which contain inflammatory cells and calcific deposits.[7] The involvement of high cholesterol levels is corroborated by studies demonstrating that patients with familial hypercholesterolemia develop aortic valve lesions that calcify with age.[8] Furthermore, preclinical studies have demonstrated atherosclerotic-like lesions in aortic valve leaflets in atherosclerosis in rabbits and mice. From the notion that CAVD and atherosclerosis might share a similar mechanism, statins (3-hydroxy-3-methylglutaryl-coenzyme A [HMG-CoA] reductase inhibitors) emerged as a potential therapy for treating CAVD. Indeed, retrospective studies have demonstrated a reduction in disease progression when patients were treated with statins.[9-11] In addition, animal studies confirmed that statin treatment inhibits calcification.[12, 13] Large prospective clinical trials however failed to demonstrate any effect on CAVD progression in patients treated with high doses of statins.[14, 15] Arguably, this may be due to the late implementation of the statins, after aortic valve calcification has progressed to the irreversible stage. However, it may also be a sign that CAVD and atherosclerosis should not be considered as similar patho-physiological entities.

The aortic valve consists of endothelial cells and valvular interstitial cells that maintain the health of the valve and are important in valvular disease. Valvular interstitial cells likely mediate

the progression of CAVD.[16] Signals in aortic valve biology that trigger activation, differentiation, or pathological change are unclear. However, in human specimens of CAVD, there is evidence that valvular interstitial cells differentiate to myofibroblasts and osteoblast-like cells, which are eventually responsible for calcium deposition.[17] Possible pathological triggers include hemodynamic shear stress, solid tissue stresses, reactive oxygen species (ROS), inflammatory cytokines and growth factors, and physiological imbalances such as the metabolic syndrome, diabetes mellitus, end-stage renal disease, and calcium or phosphate imbalance.[18-20] The cellular and molecular factors involved in the development of aortic valve stenosis, however, remain largely obscure.

The poor prognosis and increased mortality after the onset of symptoms provide a rationale for the pursuit of a better understanding of the disease process, which can lead to effective therapeutic strategies to prevent CAVD. This chapter first discusses our current understanding of the aortic valve and its physiology, risk factors, diagnosis, and clinical management of CAVD in order to set the background for this thesis.

2. THE AORTIC VALVE

Aortic heart valves maintain unidirectional blood flow throughout the cardiac cycle with minimal obstruction, without regurgitation. The aortic valve prevents retrograde flow back into the left ventricle during diastole. Heart valves open and close approximately 40 million times a year, and 3 billion times over an average lifetime. Mechanical forces exerted by the surrounding blood and heart drive the aortic valve's function. The dynamic structure and physiology of aortic heart valves enables them to avoid excess stress concentration and to withstand wear and tear over many years.[21] Aortic valve functionality must be seen in conjunction with the aortic root, and viewed as one apparatus.[18] A variety of pathological processes can lead to aortic valve malfunction, with serious clinical consequences. This malfunction usually is associated with calcific changes of the valve connective tissue, and eventually causes aortic stenosis. Before we elaborate on the pathology of CAVD, we will discuss normal aortic valve anatomy and physiology and their relationship to aortic valve function.

2.1 Aortic valve anatomy

The aortic cusps are thin, flexible structures that come together to seal the valve orifice during diastole. The aortic valve is normally composed of three cusps or leaflets. The individual cusps are attached to the aortic wall in a semilunar fashion, ascending to the commissures (where adjacent cusps come together at the aorta) and descending to the basal attachment of each cusp to the aortic wall; this anatomical structure is also called the aortic valve annulus. A portion of the annulus is attached to cardiac muscle, while the other half is continuous with the fibrous leaflets of the mitral valve. The functional unit of the aortic valve includes the cusps and their respective aortic sinus complexes, also called the aortic root. The aortic root is a bulb-shaped structure to which the aortic

cusps are attached. Behind the aortic valve cusps are dilated pockets in the aortic root known as the *sinuses of Valsalva*, from which the coronary arteries originate. The nomenclature of the aortic valve cusps and their respective sinuses are based on the position of the coronary artery ostia — the left coronary cusp, the right coronary cusp, and the non-coronary cusp (and their associated sinuses).

In the middle of the free margin of each cusp on the ventricular surface is a pronounced thickening, known as the *nodule of Arantius.* Coaptation of these three nodules ensures complete closure of the valve during diastole. Along the ventricular surface of each cusp, between the free edge and the closing edge, is a crescent shaped region called a *lunula*. These thin areas of leaflet contact the corresponding regions of both adjacent cusps to ensure a competent seal. The remainder of the cusp (noncoapting portion) is known as the *belly*. Native human aortic valves are virtually avascular, and receive nutrients through hemodynamic convection and diffusion. In most cases, the dimensions of the three leaflets are slightly unequal.[22] The dynamic, complex three-dimensional anatomy of the aortic trileaflet cusps and the aortic root allows for stress sharing between leaflets, the sinuses of Valsalva, and the aortic wall.[23, 24]

2.2 Aortic valve function

The aortic valve functions synergistically with the aortic root to maintain efficient cyclic opening and closing — opening when exposed to forward flow, and then rapidly and completely closing under minimal reverse pressure. Importantly, opening of the valve precedes, rather than responds to, the forward movement of blood from the ventricle.[25, 26] This illustrates the complex function of the valve, and is one of the reasons for considering movement of the whole root — from the level of the annulus to the sinotubular junction — when describing aortic valve functionality.

As blood decelerates in the aorta at the end of systole, vortexes in the sinuses of Valsalva behind the AV cusps facilitate valve closure. These vortexes help funnel oxygenated blood into the coronary arteries and create a small pressure gradient across the leaflet, which helps bring the leaflets to a smooth and efficient closure. The ability to prevent reverse flow of the aortic valve depends on the stretching and molding of the three cusps to fill the orifice during the closed phase of the cardiac cycle, during which back pressure from the blood is present in the aorta. Simultaneously, the valve annulus expands, pulling the cusps and thus preventing collapse.[27]

A further increase in the annular radius at end diastole and into the isovolumic contraction phase of the cardiac cycle pulls the cusps from their commissures such that a small stellate orifice results, even without the presence of transvalvular flow. The valve orifice changes quickly from stellate, to triangular, and finally a to a circular pattern, as blood is ejected from the ventricle. The aortic root adjusts from a conical to a cylindrical shape during ejection, providing optimal hemodynamics at the larger flow volume.[25] The aortic valve closes much more gradually than it opens. The total surface area of the three cusps is approximately 40% larger than the cross-sectional area of the aortic root at the annular level. This allows each cusp to bow slightly towards the left ventricular outflow tract, which prevents the cusp from inverting during diastole.[28] The normal aortic valve orifice area (AVA) is 2.6-3.5 cm^2, however depends on the body mass area of the individual.[29]

1

2.3 Aortic valve structure

The structure of the aortic valve cusps is organized into three layers: (i) the *zona ventricularis*, closest to the left ventricle chamber and composed largely of elastin, which can extend in diastole and recoil in systole to minimize cusp area; (ii) the *zona fibrosa*, closest to the outflow surface, rich in densely packed collagen organized in radial and circumferential direction, which provides the strength and stiffness of the cusps and is mainly responsible for bearing diastolic stress; and (iii) the centrally located *zona spongiosa*, which consists mainly of glycosaminoglycans (GAGs) that accommodate shear forces of the cuspal layers, and absorbs shock during the valve cycle.[18] (Figure 1)

This organization of the aortic native heart valve allows for certain unique qualities. First, accordion-like folds called corrugations, present in the valve cusps, allow for the cuspal shape and dimensions to vary with the cardiac cycle. Second, microscopic collagen folding (also known as *crimp*) allows lengthening of the valve at minimal stress. Cusp tissue also displays anisotropy, the quality conferred by collagen architecture that permits differences in radial and circumferential extensibility. Finally, the macroscopic collagen alignment enables forces from the cusps to transfer to the aortic wall.[30] By employing these properties, the native heart valve avoids excess stress concentration on the cusps and supporting tissues and can withstand biomechanical loads caused by repetitive deformations. In addition, biomechanical stress may induce the remodelling and repair of connective tissue.[21] The aortic valve tissue is comprised of a cell population that withstands a large amount of pressures and stresses.

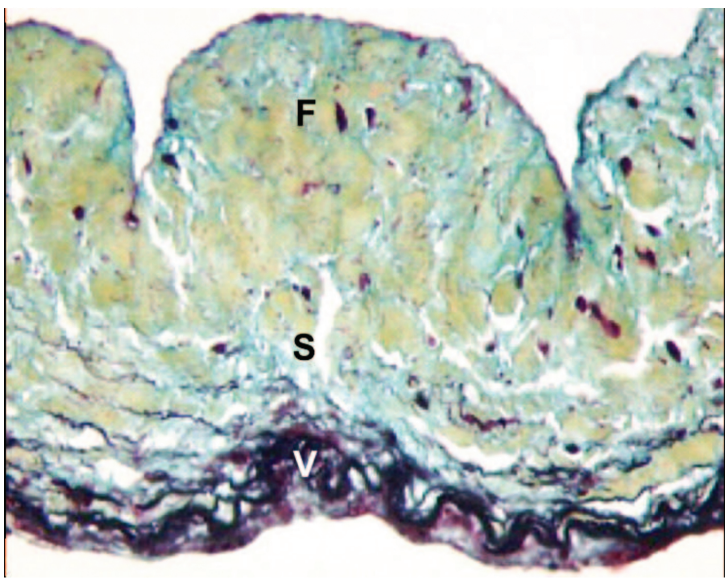

Figure 1. Human normal aortic valve histopathology depicts a tri-layered structure (F) – fibrosa, (S) – spongiosa and (V)- ventricularis.

2.4 Aortic valve cell population

The native aortic heart valve consists of two types of cells: valvular interstitial cells (VICs) that permeate the entire valve tissue, and valvular endothelial cells (VECs) that cover the surface. The components of the extracellular matrix (ECM) are synthesized, degraded, and maintained by VICs, which seem to have adaptive characteristics. In the healthy aortic valve, they have primarily quiescent fibroblast-like properties, but they can change to an activated phenotype during valvular remodelling, response to injury, or pathology. VECs regulate immune and inflammation responses and provide the native heart valve with its nonthrombogenic properties.[31] Small populations of smooth muscle cells[32] and nerve cells have also been described.[33, 34]

2.4.1 Valvular Interstitial Cells

VICs remodel ECM proteins in the aortic valve leaflet, and are of mesenchymal origin. Different phenotypes of VICs are present in the mature native valve. Five identifiable phenotypes of VICs have been described: embryonic mesenchymal cells, quiescent VICs (qVICs), activated VICs (aVICs), progenitor VICs (pVICs), and osteoblastic VICs (oVICs).[35-39] qVICs are considered to be at rest in the valvular interstitium and maintain normal valve physiology by becoming activated in response to injury or disease. It is believed that this process leads to the differentiation of VICs into activated VICs, demonstrating a fibroblast-like phenotype. More specifically, aortic valve VICs secrete and turn over proteins at a dramatically increased rate compared to other cell types in vivo, which indicates that VICs continually repair mechanically induced tissue micro-damage to enable long-term durability. ECM remodelling results from the synthesis of ECM-degrading enzymes by VICs, such as matrix metalloproteinases (e.g., MMP-1, MMP-2, MMP-9, and MMP-13) and cathepsins (e.g., cathepsins S, K, and B), and tissue inhibitors (e.g., tissue inhibitors of metalloproteinases [TIMP]).[39] The cellular and molecular mechanisms that control this phenotype differentiation also participate in aortic valve pathology. In particular, VICs become activated when stimulated by mechanical loading, and mediate connective tissue remodelling to restore a normal stress profile in the tissue.[40]

The pressure load applied to the leaflet causes an increase in circumferential and radial leaflet length, which increases strain on the tissue.[41] Valve strain seems highest at areas where leaflets attach to the aortic wall; these locations are also where calcification seems to begin in CAVD.[42, 43] Mechanical forces acting on the valve translate into biological responses at the tissue level, which in turn lead to a VIC response at the cellular level — which causes constant synthesis and renewal of the ECM.[44] Intracellular signalling leads to changes that include increased VIC stiffness and increased ECM biosynthesis. Concurrently, the higher valvular pressure gradients on the left side of the heart lead to larger local tissue stress on VICs, which in turn leads to higher VIC stiffness and collagen biosynthesis in the left-sided valves.[45]

2.4.2 Endothelial Cells

The surface of the aortic valve is lined with a single monolayer of VECs that maintain non-thrombogenicity. VECs are similar to arterial endothelial cells in the expression of von Willebrand factor

because they produce nitric oxide and have prostacyclin activity.[46] Cell junctions between VECs are also similar to those of arterial endothelial cells. VECs however seem to be phenotypically different from arterial endothelial cells,[47] based on the observation that VECs originate developmentally from sources different from arterial endothelial cells. In addition, VECs are oriented circumferentially across leaflets, perpendicular to the direction of the blood flow, in contrast to vascular endothelium, which aligns parallel to flow.[18, 48]

Comparing valvular and vascular endothelium in a static culture has led to the identification of significantly different genes.[49] In addition, although VECs and arterial endothelial cells are both prone to calcification, different mechanisms lie at the heart of the process. VECs show an increased expression of genes involved in chondrogenic differentiation, while arterial endothelial cells more strongly express osteogenic genes.[50] Due to their location at the surface of the aortic valve, VECs are important in relation to the hemodynamic forces exerted on the heart valve. The ventricularis part of the valve (inflow) is exposed to rapid, pulsatile, unidirectional shear stress. In contrast, the fibrosa part of the valve (outflow) experiences a lower, almost oscillatory shear stress.[51] Interestingly, recent evidence suggests that different transcriptional profiles are expressed by the endothelium on the opposite faces (ventricularis vs. fibrosa) of a normal adult pig aortic valve.[52] Studies have demonstrated that high pulsatile shear stress on the fibrosa side of the aortic valve increases inflammatory receptors and the expression of bone morphogenic protein (BMP),[53] but also decreases the expression of inhibitors of fibrosis and calcification, including osteoprotegerin (OPG), C-type natriuretic peptide (CNP), and chordin.[54] In addition, *in vivo* studies have demonstrated that CAVD initiates on the fibrosa side of the valve.[17, 55]

Investigators have hypothesized that these differences in endothelium between opposite sides of the aortic valve may contribute to the typical predominant localization of pathologic aortic valve calcification near the outflow surface (*zona fibrosa*).[52] VECs may also have an active role in valve tissue remodelling by migrating into the valve through endothelial-to-mesenchymal transition (EndMT) processes, akin to those during valve development. During EndMT, VECs lose endothelial markers and gain myofibroblast-like markers similar to those observed in activation of VICs. Similar to the embryological process that gives rise to VICs, these myofibroblast-like VECs invade the leaflet interstitium. In vitro evidence suggests that these EndMT changes of VECs may be dependent on mechanical strain. However, the exact role of EndMT in disease onset is unclear.

2.4.3 Cellular Interaction

VICs and VECs exist in close communication, which indicates that cellular interaction is vital for leaflet biology. Studies have demonstrated that VECs interact with VICs in a complex hemodynamic and mechanical environment to maintain aortic valve cusp tissue integrity. Additionally, VECs regulate VIC function through paracrine signals, such as controlling VIC contractility and leaflet mechanics.[56] More specifically, valvular endothelial dysfunction has been implicated as the initiator of inflammatory reactions, blood clots, and even calcification.[57] The interaction between vascular endothelial cells and vascular smooth muscle cells, and its importance to normal vessel function, has been well

documented. Such interaction likely exists between valvular endothelium and VICs, however has to date been poorly studied.

VIC–VEC co-culture studies have corroborated that VECs help maintain a qVIC phenotype.[57] Moreover, when exposed to shear stress, the presence of endothelium stabilized VIC proliferation, increased the synthesis of ECM proteins by VICs, and decreased GAG loss.[57] These results suggest that damage to or loss of valvular endothelium leads to VIC hyperplasia and myofibroblast activation. When the endothelial layer of aortic valve explants was removed, it promoted the formation of calcific nodules.[16] Studies also have demonstrated that neurogenic dilation of aortic valve cusps only occurred only when the endothelium was intact.[33] The communication between VECs and VICs is fundamental in normal and pathological signalling, but more work is needed to further delineate these relationships.

3. CLINICAL ASPECTS OF CALCIFIC AORTIC VALVE DISEASE

CAVD is a progressive disease that begins with initial changes in the cell biology of valve leaflets, develops into atherosclerotic lesions and aortic sclerosis, that eventually leads to calcification of the valve, which causes left ventricular outflow tract obstruction and eventual heart failure. This is known as calcific aortic stenosis, which is viewed as the critical end stage of this disease process, and is associated with poor outcomes.

3.1. Epidemiology

CAVD is the most common cause of aortic stenosis in the developed world. Increased aortic valve cusp thickness due to fibrosis and lipid accumulation, but without left ventricular outflow tract obstruction, is known as *aortic valve sclerosis*. Aortic valve sclerosis and aortic stenosis are generally viewed as the early stage and late stage, respectively, of the CAVD pathological process. Aortic sclerosis is common in the elderly population; the prevalence in the general population is 29%.[1] A landmark study[1] identified 26% of study population older than 65 years having aortic sclerosis, indicating that aortic sclerosis associates with age. In the same population, 2% had aortic stenosis. These numbers increase with age — those over 74 years old, 37% had aortic sclerosis, and almost 3% had aortic stenosis. Importantly, approximately 16% of patients with aortic sclerosis will develop aortic stenosis within 6 to 8 years.[58] Other studies have reported that up to 33% of patients with aortic sclerosis developed aortic stenosis within 4 years of follow-up.[59] No known therapies slow aortic valve disease progression, and surgical valve replacement currently is the only effective treatment for aortic stenosis. In addition, aortic valve sclerosis increases the risk of myocardial infarction or cardiovascular death by 50% (Lloyd-Jones, 2009). As such, aortic valve disease has a serious impact on general health.

1

3.2 Risk factors

Calcific aortic stenosis shares nearly identical risk factors with atherosclerosis. Clinical risk factors for calcific aortic stenosis include age, male sex, hypertension, smoking, elevated serum levels of lipoprotein (A), and low-density lipoprotein (LDL) levels.[1] Other studies have demonstrated that traditional risk factors that are important in atherosclerosis, including the metabolic syndrome and renal failure, also associate with calcific aortic stenosis.[60-63] This overlapping of risk factors has led to the hypothesis that calcific aortic valve disease and atherosclerosis have similar etiologies, but there are epidemiological discrepancies, as demonstrated by the inconsistency in coexisting prevalence between calcific aortic stenosis and coronary artery disease. Only 50% of patients with severe calcific aortic stenosis have significant coronary artery disease, and the majority of patients with coronary artery disease have no calcific aortic stenosis.[64] Furthermore, metabolic diseases such as hyperparathyroidism (secondary to chronic renal failure, Paget's disease) have also associated with accelerated progression of aortic valve calcification and stenosis.[65, 66] Further studies are needed to understand the differences between the pathophysiology of atherosclerosis and aortic valve disease both clinically but also at a fundamental level.

3.3 Symptoms and diagnosis

A discrepancy exists between the onset of symptoms and the onset of disease. Symptoms usually do not occur until calcific aortic stenosis has developed. The symptoms and clinical signs of CAVD are better understood by discussing the physiological changes that occur. Calcific aortic stenosis leads to left ventricular outflow tract obstruction, which causes several physiological changes, best described in a left ventricular pressure-volume loop. Ventricular emptying is impaired by outflow tract resistance, which results from a reduced aortic valve orifice area during systole. This, in turn, causes a large pressure gradient over the aortic valve — which means that ventricular pressure needs to exceed the increased aortic pressure gradient, causing increased peak systolic pressure and subsequent aortic valve closure due to an increased end-systolic volume. Consequently, stroke volume decreases. Higher end-systolic volume raises the afterload, and thus the incoming venous return, leading to increased end-diastolic volume. This process activates the Frank-Starling mechanism, which increases contraction force and thus maintains a normal stroke volume when the aortic stenosis is mild. Stenosis severity correlates with the increase of left ventricular outflow tract obstruction and afterload. When the end-systolic volume increases more than the end-diastolic volume, stroke volume will decrease, leading to a reduction in arterial pressure. The cardiovascular system will strive to maintain arterial pressure, increasing peripheral vascular resistance. In addition, the left ventricular heart muscle will demonstrate hypertrophy to compensate for a chronic increase of afterload. Most cardiovascular systems can compensate for aortic stenosis until the orifice diameter is less than 0.6 cm^2/m^2 (~1.0 cm^2).

The patient will remain relatively asymptomatic up to this point, due to adequate physiological compensatory mechanisms. Symptoms generally appear when the valve orifice is around 1.0 cm^2, and typically include shortness of breath, syncope, and chest pain. Left ventricular hypertrophy

combined with a stenotic aortic valve may lead to impaired blood flow to the heart muscle, in turn causing increased oxygen demand by the heart muscle and leading to angina pectoris. Aortic stenosis can present itself clinically with a systolic ejection murmur at the right upper sternal border, often radiating to the neck. Peaking of the murmur late in systole, a palpable delay of the carotid upstroke, and a soft second heart sound can all point to aortic stenosis. Aortic stenosis is usually confirmed using ultrasound echocardiography.[67, 68] The severity of aortic valve dysfunction is determined by the combination of the following hemodynamic indices: peak ejection velocity, effective orifice area, and mean transvalvular pressure gradient.[67] As described earlier, CAVD progression involves the narrowing of the valve orifice and increased ventricular ejection velocities and pressure gradients. Mild aortic valve stenosis is generally defined by restricted opening of the valve cusps, with a mean transvalvular pressure gradient of less than 25 mm Hg; moderate aortic valve stenosis by a mean gradient between 25 and 40 mm Hg; and severe aortic valve stenosis by a mean gradient of 40 mm Hg or more.[58] Because direct imaging of the aortic valve still involves technical challenges, echocardiography remains the gold standard for assessing aortic valve dysfunction.

3.4 Treatment

3.4.1 Surgical Treatment

Unless discovered during monitoring for other conditions, patients rarely exhibit detectable symptoms of aortic valve disease until after it has already progressed to an advanced stage.[69] Patients with severe aortic stenosis have a life expectancy of less than 10 years if untreated. Of these patients with concomitant heart failure, 50% will die within a year.[70] Aortic valve replacement is the only effective treatment, but optimal timing for surgery in asymptomatic patients remains unclear.[71] Asymptomatic patients have good survival without surgery, and combined with the surgical risk for operative mortality and post-operative complications, surgeons are reluctant to perform valve replacement in these patients.[72]

Replacement valves, be they mechanical or bioprosthetic, have several shortcomings. The body recognizes a mechanical valve as foreign material, giving rise to thromboembolic complications that require lifelong anticoagulation therapy.[73] Bioprosthetic valves are prone to reduced durability (~20 years) because of structural dysfunction resulting from progressive leaflet deterioration and calcification, eventually requiring reoperation.[73, 74] Bioprosthetic valves are the conduits of choice for patients over 60–65 years who are relatively physically inactive, and when there is a contraindication for anticoagulation therapy. Mechanical valves are chosen for active patients under 60 years, who can tolerate anticoagulation therapy.

3.4.2 Pharmacological Treatment

The need for alternatives to surgery is emphasized by the increasing age of the general population and the rising prevalence of CAVD. Therapeutic strategies to restrict disease progression are needed to delay and possibly avoid surgical valve replacement. Because CAVD and atherosclerosis have

similar disease progression and risk factors, pharmacological treatment of CAVD mostly has been focused on lipid-lowering agents (statins) and angiotensin-converting enzyme (ACE) inhibitors.[1, 75] LDLs are present in human aortic valve lesions. In addition, studies have demonstrated the presence of oxidized lipids in calcifying areas of aortic valves.[76] Statins inhibit the pathway for synthesizing cholesterol in the liver and lower plasma cholesterol levels. Animal studies and retrospective clinical studies have demonstrated that statins could potentially slow CAVD progression.[10, 77-79] However, large clinical trials have demonstrated that statins do not affect CAVD in general valve disease population.[10, 14, 77, 80] ACE, angiotensin II, and angiotensin II type 1 receptors have also been identified in aortic sclerotic lesions.[75, 81] Retrospective studies associate ACE inhibitors with a lower rate of aortic valve calcification, but ACE inhibitors do not inhibit CAVD progression.[77] Interestingly, angiotensin II type 1 antagonists have prevented aortic valve lesion formation in hypercholesterolemic rabbits.[82] Trials are ongoing to elucidate further the effect of ACE inhibitors on the progression of CAVD. As we gain more information about the specific mechanisms of CAVD, different potential pharmaceutical targets surface. The valve endothelium has received a great deal of attention and could potentially be a drug delivery platform. A recently developed method tests for the presence or absence of diseased aortic valves in atherosclerotic mice using an anti-VCAM-1 peptide to target early-stage aortic valve disease endothelium.[13] We still generally lack clinically significant pharmacological therapies for CAVD, which indicates the importance of additional research to elucidate mechanisms of CAVD progression.

4. PATHOLOGY OF CALCIFIC AORTIC VALVE DISEASE

4.1 Pathology

CAVD is a progressive disorder that ranges from mild valve thickening to severe calcification with impaired leaflet motion or aortic valve stenosis.[83] Though CAVD traditionally was viewed as a passive degenerative disease resulting from years of stress, we now recognize it as an actively regulated disease, with evidence suggesting that it follows a mechanism akin to bone formation.[17] CAVD has also been termed a fibrocalcific disease, resulting from increased collagen content found in both valve leaflets of animal models as well as human specimens. An important hallmark of CAVD progression is a fibrotic collagen accumulation, leading to thickened, stiffened valve with eventual functional deterioration. Ultimately calcific nodules form within these sclerotic leaflets, worsening loss of tissue compliance and eventually causing stenosis.

Calcification is characterized by the deposition of calcium phosphate within the extra cellular matrix. This mineralization can be considered as either a dystrophic calcification, a disorganized crystal structure often associated with precipitation of calcium phosphate on debris remaining after cell death, or as a bone-like crystal lattice of hydroxyl-appetite, indicative of an osteogenic process. Both types of mineralization have been described, however it remains uncertain how these types of mineralization relate to each other. Whether the initial fibrotic response and the calcific processes

occur in parallel during disease progression is unclear. However, it is believed that continuous activation of VICs is responsible for the persistent synthesis and deposition of collagen in the fibrotic leaflet, and that osteoblast-like cells seem to cause active mineralization. However, investigators have been unable to produce both phenotypic changes within the same *in vitro* culture conditions.

4.2 Endothelial Dysfunction

As described earlier, the surface of the aortic valve is lined with an endothelial monolayer. Although the exact initiating factors for the inflammatory process in CAVD are unclear, studies have demonstrated that the endothelium plays an important role. Because VECs are located at the surface of the aortic valve, the endothelium is subjected to hemodynamic forces. Different shear stresses are exerted on each side of the aortic valve. In vivo studies have demonstrated that early CAVD lesions initiate on the fibrosa (outflow) side of the valve.[53] Endothelium subjected to abnormal blood flow seems more susceptible to inflammatory cytokines.[40, 84] Research has shown that high pulsatile shear stress on the *fibrosa* side of the aortic valve induces up-regulation of inflammatory receptors by VECs for circulating cytokines and inflammatory monocytes, leukocytes and T-lymphocytes.[85, 86] In addition, elevated stretch loading on the aortic valve induced pro-inflammatory cytokine (bone morphogenetic protein [BMP2/4]) expression on the fibrosa part of the aortic valve. These results indicate the potential role of BMPs in early CAVD lesions.[87] Another mechanism proposed as an initiating factor in CAVD, but also in atherosclerosis, is the expression of pro-oxidant phenotypes (ROS) in VECs.[49, 53, 88] ROS, including oxidized lipids, can cause endothelial cell injury, which can lead to a loss of endothelial alignment and an increase the upregulation of cell adhesion molecules — permitting increased inflammatory infiltration.[89]

These events may together or individually initiate and/or sustain chronic inflammation, and lead to the development of CAVD.[55] The expression of endothelial nitric oxide synthase (eNOS) — a vasodilator that protects blood vessels against atherosclerosis — is reduced in conditions with oxidative stress, such as disturbed blood flow, but is elevated by antioxidant signalling. Although its role in CAVD is less clear, eNOS expression is reduced on the VECs of the fibrosa side compared to the ventricularis side of the aortic valve. This reduction indicates that eNOS might be involved in the *fibrosa* susceptibility in CAVD pathogenesis.[49] Moreover, inhibition of eNOS expression results in increased cusp stiffness of the aortic valve.[56] Statins decreased the amount of calcification and increased VEC eNOS in rabbits, which suggests that eNOS may protect against CAVD. However, during fetal valve development, an induction of eNOS expression on the fibrosa vs ventricularis sides was observed (figure 2).

4.3 Valvular Interstitial Cell Remodelling and the Role of the Extracellular Matrix

VICs are responsible for the physiological remodelling that maintains integrity and pliability in the aortic valve. In terms of CAVD, the general hypothesis is that VICs undergo myofibroblast differentiation to become osteoblast-like cells, which in turn deposit calcium in the aortic valve. This myofibroblast activation seems to be activated by invading inflammatory cells and activated endothelial cells

1

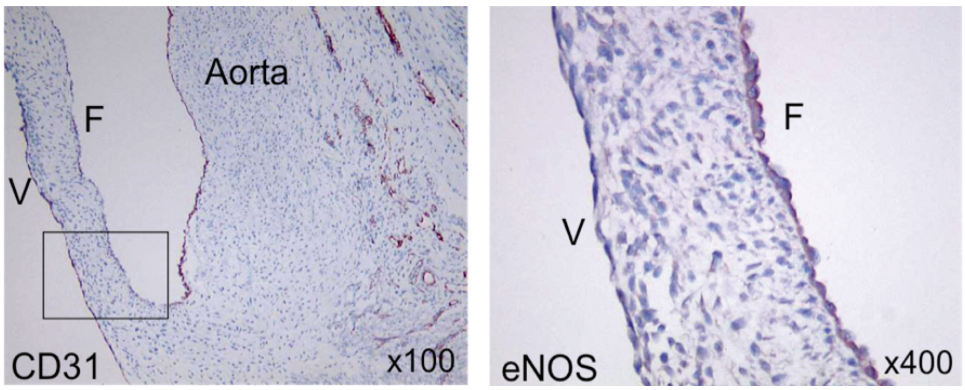

Figure 2. Human fetal aortic valve section immunostained with anti-CD31 and anti-eNOS reveals side-specific expression of eNOS. (F) – fibrosa, (V) - ventricularis.

that produce cytokines such as TGF-β1, BMP2/4, IL-1, IL- 6 and TNF-α. Increased α-smooth muscle actin (α-SMA) and smooth muscle myosin (SMM), decreased vimentin, increased migration, and increased proliferation characterize myofibroblast activation of VICs.[36, 54, 90, 91] Furthermore, studies have demonstrated that in CAVD, inflammatory cells and VICs secrete MMPs and cathepsins, which are involved in extracellular remodelling.[39, 92-94] The exact role of the inhibitors of these proteins, such as TIMPs and cystatin C, which are also expressed by VICs in CAVD, remains to be established. In CAVD, the *zona fibrosa* is especially prone to this remodelling process, characterized by disruption and disorganization of collagen bundles, fragmentation of elastin, and an increase in proteoglycan deposition. The disruption of the ECM contributes to the release of growth factors such as TGF-β1, which consequently influences VIC differentiation (as described earlier). The osteoblast-like cell differentiation of VICs is subject to a number of mechanisms, which are described in the next section.

4.4 Inflammation

Pathologically, stenotic valves are characterized by the presence of chronic inflammatory cellular infiltrates such as macrophages and T-lymphocytes, by the accumulation of lipids, and by thickening of the *fibrosa* and mineralization.[7] Early CAVD lesions are similar to atherosclerosis lesions, consisting of prominent LDL, lipoprotein (a), and apolipoproteins.[95] Inflammatory cells and lipids in stenotic valve leaflets co-localize near the surface of CAVD lesions, supporting the notion that CAVD is an active inflammatory disease process. Evidence suggests that one pathological concept of CAVD is that mechanical stress, together with atherosclerotic risk factors, leads to valvular endothelial dysfunction, followed by the deposition of LDL particles and other compounds that trigger inflammation. The inflammatory state can lead to the activation of inflammatory signalling pathways, macrophage infiltration, and T-lymphocyte activation. Activation of inflammatory pathways contributes to the disease process, which in turn activates VICs to express osteoblastic phenotypes and cause calcium deposition.

4.5 Biomechanics

The roles of mechanical and hemodynamic factors have been well studied, considering the context of designing and analyzing prosthetic valves. CAVD associates with mechanical and hemodynamic factors, as demonstrated by the correlation of CAVD lesions with regions of disturbed blood flow. Mechanical forces are vital in valve homoeostasis, but deviations from normal mechanical stress patterns can exacerbate pathological differentiation, as seen in CAVD. Contrary to the traditional belief that mechanical forces contribute to valve disease in a wear-and-tear fashion, we now see a direct relationship between mechanics and the active regulation of the aortic valve cell phenotype. This relationship is corroborated by studies that describe a side-specific pathological susceptibility of CAVD, demonstrating that the *zona fibrosa* especially suffers from mechanically induced pathological development. This relationship also reflects the difference in cellular level strains in valve tissue layers when subjected to mechanical forces. Mechanical forces and hemodynamic changes associated with CAVD exert their influence on the cells with which they are in direct contact, namely endothelial cells.

The exposure of shear stress to valve endothelial cells leads to the downregulation of genes associated with the activation and osteogenic differentiation of VICs.[49, 53] VICs exposed to pathological cyclic strain demonstrated increased expression of (α-SMA, BMP2/4, MMP, and cathepsin activity.[87] Similarly, hypertensive pressure showed increased VCAM-1 expression and decreased osteopontin.[96] Myofibroblast activation is also observed in autologous replacement valves implanted in an increased pressure environment, such as pulmonary autografts (Ross procedure) or tissue-engineered heart valves.[97, 98] Moreover, increased mechanical stiffness of the ECM occurs due to changes resulting from CAVD,[99] and VICs cultured on stiff substrates demonstrate increased myofibroblast differentiation and calcification.[54]

All in all, studies have demonstrated that changes in the mechanical environment and hemodynamic forces are important in the pathological process and changes occurring in CAVD. More specifically, biomechanics in the context of CAVD can catalyze the disease process, but are not an independent factor of osteoblastic differentiation.

4.6 Transcription Growth Factor–βeta

Transcription growth factor–βeta (TGF-β) regulates biological functions in various systems. In the aortic valve, TFG- β affects VIC differentiation, increasing the expression of α-SMA, smooth muscle myosin, and calponin.[100] TGF- β binds to its receptors (TGF- β receptors I and II), which initiates signalling through Smad proteins, which in turn interact with the transcription factors FoxH1, c-Jun, c-fos, and Gli-3. TGF- β can also initiate mitogen-activated protein kinase (MAPK) pathways. Both signalling pathways regulate cell cycle, proliferation, migration, cytokine secretion, and ECM synthesis and degradation — all of which are important in normal valvular biology.[101] The ECM components heparin and fibronectin participate in the effect of TGF- β on VICs.[102] By binding TGF- β to the pericellular environment, heparin induces α-SMA expression in VICs. Heparin also induces new TGF- β synthesis by VICs. VICs express fibronectin, a major component of the ECM that can

sequester TGF- β to activate VICs.[103] In CAVD, elevated VIC activation by TGF- β causes pathological remodelling of the ECM. More specifically, increased TGF- β1 expression increases collagen, glycosaminoglycan, and hyaluronic acid synthesis. In addition, studies of calcified valves have indicated increased expression of TGF- β in ECM. *In vitro* studies demonstrate that TGF- β promotes migration, aggregation, and formation of apoptotic alkaline phosphatase nodules. Anti-apoptotic agents prevent apoptosis and calcification in TGF-β-treated VICs. This indicates that TGF- β also promotes CAVD through a process involving apoptosis similar to atherosclerotic plaques.[90]

4.7 Lipoproteins and the Wnt signalling pathway

Landmark studies of patient aortic valve specimens with CAVD demonstrated the presence of LDLs in the valvular tissue. It became clear that lipids participate in the calcification of aortic valves relate to events leading to the eventual osteoblast-like differentiation of VICs. Lipids induce oxidative stress in the endothelium. Similar to vascular disease, endothelial dysfunction predisposes LDL migration through the endothelium. The accumulation of LDL can recruit inflammatory cells, subsequently leading to the release of inflammatory cytokines, which can activate VICs to differentiate into osteoblast-like cells.

The active role of lipids in the calcification process is confirmed in humans and in animals, which show a higher rate and severity of CAVD.[92] Interestingly, studies have demonstrated a relation between the bone formation signalling pathway and the LDL metabolism pathway. More specifically, the regulation of the LRP5/Wnt signalling has been implicated in cardiovascular calcification.[12, 104, 105] LDL receptor-related protein (LRP) signalling in bone is regulated through the canonical Wnt pathway. Wnt, a growth factor involved in bone and heart development,[106, 107] binds to receptors composed of frizzled protein and either of LRP5 or LRP6. This inhibits β-catenin degradation and leads to its accumulation and subsequent entry into the cellular nucleus. Calcified valves express elevated LRP5 and β-catenin, compared to healthy controls.[12, 104] β-catenin modulates the expression of several target genes, including cyclin D, Runx2/Cbfa1, and Sox9.[105] These transcription factors are crucial for myofibroblast differentiation to osteoblasts. The exact role of lipids in CAVD has yet to be elucidated. The recent failure in lipid-lowering pharmaceutical trials indicates that treating hyperlipidemia alone does not affect CAVD.

4.8 The OPG/RANKL/RANK signalling pathway

Calcified valves demonstrate the expression of RANKL (ligand of receptor activator of nuclear factor κ B, RANK) and osteoprotegerin (OPG), which also play a role in the cytokine system that regulates bone turnover.[108, 109] RANKL, a member of the TNF-α superfamily, is a transmembrane protein located on the surface of osteoblasts, stromal cells, T cells, and endothelial cells.[110] RANKL interacts with RANK, a transmembrane protein located on osteoclast precursors or mature osteoclasts, and induces osteoclastogenesis via NFκB. The interaction of RANKL with RANK also increases the binding of osteoblast transcription factor runx2/cbfa-1, which is essential for osteoblast differentiation.[109] This interaction can be blocked by OPG, subsequently limiting the activation of RANK and

thus preventing osteoclast differentiation. This pathway is critical in cardiovascular calcification, and provides a possible link between cardiovascular calcification and bone metabolism,[111] but determining the exact mechanism will require further investigations. Studies have shown that RANK/RANKL are highly increased in stenotic valves.[112] In VICs, RANKL treatment induces an osteoblast-like phenotype, that favours bone formation, increased nodule formation, and increased alkaline phosphatase activity, along with elevated synthesis of matrix elements and enhanced DNA binding of Runx2/Cbfa-1.[113] Treatment of VICs with TNF- α causes similar effects.[91]

Furthermore, mice deficient in OPG show calcification of large-sized and medium-sized vessels,[114] which supports the protective role of OPG against calcification. Interestingly, OPG has the opposite effect on skeletal bone, and inhibits bone resorption. Our study – as described in this thesis -demonstrated that cardiovascular calcification inversely correlates with low bone mineral density of long bones in an animal model of CAVD.[111] These results led to the hypothesis that calcium metabolites in the valve may originate from bone, and are mediated through inflammatory signalling. Further studies are needed to evaluate this hypothesis.

4.9 The renin-angiotensin system

Emerging evidence suggests that the renin-angiotensin system (RAAS) and the kallikrein-kinin system (KKS) are important in the regulation of heart valve homeostasis. In terms of CAVD, the RAAS/KKS balance seems to shift toward pro-fibrotic. ACE is a potent pro-fibrotic protein, capable of forming the equally pro-fibrotic angiotensin II (ATII).[115] ACE is produced by monocytes/macrophages and binds to circulating LDL particles. ACE can inactivate the anti-fibrotic enzyme bradykinin (BK), which is generated by the KKS.[81] Studies have demonstrated the presence of ATII receptors on VICs in CAVD; the density of these receptors is significantly higher in CAVD than in healthy aortic valves. The importance of the RAAS is demonstrated in studies where the ATII type 1 antagonist olmesartan had similar protective effects as atorvastatin in CAVD in rabbits.[82] Retrospective studies with ACE inhibitors also seem to slow calcification,[77] but randomized clinical trials are warranted.

4.10 Neoangiogenesis

Healthy human aortic valves are avascular and receive their nutrients through diffusion. In CAVD, however, neo-vessel formation or angiogenesis occurs, especially around calcified nodules. Histopathological studies have demonstrated the expression of vascular endothelial growth factor in calcified valves.[116] Furthermore, endothelial progenitor cells localize in the *zona fibrosa* of calcified native and bioprosthetic valves, indicating that cells of extra-valvular origin contribute to CAVD.[117] Whether VIC differentiation or inflammatory cells are involved in the neovascularization is unclear. Interestingly, the aortic valve also expresses anti-angiogenic factors, such as chondromodulin-1 and endostatin.[118] This observation has led to the hypothesis that the aortic valve possesses mechanisms to inhibit neovascularization in the healthy native valve, but in CAVD these mechanisms are disrupted, adding to its pathological process.

1

4.11 Genetics

The potential involvement of genes in CAVD has received much attention. Lessons learned from studies of bicuspid aortic valves, which associate with relatively quick calcific deterioration, demonstrate the potential role of a genetic component — namely, NOTCH1 and eNOS. For instance, 40% of adult mice that lack eNOS develop bicuspid aortic valves.[119] NOTCH1 is a receptor-based transcriptional activator and has been shown to promote endothelial-to-mesenchymal transformation (EndMT) and valve formation during valvular development. NOTCH1 normally inhibits calcification by inducing the expression of its target genes Hey1 and Hey2, which in turn interact with and repress the activity of Runx2/Cbfa1. Inactivation or mutations of NOTCH1 catalyze the progression of Runx2/Cbfa1-mediated calcification.[120] Much research is still needed to elucidate the role of a genetic component in CAVD, but evidence indicates that its development could be multifactorial.

4.12 Calcific Aortic Valve Disease – Status Quo

In summary, the previously discussed mechanisms lead to a suggested final common pathway of CAVD — the active mineralization of valvular matrix by activated VICs that have differentiated into osteoblast-like cells (Figure 3).

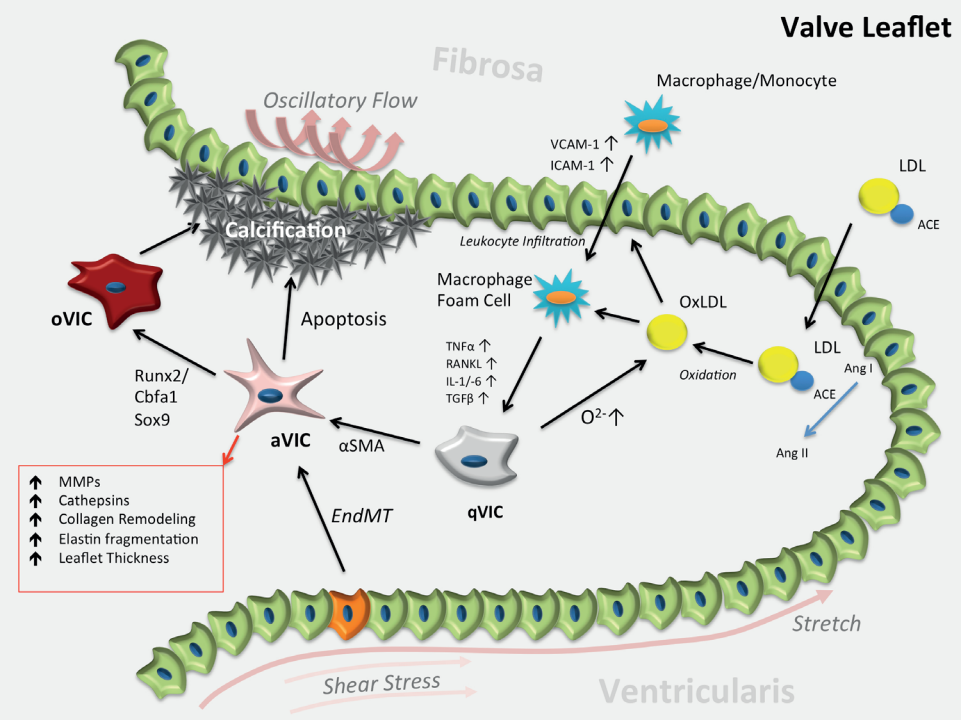

Figure 3. Schematic depiction of cellular, molecular and biomechanical mechanisms in calcific aortic valve disease (CAVD). *qVIC*: quiescent valvular interstitial cells, *aVIC*: activated valvular interstitial cells, *oVIC*: osteoblastic valvular interstitial cells. *ACE*: angiotensin-converting enzyme, *AngI/II*: angiotensin I/II; *EndMT*: endothelial-to-mesenchymal transition; *ICAM-1:* intracellular adhesion molecule-1, *VCAM-1*: vascular adhesion molecule-1; *LDL:* low-density lipoprotein; *αSMA*: alpha-Smooth Muscle Actin, *Runx2*: runt-related transcription factor 2; *TGFβ*: transforming growth factor-beta; *TNFα*: tumor necrosis factor-alpha

The calcification process initiates mainly in the *zona fibrosa*. The osteogenic differentiation of VICs is characterized by the presence of osteoblast-related genes such as osteocalcin, osteonectin, and the transcription factors runx2/cbfa1. The RANKL/RANK/OPG and Lpr5/Wnt signalling pathways can lead to the stimulation of runx2/cbfa1-mediated calcification of the aortic valve. Excess of circulatory LDL, accompanied by ACE, acts through the Lrp5/Wnt signalling pathway and induces mineralization of the valve stroma. Inflammation also stimulates VIC differentiation into osteoblast-like cells. Inflammatory cells produce cytokines that stimulate the RANKL/RANK/OPG pathway; ACE that acts through Wnt; and enzymes that degrade the ECM (e.g., MMPs, cathepsins). The inflammatory state and the degradation of ECM upregulates TGF- β, which stimulates the myofibroblast differentiation of VICs and further degrades ECM. Biomechanical forces, in which increased mechanical pressure environments can stimulate myofibroblast differentiation of VICs, also influence ECM homeostasis. CAVD should be considered a multifactorial disease for which the onset and progression to aortic valve stenosis mandate further investigation.

5. CONCLUSION

CAVD is a growing burden in the Western world. It is a progressive disease ranging from mild valve thickening to severe calcification with aortic valve stenosis. Despite its increasing prevalence and clinical significance, the mechanisms of CAVD are unclear. Fuelled by the absence of effective therapies other than aortic valve replacement, studies are needed to achieve a better understanding of CAVD — a complex disease in which multiple cellular and molecular mechanisms have been identified. The presence of additional comorbidities and clinical risk factors indicates a multifactorial pathogenesis.

The National Heart, Lung and Blood Institute Aortic Stenosis Working Group and more recently the Alliance of Investigators of Calcific Aortic Valve Disease set out recommendations for CAVD research: 1) identification of genetic, anatomic, and clinical risk factors for the distinct phases of initiation and progression of CAVD; 2) development of high-resolution and high-sensitivity imaging modalities that can identify early and subclinical CAVD, including molecular imaging and other innovative imaging approaches; 3) understanding the basic science of CAVD, including signalling pathways and the roles of valve interstitial cells and endothelial cells, autocrine and paracrine signaling, the extracellular matrix and its stiffness, interacting mechanisms of calcification, biomechanics, and hemodynamics; 4) development of suitable multi-scale *in vitro*, *ex vivo*, and animal models; 5) identification of the relationship between CAVD and bone metabolism; 6) creation of tissue banks from valve tissue acquired from surgery, pathology, and autopsy, with and without CAVD; and 7) establishing clinical studies of CAVD to determine the feasibility of pharmacological intervention and optimal timing of surgical valve replacement.

1

REFERENCES

1. Stewart BF, Siscovick D, Lind BK, Gardin JM, Gottdiener JS, Smith VE, Kitzman DW, Otto CM. Clinical factors associated with calcific aortic valve disease. Cardiovascular health study. *J Am Coll Cardiol*. 1997;29:630-634
2. Lloyd-Jones D, Adams R, Carnethon M, De Simone G, Ferguson TB, Flegal K, Ford E, Furie K, Go A, Greenlund K, Haase N, Hailpern S, Ho M, Howard V, Kissela B, Kittner S, Lackland D, Lisabeth L, Marelli A, McDermott M, Meigs J, Mozaffarian D, Nichol G, O'Donnell C, Roger V, Rosamond W, Sacco R, Sorlie P, Stafford R, Steinberger J, Thom T, Wasserthiel-Smoller S, Wong N, Wylie-Rosett J, Hong Y. Heart disease and stroke statistics--2009 update: A report from the american heart association statistics committee and stroke statistics subcommittee. *Circulation*. 2009;119:480-486
3. Iung B, Baron G, Butchart EG, Delahaye F, Gohlke-Barwolf C, Levang OW, Tornos P, Vanoverschelde JL, Vermeer F, Boersma E, Ravaud P, Vahanian A. A prospective survey of patients with valvular heart disease in europe: The euro heart survey on valvular heart disease. *Eur Heart J*. 2003;24:1231-1243
4. Takkenberg JJ, Rajamannan NM, Rosenhek R, Kumar AS, Carapetis JR, Yacoub MH. The need for a global perspective on heart valve disease epidemiology. The shvd working group on epidemiology of heart valve disease founding statement. *J Heart Valve Dis*. 2008;17:135-139
5. Rajamannan NM, Bonow RO, Rahimtoola SH. Calcific aortic stenosis: An update. *Nat Clin Pract Cardiovasc Med*. 2007;4:254-262
6. Otto CM. Calcific aortic stenosis--time to look more closely at the valve. *N Engl J Med*. 2008;359:1395-1398
7. Otto CM, Kuusisto J, Reichenbach DD, Gown AM, O'Brien KD. Characterization of the early lesion of 'degenerative' valvular aortic stenosis. Histological and immunohistochemical studies. *Circulation*. 1994;90:844-853
8. Rajamannan NM, Sangiorgi G, Springett M, Arnold K, Mohacsi T, Spagnoli LG, Edwards WD, Tajik AJ, Schwartz RS. Experimental hypercholesterolemia induces apoptosis in the aortic valve. *J Heart Valve Dis*. 2001;10:371-374
9. Aronow WS, Ahn C, Kronzon I, Goldman ME. Association of coronary risk factors and use of statins with progression of mild valvular aortic stenosis in older persons. *Am J Cardiol*. 2001;88:693-695
10. Novaro GM, Tiong IY, Pearce GL, Lauer MS, Sprecher DL, Griffin BP. Effect of hydroxymethylglutaryl coenzyme a reductase inhibitors on the progression of calcific aortic stenosis. *Circulation*. 2001;104:2205-2209
11. Bellamy MF, Pellikka PA, Klarich KW, Tajik AJ, Enriquez-Sarano M. Association of cholesterol levels, hydroxymethylglutaryl coenzyme-a reductase inhibitor treatment, and progression of aortic stenosis in the community. *J Am Coll Cardiol*. 2002;40:1723-1730
12. Rajamannan NM, Subramaniam M, Caira F, Stock SR, Spelsberg TC. Atorvastatin inhibits hypercholesterolemia-induced calcification in the aortic valves via the lrp5 receptor pathway. *Circulation*. 2005;112:I229-234
13. Aikawa E, Nahrendorf M, Figueiredo JL, Swirski FK, Shtatland T, Kohler RH, Jaffer FA, Aikawa M, Weissleder R. Osteogenesis associates with inflammation in early-stage atherosclerosis evaluated by molecular imaging in vivo. *Circulation*. 2007;116:2841-2850
14. Cowell SJ, Newby DE, Prescott RJ, Bloomfield P, Reid J, Northridge DB, Boon NA. A randomized trial of intensive lipid-lowering therapy in calcific aortic stenosis. *N Engl J Med*. 2005;352:2389-2397
15. Rossebo AB, Pedersen TR, Boman K, Brudi P, Chambers JB, Egstrup K, Gerdts E, Gohlke-Barwolf C, Holme I, Kesaniemi YA, Malbecq W, Nienaber CA, Ray S, Skjaerpe T, Wachtell K, Willenheimer R. Intensive lipid lowering with simvastatin and ezetimibe in aortic stenosis. *N Engl J Med*. 2008;359:1343-1356
16. Mohler ER, 3rd, Chawla MK, Chang AW, Vyavahare N, Levy RJ, Graham L, Gannon FH. Identification and characterization of calcifying valve cells from human and canine aortic valves. *J Heart Valve Dis*. 1999;8:254-260

17. Mohler ER, 3rd, Gannon F, Reynolds C, Zimmerman R, Keane MG, Kaplan FS. Bone formation and inflammation in cardiac valves. *Circulation*. 2001;103:1522-1528
18. Schoen FJ. Evolving concepts of cardiac valve dynamics: The continuum of development, functional structure, pathobiology, and tissue engineering. *Circulation*. 2008;118:1864-1880
19. New SE, Aikawa E. Molecular imaging insights into early inflammatory stages of arterial and aortic valve calcification. *Circulation research*. 2011;108:1381-1391
20. Miller JD, Weiss RM, Serrano KM, Castaneda LE, Brooks RM, Zimmerman K, Heistad DD. Evidence for active regulation of pro-osteogenic signaling in advanced aortic valve disease. *Arterioscler Thromb Vasc Biol*. 2010;30:2482-2486
21. Breuer CK, Mettler BA, Anthony T, Sales VL, Schoen FJ, Mayer JE. Application of tissue-engineering principles toward the development of a semilunar heart valve substitute. *Tissue Eng*. 2004;10:1725-1736
22. Roberts WC. The structure of the aortic valve in clinically isolated aortic stenosis: An autopsy study of 162 patients over 15 years of age. *Circulation*. 1970;42:91-97
23. Thubrikar MJ, Aouad J, Nolan SP. Comparison of the in vivo and in vitro mechanical properties of aortic valve leaflets. *J Thorac Cardiovasc Surg*. 1986;92:29-36
24. Katayama S, Umetani N, Sugiura S, Hisada T. The sinus of valsalva relieves abnormal stress on aortic valve leaflets by facilitating smooth closure. *J Thorac Cardiovasc Surg*. 2008;136:1528-1535, 1535 e1521
25. Thubrikar M, Bosher LP, Nolan SP. The mechanism of opening of the aortic valve. *J Thorac Cardiovasc Surg*. 1979;77:863-870
26. Higashidate M, Tamiya K, Beppu T, Imai Y. Regulation of the aortic valve opening. In vivo dynamic measurement of aortic valve orifice area. *J Thorac Cardiovasc Surg*. 1995;110:496-503
27. Thubrikar M, Nolan SP, Bosher LP, Deck JD. The cyclic changes and structure of the base of the aortic valve. *Am Heart J*. 1980;99:217-224
28. Ho SY. Structure and anatomy of the aortic root. *Eur J Echocardiogr*. 2009;10:i3-10
29. Fowler NO. Clinical aspects of acquired valvular heart disease. *Semin Roentgenol*. 1979;14:83-95
30. De Hart J, Peters GW, Schreurs PJ, Baaijens FP. Collagen fibers reduce stresses and stabilize motion of aortic valve leaflets during systole. *J Biomech*. 2004;37:303-311
31. Butcher JT, Penrod AM, Garcia AJ, Nerem RM. Unique morphology and focal adhesion development of valvular endothelial cells in static and fluid flow environments. *Arterioscler Thromb Vasc Biol*. 2004;24:1429-1434
32. Cimini M, Rogers KA, Boughner DR. Smoothelin-positive cells in human and porcine semilunar valves. *Histochem Cell Biol*. 2003;120:307-317
33. Chester AH, Kershaw JD, Sarathchandra P, Yacoub MH. Localisation and function of nerves in the aortic root. *J Mol Cell Cardiol*. 2008;44:1045-1052
34. Marron K, Yacoub MH, Polak JM, Sheppard MN, Fagan D, Whitehead BF, de Leval MR, Anderson RH, Wharton J. Innervation of human atrioventricular and arterial valves. *Circulation*. 1996;94:368-375
35. Yperman J, De Visscher G, Holvoet P, Flameng W. Molecular and functional characterization of ovine cardiac valve-derived interstitial cells in primary isolates and cultures. *Tissue Eng*. 2004;10:1368-1375
36. Taylor PM, Batten P, Brand NJ, Thomas PS, Yacoub MH. The cardiac valve interstitial cell. *Int J Biochem Cell Biol*. 2003;35:113-118
37. Liu AC, Joag VR, Gotlieb AI. The emerging role of valve interstitial cell phenotypes in regulating heart valve pathobiology. *Am J Pathol*. 2007;171:1407-1418
38. Rabkin-Aikawa E, Farber M, Aikawa M, Schoen FJ. Dynamic and reversible changes of interstitial cell phenotype during remodeling of cardiac valves. *J Heart Valve Dis*. 2004;13:841-847

39. Rabkin E, Aikawa M, Stone JR, Fukumoto Y, Libby P, Schoen FJ. Activated interstitial myofibroblasts express catabolic enzymes and mediate matrix remodeling in myxomatous heart valves. *Circulation*. 2001;104:2525-2532
40. Aikawa E, Whittaker P, Farber M, Mendelson K, Padera RF, Aikawa M, Schoen FJ. Human semilunar cardiac valve remodeling by activated cells from fetus to adult: Implications for postnatal adaptation, pathology, and tissue engineering. *Circulation*. 2006;113:1344-1352
41. Butcher JT, Simmons CA, Warnock JN. Mechanobiology of the aortic heart valve. *J Heart Valve Dis*. 2008;17:62-73
42. Thubrikar MJ, Aouad J, Nolan SP. Patterns of calcific deposits in operatively excised stenotic or purely regurgitant aortic valves and their relation to mechanical stress. *Am J Cardiol*. 1986;58:304-308
43. Levitt LC, Thubrikar MJ, Nolan SP. Patterns and pathogenesis of calcification in pathologic human aortic valves. *Curr Surg*. 1984;41:17-19
44. Mulholland DL, Gotlieb AI. Cell biology of valvular interstitial cells. *Can J Cardiol*. 1996;12:231-236
45. Merryman WD, Youn I, Lukoff HD, Krueger PM, Guilak F, Hopkins RA, Sacks MS. Correlation between heart valve interstitial cell stiffness and transvalvular pressure: Implications for collagen biosynthesis. *Am J Physiol Heart Circ Physiol*. 2006;290:H224-231
46. Butcher JT, Mahler GJ, Hockaday LA. Aortic valve disease and treatment: The need for naturally engineered solutions. *Adv Drug Deliv Rev*.
47. Jaffee OC. The development of the arterial outflow tract in the chick embryo heart. *Anat Rec*. 1967;158:35-42
48. Deck JD. Endothelial cell orientation on aortic valve leaflets. *Cardiovasc Res*. 1986;20:760-767
49. Butcher JT, Tressel S, Johnson T, Turner D, Sorescu G, Jo H, Nerem RM. Transcriptional profiles of valvular and vascular endothelial cells reveal phenotypic differences: Influence of shear stress. *Arterioscler Thromb Vasc Biol*. 2006;26:69-77
50. Butcher JT, Mahler GJ, Hockaday LA. Aortic valve disease and treatment: The need for naturally engineered solutions. *Adv Drug Deliv Rev*. 2011
51. Kilner PJ, Yang GZ, Wilkes AJ, Mohiaddin RH, Firmin DN, Yacoub MH. Asymmetric redirection of flow through the heart. *Nature*. 2000;404:759-761
52. Simmons CA, Grant GR, Manduchi E, Davies PF. Spatial heterogeneity of endothelial phenotypes correlates with side-specific vulnerability to calcification in normal porcine aortic valves. *Circulation research*. 2005;96:792-799
53. Sucosky P, Balachandran K, Elhammali A, Jo H, Yoganathan AP. Altered shear stress stimulates upregulation of endothelial vcam-1 and icam-1 in a bmp-4- and tgf-beta1-dependent pathway. *Arterioscler Thromb Vasc Biol*. 2009;29:254-260
54. Yip CY, Chen JH, Zhao R, Simmons CA. Calcification by valve interstitial cells is regulated by the stiffness of the extracellular matrix. *Arterioscler Thromb Vasc Biol*. 2009;29:936-942
55. Mohler ER, 3rd. Mechanisms of aortic valve calcification. *Am J Cardiol*. 2004;94:1396-1402, A1396
56. El-Hamamsy I, Balachandran K, Yacoub MH, Stevens LM, Sarathchandra P, Taylor PM, Yoganathan AP, Chester AH. Endothelium-dependent regulation of the mechanical properties of aortic valve cusps. *J Am Coll Cardiol*. 2009;53:1448-1455
57. Butcher JT, Nerem RM. Valvular endothelial cells regulate the phenotype of interstitial cells in co-culture: Effects of steady shear stress. *Tissue Eng*. 2006;12:905-915
58. Cosmi JE, Kort S, Tunick PA, Rosenzweig BP, Freedberg RS, Katz ES, Applebaum RM, Kronzon I. The risk of the development of aortic stenosis in patients with "benign" aortic valve thickening. *Arch Intern Med*. 2002;162:2345-2347

59. Faggiano P, Antonini-Canterin F, Erlicher A, Romeo C, Cervesato E, Pavan D, Piazza R, Huang G, Nicolosi GL. Progression of aortic valve sclerosis to aortic stenosis. *Am J Cardiol*. 2003;91:99-101
60. Aronow WS, Schwartz KS, Koenigsberg M. Correlation of serum lipids, calcium, and phosphorus, diabetes mellitus and history of systemic hypertension with presence or absence of calcified or thickened aortic cusps or root in elderly patients. *Am J Cardiol*. 1987;59:998-999
61. Katz R, Budoff MJ, Takasu J, Shavelle DM, Bertoni A, Blumenthal RS, Ouyang P, Wong ND, O'Brien KD. Relationship of metabolic syndrome with incident aortic valve calcium and aortic valve calcium progression: The multi-ethnic study of atherosclerosis (mesa). *Diabetes*. 2009;58:813-819
62. Otto CM, Burwash IG, Legget ME, Munt BI, Fujioka M, Healy NL, Kraft CD, Miyake-Hull CY, Schwaegler RG. Prospective study of asymptomatic valvular aortic stenosis. Clinical, echocardiographic, and exercise predictors of outcome. *Circulation*. 1997;95:2262-2270
63. Fox CS, Larson MG, Vasan RS, Guo CY, Parise H, Levy D, Leip EP, O'Donnell C J, D'Agostino RB, Sr., Benjamin EJ. Cross-sectional association of kidney function with valvular and annular calcification: The framingham heart study. *J Am Soc Nephrol*. 2006;17:521-527
64. Otto CM, O'Brien KD. Why is there discordance between calcific aortic stenosis and coronary artery disease? *Heart*. 2001;85:601-602
65. Horl WH. The clinical consequences of secondary hyperparathyroidism: Focus on clinical outcomes. *Nephrol Dial Transplant*. 2004;19 Suppl 5:V2-8
66. Hultgren HN. Osteitis deformans (paget's disease) and calcific disease of the heart valves. *Am J Cardiol*. 1998;81:1461-1464
67. Nakamura T, Hultgren HN, Shettigar UR, Fowles RE. Noninvasive evaluation of the severity of aortic stenosis in adult patients. *Am Heart J*. 1984;107:959-966
68. Braun HA, Comeau WJ. The importance of high-pitched squeaking systolic murmur in the diagnosis of aortic stenosis and calcification of the aortic valve. *N Engl J Med*. 1951;244:507-509
69. Rosenhek R, Binder T, Porenta G, Lang I, Christ G, Schemper M, Maurer G, Baumgartner H. Predictors of outcome in severe, asymptomatic aortic stenosis. *N Engl J Med*. 2000;343:611-617
70. Carabello BA, Paulus WJ. Aortic stenosis. *Lancet*. 2009;373:956-966
71. Stout KK, Otto CM. Indications for aortic valve replacement in aortic stenosis. *J Intensive Care Med*. 2007;22:14-25
72. Owen A, Henein MY. Challenges in the management of severe asymptomatic aortic stenosis. *Eur J Cardiothorac Surg*. 2011
73. Hammermeister K, Sethi GK, Henderson WG, Grover FL, Oprian C, Rahimtoola SH. Outcomes 15 years after valve replacement with a mechanical versus a bioprosthetic valve: Final report of the veterans affairs randomized trial. *J Am Coll Cardiol*. 2000;36:1152-1158
74. Bloomfield P, Wheatley DJ, Prescott RJ, Miller HC. Twelve-year comparison of a bjork-shiley mechanical heart valve with porcine bioprostheses. *N Engl J Med*. 1991;324:573-579
75. O'Brien KD, Shavelle DM, Caulfield MT, McDonald TO, Olin-Lewis K, Otto CM, Probstfield JL. Association of angiotensin-converting enzyme with low-density lipoprotein in aortic valvular lesions and in human plasma. *Circulation*. 2002;106:2224-2230
76. Olsson M, Thyberg J, Nilsson J. Presence of oxidized low density lipoprotein in nonrheumatic stenotic aortic valves. *Arterioscler Thromb Vasc Biol*. 1999;19:1218-1222
77. Rosenhek R, Rader F, Loho N, Gabriel H, Heger M, Klaar U, Schemper M, Binder T, Maurer G, Baumgartner H. Statins but not angiotensin-converting enzyme inhibitors delay progression of aortic stenosis. *Circulation*. 2004;110:1291-1295
78. Shavelle DM, Takasu J, Budoff MJ, Mao S, Zhao XQ, O'Brien KD. Hmg coa reductase inhibitor (statin) and aortic valve calcium. *Lancet*. 2002;359:1125-1126

1

79. Moura LM, Ramos SF, Zamorano JL, Barros IM, Azevedo LF, Rocha-Goncalves F, Rajamannan NM. Rosuvastatin affecting aortic valve endothelium to slow the progression of aortic stenosis. *J Am Coll Cardiol*. 2007;49:554-561
80. Chan KL, Teo K, Dumesnil JG, Ni A, Tam J. Effect of lipid lowering with rosuvastatin on progression of aortic stenosis: Results of the aortic stenosis progression observation: Measuring effects of rosuvastatin (astronomer) trial. *Circulation*. 2010;121:306-314
81. Helske S, Lindstedt KA, Laine M, Mayranpaa M, Werkkala K, Lommi J, Turto H, Kupari M, Kovanen PT. Induction of local angiotensin ii-producing systems in stenotic aortic valves. *J Am Coll Cardiol*. 2004;44:1859-1866
82. Arishiro K, Hoshiga M, Negoro N, Jin D, Takai S, Miyazaki M, Ishihara T, Hanafusa T. Angiotensin receptor-1 blocker inhibits atherosclerotic changes and endothelial disruption of the aortic valve in hypercholesterolemic rabbits. *J Am Coll Cardiol*. 2007;49:1482-1489
83. Freeman RV, Otto CM. Spectrum of calcific aortic valve disease: Pathogenesis, disease progression, and treatment strategies. *Circulation*. 2005;111:3316-3326
84. Sacks MS, Yoganathan AP. Heart valve function: A biomechanical perspective. *Philosophical transactions of the Royal Society of London*. 2007;362:1369-1391
85. Muller AM, Cronen C, Kupferwasser LI, Oelert H, Muller KM, Kirkpatrick CJ. Expression of endothelial cell adhesion molecules on heart valves: Up-regulation in degeneration as well as acute endocarditis. *The Journal of pathology*. 2000;191:54-60
86. Shavelle DM, Katz R, Takasu J, Lima JA, Jenny NS, Budoff MJ, O'Brien KD. Soluble intercellular adhesion molecule-1 (sicam-1) and aortic valve calcification in the multi-ethnic study of atherosclerosis (mesa). *J Heart Valve Dis*. 2008;17:388-395
87. Balachandran K, Sucosky P, Jo H, Yoganathan AP. Elevated cyclic stretch induces aortic valve calcification in a bone morphogenic protein-dependent manner. *Am J Pathol*. 2010;177:49-57
88. Sorescu GP, Song H, Tressel SL, Hwang J, Dikalov S, Smith DA, Boyd NL, Platt MO, Lassegue B, Griendling KK, Jo H. Bone morphogenic protein 4 produced in endothelial cells by oscillatory shear stress induces monocyte adhesion by stimulating reactive oxygen species production from a nox1-based nadph oxidase. *Circulation research*. 2004;95:773-779
89. Mirzaie M, Schultz M, Schwartz P, Coulibaly M, Schondube F. Evidence of woven bone formation in heart valve disease. *Ann Thorac Cardiovasc Surg*. 2003;9:163-169
90. Jian B, Narula N, Li QY, Mohler ER, 3rd, Levy RJ. Progression of aortic valve stenosis: Tgf-beta1 is present in calcified aortic valve cusps and promotes aortic valve interstitial cell calcification via apoptosis. *The Annals of thoracic surgery*. 2003;75:457-465; discussion 465-456
91. Kaden JJ, Kilic R, Sarikoc A, Hagl S, Lang S, Hoffmann U, Brueckmann M, Borggrefe M. Tumor necrosis factor alpha promotes an osteoblast-like phenotype in human aortic valve myofibroblasts: A potential regulatory mechanism of valvular calcification. *International journal of molecular medicine*. 2005;16:869-872
92. Aikawa E, Aikawa M, Libby P, Figueiredo JL, Rusanescu G, Iwamoto Y, Fukuda D, Kohler RH, Shi GP, Jaffer FA, Weissleder R. Arterial and aortic valve calcification abolished by elastolytic cathepsin s deficiency in chronic renal disease. *Circulation*. 2009;119:1785-1794
93. Soini Y, Satta J, Maatta M, Autio-Harmainen H. Expression of mmp2, mmp9, mt1-mmp, timp1, and timp2 mrna in valvular lesions of the heart. *The Journal of pathology*. 2001;194:225-231
94. Fondard O, Detaint D, Iung B, Choqueux C, Adle-Biassette H, Jarraya M, Hvass U, Couetil JP, Henin D, Michel JB, Vahanian A, Jacob MP. Extracellular matrix remodelling in human aortic valve disease: The role of matrix metalloproteinases and their tissue inhibitors. *Eur Heart J*. 2005;26:1333-1341
95. O'Brien KD, Reichenbach DD, Marcovina SM, Kuusisto J, Alpers CE, Otto CM. Apolipoproteins b, (a), and e accumulate in the morphologically early lesion of 'degenerative' valvular aortic stenosis. *Arterioscler Thromb Vasc Biol*. 1996;16:523-532

96. Warnock JN, Burgess SC, Shack A, Yoganathan AP. Differential immediate-early gene responses to elevated pressure in porcine aortic valve interstitial cells. *J Heart Valve Dis*. 2006;15:34-41; discussion 42
97. Rabkin-Aikawa E, Aikawa M, Farber M, Kratz JR, Garcia-Cardena G, Kouchoukos NT, Mitchell MB, Jonas RA, Schoen FJ. Clinical pulmonary autograft valves: Pathologic evidence of adaptive remodeling in the aortic site. *J Thorac Cardiovasc Surg*. 2004;128:552-561
98. Rabkin E, Hoerstrup SP, Aikawa M, Mayer JE, Jr., Schoen FJ. Evolution of cell phenotype and extracellular matrix in tissue-engineered heart valves during in-vitro maturation and in-vivo remodeling. *J Heart Valve Dis*. 2002;11:308-314; discussion 314
99. Weinberg EJ, Schoen FJ, Mofrad MR. A computational model of aging and calcification in the aortic heart valve. *PloS one*. 2009;4:e5960
100. ten Dijke P, Hill CS. New insights into tgf-beta-smad signalling. *Trends Biochem Sci*. 2004;29:265-273
101. Walker GA, Masters KS, Shah DN, Anseth KS, Leinwand LA. Valvular myofibroblast activation by transforming growth factor-beta: Implications for pathological extracellular matrix remodeling in heart valve disease. *Circulation research*. 2004;95:253-260
102. Taipale J, Saharinen J, Hedman K, Keski-Oja J. Latent transforming growth factor-beta 1 and its binding protein are components of extracellular matrix microfibrils. *J Histochem Cytochem*. 1996;44:875-889
103. Cushing MC, Liao JT, Anseth KS. Activation of valvular interstitial cells is mediated by transforming growth factor-beta1 interactions with matrix molecules. *Matrix Biol*. 2005;24:428-437
104. Caira FC, Stock SR, Gleason TG, McGee EC, Huang J, Bonow RO, Spelsberg TC, McCarthy PM, Rahimtoola SH, Rajamannan NM. Human degenerative valve disease is associated with up-regulation of low-density lipoprotein receptor-related protein 5 receptor-mediated bone formation. *J Am Coll Cardiol*. 2006;47:1707-1712
105. Shao JS, Cheng SL, Pingsterhaus JM, Charlton-Kachigian N, Loewy AP, Towler DA. Msx2 promotes cardiovascular calcification by activating paracrine wnt signals. *The Journal of clinical investigation*. 2005;115:1210-1220
106. Clevers H. Wnt/beta-catenin signaling in development and disease. *Cell*. 2006;127:469-480
107. Chakraborty S, Cheek J, Sakthivel B, Aronow BJ, Yutzey KE. Shared gene expression profiles in developing heart valves and osteoblast progenitor cells. *Physiological genomics*. 2008;35:75-85
108. Kaden JJ, Bickelhaupt S, Grobholz R, Haase KK, Sarikoc A, Kilic R, Brueckmann M, Lang S, Zahn I, Vahl C, Hagl S, Dempfle CE, Borggrefe M. Receptor activator of nuclear factor kappab ligand and osteoprotegerin regulate aortic valve calcification. *J Mol Cell Cardiol*. 2004;36:57-66
109. Kaden JJ, Bickelhaupt S, Grobholz R, Vahl CF, Hagl S, Brueckmann M, Haase KK, Dempfle CE, Borggrefe M. Expression of bone sialoprotein and bone morphogenetic protein-2 in calcific aortic stenosis. *J Heart Valve Dis*. 2004;13:560-566
110. Hofbauer LC, Schoppet M. Clinical implications of the osteoprotegerin/rankl/rank system for bone and vascular diseases. *Jama*. 2004;292:490-495
111. Hjortnaes J, Butcher J, Figueiredo JL, Riccio M, Kohler RH, Kozloff KM, Weissleder R, Aikawa E. Arterial and aortic valve calcification inversely correlates with osteoporotic bone remodelling: A role for inflammation. *Eur Heart J*. 2010;31:1975-1984
112. Steinmetz M, Skowasch D, Wernert N, Welsch U, Preusse CJ, Welz A, Nickenig G, Bauriedel G. Differential profile of the opg/rankl/rank-system in degenerative aortic native and bioprosthetic valves. *J Heart Valve Dis*. 2008;17:187-193
113. Kaden JJ, Dempfle CE, Grobholz R, Fischer CS, Vocke DC, Kilic R, Sarikoc A, Pinol R, Hagl S, Lang S, Brueckmann M, Borggrefe M. Inflammatory regulation of extracellular matrix remodeling in calcific aortic valve stenosis. *Cardiovasc Pathol*. 2005;14:80-87

1

114. Nanes MS. Tumor necrosis factor-alpha: Molecular and cellular mechanisms in skeletal pathology. *Gene*. 2003;321:1-15
115. Mehta PK, Griendling KK. Angiotensin ii cell signaling: Physiological and pathological effects in the cardiovascular system. *Am J Physiol Cell Physiol*. 2007;292:C82-97
116. Soini Y, Salo T, Satta J. Angiogenesis is involved in the pathogenesis of nonrheumatic aortic valve stenosis. *Human pathology*. 2003;34:756-763
117. Skowasch D, Schrempf S, Wernert N, Steinmetz M, Jabs A, Tuleta I, Welsch U, Preusse CJ, Likungu JA, Welz A, Luderitz B, Bauriedel G. Cells of primarily extra-valvular origin in degenerative aortic valves and bioprostheses. *Eur Heart J*. 2005;26:2576-2580
118. Chalajour F, Treede H, Ebrahimnejad A, Lauke H, Reichenspurner H, Ergun S. Angiogenic activation of valvular endothelial cells in aortic valve stenosis. *Experimental cell research*. 2004;298:455-464
119. Lee TC, Zhao YD, Courtman DW, Stewart DJ. Abnormal aortic valve development in mice lacking endothelial nitric oxide synthase. *Circulation*. 2000;101:2345-2348
120. Rusanescu G, Weissleder R, Aikawa E. Notch signaling in cardiovascular disease and calcification. *Curr Cardiol Rev*. 2008;4:148-156

2

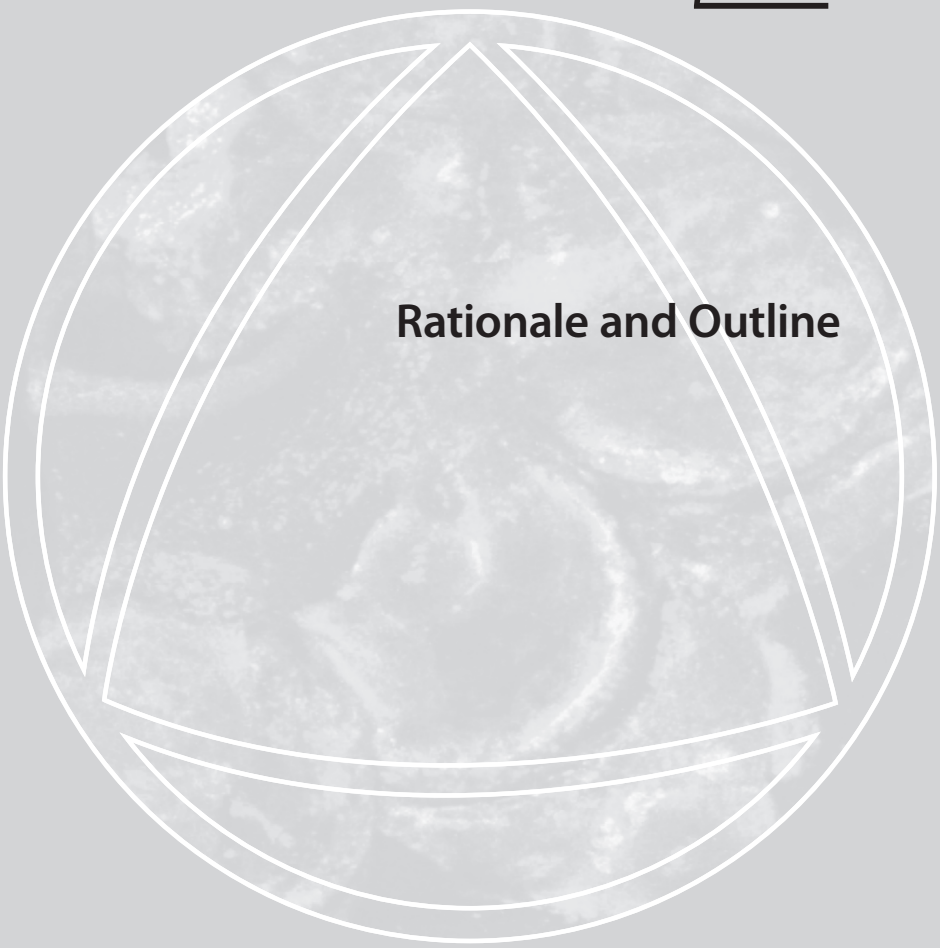

Rationale and Outline

1. RATIONALE

Calcific aortic valve disease (CAVD) has become increasingly prevalent worldwide and is associated with significant morbidity and mortality. There are currently no therapeutic options beyond surgical valve replacement, with transcatheter aortic valve replacement reserved for patients with excess operative risk. These challenges warrant better understanding of mechanisms involved in CAVD, with the eventual goal of new preventive and therapeutic strategies.

To date, our understanding of human CAVD has mostly been based on pathological specimens from patients undergoing valve replacement. However, considering that patients do not exhibit symptoms prior to significant aortic valve stenosis, these valves are almost entirely a reflection of end stage disease, providing little insight into disease onset or the progression of disease in humans. As such, most of our knowledge stems from *in vitro* cell studies or experimental *in vivo* models, which are both irrefutably important tools to study mechanisms of disease. However, *in vitro* cell studies are not accurate physiological representations of cellular behavior *in vivo*. On one hand, this is due to the inherent unnatural environment attributed to the petri dish. On the other hand, this is due to the absence of simulating the complexity of organ systems as they occur *in vivo*.

Experimental *in vivo* models are able to simulate such complexity, and provide for elucidating multiple variables that might influence disease. However, experiments performed in animal models differ significantly from humans. For instance, murine models require dietary and/or genetic manipulation to induce cardiovascular calcification and leporine models must be fed high cholesterol diet to induce disease observed in humans.[1] Considering the inability of translating beneficial effect of statins in animal models to humans, one can argue that CAVD may progress in humans differently from animals. One can also argue that our current experimental models of CAVD – *in vitro* or *in vivo*- have not yielded the understanding required to effectively translate therapeutic targets to patients. Understanding early CAVD and disease progression is vital if we are to develop new treatment strategies.

Elucidating mechanisms involved in early CAVD seems to face two important challenges. First, developing imaging modalities that can visualize the early CAVD process, and second, developing experimental models that accurately recapitulate the disease process as it may occurs *in situ*.

The clinical golden standard for detecting valvular disease in patients is visualizing valvular dysfunction by echocardiography. However, this imaging modality is unable to identify early leaflet changes mainly because regurgitant blood flow and leaflet thickening occur in subsequent stages of CAVD remodeling and calcification. As such, development of detection strategies to identify these early leaflet changes is needed. To this end optical molecular imaging has emerged as a tool to visualize progression of cardiovascular calcification, and might offer the resolution necessary to identify patients who will respond to therapy. In addition, molecular imaging has the potential to offer temporal understanding of CAVD and could thus identify hallmarks of disease progression usable to develop an optimal therapeutic strategy at each stage of CAVD.

However, understanding hallmarks of disease onset and its progression relies greatly on elucidating cellular processes of disease. Yet, cells behave differently when isolated from the complex architecture of their native tissues and cultured on Petri dishes. In particular, VICs in two dimensional culture will undergo spontaneous myofibroblast-like activation, whereas in situ they are mostly quiescent fibroblast like cells.[2] To this end, the challenge has arisen to develop experimental *in vitro* models, which are physiologically more accurate in simulating the micro-environment native to valves. Hydrogel micro engineering has emerged as a powerful tool to address this challenge by applying principles of tissue engineering to recapitulate tissue processes *in vitro*.[3] By using natural extracellular matrix proteins, hydrogel micro engineering aims to fabricate the cellular micro-environment of the heart valve. The structure and composition of these hydrogels can be tailored to deliver the appropriate chemical, biological and physical cues that resemble the native valvular milieu.

The objective of this thesis is to address current challenges in understanding CAVD and particularly develop new means of studying early CAVD. The specific aims can be defined as follows.

I Using molecular imaging as a tool to study early onset CAVD and identifying hallmarks of disease progression

II Developing an *in vitro* model that can recapitulate the process of early CAVD as it may occur in situ

2. OUTLINE

The outline of this thesis follows these goals and is partitioned in two: **(I)** visualization of early CAVD, **(II)** developing a model for early CAVD.

Part I consists firstly of *Chapter 3*, which reviews literature on visualizing novel concepts of CAVD both in animal models as well as in humans. *Chapter 4* explores molecular imaging as a tool to study mechanisms of early CAVD in a mouse model of cardiovascular calcification.

Most studies concerning pathological mechanisms of CAVD are limited by inaccurate representation of human disease. To this end, **part II** focuses on developing a physiologically more accurate model of CAVD. First, *Chapter 5* reviews literature on how to use tissue engineering – which in brief aims to fabricate human tissue in the laboratory – to create a model for valve disease. *Chapter 6* describes the technology of hydrogel micro-engineering and how to apply this to the field of heart valve research. *Chapter 7* explains our development of a micro –engineered heart valve-like tissue model, which is then used in *Chapter 8* to simulate early CAVD. *Chapter 9* is an example of how our valve-like tissue model can be used to study the effect of radiation on CAVD onset and progression. An important part of developing a valve model is the valvular endothelium. *Chapter 10* focuses on studying the interaction between valvular endothelial cells and valvular interstitial cells and their role in CAVD. Final thoughts on early CAVD are reflected in *Chapter 11* with a summary and conclusions and as a general discussion in *Chapter 12*.

REFERENCES

1. Hutcheson JD, Aikawa E, Merryman WD. Potential drug targets for calcific aortic valve disease. *Nature reviews. Cardiology*. 2014;11:218-231
2. Walker GA, Masters KS, Shah DN, Anseth KS, Leinwand LA. Valvular myofibroblast activation by transforming growth factor-beta: Implications for pathological extracellular matrix remodeling in heart valve disease. *Circulation research*. 2004;95:253-260
3. Slaughter BV, Khurshid SS, Fisher OZ, Khademhosseini A, Peppas NA. Hydrogels in regenerative medicine. *Advanced materials*. 2009;21:3307-3329

Part I

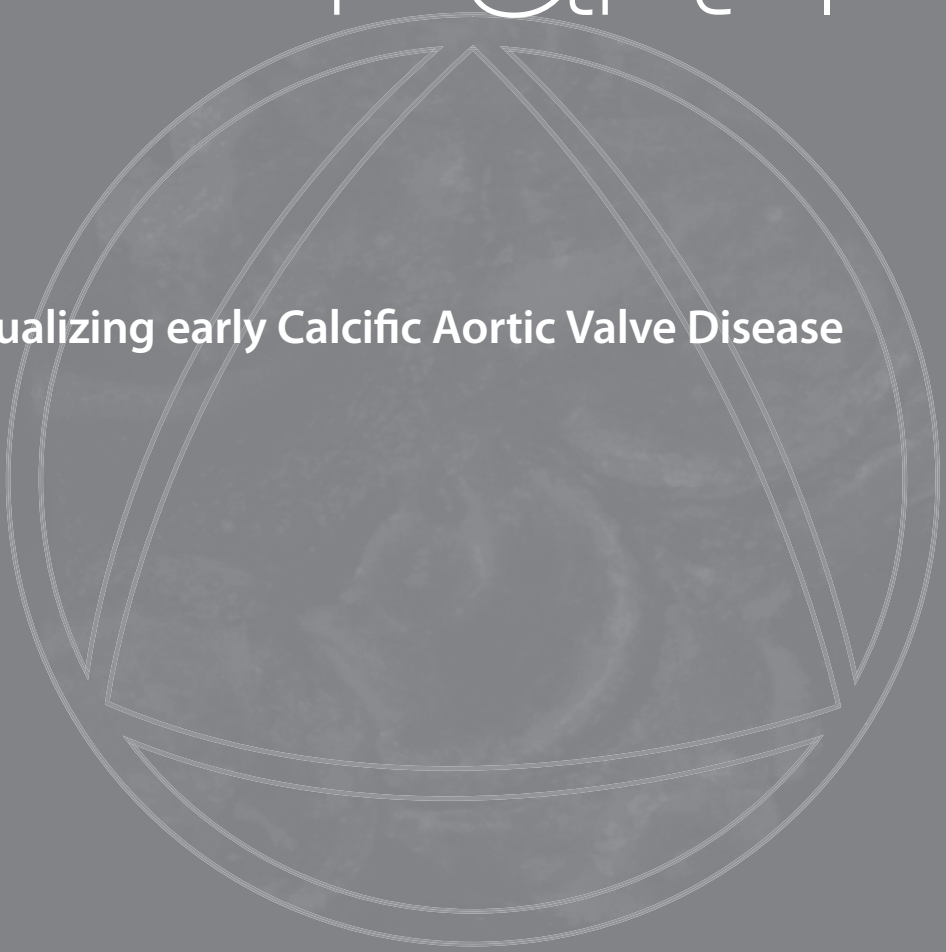

Visualizing early Calcific Aortic Valve Disease

3

Visualizing New Concepts of Cardiovascular Calcification

J. Hjortnaes[1,2], S.P. New[1], and E. Aikawa[1]

Trends in Cardiovascular Medcine 2013

[1]Center for Excellence in Vascular Biology, Brigham and Women's Hospital, Harvard Medical School, Boston, USA [2]Department of Cardiothoracic Surgery, Division of Heart and Lungs, University Medical Center Utrecht, Utrecht, The Netherlands

INTRODUCTION

Calcification, a progressive disease of dysregulated mineral metabolism, has been observed in the cardiovascular system for many decades. Ectopic calcification of the cardiovascular system predominantly affects the aorta, coronary arteries, peripheral arteries and the aortic valve. Traditionally, cardiovascular calcification has been considered a passive phenomenon associated with aging; however, it is currently viewed as an actively regulated disease process. More specifically, mounting evidence suggests that the underlying mechanisms of cardiovascular calcification are similar to embrynic bone formation.[1-3]

The pathological mineralization of the arteries is often observed in atherosclerotic plaques, which clinically translates to reduced compliance of the vessel wall, associated with hypertension.[4] In addition, studies demonstrate that microcalcifcation in the fibrous cap overlying the necrotic core of atherosclerotic plaques could lead to microfractures and plaque rupture, leading to acute thrombosis and possibly fatal myocardial infarctions.[5, 6] Furthermore, calcification poses significant challenges for the outcome of interventional strategies such as percutaneous coronary interventions for coronary artery disease.[7] Calcification of the aortic valve, or calcific aortic valve disease (CAVD), progresses from mild thickening to severe calcification and leads to stiffening of the aortic valve leaflets, eventually causing left ventricular outflow obstruction and heart failure.[3, 8, 9] Even mild aortic valve calcification is associated with increased mortality risk.[10] There are no known therapies that slow disease progression, and in case of aortic valve stenosis, surgical valve replacement and evolving transcatheter valve implantation (TAVI) are the only current treatments. Therefore, effective anti-calcification therapies are warranted.

Aortic valve calcification and arterial calcification share similar risk factors, such as age, gender, smoking, hypercholesterolemia, metabolic syndrome, end-stage renal disease, and diabetes mellitus.[11] Pathologically, explanted human stenotic aortic valves demonstrate similar lesions as observed in atherosclerotic plaques consisting of inflammatory cells and calcific deposits.[12] Patients with familial hypercholesterolemia are prone to develop atherosclerosis in addition to developing valve lesions that calcify with age.[13] Moreover, preclinical animal studies show atherosclerotic-like lesion in aortic valve leaflets of rabbits and mice with established atherosclerosis.[14] Since aortic valve calcification and atherosclerosis potentially share a similar pathological mechanism, statins (3-hydroxy-3methylglutaryl-coenzyme A [HMG-CoA] reductase inhibitors) emerged as a therapeutic agent. Although several retrospective studies demonstrate a reduction in aortic valve stenosis when treated with statins,[15-17] large prospective randomized clinical trials, do not support these findings and show no reduction in aortic valve calcification when treated with high doses of statins.[18, 19] Although, this may be due to the late implementation of statins, after aortic valve calcification has progressed to an irreversible stage, these studies underscore our lack of understanding of underlying mechanisms of cardiovascular calcification. An increasing aging population necessitate further investigation of the pathways that contribute to cardiovascular calcification. The need to develop new therapeutic targets to prevent or reverse cardiovascular calcification warrants the use of novel

imaging methods, as recently highlighted by the Working Group on Calcific Aortic Stenosis of the National heart, Lung, and Blood Institute (NHLBI).[20]

Currently cardiovascular calcification is visualized by non-invasive conventional imaging modalities such as echocardiography, computed tomography (CT) and magnetic resonance imaging (MRI). Even though, CT and echocardiography are vital diagnostic tools because of their high sensitivity and ability to quantify calcium content of soft tissues, clinical imaging is usually only performed when patients are becoming symptomatic. It should be mentioned that coronary artery calcium (CAC) scoring is used in asymptomatic patients for risk stratification for CAD. Clinical

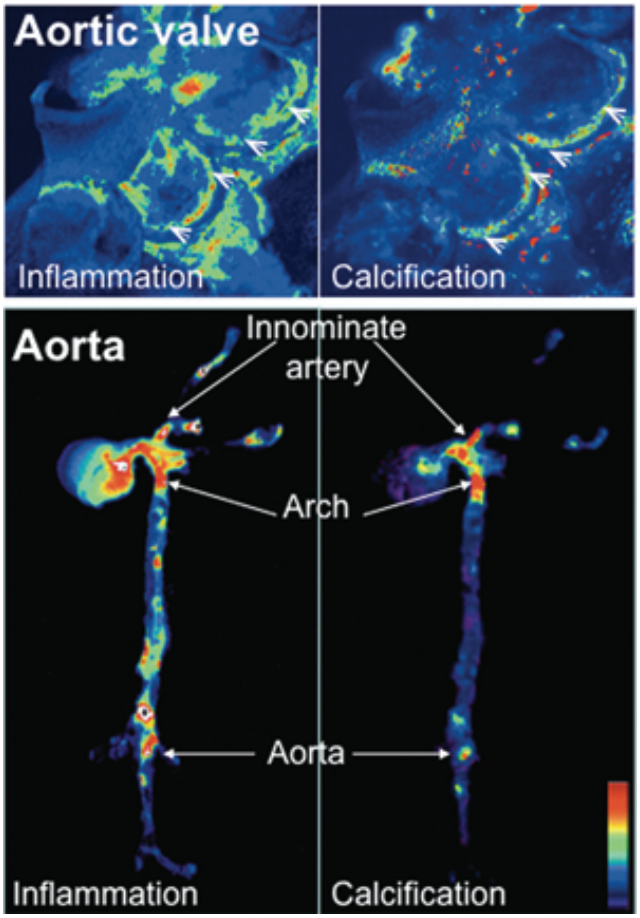

Figure 1. Molecular Imaging of Cardiovascular Calcification. Molecular imaging visualizes inflammatory activity, defined as macrophage accumulation, and osteogenesis in the aortic valves and aortas of apoE$^{-/-}$ mice. Magnetofluorescent nanoparticles were injected into mice to visualize macrophage accumulation (**left**). Spectrally distinct bisphosphonate-imaging agent that binds to hydroxyapatite were injected to detect osteogenic activity (**right**). Inflammatory and osteogenic activity colocalized in the aortic valve (**top**) and in the aorta (**bottom**), specifically in the areas of highest mechanical stresses at the aortic valve attachment (**arrowheads**) and at the atherosclerosis-prone areas, such as the innominate artery, aortic arch, and abdominal aorta (**arrows**). High signal intensities are shown in red/yellow/green. Adapted with permission from New & Aikawa Circ Res 2011 [53]

symptoms arise only at advanced stages of calcification, leaving physicians too late to reduce or prevent calcification. In addition, CT and echocardiography have a relatively low spatial resolution and cannot detect early stages of cardiovascular calcification. Early detection methods are needed to not only elucidate early mechanisms of cardiovascular calcification, but also to establish whether the disease is reversible. Imaging modalities that can visualize molecular targets can contribute to understanding important molecular and cellular aspects of cardiovascular calcification. The development of molecular imaging has enabled us to visualize early stages of calcification and piece together the mechanism of disease progression leading to calcium deposition (Figure 1). This review discusses how innovative imaging techniques have helped visualizing novel concepts of cardiovascular calcification.

INITIATION OF CALCIFICATION

The mechanistic pathways involved in the development of cardiovascular calcification remain largely unknown. In calcification research much focus is shifting toward mapping the entire process of the disease and as such determining the initiation, progression and end-stage of the disease process. The current pathological concept of cardiovascular calcification, albeit arterial or valvular in nature, is that cardiovascular risk factors lead to endothelial dysfunction, followed by the deposition of lipoprotein (LDL) particles and other compounds that trigger inflammatory response.[3, 21-23] The inflammatory state leads to the activation of inflammatory signaling pathways, macrophage infiltration and T-lymphocyte activation. Activation of inflammatory pathways contributes to the disease process, which in turn activates smooth muscle cells (SMC) in the arterial wall and valvular interstitial cells (VIC) in the aortic valve to differentiate to osteoblast-like cells and deposit calcium. Although the initiation of cardiovascular calcification is still a matter of investigation, evidence suggests that endothelial dysfunction leads to osteoblastic differentiation of underlying SMC and VIC in the arterial wall and aortic valve, respectively.

ENDOTHELIAL ACTIVATION

The endothelium maintains normal homeostasis at the vasculature-blood interface, however dysfunctional endothelial cells promote an inflammatory response and the onset of atherosclerosis/intimal calcification.[24] Noninvasive ultrasound molecular imaging, via targeted imaging agents, can detect lesion-prone vasculature before the appearance of advanced calcified atherosclerotic plaques.[25] Sites of atherosclerotic lesion formation are associated with an increased surface expression of endothelial cell adhesion molecules, such as VCAM-1 and P-selectin.[25-27] This expression of VCAM-1 by endothelial cells precedes fatty streak formation[28] and is up-regulated in response to oxidized LDL cholesterol – a hypercholesterolemic milieu.[29] VCAM-1 participates in the initiation

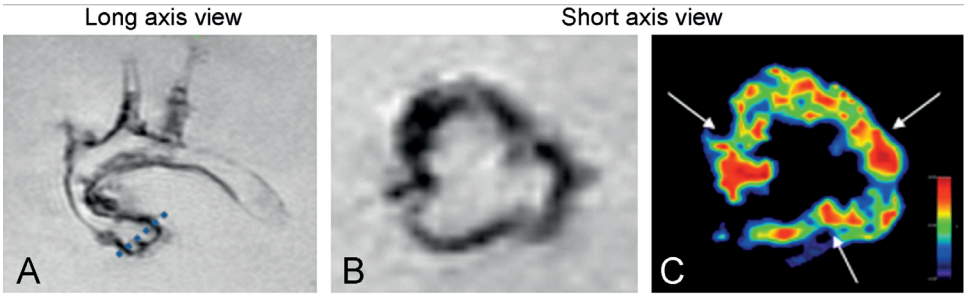

Figure 2. Visualization of VCAM-1 targeted agents. MRI visualizes endothelial activation detected by VCAM-1-targeted agent, in the commissures of aortic valves, which are regions of high flexure and mechanical stress. **(A)** dotted line = slice position of short axis view. **(B**) negative signal enhancement caused by uptake of VCAM-1-targeted nanoparticles. **(C)** color-coded signal (red) show focused uptake of VCAM-1 in commissures (arrows). (Adapted with permission from Aikawa et al. Circulation 2007 [30])

and progression of atherosclerotic plaques can be visualized *in vivo* by noninvasive molecular imaging (Figure 2).[25-27]

The mechanism of initiation of vascular calcification is proposed to be similar to that which we have suggested for calcific aortic valve disease.[23, 30] Activated endothelial cells recruit inflammatory cells, mainly in the form of monocytes/macrophages, which contribute to the progression of this pathological disorder. Our recent work used molecular imaging to detect early changes in aortic valve disease. Utilizing a similar approach as imaging arterial endothelial cells, VCAM-1 targeted agents are distributed in the commissures of the aortic valve,[27] which was validated by immunohistochemical analysis of VCAM-1 expression.[31] It has been confirmed that valvular endothelial dysfunction or injury leads to increased expression of adhesion molecules VCAM-1, ICAM-1 and E-selectin.[32, 33] Mechanically the commissures endure the greatest amount of stress during the cardiac cycle, making these areas more prone to endothelial injury than other parts of the leaflets. In addition, high pulsatile shear stress has demonstrated the upregulation of inflammatory receptors by valvular endothelial cells for circulating cytokines and inflammatory monocytes, leukocytes and T-lymphocytes.[32, 34, 35]

Another endothelial mechanism suggested a role of reactive oxygen species (ROS) as a possible initiating factor of calcification.[35-37] ROS, including oxidized lipids, can cause endothelial cell injury, leading to loss of cell alignment and upregulation of cell adhesion molecules for circulating inflammatory cells. To this end, a recent study demonstrated imaging ROS with allylhydrazine, a liquid compound that converts to nitrogen and propylene gas after reacting with ROS, in mice using a clinical echocardiography system. Allylhydrazine can be encapsulated within liposomes and is able to detect micromolar concentrations of radical oxidants.[38]

PROGRESSION OF CALCIFICATION - AN INFLAMMATORY CONCEPT

Evidence suggests that arterial and valvular calcification follows a pathway similar to that of endochondral bone formation;[39] osteoblastic differentiation of vascular SMC is via the Runx2 pathway[40] similar to VIC. A series of *in vitro* studies[41-44] demonstrate that monocytes and macrophages release inflammatory cytokines that promote cardiovascular calcification by regulating the differentiation of calcifying vascular cells. These calcifying vascular cells express a number of phenotypic markers synonymous with osteoblasts and chondrocytes.[23, 31, 45, 46] Our molecular imaging studies on arterial intimal calcification have provided the first *in vivo* evidence of the role that inflammation plays in initiating calcification.[23] Nanoparticle technology can be used to image not only the accumulation of macrophages within the intima of the atherosclerotic plaque, but also the co-localization of macrophages with osteogenic activity or active mineralization. Intravital microscopy has been performed on the carotid arteries of untreated and statin-treated cohort of apoE$^{-/-}$ mice at 20 weeks and 30 weeks of age. Macrophage number, as visualized by macrophage-targeted iron oxide nanoparticles, increased in association with osteogenic signal at 30 weeks. In this study of early calcification, anti-inflammatory statin therapy prevented both macrophage burden and osteogenic activity. Osteogenic differentiation of SMC and areas of active mineralization are effectively imaged via the use of a bisphosphonate-conjugated imaging agent (OsteoSense680).[23, 47, 48] This imaging agent binds to calcium and will accumulate where there is increased osteogenesis, as confirmed by alkaline phophatase activity.[49]

The progression of arterial calcification has shown to largely depend on an inflammatory process, which in turn associates with proteolysis and tissue remodeling. Early calcifying atherosclerotic plaques, often termed "spotty" calcifications, are associated with microcalcification and numerous macrophages undergoing proteolysis.[50] These vulnerable early atherosclerotic plaques are at risk of fatal rupture.[1, 5, 6, 51] During the progression of atherosclerosis, macrophages elaborate proteolytic activity, in the form of elastases (e.g., cathepsin S) and metalloproteinases (e.g., MMP-1, MMP-2, MMP-9). Our study utilized a novel protease-activatable imaging agent specific for cathepsin S and provided the first direct *in vivo* evidence for the role of this elastase in cardiovascular calcification.[52] Molecular imaging detected increased cathepsin S and osteogenic activities in CRD mice, induced by 5/6 nephrectomy, compared to control apoE$^{-/-}$ mice. Furthermore, calcification was decreased in atherosclerotic plaques and aortic valves in mice lacking cathepsin S. These results were corroborated using optical projection tomography and quantitative histology.

In the early stages of cardiovascular calcification, macrophage-derived elastolytic and proteolytic enzymes degrade elastin and collagen respectively, major components of the extracellular matrix (ECM) in both the aortic valve and arteries.[53] Inflammation-induced elastolysis in the atherosclerotic plaques results in the release of biologically active, soluble elastin-derived peptides.[54, 55] These biologically active peptides may regulate cell processes such as proliferation, as well as promote osteogenic differentiation of SMC and subsequent microcalcification-formation.[54-56] Microcalcifications provoke a pro-inflammatory response in macrophages via mechanisms involving protein kinase

C-α and ERK1/2 MAP kinase.[57, 58] Therefore a positive feedback loop of inflammation and calcification drives progression of arterial calcification;[57, 59] corroborated *in vivo* via the use of molecular imaging in our study.[23] Molecular imaging is capable of characterizing/diagnosing plaque activity, in the form of proteolytic activity, to identify high-risk patients. Thus the visualization of proteolytic activity, via the use of near-infrared fluorescence (NIRF) beacons/probes, may prove a valuable tool in the diagnosis of vulnerable rupture-prone plaques and onset of aortic stenosis.

The inflammatory cascade, that is initiated by the valvular endothelium, first results in excessive remodeling of the aortic valve extracellular matrix, which follows the clinical observation of aortic fibrosis preceding aortic valve stenosis.[12] Similar to the arterial wall, proteolytic enzymes and their inhibitors maintain a balance that can degrade ECM compounds such as collagen and elastin during valvular remodeling. Using macrophage targeted NIRF-conjugated iron nanoparticles and protease activatable NIRF probes, we have demonstrated that macrophages correlate with increased levels of matrix metalloproteinases (MMP-1, MMP-2, MMP-9, MMP13,), and cysteine proteases (cathepsin S, cathepsin K) in early stage calcification animal models.[23, 31, 52] In turn, we have also showed that inflammatory activity correlated with osteogenic activity using the same previously described calcification sensitive imaging probe.[47] This imaging agent uses different NIRF wavelengths than other imaging agents, allowing for the correlation of osteogenic activity with other pathological processes of the valve. Using this approach, we have correlated inflammation with early osteogenic activity in the valve, and confirmed by alkaline phosphatase specific activity and immunohistochemistry for osteocalcin, osteopontin and the osteogenic transcription factor Runx2.[23]

Furthermore, it is also possible to use these NIRF agents for MRI visualization, making the translation to clinical practice very feasible. Recently developed iron-oxide based magnetic nanoparticles, which are engulfed by tissue macrophages by phagocytosis, can be used for T2 weighted contrast MRI and PET.[60] This technology allows clinicians to discover a potential reversibility of the inflammatory response that leads to cardiovascular calcification by visualizing molecular, anatomic and physiological changes of the cardiovascular system. Another optical imaging technology, micro-optical coherence tomography (micro-OCT), has recently been developed and is able to visualize microcalcifications, cholesterol crystals, macrophages and proteins with a 1–micron resolution. It does not require the injection of molecular imaging agents and can thus be more easily translated from bench to bed. Nevertheless both NIRF imaging and micro-OCT have limited tissue penetration.

Recent evidence suggests that positron emission tomography (PET) imaging could overcome this limitation by using PET traces that target inflammation and calcification.[30, 61-63] Glucose analogue 18F-fluorodeoxyglucose (18F-FDG) is an imaging agent taken up by cells by glucose transport proteins, upon which the agent becomes trapped in macrophages. 18F-sodium fluoride (18F-NaF) binds to hydroxyapatite and is a marker for mineralization. A recent study that used this imaging approach confirmed, in patients with the full spectrum of aortic valve calcification, that inflammation and mineralization are present in early stages of aortic valve calcification.[64] It is the first clinical

study to visualize early calcification processes in patients that confirms our current understanding of aortic valve calcification.

Although the exact role of inflammation remains to be elucidated, it is clear that specific imaging agents can be used to visualize mechanisms related to cardiovascular calcification. Moreover, specific targeting imaging agents, for particular molecules of interest, may prove beneficial as a means to visualize potential biomarkers or therapeutic targets.

ALTERNATIVE MECHANISMS OF ARTERIAL CALCIFICATION

Although we are fully in support of the widely accepted concept that calcifying vascular cells play an important role in cardiovascular calcification, we also fervently believe that there are alternative mechanisms of mineralization. The apoptosis of macrophages has been proposed to contribute to plaque vulnerability.[6] In addition, macrophages induce the apoptosis of vascular SMC by direct interaction.[65, 66] The release of apoptotic bodies from macrophages and SMC undergoing apoptosis may provide a nidus for calcification and provoke the generation of microcalcification.[67, 68] Apoptosis can be monitored in the vasculature in real-time via the use of molecular imaging approaches with fluorescently tagged annexin V imaging agents.[69, 70] The clinical translation of imaging approaches such as these may prove beneficial in assessing the effectiveness of specific therapies, as well as a means to visualize disease progression.

Osteoblasts and chondrocytes release hydroxyapatite-nucleating matrix vesicles during biological skeletal tissue mineralization.[71, 72] Matrix vesicles (30-300 nm), precursors of microcalcifications, bud from the plasma membrane of living cells and also believed to serve as a nidus for mineral nucleation in ectopic calcification.[73-75] Evidence suggests that these matrix vesicles contain inhibitors of mineralization, such as Matrix Gla Protein and Fetuin-A, and a reduction in these inhibitors enhances their calcific potential.[76-78] Calcifying matrix vesicles have been stated to possess exposed phosphatidylserine.[78] Therefore some of the current molecular imaging modalities used to image apoptosis and calcification can also detect matrix vesicle accumulation. The exact role that these vesicles play in cardiovascular calcification and the mechanism by which they are released still require further investigation.

LATE-STAGE CALCIFICATION

Late-stage cardiovascular calcification is characterized by advanced tissue mineralization and diminished inflammation. It is classically reviewed as irreversible due to the development of advanced calcified material and is readily detected by conventional imaging approaches (e.g., echocardiography, CT).[79] All in all, cardiovascular calcification, albeit arterial or valvular, seems to follow similar pathways towards mineralization (Figure 3).

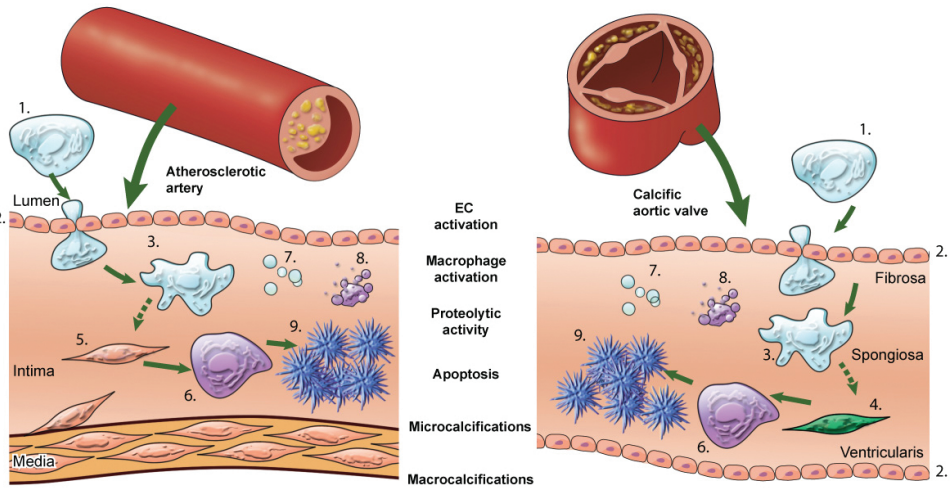

Figure 3. Mechanisms underlying arterial and aortic valve calcification. This figure depicts the theory that cardiovascular calcification follows similar pathways in both the artery and the aortic valve and summarizes how molecular imaging can visualize concepts of the calcification process. Cardiovascular calcification is an active process, initiated by endothelial dysfunction/activation and/or by inflammation and resulting in mineralization. Pro-inflammatory monocytes (**1**) are recruited to a site via activated/injured endothelial cells (ECs). (**2**) The activation of ECs causes increased expression of adhesion molecules, such as VCAM-1, which can be visualized by NIRF imaging VCAM-1 agent. Subsequent macrophage (**3**) accumulation follows, which can be analyzed with NIRF macrophage-targeted nanoparticles (AminoSPARK). The release of proteolytic enzymes, including matrix metalloproteases and cathepsins, by macrophages, which stimulates the differentiation of myofibroblasts (**4**) and smooth muscle cells (**5**) into osteoblasts, can be visualized by molecular imaging with activatable imaging agents (MMPSense, ProSense). Osteogenic activity in the form of osteoblast (**6**) formation and microcalcifications associated with generation of calcified matrix vesicles (**7**) can be identified by a bisphosphonate-conjugated imaging agent (OsteoSense) whereas apoptosis (**8**) can be detected by a fluorescently tagged Annexin A5 imaging probe. Calcification (**9**) can be readily detected by molecular imaging and conventional imaging techniques such as CT and Echocardiography. Adapted with permission from New & Aikawa Circ Res 2011 [53]

Specifically, calcification starts with endothelial dysfunction or activation due to inflammation, leading to an increased uptake of inflammatory cells. Inflammation therefore can be viewed as a propagation process eventually leading to the differentiation of SMC or VIC to actively deposit calcium in the arterial wall and aortic valve respectively. Where conventional imaging modalities are limited, this early calcification process can be visualized by molecular imaging. Table 1 depicts molecular agents used in detecting various components of cardiovascular calcification.

CONCLUSION

Cardiovascular calcification is currently viewed as an active disease process. Understanding the pathological pathways from initiation to late stage mineralization is key to identifying therapeutic targets that can potentially treat cardiovascular calcification. Especially mapping early calcification before the disease process has passed a point of no return provides the window for potential

Cardiovascular Calcification	Target	Imaging Agent	Imaging Modality
Processes associated with Early Calcification			
- Endothelial Dysfunction	VCAM-1	VINP-28	Optical Imaging†/MRI
		Microbubbles	US
	ICAM-1	NIRF Microbubbles	Optical Imaging US/MRI
	ROS	Microbubbles MPO* probe oxLDL-targeted nanoparticle	US Optical imaging MRI
- Inflammation	Macrophages	Nanoparticles (e.g. CLIO*) MMPSense	Optical Imaging/MRI/PET
	MMP Cathepsin	ProSense	Optical Imaging
Progression of Calcification			
- Inflammation	Macrophages	Nanoparticles (e.g. CLIO*) Nanoparticle	Optical Imaging/MRI/PET
- Apoptosis	Annexin-V	18F-FDG Activatable probes	Optical Imaging/MRI PET
	Caspase	OsteoSense	Optical Imaging/PET
- Microcalcification	Hydroxyapatite	18F-NaF	Optical imaging PET
Late Stage Calcification			
- Advanced Calcification	Hydroxyapatite	OsteoSense 18F-NaF	Optical Imaging PET
	Calcium	-	Echocardiography CT

Table 1. Molecular Imaging agents in Cardiovascular Calcification

*NIRF, near-infrared fluorescence; MRI, magnetic resonance imaging; US, ultrasound; ROS, reactive oxygen species; MPO, myeloperoxidase; CLIO, cross-linked iron oxide; PET, positron emission tomography; FDG, fluorodeoxyglucose; NaF, sodium fluoride; CT, computed tomography. †Optical imaging indicates one or more of the following modalities: Optical projection tomography (OPT), micro-optical coherence tomography (micro-OCT), fluorescence molecular tomography (FMT) and intravital microscopy (IVM).

treatment. Therapeutic agents have thus far not proved beneficial in the clinical setting, mainly because of late clinical diagnosis. In addition, because histopathological examination is not possible during longitudinal noninvasive imaging studies (e.g., echocardiography, CT, PET), validated high-resolution invasive imaging modalities (e.g., molecular imaging, micro-OCT) may be required to understand the mechanisms at various stages of CAVD.

The molecular imaging approach can unmask/resolve early pathophysiological changes in the cardiovascular system and may prove beneficial diagnostically in a clinical setting. Moreover, considering the amount of evidence demonstrating the role of inflammation in early stages of calcification (e.g., initiation, propagation), targeting inflammation could be beneficial in reducing and even halting subsequent mineralization. Although current clinical imaging approaches, such as echocardiography, remain essential for clinical management and for following CAVD progression once valve obstruction is present, PET may be the method of choice for detection of early calcifica-

tion and inflammation in clinical trials. Molecular imaging modalities possess great potential in visualizing *in vivo* cardiovascular calcification and will be vital in the development of therapeutic targets. Large, prospective, event-driven studies of noninvasive imaging techniques will be required to determine the place of these modalities in future clinical practice.

REFERENCES

1. Demer LL, Tintut Y. Vascular calcification: Pathobiology of a multifaceted disease. *Circulation*. 2008;117:2938-2948
2. Towler DA, Demer LL. Thematic series on the pathobiology of vascular calcification: An introduction. *Circ. Res.* 2011;108:1378-1380
3. Otto CM. Calcific aortic stenosis--time to look more closely at the valve. *N Engl J Med*. 2008;359:1395-1398
4. Abedin M, Tintut Y, Demer LL. Vascular calcification: Mechanisms and clinical ramifications. *Arterioscler. Thromb.Vasc.Biol.* 2004;24:1161-1170
5. Vengrenyuk Y, Carlier S, Xanthos S, Cardoso L, Ganatos P, Virmani R, Einav S, Gilchrist L, Weinbaum S. A hypothesis for vulnerable plaque rupture due to stress-induced debonding around cellular microcalcifications in thin fibrous caps. *Proc.Natl.Acad.Sci.U.S.A.* 2006;103:14678-14683
6. Virmani R, Burke AP, Farb A, Kolodgie FD. Pathology of the vulnerable plaque. *J.Am.Coll.Cardiol.* 2006;47:C13-C18
7. Moses JW, Carlier S, Moussa I. Lesion preparation prior to stenting. *Reviews in cardiovascular medicine*. 2004;5 Suppl 2:S16-21
8. Rajamannan NM, Bonow RO, Rahimtoola SH. Calcific aortic stenosis: An update. *Nat Clin Pract Cardiovasc Med*. 2007;4:254-262
9. Mohler ER, 3rd. Mechanisms of aortic valve calcification. *The American journal of cardiology*. 2004;94:1396-1402, A1396
10. Lloyd-Jones D, Adams R, Carnethon M, De Simone G, Ferguson TB, Flegal K, Ford E, Furie K, Go A, Greenlund K, Haase N, Hailpern S, Ho M, Howard V, Kissela B, Kittner S, Lackland D, Lisabeth L, Marelli A, McDermott M, Meigs J, Mozaffarian D, Nichol G, O'Donnell C, Roger V, Rosamond W, Sacco R, Sorlie P, Stafford R, Steinberger J, Thom T, Wasserthiel-Smoller S, Wong N, Wylie-Rosett J, Hong Y, American Heart Association Statistics C, Stroke Statistics S. Heart disease and stroke statistics--2009 update: A report from the american heart association statistics committee and stroke statistics subcommittee. *Circulation*. 2009;119:480-486
11. Stewart BF, Siscovick D, Lind BK, Gardin JM, Gottdiener JS, Smith VE, Kitzman DW, Otto CM. Clinical factors associated with calcific aortic valve disease. Cardiovascular health study. *J Am Coll Cardiol*. 1997;29:630-634
12. Otto CM, Kuusisto J, Reichenbach DD, Gown AM, O'Brien KD. Characterization of the early lesion of 'degenerative' valvular aortic stenosis. Histological and immunohistochemical studies. *Circulation*. 1994;90:844-853
13. Rajamannan NM, Sangiorgi G, Springett M, Arnold K, Mohacsi T, Spagnoli LG, Edwards WD, Tajik AJ, Schwartz RS. Experimental hypercholesterolemia induces apoptosis in the aortic valve. *The Journal of heart valve disease*. 2001;10:371-374
14. Rajamannan NM, Subramaniam M, Springett M, Sebo TC, Niekrasz M, McConnell JP, Singh RJ, Stone NJ, Bonow RO, Spelsberg TC. Atorvastatin inhibits hypercholesterolemia-induced cellular proliferation and bone matrix production in the rabbit aortic valve. *Circulation*. 2002;105:2660-2665
15. Bellamy MF, Pellikka PA, Klarich KW, Tajik AJ, Enriquez-Sarano M. Association of cholesterol levels, hydroxymethylglutaryl coenzyme-a reductase inhibitor treatment, and progression of aortic stenosis in the community. *J Am Coll Cardiol*. 2002;40:1723-1730
16. Aronow WS, Ahn C, Kronzon I, Goldman ME. Association of coronary risk factors and use of statins with progression of mild valvular aortic stenosis in older persons. *The American journal of cardiology*. 2001;88:693-695
17. Novaro GM, Tiong IY, Pearce GL, Lauer MS, Sprecher DL, Griffin BP. Effect of hydroxymethylglutaryl coenzyme a reductase inhibitors on the progression of calcific aortic stenosis. *Circulation*. 2001;104:2205-2209

18. Cowell SJ, Newby DE, Prescott RJ, Bloomfield P, Reid J, Northridge DB, Boon NA. A randomized trial of intensive lipid-lowering therapy in calcific aortic stenosis. *N Engl J Med*. 2005;352:2389-2397
19. Rossebo AB, Pedersen TR, Boman K, Brudi P, Chambers JB, Egstrup K, Gerdts E, Gohlke-Barwolf C, Holme I, Kesaniemi YA, Malbecq W, Nienaber CA, Ray S, Skjaerpe T, Wachtell K, Willenheimer R. Intensive lipid lowering with simvastatin and ezetimibe in aortic stenosis. *N Engl J Med*. 2008;359:1343-1356
20. Rajamannan NM, Evans FJ, Aikawa E, Grande-Allen KJ, Demer LL, Heistad DD, Simmons CA, Masters KS, Mathieu P, O'Brien KD, Schoen FJ, Towler DA, Yoganathan AP, Otto CM. Calcific aortic valve disease: Not simply a degenerative process: A review and agenda for research from the national heart and lung and blood institute aortic stenosis working group. Executive summary: Calcific aortic valve disease-2011 update. *Circulation*. 2011;124:1783-1791
21. Towler DA. Oxidation, inflammation, and aortic valve calcification peroxide paves an osteogenic path. *J Am Coll Cardiol*. 2008;52:851-854
22. Rajamannan NM. Mechanisms of aortic valve calcification: The ldl-density-radius theory: A translation from cell signaling to physiology. *American journal of physiology. Heart and circulatory physiology*. 2010;298:H5-15
23. Aikawa E, Nahrendorf M, Figueiredo JL, Swirski FK, Shtatland T, Kohler RH, Jaffer FA, Aikawa M, Weissleder R. Osteogenesis associates with inflammation in early-stage atherosclerosis evaluated by molecular imaging in vivo. *Circulation*. 2007;116:2841-2850
24. Gryglewski RJ, Botting RM, Vane JR. Mediators produced by the endothelial cell. *Hypertension*. 1988;12:530-548
25. Kaufmann BA, Carr CL, Belcik JT, Xie A, Yue Q, Chadderdon S, Caplan ES, Khangura J, Bullens S, Bunting S, Lindner JR. Molecular imaging of the initial inflammatory response in atherosclerosis: Implications for early detection of disease. *Arterioscler.Thromb.Vasc.Biol.* 2010;30:54-59
26. Cybulsky MI, Gimbrone MA, Jr. Endothelial expression of a mononuclear leukocyte adhesion molecule during atherogenesis. *Science*. 1991;251:788-791
27. Nahrendorf M, Jaffer FA, Kelly KA, Sosnovik DE, Aikawa E, Libby P, Weissleder R. Noninvasive vascular cell adhesion molecule-1 imaging identifies inflammatory activation of cells in atherosclerosis. *Circulation*. 2006;114:1504-1511
28. Nakashima Y, Raines EW, Plump AS, Breslow JL, Ross R. Upregulation of vcam-1 and icam-1 at atherosclerosis-prone sites on the endothelium in the apoe-deficient mouse. *Arterioscler.Thromb.Vasc.Biol.* 1998;18:842-851
29. Marui N, Offermann MK, Swerlick R, Kunsch C, Rosen CA, Ahmad M, Alexander RW, Medford RM. Vascular cell adhesion molecule-1 (vcam-1) gene transcription and expression are regulated through an antioxidant-sensitive mechanism in human vascular endothelial cells. *J.Clin.Invest*. 1993;92:1866-1874
30. Aikawa E, Otto CM. Look more closely at the valve: Imaging calcific aortic valve disease. *Circulation*. 2012;125:9-11
31. Aikawa E, Nahrendorf M, Sosnovik D, Lok VM, Jaffer FA, Aikawa M, Weissleder R. Multimodality molecular imaging identifies proteolytic and osteogenic activities in early aortic valve disease. *Circulation*. 2007;115:377-386
32. Muller AM, Cronen C, Kupferwasser LI, Oelert H, Muller KM, Kirkpatrick CJ. Expression of endothelial cell adhesion molecules on heart valves: Up-regulation in degeneration as well as acute endocarditis. *The Journal of pathology*. 2000;191:54-60
33. Ghaisas NK, Foley JB, O'Briain DS, Crean P, Kelleher D, Walsh M. Adhesion molecules in nonrheumatic aortic valve disease: Endothelial expression, serum levels and effects of valve replacement. *J Am Coll Cardiol*. 2000;36:2257-2262
34. Shavelle DM, Katz R, Takasu J, Lima JA, Jenny NS, Budoff MJ, O'Brien KD. Soluble intercellular adhesion molecule-1 (sicam-1) and aortic valve calcification in the multi-ethnic study of atherosclerosis (mesa). *The Journal of heart valve disease*. 2008;17:388-395

35. Sucosky P, Balachandran K, Elhammali A, Jo H, Yoganathan AP. Altered shear stress stimulates upregulation of endothelial vcam-1 and icam-1 in a bmp-4- and tgf-beta1-dependent pathway. *Arterioscler Thromb Vasc Biol*. 2009;29:254-260
36. Butcher JT, Nerem RM. Valvular endothelial cells regulate the phenotype of interstitial cells in co-culture: Effects of steady shear stress. *Tissue engineering*. 2006;12:905-915
37. Sorescu GP, Song H, Tressel SL, Hwang J, Dikalov S, Smith DA, Boyd NL, Platt MO, Lassegue B, Griendling KK, Jo H. Bone morphogenic protein 4 produced in endothelial cells by oscillatory shear stress induces monocyte adhesion by stimulating reactive oxygen species production from a nox1-based nadph oxidase. *Circulation research*. 2004;95:773-779
38. Perng JK, Lee S, Kundu K, Caskey CF, Knight SF, Satir S, Ferrara KW, Taylor WR, Degertekin FL, Sorescu D, Murthy N. Ultrasound imaging of oxidative stress in vivo with chemically-generated gas microbubbles. *Annals of biomedical engineering*. 2012
39. Rattazzi M, Bennett BJ, Bea F, Kirk EA, Ricks JL, Speer M, Schwartz SM, Giachelli CM, Rosenfeld ME. Calcification of advanced atherosclerotic lesions in the innominate arteries of apoe-deficient mice: Potential role of chondrocyte-like cells. *Arterioscler.Thromb.Vasc.Biol.* 2005;25:1420-1425
40. Steitz SA, Speer MY, Curinga G, Yang HY, Haynes P, Aebersold R, Schinke T, Karsenty G, Giachelli CM. Smooth muscle cell phenotypic transition associated with calcification: Upregulation of cbfa1 and downregulation of smooth muscle lineage markers. *Circ.Res.* 2001;89:1147-1154
41. Parhami F, Basseri B, Hwang J, Tintut Y, Demer LL. High-density lipoprotein regulates calcification of vascular cells. *Circ.Res.* 2002;91:570-576
42. Radcliff K, Tang TB, Lim J, Zhang Z, Abedin M, Demer LL, Tintut Y. Insulin-like growth factor-i regulates proliferation and osteoblastic differentiation of calcifying vascular cells via extracellular signal-regulated protein kinase and phosphatidylinositol 3-kinase pathways. *Circ.Res.* 2005;96:398-400
43. Tintut Y, Patel J, Territo M, Saini T, Parhami F, Demer LL. Monocyte/macrophage regulation of vascular calcification in vitro. *Circulation*. 2002;105:650-655
44. Watson KE, Bostrom K, Ravindranath R, Lam T, Norton B, Demer LL. Tgf-beta 1 and 25-hydroxycholesterol stimulate osteoblast-like vascular cells to calcify. *J.Clin.Invest*. 1994;93:2106-2113
45. Peacock JD, Levay AK, Gillaspie DB, Tao G, Lincoln J. Reduced sox9 function promotes heart valve calcification phenotypes in vivo. *Circ.Res.* 2010;106:712-719
46. El-Abbadi M, Giachelli CM. Mechanisms of vascular calcification. *Adv.Chronic.Kidney Dis.* 2007;14:54-66
47. Hjortnaes J, Butcher J, Figueiredo JL, Riccio M, Kohler RH, Kozloff KM, Weissleder R, Aikawa E. Arterial and aortic valve calcification inversely correlates with osteoporotic bone remodelling: A role for inflammation. *European heart journal*. 2010;31:1975-1984
48. Hjortnaes J, Gottlieb D, Figueiredo JL, Melero-Martin J, Kohler RH, Bischoff J, Weissleder R, Mayer JE, Aikawa E. Intravital molecular imaging of small-diameter tissue-engineered vascular grafts in mice: A feasibility study. *Tissue Eng Part C.Methods*. 2010;16:597-607
49. Kozloff KM, Weissleder R, Mahmood U. Noninvasive optical detection of bone mineral. *Journal of bone and mineral research: the official journal of the American Society for Bone and Mineral Research*. 2007;22:1208-1216
50. Ehara S, Kobayashi Y, Yoshiyama M, Shimada K, Shimada Y, Fukuda D, Nakamura Y, Yamashita H, Yamagishi H, Takeuchi K, Naruko T, Haze K, Becker AE, Yoshikawa J, Ueda M. Spotty calcification typifies the culprit plaque in patients with acute myocardial infarction: An intravascular ultrasound study. *Circulation*. 2004;110:3424-3429
51. Li R, Mittelstein D, Lee J, Fang K, Majumdar R, Tintut Y, Demer LL, Hsiai TK. A dynamic model of calcific nodule destabilization in response to monocyte- and oxidized lipid-induced matrix metalloproteinases. *Am.J.Physiol Cell Physiol*. 2012;302:C658-C665

52. Aikawa E, Aikawa M, Libby P, Figueiredo JL, Rusanescu G, Iwamoto Y, Fukuda D, Kohler RH, Shi GP, Jaffer FA, Weissleder R. Arterial and aortic valve calcification abolished by elastolytic cathepsin s deficiency in chronic renal disease. *Circulation*. 2009;119:1785-1794
53. New SE, Aikawa E. Molecular imaging insights into early inflammatory stages of arterial and aortic valve calcification. *Circ.Res.* 2011;108:1381-1391
54. Karnik SK, Brooke BS, Bayes-Genis A, Sorensen L, Wythe JD, Schwartz RS, Keating MT, Li DY. A critical role for elastin signaling in vascular morphogenesis and disease. *Development*. 2003;130:411-423
55. Simionescu A, Simionescu DT, Vyavahare NR. Osteogenic responses in fibroblasts activated by elastin degradation products and transforming growth factor-beta1: Role of myofibroblasts in vascular calcification. *Am.J.Pathol.* 2007;171:116-123
56. Saulnier JM, Hauck M, Fulop T, Jr., Wallach JM. Human aortic elastin from normal individuals and atherosclerotic patients: Lipid and cation contents; susceptibility to elastolysis. *Clin.Chim.Acta*. 1991;200:129-136
57. Nadra I, Boccaccini AR, Philippidis P, Whelan LC, McCarthy GM, Haskard DO, Landis RC. Effect of particle size on hydroxyapatite crystal-induced tumor necrosis factor alpha secretion by macrophages. *Atherosclerosis*. 2008;196:98-105
58. Nadra I, Mason JC, Philippidis P, Florey O, Smythe CD, McCarthy GM, Landis RC, Haskard DO. Proinflammatory activation of macrophages by basic calcium phosphate crystals via protein kinase c and map kinase pathways: A vicious cycle of inflammation and arterial calcification? *Circ.Res.* 2005;96:1248-1256
59. Bostrom K. Proinflammatory vascular calcification. *Circ.Res.* 2005;96:1219-1220
60. Jaffer FA, Nahrendorf M, Sosnovik D, Kelly KA, Aikawa E, Weissleder R. Cellular imaging of inflammation in atherosclerosis using magnetofluorescent nanomaterials. *Molecular imaging*. 2006;5:85-92
61. Folco EJ, Sheikine Y, Rocha VZ, Christen T, Shvartz E, Sukhova GK, Di Carli MF, Libby P. Hypoxia but not inflammation augments glucose uptake in human macrophages: Implications for imaging atherosclerosis with 18fluorine-labeled 2-deoxy-d-glucose positron emission tomography. *J Am Coll Cardiol*. 2011;58:603-614
62. Beheshti M, Saboury B, Mehta NN, Torigian DA, Werner T, Mohler E, Wilensky R, Newberg AB, Basu S, Langsteger W, Alavi A. Detection and global quantification of cardiovascular molecular calcification by fluoro18-fluoride positron emission tomography/computed tomography--a novel concept. *Hellenic journal of nuclear medicine*. 2011;14:114-120
63. Hyafil F, Messika-Zeitoun D, Burg S, Rouzet F, Benali K, Iung B, Vahanian A, Le Guludec D. Detection of 18fluoride sodium accumulation by positron emission tomography in calcified stenotic aortic valves. *The American journal of cardiology*. 2012;109:1194-1196
64. Dweck MR, Jones C, Joshi NV, Fletcher AM, Richardson H, White A, Marsden M, Pessotto R, Clark JC, Wallace WA, Salter DM, McKillop G, van Beek EJ, Boon NA, Rudd JH, Newby DE. Assessment of valvular calcification and inflammation by positron emission tomography in patients with aortic stenosis. *Circulation*. 2012;125:76-86
65. Boyle JJ, Weissberg PL, Bennett MR. Human macrophage-induced vascular smooth muscle cell apoptosis requires no enhancement of fas/fas-l interactions. *Arterioscler.Thromb.Vasc.Biol.* 2002;22:1624-1630
66. Boyle JJ, Bowyer DE, Weissberg PL, Bennett MR. Human blood-derived macrophages induce apoptosis in human plaque-derived vascular smooth muscle cells by fas-ligand/fas interactions. *Arterioscler.Thromb. Vasc.Biol.* 2001;21:1402-1407
67. Proudfoot D, Skepper JN, Hegyi L, Bennett MR, Shanahan CM, Weissberg PL. Apoptosis regulates human vascular calcification in vitro: Evidence for initiation of vascular calcification by apoptotic bodies. *Circ.Res.* 2000;87:1055-1062
68. Shanahan CM. Inflammation ushers in calcification: A cycle of damage and protection? *Circulation*. 2007;116:2782-2785

69. van Tilborg GA, Vucic E, Strijkers GJ, Cormode DP, Mani V, Skajaa T, Reutelingsperger CP, Fayad ZA, Mulder WJ, Nicolay K. Annexin a5-functionalized bimodal nanoparticles for mri and fluorescence imaging of atherosclerotic plaques. *Bioconjug.Chem.* 2010;21:1794-1803
70. Corsten MF, Bennaghmouch A. Optical characterization of arterial apoptosis. *Methods Mol.Biol.* 2011;680:117-129
71. Anderson HC. Normal and abnormal mineralization in mammals. *Trans.Am.Soc.Artif.Intern.Organs*. 1981;27:702-708
72. Anderson HC, Stechschulte DJ, Jr., Collins DE, Jacobs DH, Morris DC, Hsu HH, Redford PA, Zeiger S. Matrix vesicle biogenesis in vitro by rachitic and normal rat chondrocytes. *Am.J.Pathol.* 1990;136:391-398
73. Anderson HC. Matrix vesicles and calcification. *Curr.Rheumatol.Rep.* 2003;5:222-226
74. Bobryshev YV, Killingsworth MC, Huynh TG, Lord RS, Grabs AJ, Valenzuela SM. Are calcifying matrix vesicles in atherosclerotic lesions of cellular origin? *Basic Res.Cardiol.* 2007;102:133-143
75. Kim KM. Calcification of matrix vesicles in human aortic valve and aortic media. *Fed.Proc.* 1976;35:156-162
76. Reynolds JL, Joannides AJ, Skepper JN, McNair R, Schurgers LJ, Proudfoot D, Jahnen-Dechent W, Weissberg PL, Shanahan CM. Human vascular smooth muscle cells undergo vesicle-mediated calcification in response to changes in extracellular calcium and phosphate concentrations: A potential mechanism for accelerated vascular calcification in esrd. *J.Am.Soc.Nephrol.* 2004;15:2857-2867
77. Chen NX, O'Neill KD, Chen X, Moe SM. Annexin-mediated matrix vesicle calcification in vascular smooth muscle cells. *J.Bone Miner.Res.* 2008;23:1798-1805
78. Kapustin AN, Davies JD, Reynolds JL, McNair R, Jones GT, Sidibe A, Schurgers LJ, Skepper JN, Proudfoot D, Mayr M, Shanahan CM. Calcium regulates key components of vascular smooth muscle cell-derived matrix vesicles to enhance mineralization. *Circ.Res.* 2011;109:e1-12
79. Johnson RC, Leopold JA, Loscalzo J. Vascular calcification: Pathobiological mechanisms and clinical implications. *Circ.Res.* 2006;99:1044-1059

4

Inverse Correlation of Arterial and Aortic Valve Calcification with low Bone Mineral Density evaluated by Molecular Imaging

Jesper Hjortnaes, MD[1], Jonathan Butcher, PhD[3,4], Jose-Luiz Figueiredo, MD[1,2], Mark Riccio, ME[4], Rainer H. Kohler, PhD[1], Kenneth M. Kozloff, PhD[5], Ralph Weissleder, MD, PhD[1], and Elena Aikawa, MD, PhD[1,2]

European Heart Journal 2010

[1]Center for Molecular Imaging Research, Massachusetts General Hospital and [2]Brigham and Women's Hospital, Harvard Medical School, Boston, MA; [3]Department of Biomedical Engineering and [4]Preclinical Imaging Facility, Cornell University, Ithaca, NY; [5]Department of Orthopaedic Surgery, University of Michigan, Ann Arbor, MI

ABSTRACT

Introduction

Westernized countries face a growing burden of cardiovascular calcification and osteoporosis. Despite its vast clinical significance, the precise nature of this reciprocal relation remains obscure. We hypothesize that cardiovascular calcification progresses with inflammation and inversely correlates with bone tissue mineral density (TMD).

Methods and Results

Arterial, valvular, and bone metabolism were visualized using near-infrared fluorescence (NIRF) molecular imaging agents, targeting macrophages and osteogenesis. We detected significant arterial and aortic valve calcification in apoE$^{-/-}$ mice with or without chronic renal disease (CRD, 30 weeks old; n=28), correlating with severity of atherosclerosis. We demonstrated decreases in osteogenic activity in the femurs of apoE$^{-/-}$ mice as compared with WT mice, which was further reduced with CRD. 3D micro-CT imaging of the cortical and cancellous regions of femurs quantified structural remodeling and reductions in TMD in apoE-/- and CRD apoE-/- mice. We established significant correlations between arterial and valvular calcification and loss of TMD (R^2=0.67 and 0.71, respectively). Finally, we performed macrophage-targeted molecular imaging to explore a link between inflammation and osteoporosis *in vivo*. While macrophage burden, visualized as uptake of NIRF-conjugated iron nanoparticles, was directly related to the degree of arterial and valvular inflammation and calcification, the same method inversely correlated inflammation with TMD (R^2=0.73; 0.83; 0.75, respectively).

Conclusion

This study provides direct *in vivo* evidence that in arteries and aortic valves, macrophage burden and calcification associate with each other, while inflammation inversely correlates with bone mineralization. Thus, understanding inflammatory signaling mechanisms may offer insight into selective abrogation of divergent calcific phenomena.

INTRODUCTION

Clinical studies suggest that cardiovascular calcification, atherosclerosis, and chronic renal disease (CRD) are associated with osteoporosis.[1, 2] Emerging epidemiological evidence shows age-independent correlation between bone mineral density and cardiovascular events.[3-5] In limited mouse studies, atherosclerosis susceptibility corresponds with reduction of bone mineralization.[6, 7] Although these observations suggest common underlying mechanisms, the precise natures of the relations between arterial calcification, calcific aortic valve disease, and bone osteogenesis, as well as reciprocal regulation of these processes, remain unknown. The National Heart, Lung, and Blood Institute (NHLBI) Working Group on Calcific Aortic Stenosis has recently underscored the importance of identifying the relationship between calcification of the aortic valve and bone and the reciprocal regulation of these processes.[8]

Arterial and aortic valve calcification is a significant cause of morbidity and mortality.[9, 10] Arterial calcification not only weakens vasomotor responses, but also affects atherosclerotic plaque stability. Emerging evidence suggests that atherosclerotic plaques are prone to rupture, particularly in regions of high background stress with microcalcifications located in the thin fibrous cap.[11-13] In addition, calcification impairs the movement of aortic valve leaflets, causing life-threatening aortic stenosis and heart failure.[14] Recent studies suggest that underlying mechanisms of aortic valve calcification resemble those of atherosclerotic arterial calcification, triggered by hemodynamic stress, reactive oxygen species, and inflammatory cues.[14-17]

Cardiovascular calcification was conventionally viewed as an inevitable consequence of aging, but recent landmark studies have demonstrated that it is a highly regulated process of mineralization, akin to embryonic bone formation.[14, 18] Indeed, calcified vascular material is often indistinguishable from bone, and its formation involves cellular and molecular signaling processes found in normal osteogenesis.[19, 20] We have reported that valvular myofibroblast-like cells, due to their plasticity, respond to various stimuli by undergoing activation and sequential phenotypic differentiation. During cardiovascular calcification, macrophage-derived proteinases such as elastolytic cathepsins or metalloproteinases induce the release of biologically active, soluble elastin-derived peptides that may promote osteogenic differentiation of myofibroblasts or smooth-muscle cells (SMC).[21] This finding concurs with studies of phenotypic conversion of vascular SMC and valvular myofibroblasts into osteoblastic cells, characterized by the expression of bone-regulating proteins and osteogenic factors (e.g., alkaline phosphatase, osteopontin, osteocalcin, Runx2/Cbfa1, Osterix).[16, 22, 23]

Imaging approaches that can spatially resolve and quantify the temporal pro-osteogenic molecular processes in arteries, valves, and bones are limited. Conventional imaging modalities can identify advanced late-stage calcification, but optical molecular imaging can detect tissue mineralization at the earliest stages. The present study tested the hypothesis that arterial and aortic valve calcification is inversely correlated with low bone tissue mineral density (TMD). The specific objective was to quantify the relation between cardiovascular calcification (arterial and valvular) and long bone remodeling (cortical and trabecular) in established models of atherosclerosis and CRD,[14-16]

using optical molecular imaging and high-resolution 3D micro-CT. In addition, to demonstrate the association between inflammation, ectopic calcification, and osteoporosis, we directly compared macrophage burden and progression of osteogenic changes in each region of the same animals *in vivo* and *ex vivo*. Our results on opposing effects of inflammation in soft tissues (cardiovascular organs) and in bone agree with previous reports on accelerated osteolysis in inflamed bones.[24] Our study provides new insight into the relation between osteoporosis and cardiovascular calcification, and suggests shared inflammatory mechanisms of ectopic calcification and bone osteolysis. It also offers a unique model for exploration of *in vivo* mechanisms regulating early cardiovascular calcification and bone mineral loss.

METHODS

Animal Protocol

We studied osteogenic changes in carotid arteries, aortic valves, and femur bones obtained from 30-week-old apoE-/- mice that consumed an atherogenic diet (Teklad TD 88137; 42% milk fat, 0.2% total cholesterol, Harlan, Indianapolis, IN) from 10 weeks of age. At 20 weeks of age, mice were randomized either to continue the atherogenic diet (apoE-/-; n=10) or receive 5/6 nephrectomy procedure (CRD apoE-/-; n=10). We used 5/6 nephrectomy (left heminephrectomy, followed by right total nephrectomy one week later) to induce CRD, a procedure that also aggravates cardiovascular inflammation and calcification.[1-3] Age-matched wild-type C57/BL6 mice (WT, n=8, Jackson Laboratory, Bar Harbor, ME) served as controls. At 30 weeks of age, mice underwent intravital microscopy and were euthanized for *ex vivo* imaging following by statistical analyses. In addition to molecular imaging, the femurs of the mice underwent quantitative micro-CT imaging analyses (WT, n=3; apoE-/-, n=4; CRD apoE-/-, n=4). The Subcommittee on Research Animal Care at Massachusetts General Hospital approved all procedures.

Blood biochemical analyses

Blood was obtained from the heart, and serum levels of total cholesterol, cystatin C, creatinine and phosphate were assessed as previously described.[3]

Molecular imaging agents

To image osteogenesis, we used biphosphonate-conjugated imaging agent (Osteosense680/OS680, VisEn Medical, Inc., Woburn, MA) binding to hydroxyapatite in actively mineralized regions containing osteoblast-like cells in arteries, valves (Suppl. Figure 1A)[3-5] and bones.[6] This agent elaborates fluorescence detectable through the near-infrared (NIR) window excitation/emission 650/680nm. Macrophage-targeted near-infrared (NIR)-conjugated iron nanoparticle (Suppl. Figure 1B), producing fluorescence visible through the NIR window excitation/emission 750/780nm, was used to detect inflammation.[3, 5]

Molecular imaging of carotid arteries, aortic valves, and femurs

Mice simultaneously received two spectrally distinct imaging agents (OsteoSense680 and CLIO-750) via intravenous injection 24 hours before imaging. Dual-channel fluorescence imaging was performed using an intravital laser scanning fluorescence microscope specifically developed for imaging of small experimental animals. Excitation at 633 and 748 nm and image collection in two different channels was done serially to avoid cross talk between channels. Image stacks were processed and analyzed with ImageJ software (version 1.41, Bethesda, MD). Image post-processing was done with OsiriX imaging software (version 3.6.1, Open Source). Data was presented as region of interest (ROI; pixels) and signal intensity (SI; Arbitrary Units; AU).

Macroscopic fluorescence reflectance imaging of aortic specimens

After intravital imaging, mice were euthanized. Aortas were perfused with saline, dissected, and imaged to map the macroscopic NIR fluorescent signals elaborated from Osteosense680 using fluorescence reflectance imaging system (Omega Optical, Brattleboro, VT).[3, 4]

Micro-CT imaging of bones

Whole femurs were transferred to individual conical tubes filled with fresh PBS and imaged using micro-CT (GE eXplore Vision CT 120, GE Healthcare, Inc.). Bones were scanned at 90 KeV and 40mA, using 1200 angles and 4 images per angle to enhance clarity. Calibrations and comparison with scans by other micro-CT systems demonstrated that this protocol results in 25 µm voxel size. A calibrated bone phantom (SB3 with 1073 mg/cc, GE Healthcare, Inc.) was scanned simultaneously with the experimental samples to relate X-ray attenuation by different scans. Image stacks were reconstructed to 3D datasets using the eXplore software and transferred to MicroView v3.2 (GE Healthcare, Inc.) for post processing and analysis. The midshaft cortical region and the trabecular region in the femoral head were analyzed. For the midshaft, a 70-slice segment representing 1.75 mm axial length was processed using MicroView as previously described. Bone was identified in each slice via X-ray attenuation–based Hounsfeld unit thresholding. The average cortical and marrow areas for each bone were then determined. The 3D cortical bone volume was segmented out of the original dataset and tissue mineral density was calculated using MicroView. For the trabecular analysis, a trapezoidal zone between the epiphysis and the metaphysis containing only trabecular networks was extracted and analyzed using MicroView. Bone volume fraction, trabecular number, thickness, and spacing were quantified for each treatment. At least three femurs were analyzed for each experimental condition.

Correlative histopathological assessment

After imaging, tissue samples were frozen in OCT compound (Sakura Finetech, Torrance, CA), and 5 um sections were cut through the carotid arteries and aortic valves. Alkaline phosphatase activity was detected on cryosections that were directly incubated with conjugated antibody (Vector Labs, Burlingame, CA). The avidin-biotin peroxidase method was used for immunohistochemistry for de-

tection of macrophages (rat monoclonal antibody against mouse Mac 3, BD Biosciences, San Jose, CA). The reaction was visualized with a 3-amino-9-ethylcarbazol substrate (AEC, Sigma Chemical, St Louis, MO). Images were captured with a digital camera (Nikon DXM 1200-F, Nikon Inc, Melville, NY).

Statistical analyses

Data are presented as mean +/- standard deviation. Statistical analyses for comparison groups employed One-way ANOVA, followed by the Tukey-Kramer post hoc test performed with GraphPad prism software (version 4.0, GraphPad Software, San Diego, CA). Tests were two-sided and adjusted for variance inequality where appropriate. Linear regression with Pearson's correlation test was used to determine covariant relationships between data. Normal distribution of the data was confirmed by comparing against expected normal distributions with given means and standard deviation. In all cases, test probability values less than 0.05 were considered statistically significant. For intravital imaging, signal intensity (SI) and region of interest (ROI) were identified as positive area detected by OsteoSense680- or CLIO750-derived signals and selected in each sum-image using ImageJ imaging software (v. 1.41, Bethesda, MD) as previously described.[4]

RESULTS

Serum phosphate, creatinine, cystatin C and cholesterol levels in apoE-/- and CRD apoE-/- mice

Total cholesterol was significantly increased in apoE-/- and CRD apoE-/- mice, as compared with WT mice (467.2±51.1 mg/dL and 397.1±24.8 mg/dL vs. 56.3±9.8 mg/dL; $p<0.05$). In addition, CRD apoE-/- mice had significantly increased serum phosphate, creatinine, and cystatin C levels as compared with apoE-/- and WT mice (phosphate: 11.4±0.9 mg/dL vs. 6.3±0.4 mg/dL and 4.7±0.4 mg/dL; $p<0.05$; creatinine: 0.6±0.04 mg/dL vs. 0.4±0.01 mg/dL and 0.3±0.01 mg/dL; $p<0.05$; cystatin C: 0.9±0.01 ug/ml vs. 0.6±0.2 ug/ml, and 0.3±0.02 ug/ml; $p<0.001$). Greater serum phosphate, creatinine, and cystatin C levels suggest that 5/6 nephrectomy induced kidney failure, which in turn promotes inflammation.[15]

Osteogenic activity in mouse arteries and aortic valves associate with each other and increase with atherosclerosis severity

Fluorescence reflectance imaging was used to map mineralization in aortas of WT, apoE-/-, and CRD apoE-/- mice. Strong signals were detected at the levels of aortic valve, aortic root, aortic arch, and abdominal aorta, in apoE-/- and especially CRD apoE-/- mice as compared with WT mice (Suppl. Figure 2). Intravital imaging of carotid arteries *in vivo* showed more than 47-fold and 78-fold increases of calcified tissue area (ROI) in apoE-/- and CRD apoE-/- mice, respectively, compared to WT cohort (Figures 1A, 1B). In addition, up to 100-fold and 400-fold increases in osteogenic signal (SI) occurred in apoE-/- and CRD apoE-/- mice, respectively, when compared to the WT cohort (Figures 1A, 1C). Imaging analyses of the aortic valves in WT, apoE-/-, and CRD apoE-/- mice revealed that

ROI increased 4-fold and 20-fold in size in apoE-/- and CRD apoE-/- mice, respectively, compared to ROI in WT mice (Figures 1D, 1E). Osteogenic SI was further significantly increased in aortic valves of apoE-/- and CRD apoE-/- mice (13-fold and 50-fold, respectively) as compared with WT mice (Figures 1D, 1F). We performed a correlative analysis, in addition to a Pearson's correlation test, to evaluate an association between vascular and valvular calcification. Figure 1G shows a significant correlation of arterial and aortic valve calcific ROI ($r=0.75$; $p<0.05$). In addition, arterial osteogenic SI significantly correlated with valvular SI ($r=0.67$; $p<0.05$; Figure 1H).

Furthermore, correlative histopathology corroborated our imaging data (Suppl. Figures 3A, 3B). These imaging and histological results support the association between arterial and aortic valve calcification.

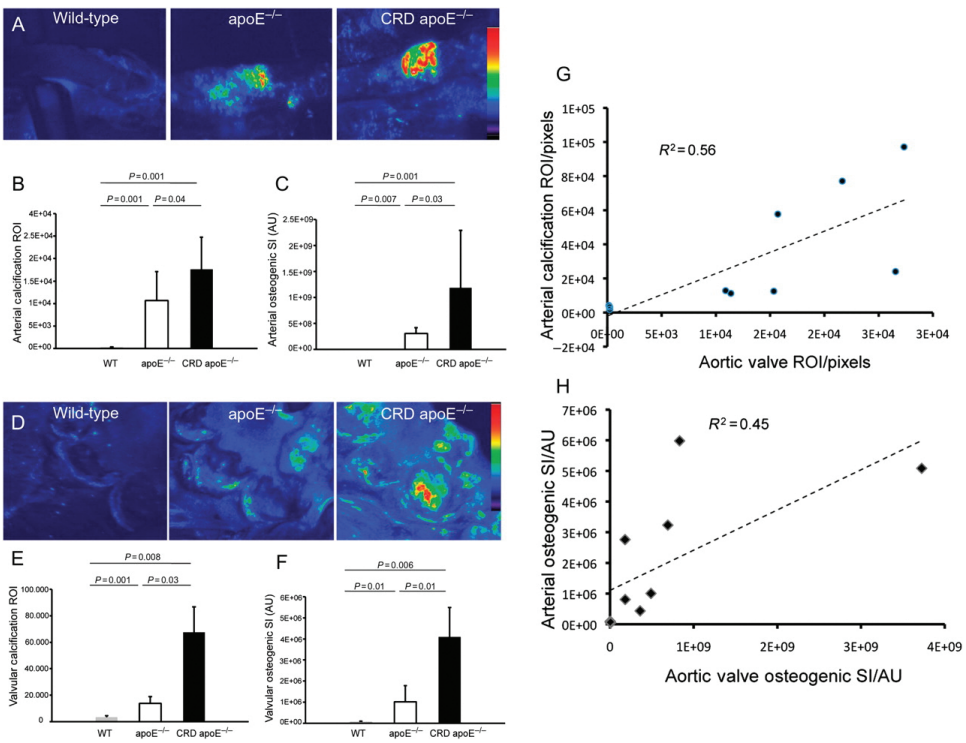

Figure 1. Induction of Osteogenesis in Carotid Arteries and Aortic Valves of apoE-/- and CRD apoE-/- Mice, Detected by Intravital Fluorescence Microscopy

(A) Calcified regions (ROI) and mineralization (signal intensities; SI) in the carotid arteries of WT, apoE-/-, and CRD apoE-/- mice injected with Osteosense680 (maximum SI shown in red). **(B)** Quantitative assessment of ROI showed significant increase in calcification in CRD apoE-/- vs. WT and apoE-/- mice. **(C)** Arterial osteogenic SI is greater in CRD apoE-/- mice, compared to other groups. **(D)** Pseudocolor mapping of mineralization ROI and SI in the aortic valves. Aortic valve calcified ROI **(E)** and osteogenic SI **(F)** are significantly higher in CRD apoE-/- mice, compared to other groups. **(A-F)** WT, n= 8; apoE-/-, n=10; CRD apoE-/-, n=10. **(G)** Correlation of arterial and valve calcified tissue area (ROI; pixels). **(H)** Correlation of arterial and valve osteogenic activity (SI; AU). **(G-H)** WT, n= 3; apoE-/-, n=4; CRD apoE-/-, n=4.

BONE MINERALIZATION DECREASES IN FEMURS OF ATHEROSCLEROTIC MICE AND INVERSELY CORRELATES TO ARTERIAL AND AORTIC VALVE CALCIFICATION

Figure 2 shows mineralization in the midshaft region of femurs in WT, apoE-/-, and CRD apoE-/- mice, detected by molecular imaging *ex vivo*. We observed significantly decreased osteogenic SI in apoE-/- mice and CRD apoE-/- mice as compared with WT mice, and in apoE-/- mice as compared with CRD apoE-/- mice (Figure 2A, 2B). Micro-CT imaging further showed a decrease in bone tissue mineral density (TMD) in the midshaft region of femurs from apoE-/- mice as compared with WT mice (Figures 2C-2F), which supports our molecular imaging results. Quantitative analyses demonstrated a significant difference in TMD between apoE-/- mice and WT mice, and between CRD apoE-/- mice and WT mice (Figure 2E). Albeit not significant (p=0.057), the difference between CRD apoE-/- mice and WT mice showed a tendency toward decreased cortical/marrow area ratio in CRD apoE-/- mice, suggesting more severe loss of bone structure in the CRD cohort (Figure 2F). Periosteal perimeters were not different between conditions, suggesting that the endosteal dimensions expanded through osteoclast activity. Micro-CT showed a decrease in tissue mineral density in the femur heads of apoE-/- mice as compared with WT mice (Figures 2G, 2H), though bone volume fraction was not significantly changed (Suppl. Figure 4). Further statistical analyses of trabecular microarchitecture showed a significant decrease in trabecular number (Figure 2I) and a significant increase in trabecular spacing (Figure 2J) between CRD apoE-/- mice and WT mice, but there was no significant difference in trabecular thickness between groups (Figure 2K). These results suggest that osteoporotic remodeling may occur as a consequence of calcific cardiovascular disease. To test this, we applied linear regression analysis comparing arterial and valvular calcification to bone TMD (Figure 3). TMD inversely correlates with arterial and aortic valve regions of calcification (ROI: R^2=0.86, R^2=0.34; respectively; Figures 3A, 3B). Furthermore, TMD is inversely correlated to osteogenic SI in carotid arteries and aortic valves (SI: R^2=0.67, R^2=0.72, respectively; Figures 3C, 3D). These data suggest a strong inverse correlation between cardiovascular calcification and bone mineralization.

Figure 2. Loss of Bone Mineral Density and Alterations in Microarchitecture in Mouse Femurs, Detected by 3D Micro-CT and Molecular Imaging

(A) Fluorescence microscopy of midshaft region of femurs of mice injected with Osteosense680. **(B)** Quantification analysis of bone mineralization SI showed significant reduction in CRD apoE-/- mice, compared to other groups. **(A-B)** WT, n= 8; apoE-/-, n=10; CRD apoE-/-, n=10. **(C, D)** Micro-CT imaging of femur midshaft region (normal bone=red; loss of bone mineralization=green-blue). **(E)** Quantification assessment of bone TMD shows significant bone loss in apoE-/- and CRD apoE-/- mice. **(F)** Cortical/marrow area shows tendency toward decrease of cortical/marrow ratio in CRD apoE-/- mice. **(G, H)** Micro-CT imaging of femur head. Quantification assessment of microarchitecture demonstrates **(I)** decrease in trabecular number and **(J)** increase in trabecular spacing in CRD apoE-/- mice. **(K)** No changes in trabecular thickness were detected. **(C-K)** WT, n= 3; apoE-/-, n=4; CRD apoE-/-, n=4.

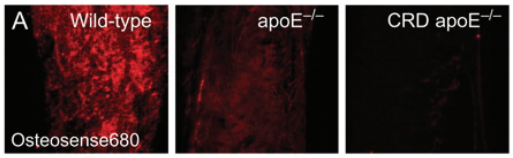
A
Wild-type
apoE−/−
CRD apoE−/−
Osteosense680

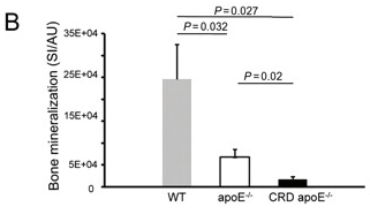
B
P=0.027
P=0.032
P=0.02
Bone mineralization (SI/AU)
35E+04
25E+04
15E+04
5E+04
0
WT
apoE-/-
CRD apoE-/-

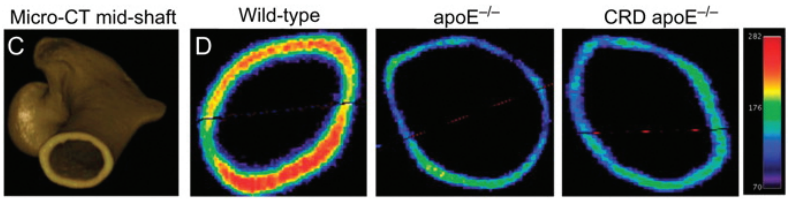
Micro-CT mid-shaft
Wild-type
apoE−/−
CRD apoE−/−
C
D

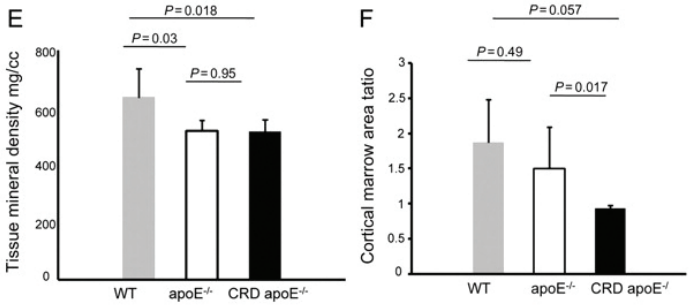
E
P=0.018
P=0.03
P=0.95
Tissue mineral density mg/cc
800
600
400
200
0
WT
apoE-/-
CRD apoE-/-
F
P=0.057
P=0.49
P=0.017
Cortical marrow area tatio
3
2.5
2
1.5
1
0.5
0
WT
apoE-/-
CRD apoE-/

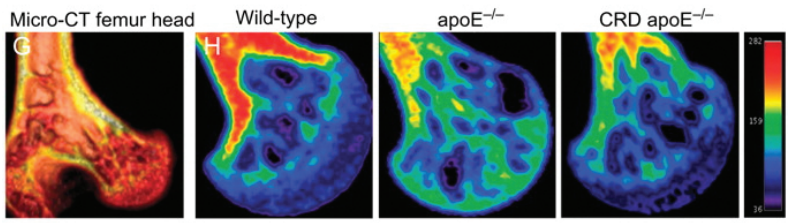
Micro-CT femur head
Wild-type
apoE−/−
CRD apoE−/−
G
H

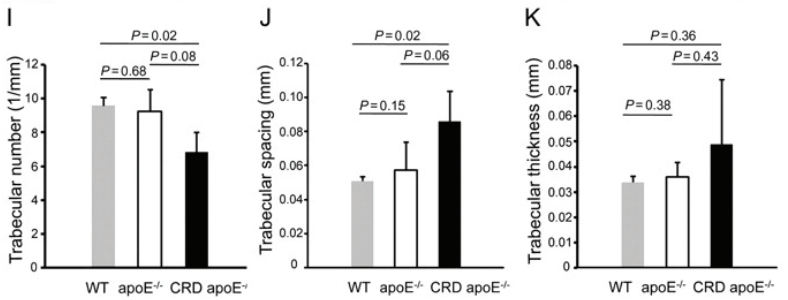
I
P=0.02
P=0.08
P=0.68
Trabecular number (1/mm)
12
10
8
6
4
2
0
WT
apoE-/-
CRD apoE-/-
J
P=0.02
P=0.06
P=0.15
Trabecular spacing (mm)
0.12
0.10
0.08
0.06
0.04
0.02
0
WT
apoE-/-
CRD apoE-/-
K
P=0.36
P=0.43
P=0.38
Trabecular thickness (mm)
0.08
0.07
0.06
0.05
0.04
0.03
0.02
0.01
0
WT
apoE-/-
CRD apoE-/-

4

Enhanced inflammation correlates with calcification in arteries and aortic valves

Macrophage-targeting molecular imaging agent (CLIO750) showed negligible inflammatory signal in WT arteries, which were substantially increased in apoE-/- and CRD apoE-/- mice (Figure 4A). Quantitative assessment of arterial inflammatory ROI determined a 44-fold and 95-fold increase in inflammation tissue area in apoE-/- mice and CRD apoE-/- mice as compared with WT mice, which was further confirmed with significant 326-fold and 718-fold increases in SI (Figures 4B, 4C). Likewise, enhanced expression of inflammation was found in the aortic valves of apoE-/- and CRD apoE-/- mice (Figure 4D). Quantitative analyses demonstrated statistically significant increases in inflammatory valvular ROI and SI between WT, apoE-/-, and CRD apoE-/- groups (ROI: 1.5-fold and 5.7-fold increase, Figure 4E; SI: 2.6-fold and 11.6-fold increase, Figure 4F). Further, we found a statistically significant correlation between cardiovascular calcification and inflammation in both arteries (ROI: R^2=0.73; SI: R^2=0.54; Figures 4G, 4H) and valves (ROI: R^2=0.84; SI: R^2=0.81; Figures 4I, 4J). Macrophage staining confirmed our molecular imaging findings (Suppl. Figures 5A, 5B). Overall, these results suggest that the extent of cardiovascular inflammation correlates with the severity of calcification.

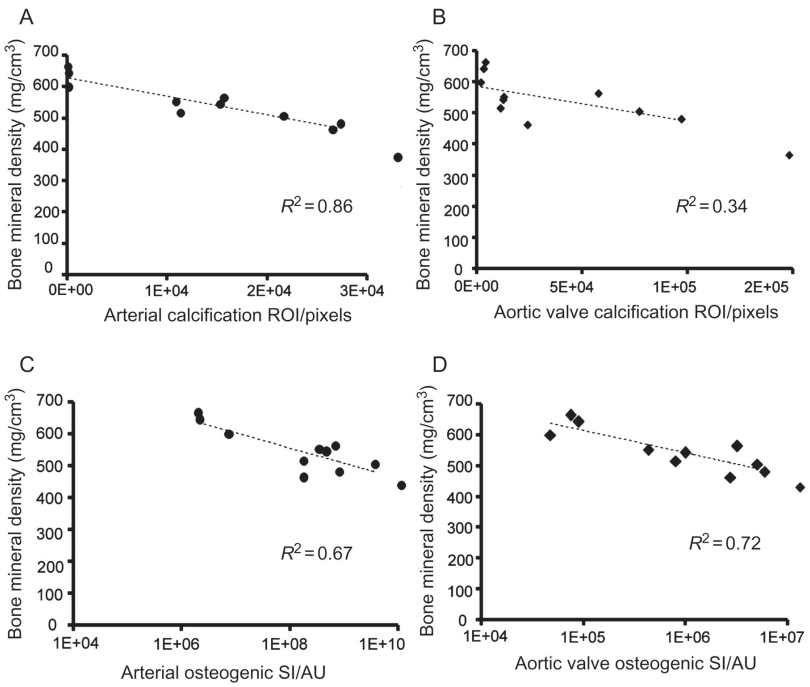

Figure 3. Inverse Correlation of Bone TMD with Arterial and Aortic Valve Calcification

Relation of bone TMD to arterial **(A)** and valve **(B)** calcified area (ROI). Relation of TMD to arterial **(C)** and valve **(D)** osteogenic activity (SI). n=11.

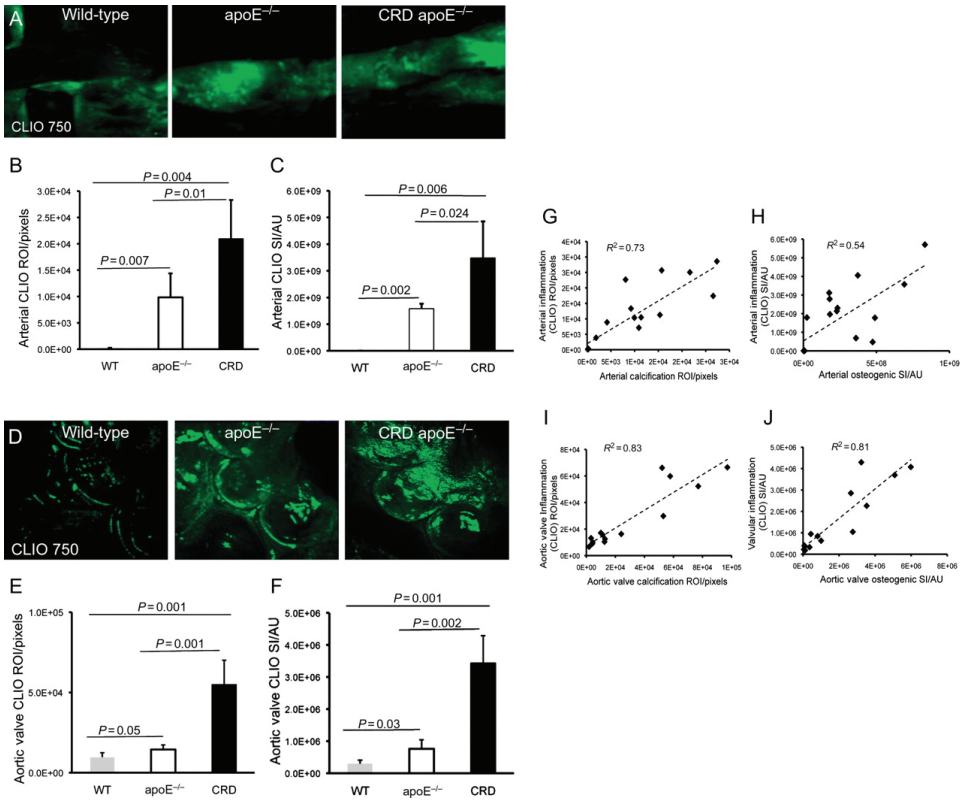

Figure 4. Induction of Inflammatory Signal in Carotid Arteries and Aortic Valves of apoE-/- and CRD apoE-/- Mice, Detected by Intravital Fluorescence Microscopy

(A) Intravital microscopy detected CLIO750-derived inflammatory signals in the carotid arteries of mice. **(B)** Significant increase in arterial inflammation area (ROI) and **(C)** inflammatory signal (SI) in CRD apoE-/- mice vs. WT and apoE-/- mice. **(D)** Fluorescence microscopy detected CLIO750-derived inflammatory signals in the aortic valves. **(E)** Significant increase in aortic valve inflammation area (ROI) and **(F)** signal (SI) in CRD apoE-/- mice, compared to WT and apoE-/- mice. (A-F) WT, n= 8; apoE-/-, n=10; CRD apoE-/-, n=10. **(G)** Relation between arterial inflammation area (CLIO750; ROI) and arterial calcified tissue area (Osteosense680; ROI). **(H)** Association of arterial inflammatory activity (CLIO750; SI) with arterial osteogenic activity (Osteosense680; SI). **(I)** Relation between valvular inflammation (CLIO750; ROI) and aortic valve calcification (Osteosense680; ROI). **(J)** Association of valvular inflammatory signal (CLIO750; SI) with valvular osteogenic activity (Osteosense680; SI). **(G-J)** n=14.

Long bone inflammation correlates inversely with decreased bone mineral signal and associates positively with cardiovascular calcification

Evidence suggests that inflamed or infected bones shift toward an osteolytic environment. To address further the mechanisms for osteoporotic changes, we attempted to link inflammation and TMD in the same mice used for imaging of cardiovascular calcification. Molecular imaging demonstrated robust inflammation signal in the long bones of both apoE-/- mice and CRD apoE-/- mice, while WT mice demonstrated virtually no inflammation (Figure 5A). Using the same approach as before, we found 7.6-fold and 22-fold increases in long bone inflammation (CLIO SI) for apoE-/- mice and CRD

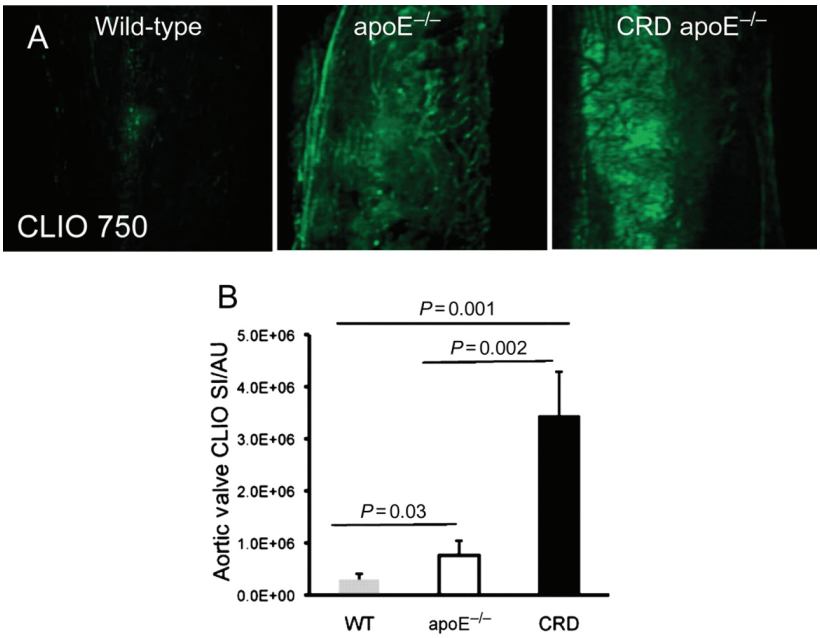

Figure 5. Correlation of Long Bone Inflammation with Osteogenic Activity
(A) Molecular imaging of inflammation in the long bones of mice injected with CLIO750. **(B)** Significant increase of bone inflammation in CRD apoE-/- mice vs. WT and apoE-/- mice. (A-B) WT, n= 8; apoE-/-, n=10; CRD apoE-/-, n=10.

apoE-/- mice, as compared with WT mice (Figure 5B). In contrast to the cardiovascular condition, this increased inflammation correlated with decreased bone mineral signal (R^2=0.75; Figure 6A).

These results strongly suggest that the inflammatory responses in long bones contribute to loss of bone mineralization. Finally, we found strong positive correlations in signal intensity between the degree of arterial or valvular inflammation and bone inflammation (R^2=0.97; Figures 6B, 6C). These results support our hypothesis that systemic inflammatory signal simultaneously acts to decrease bone mass and increase cardiovascular calcification.

DISCUSSION

This study establishes direct *in vivo* evidence that the calcification of arteries and aortic valves in atherosclerosis and CRD correlates inversely with bone tissue mineralization. We demonstrate an association between aortic valve calcification and arterial calcification, and that the degree of cardiovascular calcification correlates directly with loss of bone mineral. The increased inflammatory activity in arteries, aortic valves, and long bones in atherosclerosis and renal failure demonstrates that inflammation at these three locations is related probably via systemic or circulating inflammatory cues. Furthermore, our study reveals that while macrophage burden positively correlates with the extent of early cardiovascular calcification, inflammation inversely associates with bone miner-

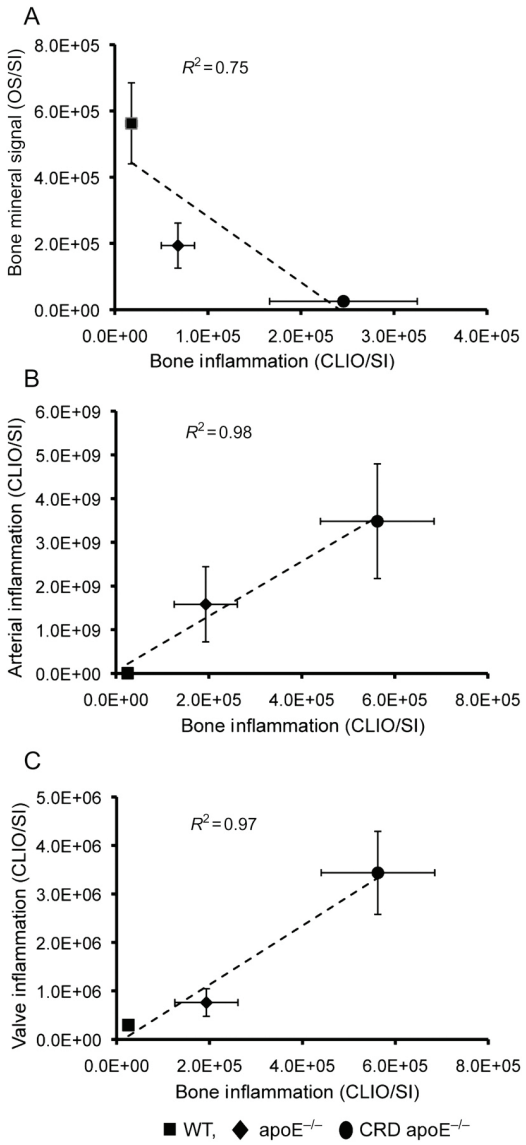

Figure 6. Relation between Bone Osteogenic Activity and Inflammation

(A) Inverse association of bone osteogenic activity (Osteosense680; SI) with bone inflammation (CLIO750; SI). **(B)** Positive relation between arterial inflammation (CLIO750; SI) and bone inflammation (CLIO750; SI). **(C)** Positive correlation of aortic valve inflammation (CLIO750; SI) and bone inflammation (CLIO750; SI). **(A-C)** WT, n= 8; apoE-/-, n=10; CRD apoE-/-, n=10

alization. These results build on previous studies of the pathogenesis of cardiovascular calcification, in which advanced molecular imaging approaches demonstrated that atherosclerotic and aortic valve calcification share similar risk factors and are induced by similar pro-inflammatory molecular and cellular processes.[14-16] Our seemingly paradoxical *in vivo* evidence on inflammation and bone mineralization concur well with previous reports on osteolytic environment in inflamed bones.[24]

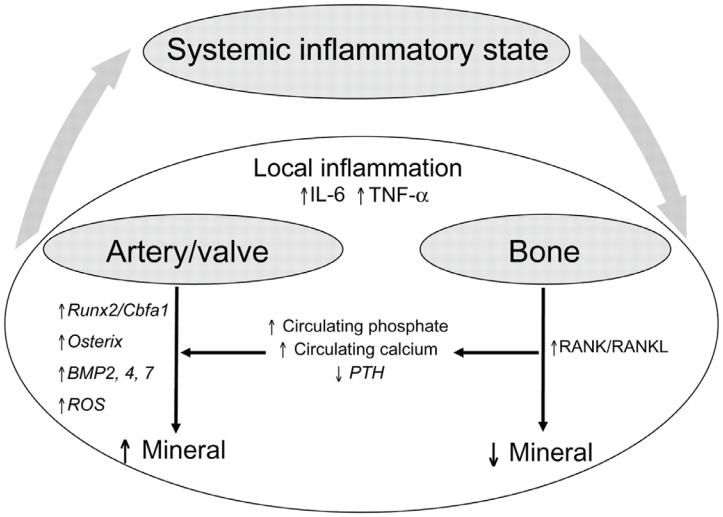

Figure 7. Schematic presentation of a hypothetical model on the paradoxical relationship between cardiovascular calcification and bone mineral loss, associated with local and systemic inflammation

Atherosclerosis and CRD-associated systemic inflammatory stimuli enhance local inflammation in the cardiovascular system. Local pro-inflammatory microenvironmental cues in atherosclerotic plaques and diseased valves may shift vascular and valvular cells towards an osteogenic phenotype, resulting in increased mineral deposition. In the bone, the inflammatory milieu may increase the number/activity of bone-resorbing osteoclasts, leading to decreased mineral. Additional factors arising from bone could further influence cardiovascular calcification.

Arterial calcification occurs in two different forms — intimal calcification, typically associated with atherosclerosis, and medial calcification, an ossification process associated with renal failure and diabetes.[9] In dysmetabolic patient populations, both types of arterial calcification often develop simultaneously. Intimal calcification increases the risk of plaque rupture, while medial calcification increases arterial stiffness and impairs cardiovascular hemodynamics.[9] Although the mechanism remains incompletely understood, it is generally agreed that cardiovascular calcification is a more active biological process than previously considered.[26] Clinicopathological studies have shown similarity between calcified vascular material and bone material,[20] have observed osteoblasts and osteoclast-like cells in the arterial wall,[19] and have demonstrated the presence of various bone-regulating proteins in calcified arteries.[27] Osteogenic differentiation of vascular SMC or valvular myofibroblasts is likely caused by various mechanisms, including proinflammatory cytokines (e.g., IL-6, TNF-α),[10] oxidized lipids,[17] and microenvironmental and mechanical cues.[28] Biochemical imbalances also accelerate calcification. Studies show that excess phosphate levels in CRD accelerate calcification of vascular SMC or valvular myofibroblasts through phosphate-induced release of matrix vesicles and apoptosis.[15, 29]

Systemic factors associated with CRD, including reduced circulating levels of erythropoietin, have been shown to reduce osteoblast quantity and bone mineral density via Jak-Stat signaling in hematopoietic stem cells.[30] Furthermore, the kidneys represent the site of vitamin D activation, and therefore CRD-associated reductions in activated vitamin D may also induce parallel reductions

in bone mass. Whether CRD-induced anemia or activated vitamin D deficiency play a role in the reduced bone mass or increased cardiovascular calcification remains uncertain.

Our results directly quantified a paradox of simultaneous osteolysis and ectopic calcification *in vivo* in the same animals. While both correlate with age in humans, some clinical studies have shown the association of cardiovascular calcification and osteoporosis to be independent of age.[3, 31] Research has demonstrated that patients with lower bone density and osteoporosis have more severe atherosclerosis.[32, 33] Dyslipidemia also may link bone loss with cardiovascular calcification. Preclinical studies suggest that hyperlipidemia reduces bone mineral density[34] and promotes arterial and valvular calcification in mice,[14, 16] and that statins reduce calcification.[14, 35] Moreover, loss of bone mass leads to increased circulating phosphate and calcium and decreased parathyroid hormone, which stimulates the Cbfa1-dependent mineralization of cardiovascular tissue.[36] This evidence suggests that osteoporosis may contribute to cardiovascular calcification by adding to a pathological microenvironment that promotes osteogenesis of the arterial wall and aortic valve. During bone resorption, biochemical factors are released into the circulation, contributing to vascular calcification; this observation agrees with studies showing that agents that block bone resorption in animal models also block vascular calcification.[37]

Our findings strongly suggest *in vivo* that systemic and local inflammation drives both cardiovascular calcification and bone loss. In general, inflammation causes "hardening" of soft tissue and "softening" of hard tissue,[34] but it is unclear whether the pathways are similar. Connections between inflammation and osteolysis were recently established in arthritic and periodontal diseases.[24] Pro-inflammatory cytokines such as IL-6 and TNF-α have been shown to increase osteoclast activity through the NF-kB pathway.[38] Osteoprotegerin — normally produced by vascular SMC and osteoblasts — functions as a decoy receptor for the receptor activator of NF-kB ligand RANKL.[26] RANKL, a cytokine that induces osteoclast differentiation and activation, stimulates bone resorption, whereas osteoprotegerin neutralizes the binding of RANKL to RANK and prevents bone loss. Osteoprotegerin-deficient mice demonstrated severe bone loss in addition to medial calcifications.[39] Taken together, these studies suggest that inflammation in cardiovascular and bone regions acts through the NF-kB-RANKL pathway, but whether this pathway is utilized simultaneously for ectopic calcification and bone loss is unknown.

Figure 7 shows a schematic illustration of our working hypothesis. The presence of atherosclerosis or CRD likely associates with systemic inflammatory signals, as described above. Local inflammation, as detected by macrophage-targeted NIRF nanoparticles, associates with increased mineral in cardiovascular tissues and decreased mineral in bone, as detected by Osteosense. Potential mediators associated with systemic and local inflammatory processes are shown, as are possible factors arising from bone, which could further influence cardiovascular calcification. Studies are needed to further establish the relation between cardiovascular calcification and osteoporosis, and to dissect the complex mechanisms for reciprocal regulation of these processes.

Unraveling the mechanisms underlying cardiovascular calcification is an important step towards future strategies. Therapeutic agents that selectively increase or inhibit osteogenesis will be much

preferred over current systemic approaches like statin therapy. The identification of high-risk patients at subclinical stages is an equally important task, requiring new imaging modalities or biomarkers targeting calcification.[8] Molecular imaging provides appealing new means to identify early-stage calcifying atherosclerotic plaques and aortic valve lesions, and offers a powerful tool in personalized preventive cardiovascular medicine.

FUNDING SUPPORT

This study was supported in part by Wijck-Casper-Stam Foundation (JH), American Heart Association Scientist Development Grants (0835460N, EA; 0830384N,JB), NYSTAR CAT Award (JB, MR), Donald W. Reynolds Foundation (RW, EA), Leducq Foundation (07CVD04; EA, JB) and Translational Program of Excellence in Nanotechnology (5-UO1-HL080731; RW).

ACKNOWLEDGEMENTS

The authors would like to thank Dr. Masanori Aikawa for critical reading of the manuscript and Sara Karwacki for excellent editorial assistance.

DISCLOSURES

Dr. Weissleder reports serving as a consultant for Visen Medical. Other authors report no disclosures.

REFERENCES

1. Banks LM, Lees B, MacSweeney JE, Stevenson JC. Effect of degenerative spinal and aortic calcification on bone density measurements in post-menopausal women: Links between osteoporosis and cardiovascular disease? *European journal of clinical investigation*. 1994;24:813-817
2. Stehman-Breen C. Osteoporosis and chronic kidney disease. *Seminars in nephrology*. 2004;24:78-81
3. Farhat GN, Cauley JA, Matthews KA, Newman AB, Johnston J, Mackey R, Edmundowicz D, Sutton-Tyrrell K. Volumetric bmd and vascular calcification in middle-aged women: The study of women's health across the nation. *J Bone Miner Res*. 2006;21:1839-1846
4. Farhat GN, Strotmeyer ES, Newman AB, Sutton-Tyrrell K, Bauer DC, Harris T, Johnson KC, Taaffe DR, Cauley JA. Volumetric and areal bone mineral density measures are associated with cardiovascular disease in older men and women: The health, aging, and body composition study. *Calcified tissue international*. 2006;79:102-111
5. Frost ML, Grella R, Millasseau SC, Jiang BY, Hampson G, Fogelman I, Chowienczyk PJ. Relationship of calcification of atherosclerotic plaque and arterial stiffness to bone mineral density and osteoprotegerin in postmenopausal women referred for osteoporosis screening. *Calcified tissue international*. 2008;83:112-120
6. Tintut Y, Morony S, Demer LL. Hyperlipidemia promotes osteoclastic potential of bone marrow cells ex vivo. *Arteriosclerosis, thrombosis, and vascular biology*. 2004;24:e6-10
7. Hirasawa H, Tanaka S, Sakai A, Tsutsui M, Shimokawa H, Miyata H, Moriwaki S, Niida S, Ito M, Nakamura T. Apoe gene deficiency enhances the reduction of bone formation induced by a high-fat diet through the stimulation of p53-mediated apoptosis in osteoblastic cells. *J Bone Miner Res*. 2007;22:1020-1030
8. Rajamannan NM AE, Grande-Allen KJ, Heistad DD, Masters KS, Mathieu P, O'Brien K, Otto CM, Schoen FJ, Simmons G, Towler D, Yoganathan A. . National heart, lung and blood institute (nhlbi) working group on calcific aotic stenosishttp://www.Nhlbi.Nih.Gov/meetings/workshops/cas.Htm. 2010
9. Wayhs R, Zelinger A, Raggi P. High coronary artery calcium scores pose an extremely elevated risk for hard events. *Journal of the American College of Cardiology*. 2002;39:225-230
10. Abedin M, Tintut Y, Demer LL. Vascular calcification: Mechanisms and clinical ramifications. *Arteriosclerosis, thrombosis, and vascular biology*. 2004;24:1161-1170
11. Virmani R, Burke AP, Farb A, Kolodgie FD. Pathology of the vulnerable plaque. *Journal of the American College of Cardiology*. 2006;47:C13-18
12. Vengrenyuk Y, Cardoso L, Weinbaum S. Micro-ct based analysis of a new paradigm for vulnerable plaque rupture: Cellular microcalcifications in fibrous caps. *Mol Cell Biomech*. 2008;5:37-47
13. Hoshino T, Chow LA, Hsu JJ, Perlowski AA, Abedin M, Tobis J, Tintut Y, Mal AK, Klug WS, Demer LL. Mechanical stress analysis of a rigid inclusion in distensible material: A model of atherosclerotic calcification and plaque vulnerability. *American journal of physiology*. 2009;297:H802-810
14. Aikawa E, Nahrendorf M, Sosnovik D, Lok VM, Jaffer FA, Aikawa M, Weissleder R. Multimodality molecular imaging identifies proteolytic and osteogenic activities in early aortic valve disease. *Circulation*. 2007;115:377-386
15. Aikawa E, Aikawa M, Libby P, Figueiredo JL, Rusanescu G, Iwamoto Y, Fukuda D, Kohler RH, Shi GP, Jaffer FA, Weissleder R. Arterial and aortic valve calcification abolished by elastolytic cathepsin s deficiency in chronic renal disease. *Circulation*. 2009;119:1785-1794
16. Aikawa E, Nahrendorf M, Figueiredo JL, Swirski FK, Shtatland T, Kohler RH, Jaffer FA, Aikawa M, Weissleder R. Osteogenesis associates with inflammation in early-stage atherosclerosis evaluated by molecular imaging in vivo. *Circulation*. 2007;116:2841-2850

17. Miller JD, Chu Y, Brooks RM, Richenbacher WE, Pena-Silva R, Heistad DD. Dysregulation of antioxidant mechanisms contributes to increased oxidative stress in calcific aortic valvular stenosis in humans. *Journal of the American College of Cardiology*. 2008;52:843-850
18. Rajamannan NM, Nealis TB, Subramaniam M, Pandya S, Stock SR, Ignatiev CI, Sebo TJ, Rosengart TK, Edwards WD, McCarthy PM, Bonow RO, Spelsberg TC. Calcified rheumatic valve neoangiogenesis is associated with vascular endothelial growth factor expression and osteoblast-like bone formation. *Circulation*. 2005;111:3296-3301
19. Bostrom K, Watson KE, Stanford WP, Demer LL. Atherosclerotic calcification: Relation to developmental osteogenesis. *The American journal of cardiology*. 1995;75:88B-91B
20. Duer MJ, Friscic T, Proudfoot D, Reid DG, Schoppet M, Shanahan CM, Skepper JN, Wise ER. Mineral surface in calcified plaque is like that of bone: Further evidence for regulated mineralization. *Arteriosclerosis, thrombosis, and vascular biology*. 2008;28:2030-2034
21. Rabkin E, Aikawa M, Stone JR, Fukumoto Y, Libby P, Schoen FJ. Activated interstitial myofibroblasts express catabolic enzymes and mediate matrix remodeling in myxomatous heart valves. *Circulation*. 2001;104:2525-2532
22. Rattazzi M, Bennett BJ, Bea F, Kirk EA, Ricks JL, Speer M, Schwartz SM, Giachelli CM, Rosenfeld ME. Calcification of advanced atherosclerotic lesions in the innominate arteries of apoe-deficient mice: Potential role of chondrocyte-like cells. *Arteriosclerosis, thrombosis, and vascular biology*. 2005;25:1420-1425
23. Steitz SA, Speer MY, Curinga G, Yang HY, Haynes P, Aebersold R, Schinke T, Karsenty G, Giachelli CM. Smooth muscle cell phenotypic transition associated with calcification: Upregulation of cbfa1 and downregulation of smooth muscle lineage markers. *Circ Res*. 2001;89:1147-1154
24. Lerner UH. Inflammation-induced bone remodeling in periodontal disease and the influence of postmenopausal osteoporosis. *Journal of dental research*. 2006;85:596-607
25. Kozloff KM, Volakis LI, Marini JC, Caird MS. Near-infrared fluorescent probe traces bisphosphonate delivery and retention in vivo. *J Bone Miner Res*.
26. Demer LL, Tintut Y. Vascular calcification: Pathobiology of a multifaceted disease. *Circulation*. 2008;117:2938-2948
27. El-Abbadi M, Giachelli CM. Mechanisms of vascular calcification. *Advances in chronic kidney disease*. 2007;14:54-66
28. Yip CY, Chen JH, Zhao R, Simmons CA. Calcification by valve interstitial cells is regulated by the stiffness of the extracellular matrix. *Arteriosclerosis, thrombosis, and vascular biology*. 2009;29:936-942
29. Reynolds JL, Joannides AJ, Skepper JN, McNair R, Schurgers LJ, Proudfoot D, Jahnen-Dechent W, Weissberg PL, Shanahan CM. Human vascular smooth muscle cells undergo vesicle-mediated calcification in response to changes in extracellular calcium and phosphate concentrations: A potential mechanism for accelerated vascular calcification in esrd. *J Am Soc Nephrol*. 2004;15:2857-2867
30. Shiozawa Y, Jung Y, Ziegler AM, Pedersen EA, Wang J, Wang Z, Song J, Wang J, Lee CH, Sud S, Pienta KJ, Krebsbach PH, Taichman RS. Erythropoietin couples hematopoiesis with bone formation. *PloS one*.5:e10853
31. Hak AE, Pols HA, van Hemert AM, Hofman A, Witteman JC. Progression of aortic calcification is associated with metacarpal bone loss during menopause: A population-based longitudinal study. *Arteriosclerosis, thrombosis, and vascular biology*. 2000;20:1926-1931
32. Browner WS, Seeley DG, Vogt TM, Cummings SR. Non-trauma mortality in elderly women with low bone mineral density. Study of osteoporotic fractures research group. *Lancet*. 1991;338:355-358
33. Uyama O, Yoshimoto Y, Yamamoto Y, Kawai A. Bone changes and carotid atherosclerosis in postmenopausal women. *Stroke; a journal of cerebral circulation*. 1997;28:1730-1732
34. Demer LL. Vascular calcification and osteoporosis: Inflammatory responses to oxidized lipids. *International journal of epidemiology*. 2002;31:737-741

35. Rajamannan NM, Subramaniam M, Springett M, Sebo TC, Niekrasz M, McConnell JP, Singh RJ, Stone NJ, Bonow RO, Spelsberg TC. Atorvastatin inhibits hypercholesterolemia-induced cellular proliferation and bone matrix production in the rabbit aortic valve. *Circulation*. 2002;105:2660-2665
36. Jono S, Nishizawa Y, Shioi A, Morii H. 1,25-dihydroxyvitamin d3 increases in vitro vascular calcification by modulating secretion of endogenous parathyroid hormone-related peptide. *Circulation*. 1998;98:1302-1306
37. Price PA, June HH, Buckley JR, Williamson MK. Osteoprotegerin inhibits artery calcification induced by warfarin and by vitamin d. *Arteriosclerosis, thrombosis, and vascular biology*. 2001;21:1610-1616
38. Crotti TN, Smith MD, Findlay DM, Zreiqat H, Ahern MJ, Weedon H, Hatzinikolous G, Capone M, Holding C, Haynes DR. Factors regulating osteoclast formation in human tissues adjacent to peri-implant bone loss: Expression of receptor activator nfkappab, rank ligand and osteoprotegerin. *Biomaterials*. 2004;25:565-573
39. Bucay N, Sarosi I, Dunstan CR, Morony S, Tarpley J, Capparelli C, Scully S, Tan HL, Xu W, Lacey DL, Boyle WJ, Simonet WS. Osteoprotegerin-deficient mice develop early onset osteoporosis and arterial calcification. *Genes & development*. 1998;12:1260-1268

SUPPLEMENTAL FIGURES

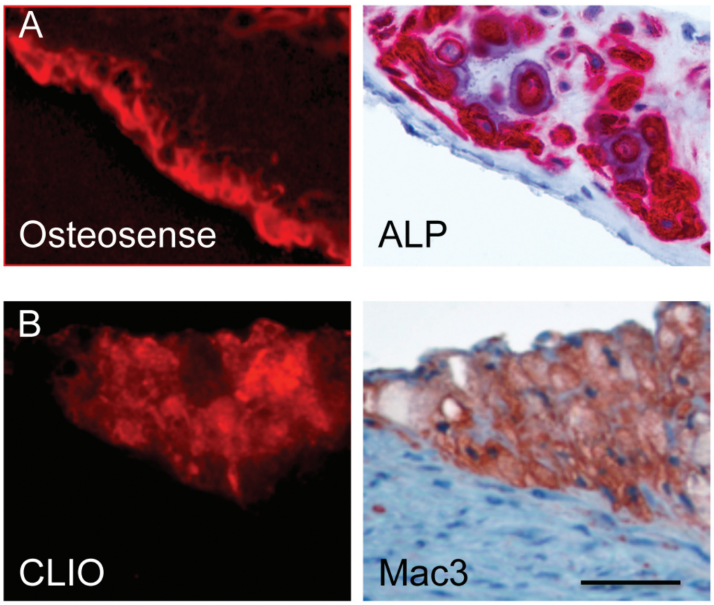

Supplemental Figure I. Molecular imaging agents. A) Co-localization of osteogenic signal (red fluorescence, left) with osteoblast-like cells (alkaline phosphatase activity, ALP, right) in the tissue section through the area of active mineralization in atherosclerotic lesion of mouse injected with Osteosense680. **(B)** Co-localization of fluorescence NIR nanoparticle (red fluorescence, left) with macrophages shown as mac-3-positive cells (right) in atherosclerotic lesion. Bar=50um.

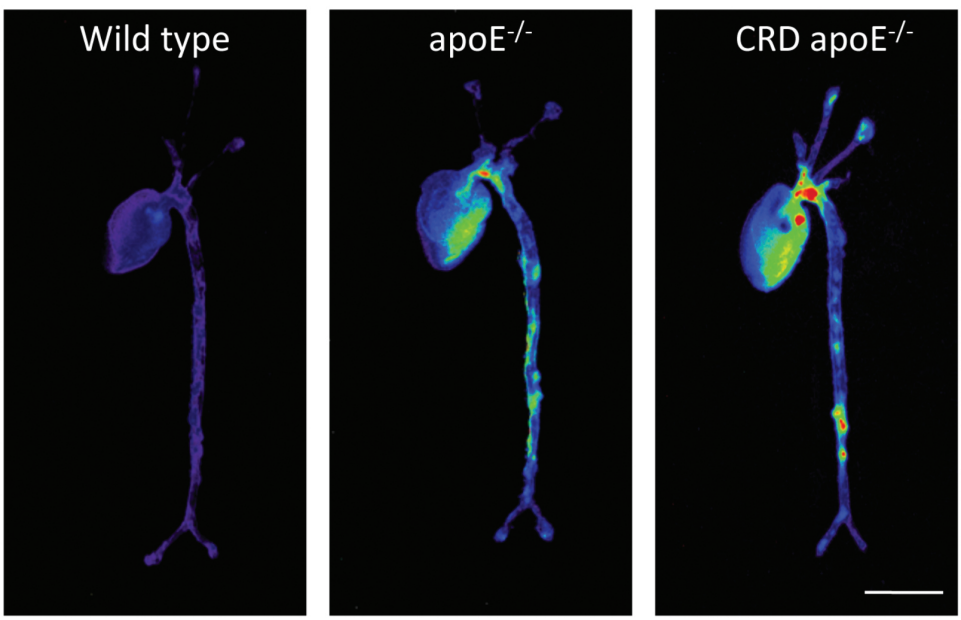

Supplemental Figure II. Calcification increased in aortas of CRD apoE-/- mice. Macroscopic fluorescence reflectance imaging of calcification yielded strong Osteosense680-derived osteogenic signal in atherosclerotic mice with CRD. Bar=1cm

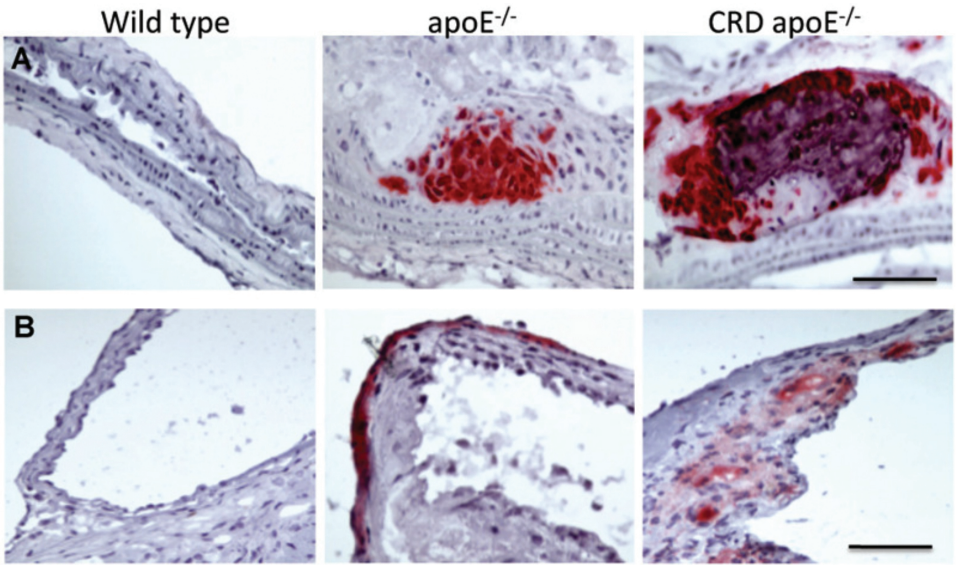

Supplemental Figure III. (A) Carotid arteries and **(B)** aortic valves showed notable increase in alkaline phosphatase activity (red reaction product) in apoE-/- and CRD apoE-/- mice compared to wild type mice. Bar=50um.

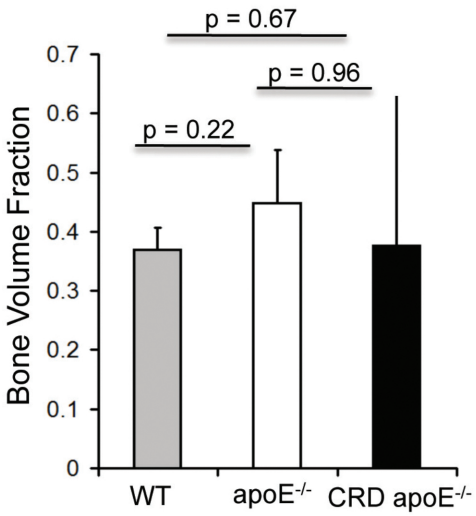

Supplemental Figure IV. Micro-CT showed no significant changes in bone volume fraction between three groups.

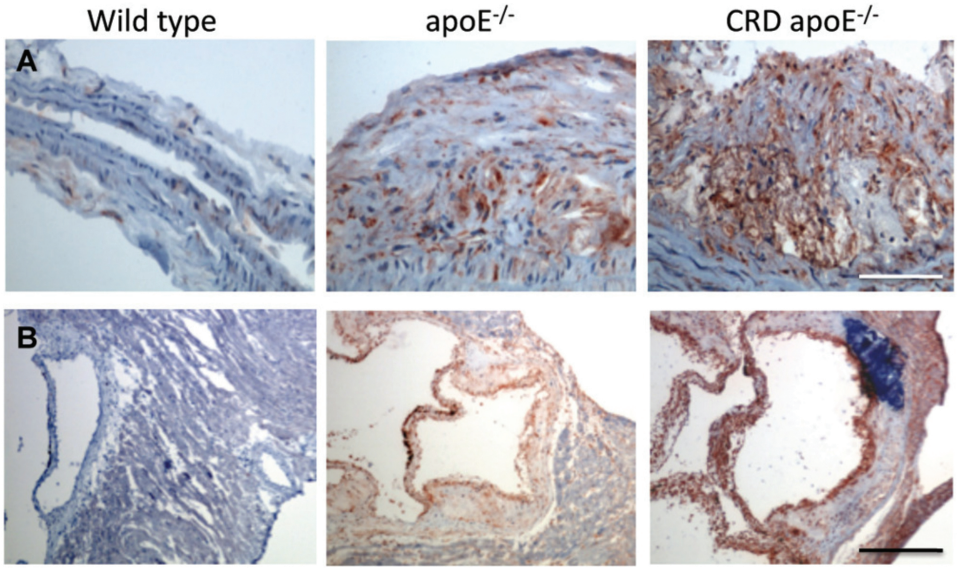

Supplemental Figure V. (A) Carotid arteries (bar=50um) and **(B)** aortic valves (bar=100um) demonstrate increase in macrophage accumulation (mac-3 staining, brown-red reaction product) particularly in CRD apoE-/- mice. Note higher numbers of macrophages in the aortic valves and myocardium in CRD apoE-/- mice compared to apoE-/- and WT mice.

Part II

Modeling early Calcific Aortic Valve Disease

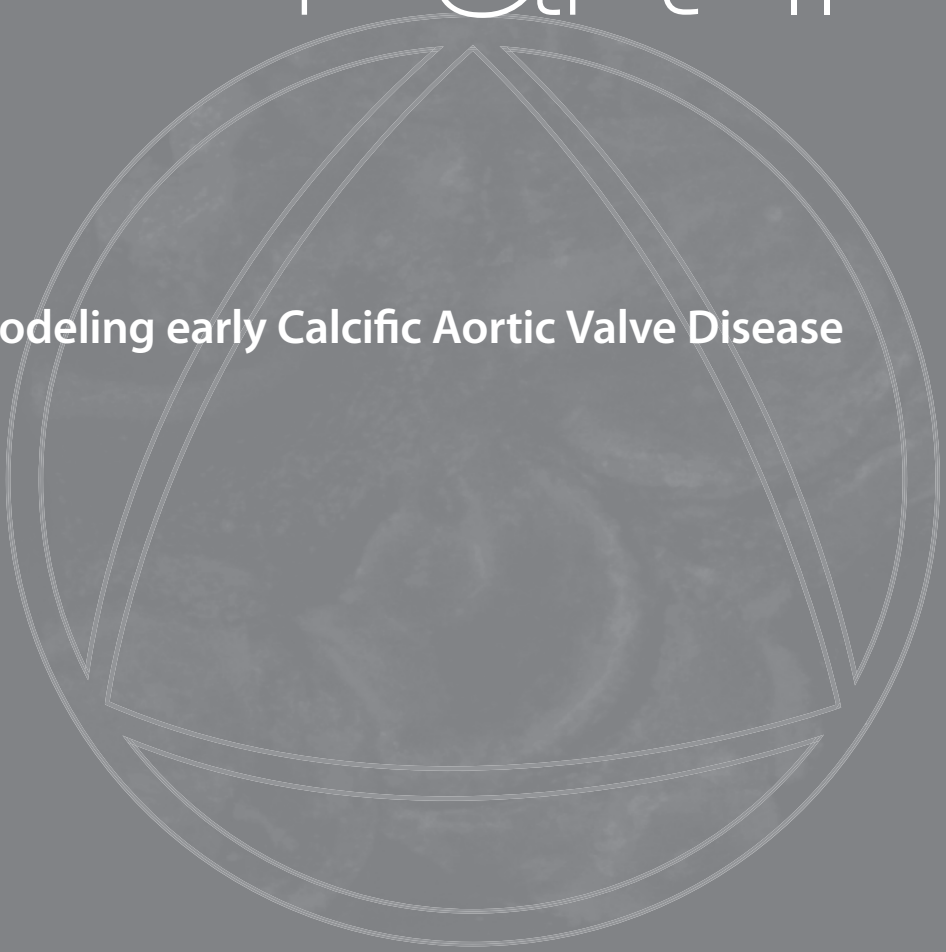

5

Microfabricated Gels for Tissue Engineering

Gulden Camci-Unal[1,2], Jesper Hjortnaes[1,3,4], Hojae Bae[1,2], Mehmet Remzi Dokmeci[1,2] and Ali Khademhosseini[1,2,5]

Biomaterials and Regenerative Medicine

Cambridge University Press 2013

[1] Center for Biomedical Engineering, Department of Medicine, Brigham and Women's Hospital, Harvard Medical School, Cambridge, USA. [2] Harvard-MIT Division of Health Sciences and Technology, Massachusetts Institute of Technology, 77 Massachusetts Avenue, Cambridge, USA. [3] Division of Cardiovascular Medicine, Brigham and Women's Hospital, Harvard Medical School, Boston, USA. [4] Department of Cardiothoracic Surgery, Division of Heart and Lungs, University Medical Center Utrecht, Utrecht, the Netherlands.[5] Wyss Institute for Biologically Inspired Engineering, Harvard University, Boston, USA.

ABSTRACT

Microfabrication techniques are powerful approaches to produce tissue engineered constructs for *in vitro* studies and potentially to replace damaged or malfunctioning tissues. To fabricate microengineered cell-laden hydrogels, which have the ability to mimic living structures, one needs to control a number of factors, such as shape, size, architectural organization and distribution of the cells throughout the engineered construct. This challenge can be addressed by the use of various microfabrication techniques, which enable three-dimensional encapsulation of cells within biocompatible hydrogels. In this chapter, we describe some of the emerging techniques to micro-engineered hydrogels for tissue engineering. Furthermore, we discuss specific examples for tissue engineering applications focusing on two main approaches, top-down and bottom-up strategies.

1. INTRODUCTION

Tissue engineering aims to develop biological substitutes that repair or replace damaged tissues or whole organs by combining technologies from engineering and medical sciences.[1] Although tissue engineering has enabled successful generation of various artificial tissue substitutes, such as skin,[2] bladder,[3] cartilage,[4] bone,[5] heart valves[6] and blood vessels,[7] a number of challenges remain to be solved. It has been challenging to engineer large and vascularized organs such as the heart or liver. These tissues depend on adequate vascularization of the supply of nutrients and oxygen. In tissue engineering, this translates into not only creating the specific tissue but also making the often highly organized vasculature. On the other hand, avascular tissues, such as a heart valve or cartilage, depend on adequate diffusion for their supply of nutrients and oxygen. In terms of engineering, the biomimetic construct cannot be too thick,[8, 9] as this would lead to a limited supply of nutrients and oxygen.[1] Microfabrication strategies aim to overcome these limitations by controlling size, geometry and features of 3D *in vitro* tissue engineered constructs. Recent advances in biomaterials are expected to render the generation of microvascular structures, engineering macroscale constructs from individual building blocks, and creating tissue constructs with properties similar to native tissues.[10]

Native tissues consist of cells that reside in a framework called the extracellular matrix (ECM). The ECM is composed of proteins (e.g. collagen), fibers (e.g. elastin), polysaccharides (e.g. hyaluronic acid), glycosaminoglycans (e.g. heparan sulfate), and growth factors (e.g. fibroblast growth factor). The ECM functions as a support system for cells to exert their biological function and it can be viewed as the scaffolding of tissues. Traditional tissue engineering uses synthetic scaffolds or biomaterials as molds to create tissue constructs. These scaffolds are typically porous, biocompatible, degradable and allow for sufficient diffusion.[11] Furthermore, such scaffolds enable cell adhesion, proliferation, differentiation, and tissue organization that are similar to their native counterparts.[12] Over time, the synthetic scaffold will degrade while the cells deposit new natural scaffolding (ECM) and thus lead to the formation of the new tissue.

Some of the most common biomaterials used in tissue engineering are hydrogels. Hydrogels are generated by crosslinking hydrophilic polymer precursors using a range of external stimuli, such as ultra-violet (UV) light, pH or temperature. Hydrogels resemble native ECM[13] because they possess high water content,[12, 14] are sufficiently flexible and can be fabricated using natural ECM components, such as collagen, hyaluronic acid (HA), chondroitin sulfate, heparin, or elastin. Hydrogels are used as 3D scaffolds or matrices to entrap cells[15] and provide for a sufficiently hydrophilic environment for cell survival, growth and new ECM production.[12] Hydrogels can also be used as building blocks to fabricate scaffolds,[15] which provide structural support and regulate cellular function and signaling.[12]

The chemical, biological and mechanical features of hydrogels can be tailored to modulate cellular function. For example, various growth factors, adhesive peptides, proteins, fibers and degradable peptides, have been used to modify hydrogels for tissue engineering applications.[12] Additionally,

modifications in degradation or mechanical properties of hydrogels generate alterations in cell response in the final engineered construct due to the resulting changes in the substrate properties. Such tunable hydrogels can potentially be useful for a number of different tissue engineering applications,[12, 16] such as bone[17] or cartilage[14] tissue engineering.

Communication between cells is essential for them to function properly,[18] and this is largely facilitated by integration and interaction of cells with the ECM.[16] In an ideal engineered tissue, cells are homogeneously distributed and sufficiently organized to allow for the transport of oxygen, nutrients and waste throughout the porous scaffold. In addition, such constructs should possess adequate mechanical properties to support the growing tissue. Cell-cell, cell-substrate and cell-soluble factor interactions can be manipulated by controlling cellular microenvironments with the aid of microfabrication techniques.[19, 20] For instance, the alignment of cells or behavior of co-cultures can be controlled by these strategies. Additionally, patterned substrates, which are generated by these techniques, can be used to influence cellular behavior, such as adhesion, survival, spreading, migration, proliferation, elongation, biological function and direction of stem cell fate.

In tissue engineering, selecting the appropriate biomaterial is crucial for directing interactions between cells and the surrounding microenvironment. Cell-biomaterial interactions on hydrogel surfaces play a significant role in influencing cellular behavior. For instance, photocured HA-gelatin methacrylate hydrogels have been synthesized to capture endothelial progenitor cells (EPCs).[21] Similarly, HA-heparin containing hydrogels were generated to promote adhesion and spreading of EPCs for endothelialization purposes.[22] Furthermore, cells or biological molecules have been patterned on surfaces to study cellular interactions in two dimensions (2D) by utilizing various microfabrication techniques.[23-31] However, 2D cultures are not suitable for simulating the natural environment of cells, because they lack the complexity and organization present in native tissues. To address this need, cells have been embedded in 3D hydrogels.[32, 33]

Hydrogel microengineering strategies are potentially powerful tools to create 3D tissue models to mimic the natural environment of living tissues. The ability to engineer hydrogels laden with cells or other biological molecules has enabled the fabrication of *in vitro* tissue constructs. Microengineered hydrogels can be produced by a number of techniques, such as bioprinting, micromolding, photopatterning, emulsification and microfluidics. Cells are encapsulated in the hydrogel precursors with these techniques to create controlled architectures for different tissue engineering applications.[34]

In this chapter, we will classify hydrogel microfabrication strategies and highlight tissue engineering applications by discussing top-down and bottom-up tissue engineering approaches.

2. MICROFABRICATION TECHNIQUES

Microfabrication strategies for the generation of hydrogels have emerged as powerful tools in tissue engineering and regenerative medicine. These fabrication techniques may yield complex features resembling highly organized architectures in native organs. For instance, micropatterned co-cultures can control homotypic and heterotypic cellular interactions in engineered tissue constructs.[18] The major microfabrication techniques to synthesize engineered hydrogels can be classified into the following groups: bioprinting, micromolding, photolithograpy, emulsification and microfluidics.

2.1. Bioprinting

Bioprinting is a technique that uses printing technology to engineer tissue-like structures. In essence, this technology 'prints' tissue. Cells or biological molecules can be embedded within hydrogels and used as 'ink' to generate engineered constructs.[12] More specifically, gels with or without cells/biological factors are printed on predefined positions utilizing a layer-by-layer approach (Figure 1).[35]

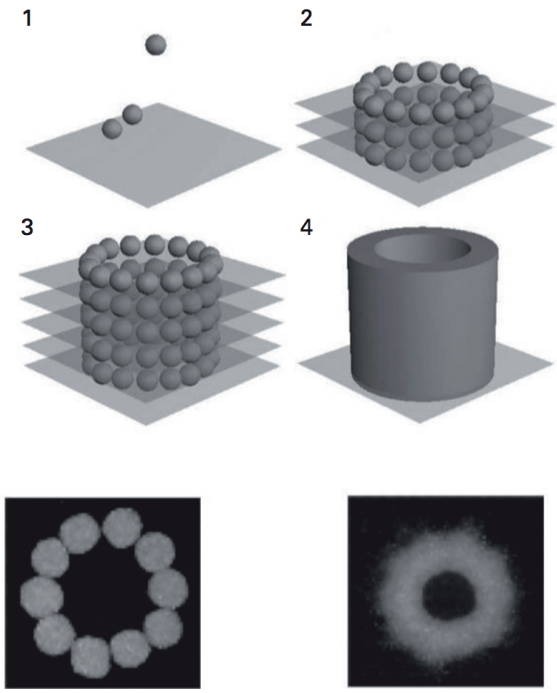

Figure 1. Bioprinting strategy to build tissues and organs by making use of hydrogel precursors (35). Reproduced by permission of The Royal Society of Chemistry.

This technique allows for creation of 3D tissue constructs, which could be used to repair damaged or diseases tissues.[11, 12] Using this technique, cells can be homogeneously distributed within

a hydrogel matrix on predefined positions. To alter physical, chemical or mechanical properties of printed gels, such as size, shape or stiffness, one can change nozzle diameter, cell density, fluid flow rate, liquid rheology and operation temperature[13, 36, 37] in bioprinting based systems.

The hydrogel precursors for bioprinting are chosen based on the targeted application. The following polymers are commonly used as hydrogel precursors in bioprinting studies: gelatin,[38] chitosan,[39] Matrigel,[40-43] alginate,[44-46] HA,[47] starch,[48] collagen,[40, 49-51] fibrin,[13] polyethylene glycol diacrylate (PEGDA),[52] and agarose.[13] Numerous cell types have been utilized in bioprinting techniques to build artificial tissue units. For example, endothelial cells,[42] smooth muscle cells[40] and osteoblasts[45] have been successfully encapsulated in hydrogel based matrices. Moreover, nerve, bone, and cartilage tissues have also been fabricated using bioprinting.[11] Although bioprinting enables precise placement of cells in the hydrogels, such rapid prototyping techniques have some limitations. For instance, due to harsh printing conditions, such as shear stress, variation in pH or elevated temperatures, it may be challenging to maintain high cell viability during the printing process.[53]

Printing strategies can also be used for cell-patterning or creating biological molecule loaded hydrogels.[54] In these approaches, cells or biological molecules, such as growth factors, are resuspended in the prepolymer solution and dispensed by a printing mechanism on predetermined positions on a solid surface. The resulting droplets are subsequently crosslinked to form individual building blocks and this process is repeated to form layers for the final tissue construct. This approach enables the deposition of multiple cell types or aggregates of cells encapsulated in hydrogels.[53] Ten to several hundreds of micrometers is typically the range for spatial resolution obtained by computer assisted design (CAD) strategies.[55]

Stereolithography, another bioprinting technique, is also used to generate cell-laden hydrogels and print *in vitro* tissue engineered constructs. In stereolithography, selective polymerization of the hydrogel precursor is carried out by an ordered layer-by-layer procedure to obtain multilayered cell embedded scaffolds[12] utilizing photocrosslinking (Please see Section 2.3 for details of this technique) via exposure to UV light.[11, 13, 56-58]

2.2. Micromolding

Creating highly organized complex tissue architectures is one of the main challenges in tissue engineering.[16, 59-61] Especially, because the spatial distribution of cells modulate tissue function.[62] Micromolding techniques are used to control spatial distribution of cells in 3D tissue-like structures[23, 63, 64] by regulating the size and shape of microscale hydrogels.[16, 19, 32] This technique can produce hydrogel patterns with micron or nanometer resolutions.[65] Basically, this technology utilizes the shape of molds to create the desired features for different materials. More specifically, with micromolding, prepolymer solutions are crosslinked within patterns of elastomeric molds,[16, 66] to regulate the dimensions, shapes and sizes of the resulting hydrogels.[67] Micromolding is a simple and low-cost technique[67, 68] and has extensively been used to fabricate microengineered constructs.[19, 23, 62, 64, 69-71] However, the major limitation of micromolding is that it is challenging to use this technique for chemically crosslinked hydrogels.[66]

The micromolds are typically made from poly-dimethoxysilane (PDMS), which is a broadly used elastomer to transfer specific patterns from silicon wafers[67, 70, 72] (Figure 2). PDMS is a highly porous, transparent and biocompatible substrate. In addition to PDMS, polyimines or polyurethanes also are used as molds in micromolding based techniques. Additionally, fluoropolymers (e.g. perfluoropolyether) have been utilized as molding materials to obtain easily harvestable hydrogel units due to their unique non-adhesive properties.[73] Micromolding is used to fabricate gels for a variety of polymer precursors, such as chitosan,[19] PEG,[32, 70, 74] HA[23, 32] and agarose.[75] Micromolding has successfully been used to create 3D tissue-like structures[23, 63, 64, 76] by means of cell-laden hydrogels. For example, spatial distribution of NIH-3T3 fibroblast cells in PEG and HA-based hydrogel patterns have been controlled by micromolding strategies.[32] In another study, microvasculature patterns in hepatocyte-laden agarose based hydrogel channels were created.[77] Additionally, alignment and differentiation of skeletal muscle cells were studied in fibrin-collagen gels by micromolding techniques.[64]

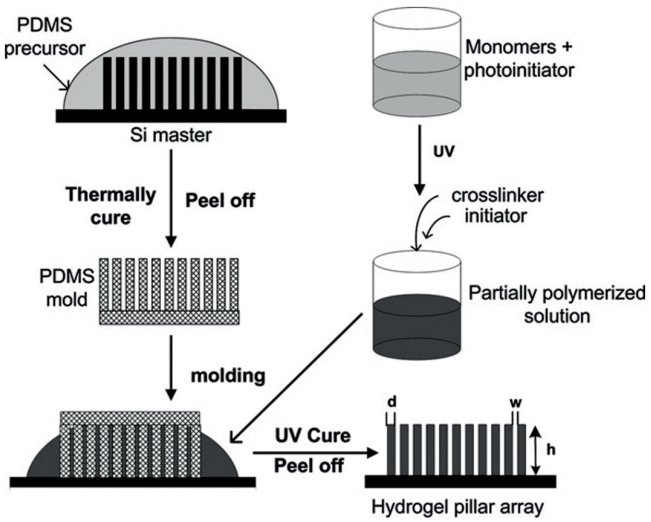

Figure 2. Soft lithographic fabrication process for PDMS molds (70). Reproduced by permission of The Royal Society of Chemistry.

2.3. Photolithography

Another strategy to fabricate controlled size and shape hydrogels is by using photolithography.[72] In this process, photolabile hydrogel precursors are crosslinked via exposure to light. A photomask with predefined patterns is placed above the prepolymer mixture and crosslinked via radical polymerization by means of UV light[66, 78] (Figure 3). As a result, patterns from the photomask are transferred on the polymer substrate. Once the polymerization is complete, the unreacted polymer mixture is rinsed away. Resolution of photolithographic techniques varies between a sub-micron to millimeter range.[16] Photolithography is a simple technique enabling spatial control,[16] however, the major drawback of photolithography is that it often uses exposure to UV light to induce crosslink-

ing which can be cytotoxic.[66] There are a variety of hydrogel precursors, which can be modified with photocrosslinkable functional groups. Photolithography is a simple procedure to fabricate micropatterns with varying size and shapes.[72, 79, 80] In addition, photolithographic approaches enable immobilization of cells in patterned hydrogels with spatial control.[16] For instance, micropatterns of PEG-based hydrogels have been generated by encapsulating hepatocytes, fibroblasts or macrophages.[80, 81] Similarly, NIH-3T3 fibroblasts have been encapsulated in microchannel patterns made of gelatin methacrylate hydrogel to study cell alignment.[82]

Scanning or focusing light are other approaches to generate 3D hydrogel patterns.[66] For example, photocurable polymers have been crosslinked using scanning laser lithography.[83-85] In another study, a similar approach has been utilized to generate 3D hydrogel scaffolds with heterogeneous properties.[52] In this report, porous scaffolds in honeycomb or woodpile geometries were fabricated with protein-modifiable sites to study cell adhesion.

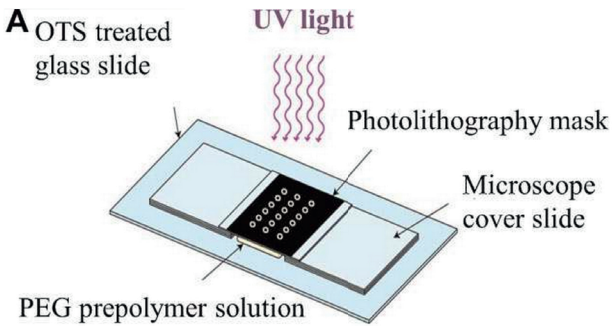

Figure 3. Photolithography utilizes photocurable hydrogel precursors with a photomask with desired shapes on it to generate microfabricated structures (78). Reproduced by permission of John Wiley and Sons

2.4. Other techniques

2.4.1. Emulsification

Emulsification is a technique used to produce micron size hydrogel particles.[16] In emulsification, two phase separating liquids[72] are mixed by agitation[66] to generate droplets which can subsequently be crosslinked (Figure 4).[86] For example, water-in-oil emulsion systems are often used to obtain emulsified phases.[67] Mineral oil, hexane and cyclohexane are commonly used as the hydrophobic phase to produce emulsions.[67, 72] In this process, shape and size of the hydrogel particles can be controlled by manipulating a number of factors, such as rotation speed, surface tension and viscosity[16] of the liquid phases. The droplets, which are formed as a result of mixing, can then be crosslinked using different stimuli, such as temperature, pH or UV exposure.[16] Although emulsification is a simple technique, size distribution of hydrogel particles vary more than that in the other microfabrication methods.[16, 66] Additionally, there is less control over the shapes of the gels produced by this technique.

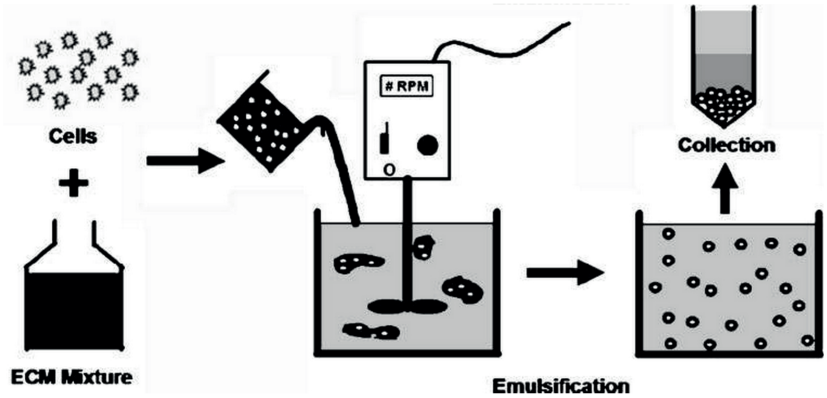

Figure 4. The process of emulsification yielding cell-loaded hydrogel particles (86). Reproduced by permission of John Wiley and Sons.

Common hydrogel precursors used to generate droplets by emulsification based techniques are agarose,[16] alginate,[16] collagen,[16] HA,[67, 87, 88] and gelatin.[67, 89] In addition to producing hydrogel beads, cells can easily be incorporated within hydrogels by means of emulsification.[16, 67, 90, 91] For instance, in one study, embryoid bodies have been encapsulated in alginate based hydrogels by emulsification, which promoted cardiomyogenic differentiation resulting in spontaneous beating areas in the hydrogel beads.[92] Another study has demonstrated successful encapsulation of human mesenchymal stem cells (hMSCs) in agarose-collagen based hydrogel beads by emulsification.[86]

2.4.2. Microfluidics

Microfluidics is another technology used for the fabrication of microscale hydrogels. The most common microfluidic strategies to make microgels are based on single phase flows or two-phase immiscible liquid mixtures.[16] In single phase systems, UV light is exposed to a particular area of the flowing prepolymer to form hydrogels. In multiphase systems, first the droplets are formed under continuous fluid flow and then these droplets are crosslinked using a variety of methods, such as UV or ionic stimuli.[67] Surface tension and viscosity[16] of the fluids and reaction time[67] are the main parameters to control the droplet fabrication process. Microfluidic channels are commonly produced from elastomeric PDMS molds. Flow rate of the fluids and dimensions of microfluidic channels also affect the final properties of the hydrogels.[16] This method enables precise production of size and shape-controlled hydrogel particles.[93] The major limitation of microfluidic systems is that they widely use photoliabile polymer precursors to form hydrogels.[94]

Recently, new technologies to produce hydrogel units based on microfluidic strategies have been reported. For example, stop-flow lithography is developed by combining microfluidics and photopatterning approaches.[16] This method can be used to create gels under continuous flow conditions via exposure to UV light.[95] Optofluidic maskless lithography (OFML) is another microfluidic approach, which enables *in situ* formation of hydrogels in microfluidic channels under continuous flow.[96] In this technique, projection of UV light on the flowing photocrosslinkable resin is controlled

by a computer. Hydrogel patterns are formed by selective crosslinking of photocurable resin induced by UV light exposure. In one study, OMFL has been utilized with the addition of a membrane to control the size of the hydrogels by manipulating the height of the channel (Figure 5).[97]

In addition to plain hydrogel units, cell-encapsulated hydrogels can be generated by microfluidic techniques.[81, 98, 99] For example, layer-by-layer fabrication of co-cultures within different polymers have been performed.[100] Similarly, another layer-by-layer study was carried out by encapsulating HeLa cells within PEGDA hydrogels using OMFL technique to demonstrate the feasibility of the approach to potentially study cellular interactions in co-cultures.[97]

Microfluidics is also used to generate concentration gradients of soluble or growth factors along the hydrogel channels. This has important implications for tissue engineering applications where production of a gradient is needed.[72, 101] For example, NIH-3T3 fibroblasts have been encapsulated in a gelatin-HA gradient within a microchannel demonstrating gradient dependent cell spreading.[102] This result is observed due to the adhesive and non-adhesive nature of gelatin and HA hydrogels, respectively. Similarly, elasticity gradients have been generated using microfluidic systems to control cellular behavior, such as adhesion and spreading, based on substrate stiffness.[103]

3. TISSUE ENGINEERING APPLICATIONS

Due to the complexity of interactions between cells, ECM and soluble factors of the cellular niche, it has been challenging to mimic the 3D organization of native microenvironments. To address these issues, different approaches were developed to fabricate biomimetic tissue constructs *in vitro*. There are two main strategies to utilize microfabrication techniques in tissue engineering: top-down and bottom-up approaches.

3.1. Top-down approach

Traditionally in tissue engineering cells are seeded onto a 3D scaffold and stimulated to deposit their own ECM structure while the scaffold degrades. Theoretically, the resulting structure would have the shape of the scaffold.[1] However, it has shown that this approach may not recreate all the complex tissue structure that exists in native tissues. The most successful applications of tissue engineering using this approach are relatively simple tissues such as cartilage and skin due to their relatively simple structures, low requirements for oxygen and nutrients and their ability to be supported by vascular structures in the host. Creating connective tissues such as the bladder and bone has also been successful over the past decades using this tissue engineering approach. In addition, several successful applications have been reported in heart valve and vascular tissue engineering.[7, 58, 104-107]

Top-down microfabrication strategies aim to control and modify the properties of relatively large hydrogel units in microscale. To achieve this goal, researchers have engineered controlled features within macroscale scaffolds. Principally, the goal of this approach is to engineer a tissue's

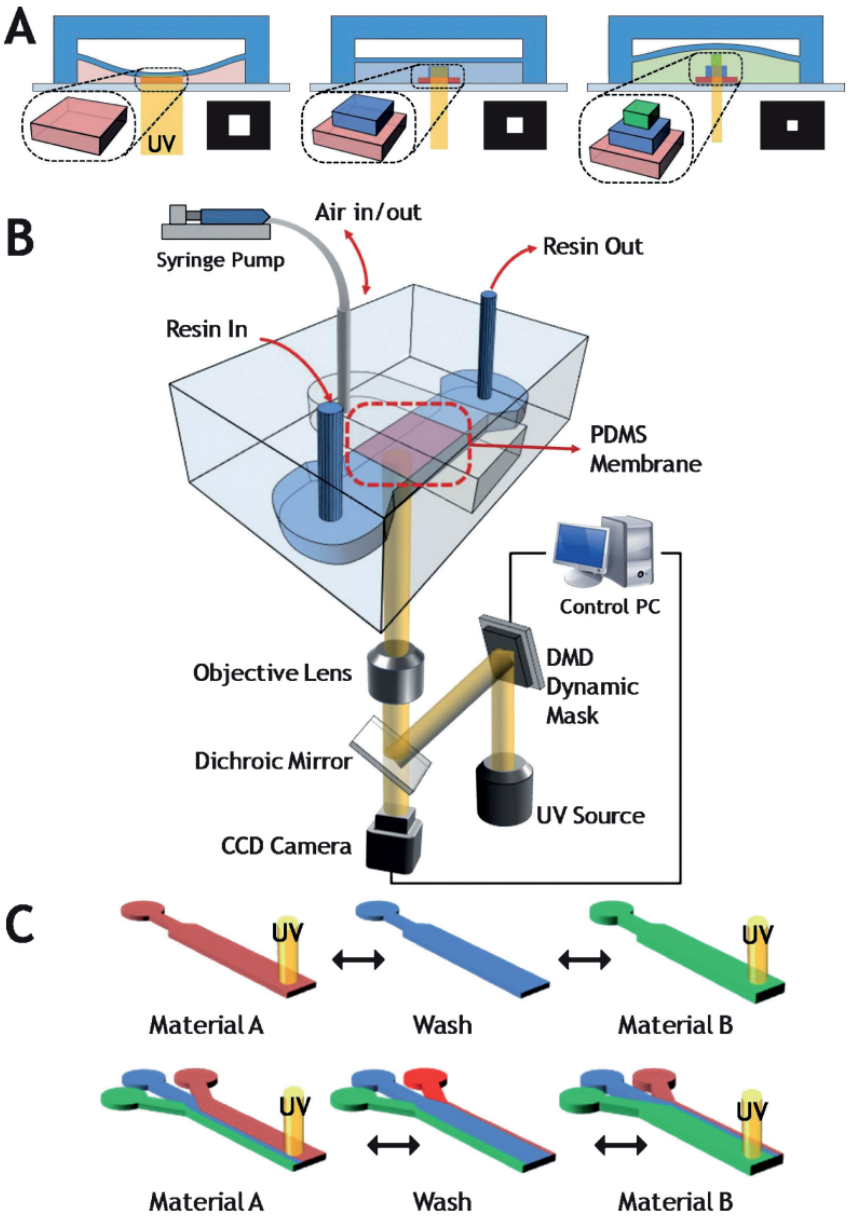

Figure 5. Fabrication of hydrogel units by a microfluidics method using the optofluidic maskless lithography (OFML). A two-layered OFML is performed to control the thickness of the hydrogel (97). Reproduced by permission of The Royal Society of Chemistry.

vasculature *in vitro*.[61, 108] For instance, microvasculature structures are engineered within tissue engineering scaffolds.[108] Similarly, microfluidic channels can be created to form vasculature geometries

by generating size and shape-controlled patterns.[109-111] Additionally, microtubular structures have been generated in collagen gels and endothelialization on the walls of the lumens was achieved.[112]

A different approach to engineer microvascular structures has been used to fabricate a HepG2-laden agarose hydrogel system containing micropores (Figure 6) that are created by dissolving sucrose crystals which causes leaching.[77] These porous structures can improve oxygen, protein transport and nutrient diffusion and thus provide for a synthetic environment able to mimic native tissue structures. In addition, this technique is able to control the microporosity of the scaffold. Similarly, AML-12 murine hepatocytes have been encapsulated within hydrogel channels fabricated from agarose.[110] Media is perfused through the channels to demonstrate the effect of oxygen and nutrient delivery on viability of cells. Creating microfluidic channels within macroscaffolds holds great potential in creating biomimetic synthetic vasculature.[110]

Another top-down strategy has been demonstrated by using microengineering to yield 3D scaffolds with appropriate tissue architecture. For instance, layers of hydrogels, with or without cells, are

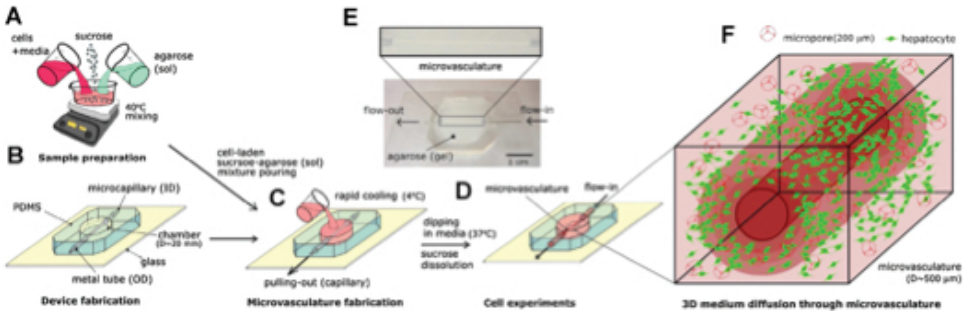

Figure 6. Production process to obtain microporous hydrogel construct with potential tissue engineering applications to mimic vasculatures. Cell-encapsulated hydrogel block was perfused with media to maintain high cell viability (77). Reproduced by permission of John Wiley and Sons.

fabricated by controlled porosity. Then the layers are combined to create 3D scaffolds, which result in specific architectures. By using a layer-by-layer microfluidic approach studies have immobilized cell-loaded hydrogel units to build multilayered constructs. By using three different types of cells with vascular origin, the constructs can mimic the arterial structure.[100]

Studies have also used photolithography to pattern bioactive features into photolabile materials using an adaptation of established photolithographic techniques.[84] For example, single-photon absorption photolithography has been used to generate biochemical and mechanical patterns in hydrogels in 3D, but this method results in limited pattern complexity. To overcome this limitation, studies have created complex 3D patterns and gradients in photoactive biomaterials by using two-photon absorption lithography.[84]

Top-down approaches in microengineering aims to control features of macroscale scaffolds. This has led to the fabrication of functional capillary networks on scaffold materials and also to controlling biochemical and mechanical features of existing scaffold materials. Although more research

is warranted before translation from bench to bed, these techniques are a vital addition for the engineering of vascularized tissue constructs.

3.2. Bottom-up approach

Bottom-up approaches are used to engineer tissues by assembling microscale building blocks made of only cells or cell-laden biomaterials.[113] This is an efficient strategy to create biomimetic structures, because some of the complex organs in the body, such as pancreas, kidney, muscles or liver, consist of repeating functional units. For example, hepatocytes have been encapsulated in hydrogels to mimic one lobule of liver.[114] Although bottom-up strategies provide unique opportunities to generate engineered constructs, it is challenging to assemble the individual building blocks with sufficient mechanical strength. For example, secondary crosslinking step to attach the individual building blocks should be optimized in such a way that it mechanically supports the entire tissue construct.[115] In addition, feasibility and reproducibility of the assembly processes require improvements to fabricate successfully functioning tissue constructs.[116]

Geometrical architecture of the tissues in the body consist of small vascularized repeating functional units.[115] Tightly assembled tissue-like building blocks provide precisely organized elements, which may resemble actual tissues. To accomplish this aim, lock and key approaches have been developed to create highly organized engineered constructs, which could potentially yield clinically relevant tissue units.[54] Hydrogels with controlled sizes and shapes created by microfabrication techniques can be assembled using such lock and key approaches. For instance, different geometries, such as solid ball, casquet or cylindrical tubes can be formed by directed aggregation of small hydrogel units.[117] Once micron size hydrogels have been fabricated by photolithography, a small amount of prepolymer is added to the gels and then they are transferred onto a PDMS mold with the desired final geometry. The excess prepolymer is removed, gels are allowed to assemble, and subsequently crosslinked to stabilize the shape. Then, PDMS mold is removed to obtain the final geometry of tightly packed building blocks. In this work, capillary forces are considered as the major driving force of the assembly process. In addition, hydrophilicity and the viscosity of prepolymer can be participating factors in the hydrogel packing. To demonstrate the applicability of this strategy in tissue engineering, cell-laden gels have been fabricated and allowed to assemble for the desired geometries. Hepatocytes have been encapsulated in 20% (w/v) PEG dimethacrylate (PEGDM) to form 500 um size cubic units and these gel units are assembled to form a cylindrical tube structure with a 5 mm inner diameter. Moreover, the lock and key approach has been utilized to assemble microgels with different shapes (e.g. rods and crosses) to obtain final geometries as blocks or tubes. This is a useful technique to fabricate cell encapsulated artificial tissue-like structures.

In another bottom-up approach, surface tension is used as a driving force to assemble individual cell-laden hyrogels.[118] Macroscale constructs are fabricated from cuboidic hydrogels with dimensions ranging from 100 to 200 um. Such scalable approaches promote incorporation of multiple types of cells in different types of hydrogels to study co-cultures. Secondary UV-crosslinking is used to stabilize the assembled hydrogel units. Similarly, directed assembly of PEGDM based hydrogel

units is achieved in a mineral oil/water system following a bottom-up strategy.[119] Once hydrogels are generated by UV light exposure, they are placed in a petri dish with mineral oil. By agitation, directed assembly of hydrogels is promoted and the gels are stabilized by a secondary UV light exposure. In this approach, hydrophilic/hydrophobic effects are considered to be dominant by minimizing the surface energy. This method enables fabrication of co-cultured hydrogels by encapsulation of different cell types. Another scalable example of a bottom-up strategy is used to form fibroblast-loaded hydrogels with a size range of 200-1,000 um with 150 um thickness.[120]

Bottom-up strategies have also been utilized to fabricate millimeter size 3D tissue-like structures.[121] For example, directed assembly of cell-laden photocured PEGDA hydrogels was performed. Hexagonal shaped micron size hydrogel patterns have been created using PDMS stencils (Figure 7). Then by addition of prepolymer, hydrogel units are packed followed by secondary crosslinking. In the last step, individual layers of hydrogels are stacked together by additional crosslinking via UV exposure yielding larger than 3 mm thick constructs.

Furthermore, alginate is used as sacrificial element to create pores throughout the engineered unit. In addition to assembling hydrogel units, bottom-up approaches can also be utilized to generate vascular tissue engineered constructs. Vascularized structures have been fabricated by packing collagen gels in a tube where blood or media is passed through the gel units.[33] For instance, HepG2 cells have been encapsulated in micron-size collagen rods and are seeded with human umbilical vein endothelial cells (HUVECs) to obtain endothelialized constructs taking advantage of their non-thrombogenic properties. Then endothelialized gels are packed in a tube and subsequently perfused with blood or media. The resulting tissue units demonstrate high viability offering opportunities towards creation of functional tissue units with potential use for *in vivo* studies.

In another attempt to create vasculature-like hydrogel structures, microgel units from 20% (w/v) PEGDA have been assembled to obtain cylindrical tubes with connected lumens.[78] These hydrogels are assembled sequentially to mimic vasculature geometries. First, NIH-3T3 cells are encapsulated to optimize the viability in the engineered units. Then, endothelial cells and smooth muscle cells are encapsulated in PEGDA hydrogels to fabricate a final geometry resembling a blood vessel. This strategy allows for fabrication of engineered structures with potential applications in vascular tissue engineering.

All in all, bottom-up tissue engineering strategies enable formation of multicellular tissue structures, which can improve the existing methods to generate medically relevant biomimetic constructs.

4. CONCLUSIONS

In this chapter, we described various microfabrication strategies to produce cell-laden microscale hydrogels and provide detailed examples related to their use in tissue engineering. We have re-

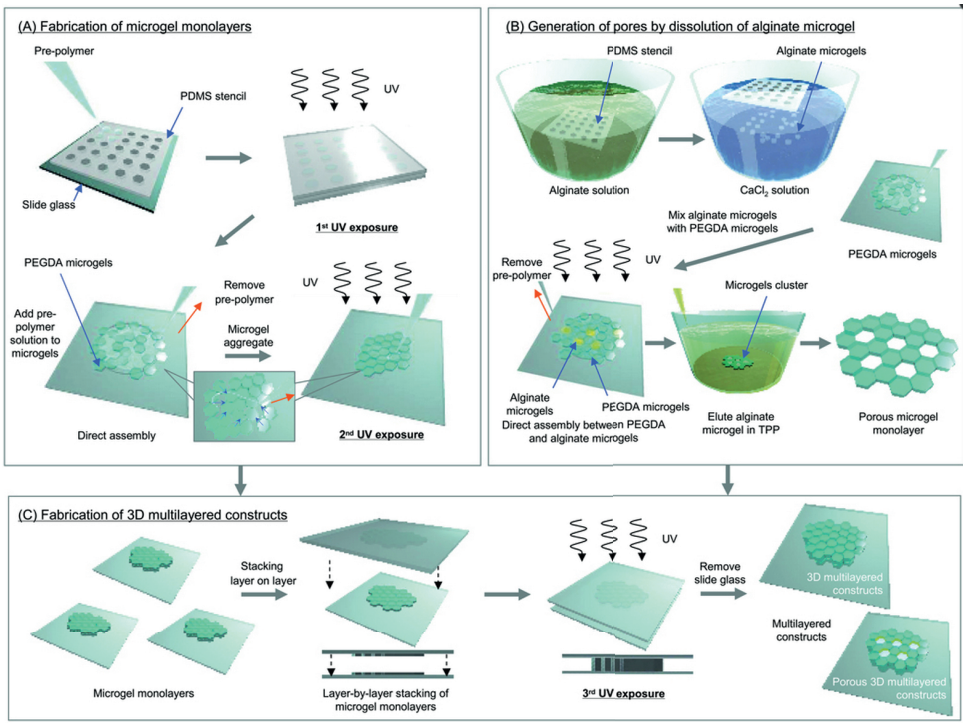

Figure 7. Fabrication and assembly of PEGDA based hydrogel units. Photolithography was used to generate individual hydrogel building blocks. Then the gels were exposed the UV second time to stabilize assembled groups. Alginate was used as an additional component to generate pores throughout the construct. 3D layered hydrogels were prepared by stacking the monolayers on top of each other and crosslinking further to stabilize the entire construct (121). Reproduced by permission of John Wiley and Sons.

viewed bottom-up and top-down tissue engineering strategies for their applications in controlling cellular microenvironments, such as differentiation, vascularization and cell guidance. Fabrication of complex engineered constructs is considered a challenge, however, this can be addressed by the use of flexible hydrogels with tunable features and patterns to direct cellular behavior. For this reason, new biomaterial design strategies are becoming popular for specific tissue engineering applications. Future success of engineering artificial organs is closely related to fabrication of biomimetic cell-loaded constructs. Adequately controlled cell-laden hydrogel systems are expected to lead significant developments for *in vitro* tissue models, which could potentially be transformed into applications related to *in vivo* systems.

ACKNOWLEDGEMENTS

This work was supported by the US Army Corps of Engineers, the Institute for Soldier Nanotechnologies, National Science Foundation (DMR0847287) and the National Institutes of Health (AR057837; HL092836; EB008392; HL099073; DE019024).

REFERENCES

1. Langer R, Vacanti JP. Tissue engineering. *Science*. 1993;260:920-926
2. Auger FA, Lacroix D, Germain L. Skin substitutes and wound healing. *Skin Pharmacology and Physiology*. 2009;22:94-102
3. Atala A, Bauer SB, Soker S, Yoo JJ, Retik AB. Tissue-engineered autologous bladders for patients needing cystoplasty. *Lancet*. 2006;367:1241-1246
4. Ashiku SK, Randolph MA, Vacanti CA. Tissue engineered cartilage. *Porous Materials for Tissue Engineering*. 1997;250:129-150
5. Petite H, Viateau V, Bensaid W, Meunier A, de Pollak C, Bourguignon M, Oudina K, Sedel L, Guillemin G. Tissue-engineered bone regeneration. *Nature Biotechnology*. 2000;18:959-963
6. Cebotari S, Lichtenberg A, Tudorache I, Hilfiker A, Mertsching H, Leyh R, Breymann T, Kallenbach K, Maniuc L, Batrinac A, Repin O, Maliga O, Ciubotaru A, Haverich A. Clinical application of tissue engineered human heart valves using autologous progenitor cells. *Circulation*. 2006;114:I132-I137
7. L'Heureux N, Dusserre N, Konig G, Victor B, Keire P, Wight TN, Chronos NAF, Kyles AE, Gregory CR, Hoyt G, Robbins RC, McAllister TN. Human tissue-engineered blood vessels for adult arterial revascularization. *Nature Medicine*. 2006;12:361-365
8. Liu B, Liu Y, Lewis AK, Shen W. Modularly assembled porous cell-laden hydrogels. *Biomaterials*. 2010;31:4918-4925
9. Muschler GE, Nakamoto C, Griffith LG. Engineering principles of clinical cell-based tissue engineering. *Journal of Bone and Joint Surgery-American Volume*. 2004;86A:1541-1558
10. Nichol JW, Bae H, Kachouie N, Zamanian B, Masaeli M, Khademhosseini A. Microscale technologies for tissue engineering and stem cell differentiation. In: Song Li NLHaJE, ed. *Stem cell and tissue engineering*. World scientific publishing company (WSPC); 2010.
11. Pescosolido L, Schuurman W, Malda J, Matricardi P, Alhaique F, Coviello T, van Weeren PR, Dhert WJA, Hennink WE, Vermonden T. Hyaluronic acid and dextran-based semi-ipn hydrogels as biomaterials for bioprinting. *Biomacromolecules*. 2011;12:1831-1838
12. Fedorovich NE, Alblas J, de Wijn JR, Hennink WE, Verbout AJ, Dhert WJ. Hydrogels as extracellular matrices for skeletal tissue engineering: State-of-the-art and novel application in organ printing. *Tissue Eng*. 2007;13:1905-1925
13. Landers R, Hubner U, Schmelzeisen R, Mulhaupt R. Rapid prototyping of scaffolds derived from thermoreversible hydrogels and tailored for applications in tissue engineering. *Biomaterials*. 2002;23:4437-4447
14. DeKosky BJ, Dormer NH, Ingavle GC, Roatch CH, Lomakin J, Detamore MS, Gehrke SH. Hierarchically designed agarose and poly(ethylene glycol) interpenetrating network hydrogels for cartilage tissue engineering. *Tissue Engineering: Part C*. 2010;16:1533-1542
15. Lutolf MP. Spotlight on hydrogels. *Nature Materials*. 2009;8:451-453
16. Khademhosseini A, Langer R. Microengineered hydrogels for tissue engineering. *Biomaterials*. 2007;28:5087-5092
17. Benoit DSW, Durney AR, Anseth KS. Manipulations in hydrogel degradation behavior enhance osteoblast function and mineralized tissue formation. *Tissue Engineering*. 2006;12:1663-1673
18. Kaji H, Camci-Unal G, Langer R, Khademhosseini A. Engineering systems for the generation of patterned co-cultures for controlling cell-cell interactions. *Biochim Biophys Acta*. 2011;1810:239-250
19. Fukuda J, Khademhosseini A, Yeo Y, Yang X, Yeh J, Eng G, Blumling J, Wang C-F, Kohane DS, Langer R. Micromolding of photocrosslinkable chitosan hydrogel for spheroid microarray and co-cultures. *Biomaterials*. 2006;27:5259-5267

20. Wheeldon I, Fernandez J, Bae H, Kaji H, Khademhosseini A. Microscale biomaterials for regenerative medicine and engineered cellular microenvironments. In: Mauck JBaR, ed. *Biomaterials for tissue engineering: A review of the past and future trends*. Springer -Verlag/Wien; 2011:119-138.
21. Camci-Unal G, Aubin H, Ahari AF, Bae H, Nichol JW, Khademhosseini A. Surface-modified hyaluronic acid hydrogels to capture endothelial progenitor cells. *Soft Matter*. 2010;6:5120-5126
22. Camci-Unal G, Nichol JW, Bae H, Tekin H, Bischoff J, Khademhosseini A. Hydrogel surfaces to promote attachment and spreading of endothelial progenitor cells. *Journal of Tissue Engineering and Regenerative Medicine*. 2011;accepted
23. Khademhosseini A, Eng G, Yeh J, Fukuda J, Blumling J, 3rd, Langer R, Burdick JA. Micromolding of photocrosslinkable hyaluronic acid for cell encapsulation and entrapment. *J Biomed Mater Res A*. 2006;79:522-532
24. Chung BG, Kang L, Khademhosseini A. Micro- and nanoscale technologies for tissue engineering and drug discovery applications. *Expert Opinion on Drug Discovery*. 2007;2:1653-1668
25. Karp JM, Yeh J, Eng G, Fukuda J, Blumling J, Suh KY, Cheng J, Mahdavi A, Borenstein J, Langer R, Khademhosseini A. Controlling size, shape and homogeneity of embryoid bodies using poly(ethylene glycol) microwells. *Lab Chip*. 2007;7:786-794
26. Moeller HC, Mian MK, Shrivastava S, Chung BG, Khademhosseini A. A microwell array system for stem cell culture. *Biomaterials*. 2008;29:752-763
27. Yamazoe H, Uemura T, Tanabe T. Facile cell patterning on an albumin-coated surface. *Langmuir*. 2008;24:8402-8404
28. WojciakStothard B, Curtis A, Monaghan W, Macdonald K, Wilkinson C. Guidance and activation of murine macrophages by nanometric scale topography. *Experimental Cell Research*. 1996;223:426-435
29. Meyle J, Gultig K, Wolburg H, Vonrecum AF. Fibroblast anchorage to microtextured surfaces. *Journal of Biomedical Materials Research*. 1993;27:1553-1557
30. Rajnicek AM, Britland S, McCaig CD. Contact guidance of cns neurites on grooved quartz: Influence of groove dimensions, neuronal age and cell type. *Journal of Cell Science*. 1997;110:2905-2913
31. Chen CS, Mrksich M, Huang S, Whitesides GM, Ingber DE. Geometric control of cell life and death. *Science*. 1997;276:1425-1428
32. Yeh J, Ling Y, Karp JM, Gantz J, Chandawarkar A, Eng G, Blumling J, 3rd, Langer R, Khademhosseini A. Micromolding of shape-controlled, harvestable cell-laden hydrogels. *Biomaterials*. 2006;27:5391-5398
33. McGuigan AP, Sefton MV. Vascularized organoid engineered by modular assembly enables blood perfusion. *Proceedings of the National Academy of Sciences of the United States of America*. 2006;103:11461-11466
34. Nguyen KT, West JL. Photopolymerizable hydrogels for tissue engineering applications. *Biomaterials*. 2002;23:4307-4314
35. Mironov V, Prestwich G, Forgacs G. Bioprinting living structures. *Journal of Materials Chemistry*. 2007;17:2054-2060
36. Fedorovich NE, Swennen I, Girones J, Moroni L, van Blitterswijk CA, Schacht E, Alblas J, Dhert WJA. Evaluation of photocrosslinked lutrol hydrogel for tissue printing applications. *Biomacromolecules*. 2009;10:1689-1696
37. Seitz H, Rieder W, Irsen S, Leukers B, Tille C. Three-dimensional printing of porous ceramic scaffolds for bone tissue engineering. *Journal of Biomedical Materials Research Part B-Applied Biomaterials*. 2005;74B:782-788
38. Wang XH, Yan YN, Pan YQ, Xiong Z, Liu HX, Cheng B, Liu F, Lin F, Wu RD, Zhang RJ, Lu QP. Generation of three-dimensional hepatocyte/gelatin structures with rapid prototyping system. *Tissue Engineering*. 2006;12:83-90
39. Ang TH, Sultana FSA, Hutmacher DW, Wong YS, Fuh JYH, Mo XM, Loh HT, Burdet E, Teoh SH. Fabrication of 3d chitosan-hydroxyapatite scaffolds using a robotic dispensing system. *Materials Science & Engineering C-Biomimetic and Supramolecular Systems*. 2002;20:35-42

40. Wilson WC, Jr., Boland T. Cell and organ printing 1: Protein and cell printers. *The anatomical record*. 2003;272:491-496
41. Odde DJ, Renn MJ. Laser-guided direct writing of living cells. *Biotechnology and Bioengineering*. 2000;67:312-318
42. Barron JA, Wu P, Ladouceur HD, Ringeisen BR. Biological laser printing: A novel technique for creating heterogeneous 3-dimensional cell patterns. *Biomedical Microdevices*. 2004;6:139-147
43. Ringeisen BR, Kim H, Barron JA, Krizman DB, Chrisey DB, Jackman S, Auyeung RYC, Spargo BJ. Laser printing of pluripotent embryonal carcinoma cells. *Tissue Engineering*. 2004;10:483-491
44. Cohen DL, Malone E, Lipson H, Bonassar LJ. Direct freeform fabrication of seeded hydrogels in arbitrary geometries. *Tissue Engineering*. 2006;12:1325-1335
45. Varghese D, Deshpande M, Xu T, Kesari P, Ohri S, Boland T. Advances in tissue engineering: Cell printing. *Journal of Thoracic and Cardiovascular Surgery*. 2005;129:470-472
46. Landers R, Pfister A, Hubner U, John H, Schmelzeisen R, Mulhaupt R. Fabrication of soft tissue engineering scaffolds by means of rapid prototyping techniques. *Journal of Materials Science*. 2002;37:3107-3116
47. Skardal A, Zhang JX, Prestwich GD. Bioprinting vessel-like constructs using hyaluronan hydrogels crosslinked with tetrahedral polyethylene glycol tetracrylates. *Biomaterials*. 2010;31:6173-6181
48. Lam CXF, Mo XM, Teoh SH, Hutmacher DW. Scaffold development using 3d printing with a starch-based polymer. *Materials Science & Engineering C-Biomimetic and Supramolecular Systems*. 2002;20:49-56
49. Nahmias Y, Schwartz RE, Verfaillie CM, Odde DJ. Laser-guided direct writing for three-dimensional tissue engineering. *Biotechnology and Bioengineering*. 2005;92:129-136
50. Boland T, Mironov V, Gutowska A, Roth EA, Markwald RR. Cell and organ printing 2: Fusion of cell aggregates in three-dimensional gels. *Anatomical Record Part A-Discoveries in Molecular Cellular and Evolutionary Biology*. 2003;272A:497-502
51. Smith CM, Stone AL, Parkhill RL, Stewart RL, Simpkins MW, Kachurin AM, Warren WL, Williams SK. Three-dimensional bioassembly tool for generating viable tissue-engineered constructs. *Tissue Engineering*. 2004;10:1566-1576
52. Han LH, Suri S, Schmidt CE, Chen SC. Fabrication of three-dimensional scaffolds for heterogeneous tissue engineering. *Biomedical Microdevices*. 2010;12:721-725
53. Chen CY, Barron JA, Ringeisen BR. Cell patterning without chemical surface modification: Cell-cell interactions between printed bovine aortic endothelial cells (baec) on a homogeneous cell-adherent hydrogel. *Applied Surface Science*. 2006;252:8641-8645
54. Guillotin B, Guillemot F. Cell patterning technologies for organotypic tissue fabrication. *Trends Biotechnol.* 2011;29:183-190
55. Ovsianikov A, Gruene M, Pflaum M, Koch L, Maiorana F, Wilhelmi M, Haverich A, Chichkov B. Laser printing of cells into 3d scaffolds. *Biofabrication*. 2010;2
56. Kikuchi A, Okano T. Nanostructured designs of biomedical materials: Applications of cell sheet engineering to functional regenerative tissues and organs. *Journal of Controlled Release*. 2005;101:69-84
57. Shimizu T, Sekine H, Isoi Y, Yamato M, Kikuchi A, Okano T. Long-term survival and growth of pulsatile myocardial tissue grafts engineered by the layering of cardiomyocyte sheets. *Tissue Engineering*. 2006;12:499-507
58. L'Heureux N, Paquet S, Labbe R, Germain L, Auger FA. A completely biological tissue-engineered human blood vessel. *Faseb Journal*. 1998;12:47-56
59. Mikos AG, Herring SW, Ochareon P, Elisseeff J, Lu HH, Kandel R, Schoen FJ, Toner M, Mooney D, Atala A, Van Dyke ME, Kaplan D, Vunjak-Novakovic G. Engineering complex tissues. *Tissue Engineering*. 2006;12:3307-3339
60. Lee KY, Mooney DJ. Hydrogels for tissue engineering. *Chemical Reviews*. 2001;101:1869-1879

61. Kaihara S, Borenstein J, Koka R, Lalan S, Ochoa ER, Ravens M, Pien H, Cunningham B, Vacanti JP. Silicon micromachining to tissue engineer branched vascular channels for liver fabrication. *Tissue Engineering*. 2000;6:105-117
62. Stevens MM, Mayer M, Anderson DG, Weibel DB, Whitesides GM, Langer R. Direct patterning of mammalian cells onto porous tissue engineering substrates using agarose stamps. *Biomaterials*. 2005;26:7636-7641
63. Tekin H, Ozaydin-Ince G, Tsinman T, Gleason KK, Langer R, Khademhosseini A, Demirel MC. Responsive microgrooves for the formation of harvestable tissue constructs. *Langmuir*. 2011;27:5671-5679
64. Bian WN, Bursac N. Engineered skeletal muscle tissue networks with controllable architecture. *Biomaterials*. 2009;30:1401-1412
65. Xia YN, Whitesides GM. Soft lithography. *Annual Review of Materials Science*. 1998;28:153-184
66. Slaughter BV, Khurshid SS, Fisher OZ, Khademhosseini A, Peppas NA. Hydrogels in regenerative medicine. *Advanced Materials*. 2009;21:3307-3329
67. Oh JK, Lee DI, Park JM. Biopolymer-based microgels/nanogels for drug delivery applications. *Progress in Polymer Science*. 2009;34:1261-1282
68. Folch A, Toner M. Microengineering of cellular interactions. *Annu rev biomed eng*. United States; 2000:227-256.
69. Suh KY, Choi SJ, Baek SJ, Kim TW, Langer R. Observation of high-aspect-ratio nanostructures using capillary lithography. *Advanced Materials*. 2005;17:560-+
70. Chandra D, Taylor JA, Yang S. Replica molding of high-aspect-ratio (sub-)micron hydrogel pillar arrays and their stability in air and solvents. *Soft Matter*. 2008;4:979-984
71. Johann RM, Baiotto C, Renaud P. Micropatterned surfaces of pdms as growth templates for hek 293 cells. *Biomedical Microdevices*. 2007;9:475-485
72. Rivest C, Morrison DWG, Ni B, Rubin J, Yadav V, Mahdavi A, Karp JM, Khademhosseini A. Microscale hydrogels for medicine and biology: Synthesis, characteristics and applications. *Journal of Mechanics of Materials and Structures*. 2007;2:1103-1119
73. Rolland JP, Maynor BW, Euliss LE, Exner AE, Denison GM, DeSimone JM. Direct fabrication and harvesting of monodisperse, shape-specific nanobiomaterials. *Journal of the American Chemical Society*. 2005;127:10096-10100
74. Khademhosseini A, Yeh J, Jon S, Eng G, Suh KY, Burdick JA, Langer R. Molded polyethylene glycol microstructures for capturing cells within microfluidic channels. *Lab Chip*. 2004;4:425-430
75. Tekin H, Tsinman T, Sanchez JG, Jones BJ, Camci-Unal G, Nichol JW, Langer R, Khademhosseini A. Responsive micromolds for sequential patterning of hydrogel microstructures. *JACS*. 2011;in press
76. Khademhosseini A, Ferreira L, Blumling Iii J, Yeh J, Karp JM, Fukuda J, Langer R. Co-culture of human embryonic stem cells with murine embryonic fibroblasts on microwell-patterned substrates. *Biomaterials*. 2006;27:5968-5977
77. Park JH, Chung BG, Lee WG, Kim J, Brigham MD, Shim J, Lee S, Hwang CM, Durmus NG, Demirci U, Khademhosseini A. Microporous cell-laden hydrogels for engineered tissue constructs. *Biotechnology and Bioengineering*. 2010;106:138-148
78. Du YA, Ghodousi M, Qi H, Haas N, Xiao WQ, Khademhosseini A. Sequential assembly of cell-laden hydrogel constructs to engineer vascular-like microchannels. *Biotechnology and Bioengineering*. 2011;108:1693-1703
79. Koh WG, Revzin A, Pishko MV. Poly(ethylene glycol) hydrogel microstructures encapsulating living cells. *Langmuir*. 2002;18:2459-2462
80. Liu VA, Bhatia SN. Three-dimensional photopatterning of hydrogels containing living cells. *Biomedical Microdevices*. 2002;4:257-266
81. Koh WG, Itle LJ, Pishko MV. Molding of hydrogel multiphenotype cell microstructures to create microarrays. *Analytical Chemistry*. 2003;75:5783-5789

82. Aubin H, Nichol JW, Hutson CB, Bae H, Sieminski AL, Cropek DM, Akhyari P, Khademhosseini A. Directed 3d cell alignment and elongation in microengineered hydrogels. *Biomaterials*. 2010;31:6941-6951
83. Mapili G, Lu Y, Chen SC, Roy K. Laser-layered microfabrication of spatially patterned functionalized tissue-engineering scaffolds. *Journal of Biomedical Materials Research Part B-Applied Biomaterials*. 2005;75B:414-424
84. Hahn MS, Miller JS, West JL. Three-dimensional biochemical and biomechanical patterning of hydrogels for guiding cell behavior. *Advanced Materials*. 2006;18:2679-+
85. Fozdar DY, Soman P, Lee JW, Han LH, Chen SC. Three-dimensional polymer constructs exhibiting a tunable negative poisson's ratio. *Advanced Functional Materials*. 2011;21:2712-2720
86. Batorsky A, Liao JH, Lund AW, Plopper GE, Stegemann JP. Encapsulation of adult human mesenchymal stem cells within collagen-agarose microenvironments. *Biotechnology and Bioengineering*. 2005;92:492-500
87. Jia XQ, Yeo Y, Clifton RJ, Jiao T, Kohane DS, Kobler JB, Zeitels SM, Langer R. Hyaluronic acid-based microgels and microgel networks for vocal fold regeneration. *Biomacromolecules*. 2006;7:3336-3344
88. Laroui H, Grossin L, Leonard M, Stoltz JF, Gillet P, Netter P, Dellacherie E. Hyaluronate-covered nanoparticles for the therapeutic targeting of cartilage. *Biomacromolecules*. 2007;8:3879-3885
89. Ethirajan A, Ziener U, Chuvilin A, Kaiser U, Colfen H, Landfester K. Biomimetic hydroxyapatite crystallization in gelatin nanoparticles synthesized using a miniemulsion process. *Advanced Functional Materials*. 2008;18:2221-2227
90. Dang SM, Kyba M, Perlingeiro R, Daley GQ, Zandstra PW. Efficiency of embryoid body formation and hematopoietic development from embryonic stem cells in different culture systems. *Biotechnology and Bioengineering*. 2002;78:442-453
91. Dang S, Zandstra P. Scalable production of embryonic stem cell-derived cells. *Methods in Molecular Biology*. 2005;290:353–364
92. Magyar JP, Nemir M, Ehler E, Suter N, Perriard JC, Eppenberger HM. Mass production of embryoid bodies in microbeads. In: Hunkeler D, Cherrington A, Prokop A, Rajotte R, eds. *Bioartificial organs iii: Tissue sourcing, immunoisolation, and clinical trials*. 2001:135-143.
93. Xu S, Nie Z, Seo M, Lewis P, Kumacheva E, Stone HA, Garstecki P, Weibel DB, Gitlin I, Whitesides GM. Generation of monodisperse particles by using microfluidics: Control over size, shape, and composition (vol 44, pg 724, 2005). *Angewandte Chemie-International Edition*. 2005;44:3799-3799
94. Franzesi GT, Ni B, Ling YB, Khademhosseini A. A controlled-release strategy for the generation of cross-linked hydrogel microstructures. *Journal of the American Chemical Society*. 2006;128:15064-15065
95. Dendukuri D, Pregibon DC, Collins J, Hatton TA, Doyle PS. Continuous-flow lithography for high-throughput microparticle synthesis. *Nature Materials*. 2006;5:365-369
96. Chung SE, Park W, Park H, Yu K, Park N, Kwon S. Optofluidic maskless lithography system for real-time synthesis of photopolymerized microstructures in microfluidic channels. *Applied Physics Letters*. 2007;91
97. Lee SA, Chung SE, Park W, Lee SH, Kwon S. Three-dimensional fabrication of heterogeneous microstructures using soft membrane deformation and optofluidic maskless lithography. *Lab on a Chip*. 2009;9:1670-1675
98. Panda P, Ali S, Lo E, Chung BG, Hatton TA, Khademhosseini A, Doyle PS. Stop-flow lithography to generate cell-laden microgel particles. *Lab Chip*. 2008;8:1056-1061
99. Braschler T, Johann R, Heule M, Metref L, Renaud P. Gentle cell trapping and release on a microfluidic chip by in situ alginate hydrogel formation. *Lab on a Chip*. 2005;5:553-559
100. Tan W, Desai TA. Layer-by-layer microfluidics for biomimetic three-dimensional structures. *Biomaterials*. 2004;25:1355-1364
101. Burdick JA, Khademhosseini A, Langer R. Fabrication of gradient hydrogels using a microfluidics/photopolymerization process. *Langmuir*. 2004;20:5153-5156

102. Hancock MJ, Piraino F, Camci-Unal G, Rasponi M, Khademhosseini A. Anisotropic material synthesis by capillary flow in fluid stripes. *Biomaterials*. 2011;32:6493-6504
103. Zaari N, Rajagopalan P, Kim SK, Engler AJ, Wong JY. Photopolymerization in microfluidic gradient generators: Microscale control of substrate compliance to manipulate cell response. *Advanced Materials*. 2004;16:2133-2137
104. Hoerstrup SP, Zund G, Sodian R, Schnell AM, Grunenfelder J, Turina MI. Tissue engineering of small caliber vascular grafts. *European Journal of Cardio-Thoracic Surgery*. 2001;20:164-169
105. Shin'oka T, Matsumura G, Hibino N, Naito Y, Watanabe M, Konuma T, Sakamoto T, Nagatsu M, Kurosawa H. Midterm clinical result of tissue-engineered vascular autografts seeded with autologous bone marrow cells. *Journal of Thoracic and Cardiovascular Surgery*. 2005;129:1330-1338
106. Hjortnaes J, Gottlieb D, Figueiredo JL, Melero-Martin J, Kohler RH, Bischoff J, Weissleder R, Mayer JE, Aikawa E. Intravital molecular imaging of small-diameter tissue-engineered vascular grafts in mice: A feasibility study. *Tissue Engineering Part C-Methods*. 2010;16:597-607
107. L'Heureux N, Germain L, Labbe R, Auger FA. In vitro construction of a human blood-vessel from cultured vascular cells - a morphologic study. *Journal of Vascular Surgery*. 1993;17:499-509
108. Borenstein JT, Terai H, King KR, Weinberg EJ, Kaazempur-Mofrad MR, Vacanti JP. Microfabrication technology for vascularized tissue engineering. *Biomedical Microdevices*. 2002;4:167-175
109. Fidkowski C, Kaazempur-Mofrad MR, Borenstein J, Vacanti JP, Langer R, Wang Y. Endothelialized microvasculature based on a biodegradable elastomer. *Tissue Eng*. 2005;11:302-309
110. Ling Y, Rubin J, Deng Y, Huang C, Demirci U, Karp JM, Khademhosseini A. A cell-laden microfluidic hydrogel. *Lab Chip*. 2007;7:756-762
111. Golden AP, Tien J. Fabrication of microfluidic hydrogels using molded gelatin as a sacrificial element. *Lab on a Chip*. 2007;7:720-725
112. Chrobak KM, Potter DR, Tien J. Formation of perfused, functional microvascular tubes in vitro. *Microvascular Research*. 2006;71:185-196
113. Nichol JW, Khademhosseini A. Modular tissue engineering: Engineering biological tissues from the bottom up. *Soft Matter*. 2009;5:1312-1319
114. Tsang VL, Chen AA, Cho LM, Jadin KD, Sah RL, DeLong S, West JL, Bhatia SN. Fabrication of 3d hepatic tissues by additive photopatterning of cellular hydrogels. *Faseb Journal*. 2007;21:790-801
115. Wheeldon I, Ahari AF, Khademhosseini A. Microengineering hydrogels for stem cell bioengineering and tissue regeneration. *JALA Charlottesv Va*. 2010;15:440-448
116. Peppas NA, Hilt JZ, Khademhosseini A, Langer R. Hydrogels in biology and medicine: From molecular principles to bionanotechnology. *Advanced Materials*. 2006;18:1345-1360
117. Fernandez JG, Khademhosseini A. Micro-masonry: Construction of 3d structures by microscale self-assembly. *Advanced Materials*. 2010;in press
118. Du Y, Ghodousi M, Lo E, Vidula MK, Emiroglu O, Khademhosseini A. Surface-directed assembly of cell-laden microgels. *Biotechnol Bioeng*. 2010;105:655-662
119. Du Y, Lo E, Vidula MK, Khabiry M, Khademhosseini A. Method of bottom-up directed assembly of cell-laden microgels. *Cellular and Molecular Bioengineering*. 2008;1:157-162
120. Du Y, Lo E, Ali S, Khademhosseini A. Directed assembly of cell-laden microgels for fabrication of 3d tissue constructs. *Proceedings of the National Academy of Sciences*. 2008;105:9522-9527
121. Yanagawa F, Kaji H, Jang YH, Bae H, Du YA, Fukuda J, Qi H, Khademhosseini A. Directed assembly of cell-laden microgels for building porous three-dimensional tissue constructs. *J. Biomed. Mater. Res. Part A*. 2011;97A:93-102

6

Application of Hydrogels in Heart Valve Tissue Engineering

J. Hjortnaes[1,2] & F. J. Schoen[3]

Gels Handbook - Fundamentals, Properties and Applications (Vol 2)

World Scientific Publishing Company, 2015.

[1]Department of Cardiothoracic Surgery, Division of Heart and Lungs, University Medical Center Utrecht, Utrecht, The Netherlands [2] Center of Excellence in Vascular Biology, Department of Medicine, Brigham and Women's Hospital, Harvard Medical School, Boston, USA [3] Department of Pathology, Brigham and Women's Hospital, Harvard Medical School, Boston, USA

INTRODUCTION

Heart valve disease is a leading cause of mortality and morbidity in the Western world.[1] Nearly 300,000 valve repair and replacement surgeries are performed each year worldwide, and this number is expected to increase sharply as life expectancy rises, and the aging population increases over the next 30 years.[2] Commercially available mechanical and bioprosthetic heart valves, and cryopreserved homograft valves are the standard of practice in surgical valve replacement.[3] However, contemporary valve substitutes are associated with significant shortcomings.

Firstly, mechanical valves generally have excellent durability, but are thrombogenic, which necessitates life-long anti coagulation therapy.[4] Conversely, bioprosthetic valves do not generally require anti-coagulation treatment. However, these valves have limited durability (on average approximately 15 years) due to valve leaflet mineralization and structural deterioration over time.,[5] necessitating reoperation. In addition, both mechanical and bioprosthetic valves are obstructive relative to native valves and both types are susceptible to infection, which often requires another replacement surgery as this complication may be difficult to treat medically. Cryopreserved homografts, which are valves derived from human cadavers and non-viable when implanted, share similar durability limitations with bioprosthetic valves, in addition to being of very limited supply.[6] Finally, all existing valve substitutes are particularly unsuitable for congenital valve disease. Not only are very small valve sizes required, and bioprosthetic valves subject to accelerated calcification in the young but also because growth and enlargement of a valve replacement, essential to eliminate the need for reoperations in the rapidly growing pediatric patient, cannot occur with conventional valve replacement.[7]

The development of tissue engineered heart valves (TEHV) aims to overcome these limitations by permitting living heart valve substitutes that are (1) non-obstructive, (2) non-thrombogenic, (3) provide for ongoing remodel to maintain tissue homeostasis, (4) repair any injury occurring during function, and importantly (5) grow with the patient.[8, 9]

Various approaches have been utilized in the pursuit of developing a TEHV. A widely studied paradigm is to pre-seed autologous cells on synthetic biodegradable polymer scaffolds, which are fabricated in the shape of a trileaflet valve. These are then conditioned in an *in vitro* bioreactor, which simulates the physiological mechanical and hemodynamic environment of a native heart valve.[7, 10] This approach stimulates tissue growth *in vitro* prior to surgical implantation, followed by remodeling *in vivo* after implantation. TEHVs grown from autologous cells seeded on biodegradable synthetic polymers have typically been implanted in the pulmonary circulation of growing lambs and evaluated in experimental models for up to five months. In some cases, the constructs seem to have evolved into functionally appropriate structures that mimic the complex architecture of native semilunar vales.[11-14] However, long-term evaluation of this approach is needed.

Other approaches to engineer TEHV are also being investigated; these approaches include *'in situ* tissue regeneration' (13), in which an implanted scaffold of degradable biomaterial or a decellularized nonaldehyde-fixed or otherwise chemically preserved valve is either seeded with cells in-

vitro, or is functionalized, in an effort to attract endogenous circulating precursor cells as the source of cells. Decellularized tissue scaffolds derived from porcine valves have been successfully used in clinical studies in the pulmonary position[15] but have suffered mechanical failure in the systemic circulation.[16] Decellularized valves pre-seeded with autologous vascular endothelial cells prior to orthotopic implantation and implanted onto the aortic valve position in a growing lamb model demonstrated favorable functionality compared to cryopreserved allografts for up to 9 months. However, in some cases predisposition to mineralization of the tissue engineered constructs were observed in these animal models.[17] Moreover, and importantly these studies have not shown that preseeding is either necessary or advantageous to function or that appropriate cellular repopulation occurs in vivo. Thus, despite the exciting possibility of TEHV, many significant challenges remain before this form of therapy can be validated, and shown to be sufficiently safe and effective to warrant successful translation to clinical use.[18]

The scaffold material is a paramount consideration in fabricating a valve substitute by tissue engineering approaches. Moreover, an emerging area of biomaterials research is focused on fusing techniques of engineering with developmental heart valve biology. Specifically, there has been increased focus on finding materials that simulate the natural physiological environment that lead to fetal heart valve development.[19] This could lead to better understanding and harnessing of the environmental signals that control heart valve development and regeneration. Indeed, focusing on re-creating the natural valve micro-environment has helped to understand and potentially facilitate valve tissue remodeling, and hydrogel micro-engineering holds promise as a new approach to engineer heart valve substitutes.

Hydrogels are colloidal polymers composed of particles and water. In the present context hydrogels are defined as 'three-dimensional (3D) *in vitro* culture platforms that enable cell growth in or on user-defined microenvironments that mimic critical aspects of native tissue'.[20] Chemical and mechanical properties of hydrogels can be tuned by engineering methodology. This allows for a predictable functionality, which directly influences cell fate. Theoretically, by mimicking the native cellular microenvironment or niche within the native, developing and mature, healthy heart valve, tissue heart valve regeneration can be understood and mimicked, and thus provide a potential means to engineer a heart valve substitute.

This chapter summarizes the application of hydrogels in heart valve tissue engineering and discusses how the imaginative use of hydrogels can further the development of a successful tissue engineered therapeutic option.

HEART VALVE STRUCTURE, FUNCTION AND DEVELOPMENT: RELEVANCE TO ENGINEERING

Aortic Valve Structure and Function

We provide a brief overview of valve function and structure as a scientific context for TEHV. Normal heart valves ensure unidirectional blood flow through the heart. The semilunar valves – the pulmonary valve and the aortic valve – prevent backflow into the ventricles during diastole (when they are closed), whereas the atrioventricular valves – the mitral valve and the tricuspid valve – prevent reverse flow from the ventricles into the atria during systole (when these valves are closed and the semilunar valves are open). Human heart valves open and close approximately 40 million times annually and thus 3 billion times over a lifetime. The cyclical opening and closing of the valves with each cardiac cycle is facilitated by a synergistic process of mechanical forces exerted by the surrounding blood and heart onto the mobile part of the valves, termed their cusps (semilunar valves) or leaflets (for atrioventricular valves).[7] The ability of valves to maintain structural and mechanical integrity is largely attributed to the unique and complex organization of valve in which both the extracellular matrix (ECM), and cells are highly specialized. (Figure 1)

Heart valve leaflets demonstrate a similar layered ECM architecture: (i) near the outflow side of the valve, there is a layer with densily packed collagen, giving the leaflets their strength, called the *fibrosa*; (ii) a middle layer of loose connective tissue enriched in glycosaminoglycans (GAG), named the *spongiosa*; and (iii) a layer below the inflow surface of the leaflet rich in elastin, known as the *ventricularis*.[21] This unique organization of ECM proteins contributes to the structural and functional integrity of the heart valve. Collagen is the major stress-bearing component of the heart valve ECM. It maintains apposition of the cusps during the cardiac cycle in addition to transferring mechanical load from the cusps to the aortic wall when the valve is closed and needs to withstand the pressure of backflow. Since collagen fibrils cannot be stretched, the changes of cusp shape and size during the cardiac cycle is attributed to rearrangements in collagen structure such as crimping in systole and straightening of the crimp in diastole (similar to an accordion).[22] These rearrangements of collagen during opening and closing are facilitated by the pull of the elastin in the *ventricularis* that was stretched during valve closure. Finally, GAGs in the *spongiosa* function as a shock absorber to the mechanical forces and a lubricant for internal tissue reaugmentation that occurs during the cardiac cycle.[21]

Valvular Cell Population

The surfaces of the valve are covered with an endothelial monolayer comprised of valvular endothelial cells (VECs) and the entire internal valve cross section is composed of valvular interstitial cells (VICs) embedded in ECM. VECs contribute to the nonthrombogenic properties of the valve. Moreover, VECs have shown to be able to undergo endothelial to mesenchymal transformation (EMT) in response to pathological levels of mechanical strain, increased TGF-β signaling, or Notch-1 activation,[23] which in turn may play a role in valve morphogenesis and development,, adaptive

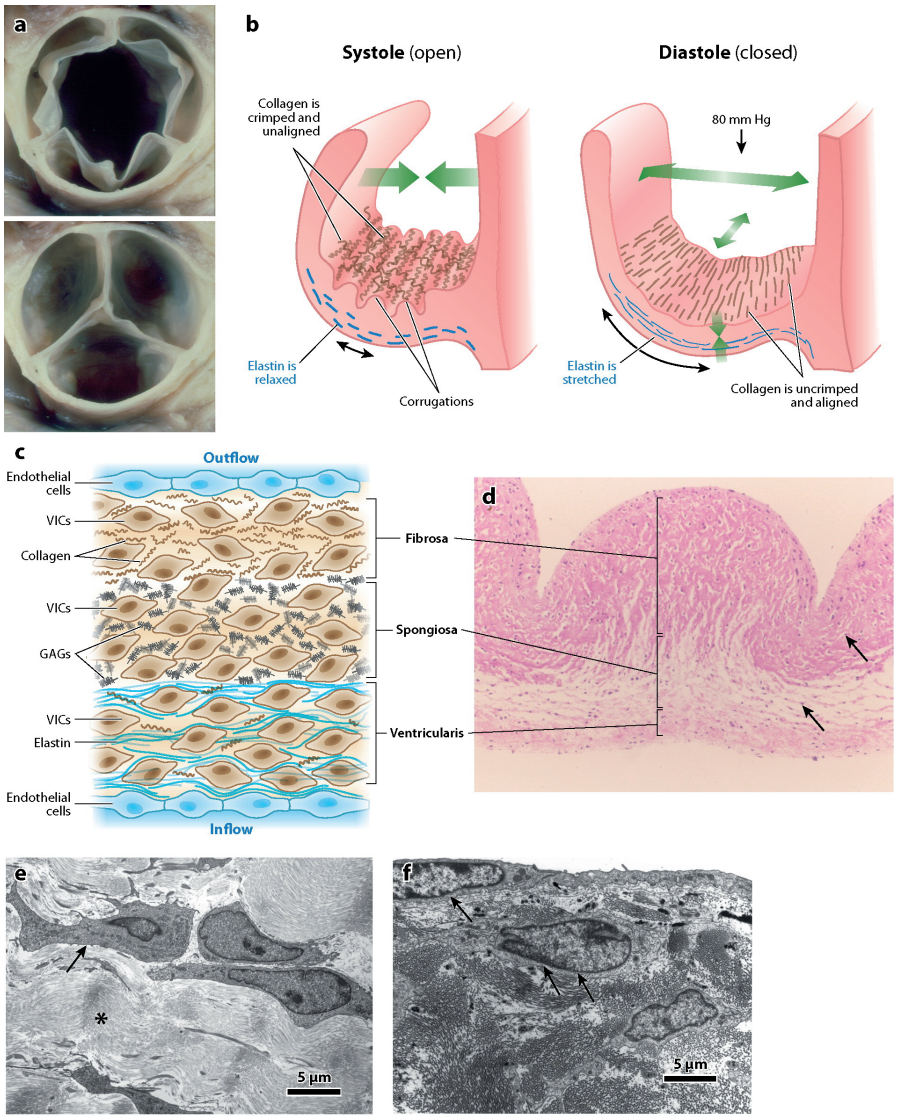

Figure 1. Aortic valve functional structure at macroscopic and microscopic levels. (A) Outflow aspect of aortic valve in open (top) and closed (bottom) configurations, corresponding to systole and diastole, respectively. **(B)** Schematic representation of architecture and configuration of aortic valve cusp in cross section and of collagen and elastin in systole and diastole. Modified from Ref. 11. **(C)** Schematic diagram of the detailed cellular and extracellular matrix architecture of a normal aortic valve. Modified with permission from Ref. 12. **(D)** Tissue architecture, shown as low magnification photomicrograph of cross-section cuspal configuration in the non-distended state (corresponding to systole), emphasizing three major layers: ventricularis, spongiosa, and fibrosa. Valvular interstitial cells (VICs) are denoted by arrows. The outflow surface is at the top. Original magnification: 100×. Hematoxylin and eosin stain. **(E)** Transmission electron photomicrograph of relaxed fresh porcine aortic valve (characteristic of the systolic configuration), demonstrating the fibroblast morphology of VICs (arrow); the dense, surrounding closely apposed collagen (asterisk) with wavy crimp; and the potential for VIC-collagen and VIC-VIC interactions. Reproduced with permission from Ref. 2. **(F)** Transmission electron photomicrograph of surface of aortic valve demonstrating valvular endothelial cell (VEC; arrow) and proximity of deeper VICs (double arrows) and potential for VEC–VIC interactions. Reproduced with permission from Ref. 14. Abbreviation: GAG, glycosoaminoglycan. Source: Reproduced with permission from Annu. Rev. Pathol. Mech. Dis., 7, 161–183.

remodeling, and sometimes pathology.[24] VICs are crucial to maintaining valvular function. VICs continuously repair and remodel the valvular ECM, by synthesizing ECM proteins, expressing matrix degrading enzymes (e.g. matrix metalloproteinases (MMPs) and tissue inhibitors of metalloproteinases (TIMPs)).[25, 26]

VICs are a very heterogeneous cell population characterized by five specifically identifiable phenotypes: embryonic progenitor endothelial VICs, adult progenitor VICs, quiescent VICs, activated VICs and osteoblastic VICs.[27] Valvular homeostasis and the ability to repair/remodel as a consequence of injury is considered to be mediated primarily by active VIC phenotype transition primarily driven by environmental cues.[28] It is believed that the transition of quiescent fibroblast-like cells to activated myofibroblast-like cells is key to maintaining valvular homeostasis. For example, VICs are activated during embryonic development and valvular maturation.[26] In addition, mechanical stress changes or transforming growth factor (TGF)-β increase VIC activation and ECM protein synthesis by isolated VICs in vitro.[29-32] VIC activation, marked by expression of alpha smooth muscle actin (α-SMA), increases stress fiber formation causing enhanced contractility of cells onto the surrounding ECM. In turn this may promote physiological and pathological remodeling of the valve.[28] In addition, although VECs may interact with VICs to contribute to valvular tissue integrity, the exact mechanisms of the functional interactions between VECs and VICs are uncertain.

Consistent with the rapidly evolving view that mechanical environment is a major determinant of stem and cell differentiated cell phenotype, the interplay between VIC phenotypical transitions and the surrounding ECM, vital to the understand of valvular physiology and even pathology, is under active investigation. More specifically, in the pursuit of engineering a valve substitute that is able to grow, remodel and repair, an understanding of both the effects of VICs on their environment in addition to the VIC response to their environment, is crucial.

Cardiac Valve Development

Since creating a tissue engineered heart valve may in large measure recapitulate normal cardiac morphogenesis, mechanisms of embryonic and foetal heart valve development are important to consider. Valves develop within the atrioventricular canal and ventricular outflow tracts, and mature in the fetus.[33, 34] During normal development of the heart, the heart tube consists of endocardium and myocardium separated by a primitive acellular amorphous extracellular matrix called the cardiac jelly. After the completion of heart looping, the valve cusps/leaflets originate from endocardial cushions, the precursors of valves and the cardiac septums.[35] A subset of endothelial cells of the endocardial cushion, driven by signals from the underlying myocardium, transform to mesenchymal cells and migrate into the cardiac jelly to form VICs (through EndMT as described above).

Experimental studies have suggested that VICs in adult valves may be also replenished via circulating endothelial or mesenchymal cell precursors derived from the bone marrow[36] and subsequently undergo EMT.[37] Even though the role of specific ECM components in remodeling of the endocardial cushions into heart valves is poorly understood, it is clear that the temporal and spatial patterns of collagen expression are vital to function.[38] In addition, the glycosaminoglycan

hyaluronic acid (HA) is well documented to have important function in EMT and subsequent valve development.[39]

BIOMATERIALS IN HEART VALVE TISSUE ENGINEERING

Investigators in the field of heart valve tissue engineering have focused on either 1) shaping a valve and leaflet geometries out of synthetic polymer scaffolds and seeding these with cells prior to implantation into animal models, 2) using decellularized natural valve materials or 3) using fabricated extracellular matrix with or without embedded cells. The biggest challenge to overcome before TEHV can successfully be translated to patients is to exactly formulate which are the optimal components and conditions (e.g. scaffold material, cell source, in-vitro manipulation, animal models) for tissue engineering to yield progress toward an adequate valve substitute in a bioreactor. Other key challenges have been discussed.[18]

As a cornerstone in tissue engineering over the last three decades, biomaterials science has focused on how to create scaffolds to promote natural tissue regeneration.[40] A wide range of synthetic polymers have been developed and used in heart valve tissue engineering. Widely used polymers include poly(lactic acid) (PLA), poly(glycoclic acid) (PGA) and poly (lactic-co-glycolic acid) (PLGA), which are clinically used as biodegradable sutures.[41-43] Because they were already FDA approved and accepted as biocompatible and biodegradable polymers over a reasonable interval, initial heart valve tissue engineering research focused on these materials. However, the early studies into using PLA:PGA scaffolds revealed inadequate mechanical properties suitable for TEHV, which lead to the addition of other polymers to the PGA based scaffolds. The most common modification used was the addition of poly-4-hydroxybutyrate (P4HB), a bioresorbable thermoplastic that can be molded into the complex shape of a heart valve and sealed without the use of sutures.[44] One study seeded these scaffolds with amniotic fluid-derived stem cells and conditioned them in an in vitro pulsatile system,[45] resulting in endothelialization, cell proliferation and ECM synthesis. Upon evaluation in a lamb model, PGA:P4HB scaffolds seeded with ovine VICs and VECs, yielded ECM protein synthesis and mechanical properties similar to the native valve after 20 weeks of implantation.[41]

Despite what seems like initial short-term success, long-term function remains to be evaluated and reliably reproduced. Using these synthetic polymers for TEHV has yet to produce a viable tissue engineered valve substitute that is close to human trials. In addition, these materials possess certain limitations. While these materials exhibit good mechanical properties, they usually possess high initial stiffness compared with native tissues. In addition, they require considerable time for the polymer to undergo degradation by hydrolysis and resorption.[46] Moreover, these materials do not possess any functional biological moieties that could direct cell signaling, ECM production or enzymatic material degradation. Some of these materials can be functionalized with such tissue guiding motifs; however, there has been no control over functional molecule localization.[47, 48] Moreover, this approach does not uniformly lead to a physiologically relevant environment that

can be invaded and remodeled by cells. To this end, alternative approaches are being pursued to controllably provide requisite environmental cues to promote and control cell growth and provide functional ECM.

HYDROGELS: TUNABLE, CONTROLLABLE, BIO-MIMETIC SCAFFOLDS

Hydrogels

Cells often behave very differently when they are isolated from the complex architecture of their native tissues and cultured in Petri dishes. In particular, VICs in two-dimensional culture will undergo spontaneous myofibroblast-like differentiation (aVICs), whereas in situ they are mostly quiescent fibroblast like cells (qVICs).[27] This difference in cell behavior has constituted a major obstacle for tissue engineers. However, in the past 15 years the field has made progress in creating successful 3D cellular microenvironments with hydrogels that possess elasticity similar to that of natural tissues.[49] The structure and composition of these hydrogels can be tailored to deliver the appropriate chemical, biological, and physical cues that encourage the development of tissue-like structures *in vitro*. Hydrogels can be fabricated from synthetic and from natural biomaterials. Both have been applied in the field of heart valve tissue engineering.

Synthethic hydrogel: poly(ethylene glycol)

One of the most common polymers used in hydrogels for heart valve tissue engineering is poly(ethylene glycol) (PEG).[50-52] PEG hydrogels are intrinsically biocompatible due to biologically neutral base gels, resistance to protein adsorption, no release of acidic products during degradation, and allow for polymer crosslinking with low toxicity. In turn, this allows for high-density cellular encapsulation. PEG hydrogels can be chemically tuned by crosslinking bioactive moieties such as peptides, glycosaminoglycans or growth factors. More specifically, peptides attached to the surface or bulk of PEG will retain their bioactivity.[53] Mechanical properties can also be altered by changing the amount of polymer crosslinking, or copolymerization. As such, the properties of PEG hydrogels can be modified to mimic tissue function or even a specific pericellular environment. Changing the molecular weight or the weight fraction in solution of the macromere or altering crosslinking time can control physical properties of PEG hydrogels.[54, 55] Hence, dynamically tunable PEG-based hydrogel platforms have been developed to understand valve cellular biology.[56] A photosensitive PEG hydrogel was functionalized with an MMP-sensitive peptide to study the response of VICs.[50] A similar approach was used to tune mechanical properties of PEG-based hydrogels. Interestingly, this work showed that VIC differentiation can be directed by gradients in substrate stiffness. Moreover, whereas it was previously thought that stiff environments would favor activation of VICs, this work showed that soft substrates could also facilitate activation of VICs.[57, 58] However, PEG synthetic hydrogels have the significant drawback of being devoid of cell binding motifs. Functionalization

with cell-adhesive peptides is thus necessary to facilitate cell attachment. The potential of using this material thus mostly lies in the tunability of such a platform to a specific purpose.

'Natural' Hydrogels

Increased interest has risen to use so-called 'natural materials' which are based on valvular ECM components. Although they have less flexibility in functionalization, they do provide mechanical properties comparable to native tissue and the possibility of biological cues needed to direct and control cell growth. Most importantly, natural materials allow for the fabrication of a more *in situ*-like environment analogous to the native heart valve. Cells surrounded by a native-like environment mimicking their natural state may be presented with proteins similar to those of fetal and adult heart valves, which could promote *in vitro* and *in vivo* remodeling. In turn, this may be beneficial in creating a viable heart valve replacement. In addition, such an approach can be used *in vitro* to controllably study the mechanism of valvular physiology and disease as it may occur in vivo.

Native valve ECM components such as collagen, hyaluronic acid, fibronectin and elastin have been used as biomaterials to fabricate hydrogels. The two most studied natural biomaterials for hydrogel based heart valve tissue engineering are hyaluronic acid and collagen.[59-63] Both collagen and hyaluronic acid are abundant in adult heart valve ECM, but also not only are vital for valve maturation.

Hyaluronic Acid

As mentioned before, the endocardial cushions from which heart valves develop contain a significant amount of HA, playing a key role in regulating ECM production and control of EMT by endocardial cells. From an engineering point of view HA hydrogels are promising scaffolds for *in vitro* and *in vivo* remodeling, due to their inherent slow biodegradation by VIC secreted hyaluronases. The *spongiosa* of native valves contain more than ninety percent HA. HA is also a non-thrombogenic and non-immunogenic material. Using HA in hydrogel scaffolds also seems to provide for biological cues to promote specific ECM production. For example, in a study where neonatal rat smooth muscle cells were cultured on HA hydrogels, results demonstrated increased elastin production compared to cells grown on a petri-dish.[60] In addition, photo-crosslinkable HA hydrogels modified with methacrylate groups showed that ECM protein production of encapsulated VICs is based on the molecular weight of the HA degradation products.[64] This is by itself very promising, since lack of elastin production seems to hinder the successful long term performance synthetic based heart valve tissue engineering.

Collagen

Collagen is the main ECM protein produced in developing valves and maintained in mature valves through a homeostatic process described earlier. Collagen is largely responsible for the mechanical strength of heart valves, and seems logical to be considered a scaffold.[65] However, on its own, collagen lacks the necessary mechanical properties to fabricate a strong enough heart valve sub-

stitute. It is thus often used as one component of a composite material. Collagen has been used in combination with photocrosslinkable methacrylated HA.[66] Interestingly, such a composite material which provides for a similar fibrous structure of native valve leaflets, through collagen, together with increased mechanical properties of HA, has shown to promote proliferation of fibroblasts, analogous to quiescent VICs, predominantly present in healthy heart valves.[67] By adding HA, the formation of a collagen fiber network is altered, meaning that cells cannot contract the composite gels, compared with collagen gels alone. Collagen has also been combined with the GAG chondroitin sulfate to create valve replacements.[61] This composite scaffold demonstrated *in vitro* development into similar architecture as native valves when seeded with porcine VICs and VECs.

Alternatively, a technique has been developed to create collagen-based valve scaffolds *in vivo* using fibrous encapsulation of an implanted foreign body by an organism.[68, 69] First, silicone rods were shaped into valve molds and wrapped in polyurethane or autologous connective tissue from white rabbits. Then, these constructs were implanted subcutaneously in the same animals. After four weeks, the host response to the implant was to secrete connective tissue primarily in the form of collagen, which would coat the valve-shaped mold. Results demonstrated a tri-leaflet valve composed primarily of collagen, which performed well in bioreactors simulating the pulmonary circulation.[69] Future studies are ongoing on using this approach to create an autologous valve substitute.

Another approach using collagen-based hydrogels is to use its hydrolyzed form, gelatin. Gelatin is synthesized upon the partial breakdown of the natural triple-helical structure of collagen and is considered safe by the FDA, which made it an attractive material to explore. It maintains similar bioactivity as collagen, however unmodified gelatin as a hydrogel platform is mechanically very weak and the gelation temperature is below 37°C, the physiological temperature. Gelatin is therefore altered with methacrylate groups (GelMA), which when exposed to light in the presence of a photo-initiatior, polymerizes to form covalently and physically crosslinked hydrogels. Changing macromer molecular weight or percentage per volume or crosslinking time can alter its physical mechanical properties, making it an attractive scaffold. Encapsulating VICs into GelMA hydrogels resulted in high viability, myofibroblast differentiation and matrix remodeling in 3D.[70] However, similar to collagen, GelMA is an intrinsically weak material, which is not at par with the mechanical properties required for a tissue engineered valve substitute. To what extent GelMA can be explored in combination with other materials to address this limitation remains to be studied.

Fibrin

Fibrin based hydrogels present another viable alternative for TEHVs, since they can be derived from the patient. This would eliminate the worry of an adverse immunogenic response. Although studies of fibroblasts encapsulated in fibrin gels show increased collagen production and anisotropic mechanical properties, these materials are not strong enough to be considered sustainable heart valve scaffold materials.[71, 72] However, when mechanical conditioning in the form of cyclic distension is performed, fibrin-based scaffolds with porcine VICs or fibroblasts showed improved mechanical

properties and collagen production compared to statically grown control samples.[73] This could mean that fibrin-based scaffolds may facilitate increased remodeling and thus eventually aid in generating mechanical properties needed for *in vivo* implantation.

3D Printing

A technique that has recently gained a great deal of attention, particularly in organ tissue engineering is 3D printing. Considering that hydrogels can be designed to mimic mechanical and biological properties of soft tissues, they are very suitable to be used and controlled for 3D printing. The technology that can print clinically sized, geometrically, complex constructs with hydrogels exist. This technique has primarily been demonstrated for hard tissues such as bone and cartilage.[74] However, a recent study used this approach to print aortic valves.[75] (Figure 2)

By using PEG-diacrylate (PEGDA) as a base polymer hydrogel, aortic valves including leaflets, coronary sinus and root geometry at different scales were printed. Briefly, the valves were fabricated by was simultaneously printing and crosslinking small hydrogel paths by exposing the hydrogel paths to light. Each small path would then brick-wise be printed to form an aortic valve. These constructs exhibited tunable mechanical properties, and adequate cytocompatibility of seeded porcine VICs.

Although this approach is in its infancy, this use of hydrogels could prove an enabling technique for heart valve tissue engineering, because the 3D printed heart valve can be sized and shaped according to the specific patient's needs. In essence, this is personalized medicine applied to cardiac valve replacement. In addition, 3D printing hydrogels has been utilized in creating vascularized constructs using thermal gelation after printing. Using different biomaterial inks and print-heads

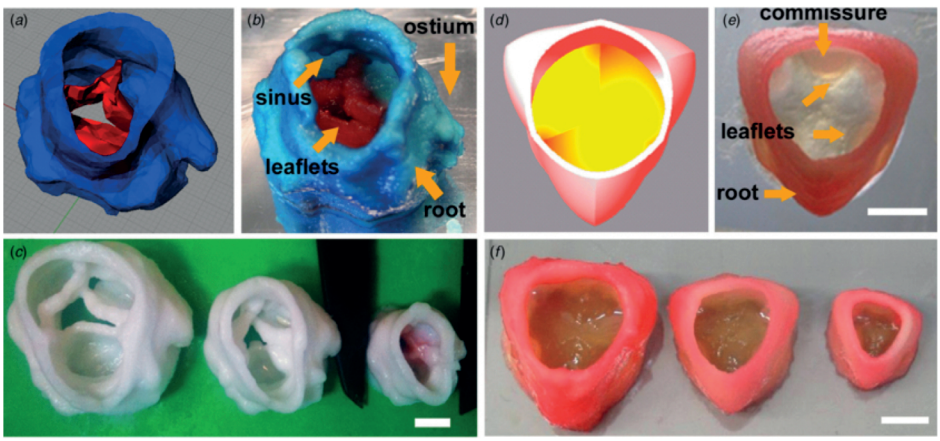

Figure 2. Printing heterogeneous valve constructs. (A) Porcine aortic valve model was **(B)** Printed, where root was formed with 700 MW PEG-DA hydrogel while the leaflets were formed with 700/8000 MW PEG-DA hydrogels. Key features such as the coronary ostium and sinuses were present. **(C)** Scaffolds were printed with 700 MW PEG-DA at different scale for fidelity analysis, where the inner diameters (ID) were 22, 17 and 12 mm. **(D)** Axisymmetric valve model was **(E)** Printed with two blends of hydrogels **(F)** And at 22, 17, and 12 mm ID. Scale bar = 1 cm. Source: With permission from Hockaday et al. Biofabrication (2013)

simultaneously, vascularized multicellular heterogeneous tissue constructs were printed, demonstrating good viability and little no damage to encapsulated cells.[76] This approach may open up new avenues for research on angiogenesis, drug screening and stem cell niches.

HYDROGELS AS MODEL SYSTEMS TO STUDY BIOLOGY AND PATHOPHYSIOLOGY OF VICS IN HEALTH AND DISEASE

The chemical and mechanical tunability of hydrogels – as described previously – does not only harbor potential in creating functional tissue engineered valve substitutes, but also facilitates the ability to capture the native cellular niche as it may occur in the heart valve. More specifically, hydrogels provide for a 3D *in vitro* platform to study the biology and pathophysiology of valvular cells, in a model which may be much more physiological than standard culture. (Figure 3) Indeed, this is an active area of investigation.[77, 78] Of special interest is the pursuit of understanding the mechanisms of calcific aortic valve disease (CAVD). CAVD is the most common valve disease in the Western world[2] and is characterized by progressive fibrosis and mineralization of the aortic valve cusps, causing aortic valve stenosis.[21] Traditionally viewed as a degenerative disease, CAVD is now seen as a dynamic process involving phenotypic modulation of resident VICs .[79] As described before, VICs are responsible for maintaining valve tissue homeostasis. However, when repeated valve injury or chronic exposure to exogenous pathogenic stimuli such as inflammation or excessive mechanical stress occur, regulation of healthy VIC phenotypes can be altered.

One of the postulated mechanisms is that with changes in valve architecture that occur with age and upon persistent VIC myofibroblastic activation, VICs can increase valve stiffness through excess remodeling of the valve, and eventually cause VICs to express genes and proteins associated with osteogenesis.[80] This process of osteogenic activation is subject to several factors amongst which the potent cytokine transforming growth factor β1 (TGFβ1) has been well documented.[81] Because symptoms do not occur until there is a significant aortic valve stenosis caused by severe calcification with CAVD, clinical specimens obtained at surgery have end-stage calcific valve disease in humans. In addition, animal models have failed to truly recapitulate the human disease, and *in vitro* standard culture experiments are arguably unable to simulate the cellular processes that occur *in vivo*. As such, hydrogels have been explored to simulate specific biological and pathophysiological processes to gain insight into underlying mechanisms. (Figure 3) A key advance was on seeding VICs onto HA-based hydrogels, demonstrating the feasibility of utilizing natural material based hydrogel microengineering as an *in vitro* culture platform.[59] GelMA based hydrogel platforms have also been widely explored as hydrogel culture systems as a tool to understand and direct VIC phenotypic fate,[20, 70] in addition to synthetic polymers such as PEG. After the feasibility of using various materials to create relevant 3D cellular micro-environments was demonstrated, investigators started using these system to understand the phenotypic change of VICs that may occur in heart valve biology and pathophysiology. Understanding the phenotypic switch from quiescent

fibroblast-like VIC to activated myofibroblastic VIC is of vital importance in unraveling mechanisms of disease. For instance, it became clear that matrix elasticity is able to regulate proliferation and differentiation of quiescent fibroblastic VIC;[57, 77] particularly stiffened matrix in fibrotic lesions are thought to promote pathogenic myofibroblast activation.[80] PEG based hydrogels have been modulated to simulate physiological matrix elasticities, demonstrating that soft hydrogels are able to preserve the quiescent fibroblast phenotype of VICs much better than stiff surfaces.[82, 83] Decreasing matrix elasticity during culture even facilitated a phenotypic change from activated myofibroblasts to quiescent fibroblasts.[58, 77, 78] In addition to controlling the mechanical characteristics of hydrogels, the chemical composition of matrices and its effect on VIC phenotype can also be modulated. Indeed, hydrogels have been functionalized with other valve matrix molecules such as fibronectin and fibrin, which revealed that fibronectin had an inhibitory effect on calcification markers of VICs, whereas fibrin seemed to enhance them.[72] Hydrogels can also be used as a platform to test the

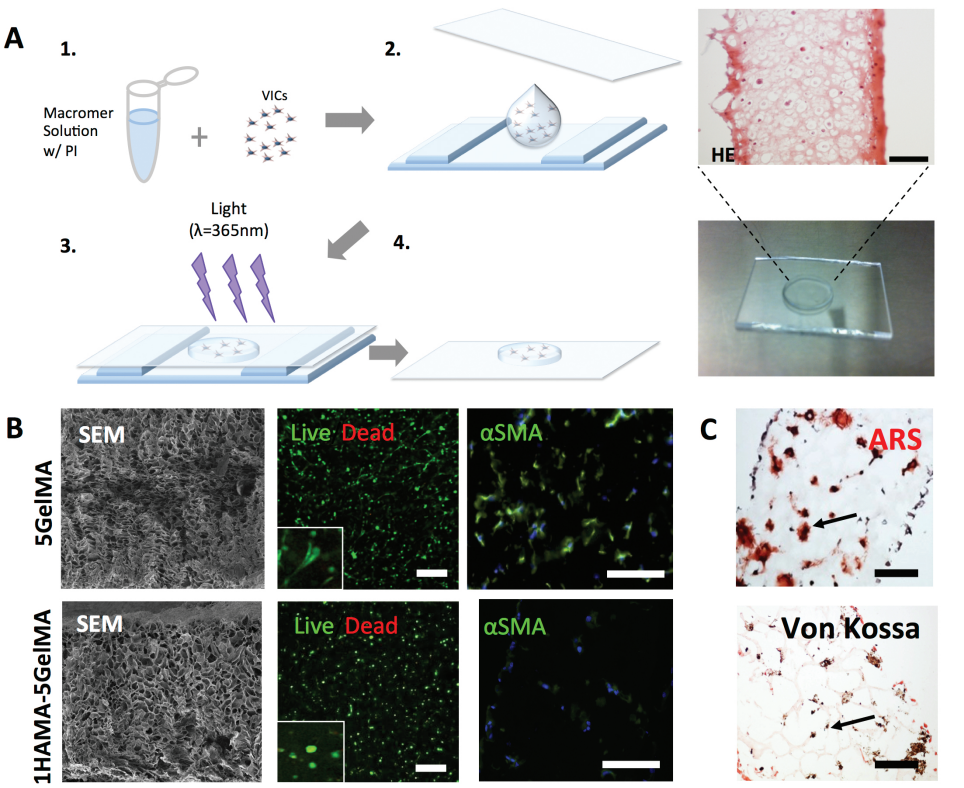

Figure 3. Using hydrogels as model systems for valve pathobiology. (A) Typical fabrication technique of photo-crosslinkable hydrogels in which VICs are resuspended in a macromer solution which in the presence of PI solution can crosslink when exposed to UV light. **(B)** Changing material composition affects VIC behavior. When HAMA was added to GelMA it facilitated a quiescent VIC phenotype, contrary to VICs encapsulated in GelMA alone, which demonstrate spreading and myofibroblast-like differentiation. **(C)** When exposed to osteogenic environment VICs encaspulated in hybrid hydrogels undergo osteoblastic differentiation and deposit calcium as visualized by Alizarin Red S and Von Kossa staining. Arrows indicate positive staining Bar 50 um. (This thesis, Chapter 7,8)

effect of exogenous stimuli such as cytokines on VIC phenotype. The addition of TGFβ1 revealed an increased myofibroblastic differentiation of VICs encapsulated in hydrogels,[29] whereas FGF-2 has demonstrated an inhibitory effect on myofibroblastic differentiation of VICS. All in all, hydrogels are dynamic substrates, which hold great potential in deciphering the complex role of matrix composition and cues on the phenotypic plasticity of VICs and the role of this most influential cell type in valve homeostasis and disease.

CONCLUSION

The success of TEHV depends on living functional tissue that is able to adapt to a viable and durable homeostatic state. In addition there must be an intricate ability to repair and remodel when needed, whether it is as a response to injury or growth. Valvular homeostasis is a complex interaction between the endothelium, VIC phenotypes, the extracellular matrix and biomechanics. Using natural materials to fabricate hydrogels and generate living heart valves is a relatively new approach in heart valve tissue engineering. Even though hydrogels have substantial potential due to their tunable, controllable and biomimetic nature caused by using the body's own ECM proteins, significant challenges need to be overcome. Up until this point the use of hydrogels in TEHV has mostly been *in vitro* and used to understand cell-material relationships in three-dimensional platforms. In addition, even with the advent of tissue controlling natural materials, biocompatibility alone will not be enough to create the 'perfect' heart valve replacement. The valve substitute must have sufficient mechanical properties to withstand the hemodynamic demands of a beating heart. The combination of cell-instructive biomaterials with other techniques that introduce mechanical strength could create such a scaffold system. Although considerable progress has been made in developing, characterizing and using hydrogel-based tissue engineering for heart valve replacement, the approach is still in its rudimentary stages and far short of clinical implementation. Nevertheless, considering the premise that hydrogel engineering can use the body's own ECM proteins to stimulate a living, durable valve substitute, hydrogels hold exciting potential.

REFERENCES

1. Otto CM, Lind BK, Kitzman DW, Gersh BJ, Siscovick DS. Association of aortic-valve sclerosis with cardiovascular mortality and morbidity in the elderly. *The New England journal of medicine*. 1999;341:142-147
2. Takkenberg JJ, Rajamannan NM, Rosenhek R, Kumar AS, Carapetis JR, Yacoub MH. The need for a global perspective on heart valve disease epidemiology. The shvd working group on epidemiology of heart valve disease founding statement. *J Heart Valve Dis*. 2008;17:135-139
3. Rahimtoola SH. Choice of prosthetic heart valve in adults an update. *Journal of the American College of Cardiology*. 2010;55:2413-2426
4. Hammermeister K, Sethi GK, Henderson WG, Grover FL, Oprian C, Rahimtoola SH. Outcomes 15 years after valve replacement with a mechanical versus a bioprosthetic valve: Final report of the veterans affairs randomized trial. *Journal of the American College of Cardiology*. 2000;36:1152-1158
5. Schoen FJ, Levy RJ. Calcification of tissue heart valve substitutes: Progress toward understanding and prevention. *The Annals of thoracic surgery*. 2005;79:1072-1080
6. Mitchell RN, Jonas RA, Schoen FJ. Pathology of explanted cryopreserved allograft heart valves: Comparison with aortic valves from orthotopic heart transplants. *The Journal of thoracic and cardiovascular surgery*. 1998;115:118-127
7. Sacks MS, Schoen FJ, Mayer JE. Bioengineering challenges for heart valve tissue engineering. *Annual review of biomedical engineering*. 2009;11:289-313
8. Vesely I. Heart valve tissue engineering. *Circulation research*. 2005;97:743-755
9. Harken DE. Heart valves: Ten commandments and still counting. *The Annals of thoracic surgery*. 1989;48:S18-19
10. Schoen FJ. Heart valve tissue engineering: Quo vadis? *Current opinion in biotechnology*. 2011;22:698-705
11. Sutherland FW, Perry TE, Yu Y, Sherwood MC, Rabkin E, Masuda Y, Garcia GA, McLellan DL, Engelmayr GC, Jr., Sacks MS, Schoen FJ, Mayer JE, Jr. From stem cells to viable autologous semilunar heart valve. *Circulation*. 2005;111:2783-2791
12. Hoerstrup SP, Kadner A, Melnitchouk S, Trojan A, Eid K, Tracy J, Sodian R, Visjager JF, Kolb SA, Grunenfelder J, Zund G, Turina MI. Tissue engineering of functional trileaflet heart valves from human marrow stromal cells. *Circulation*. 2002;106:I143-150
13. Gottlieb D, Kunal T, Emani S, Aikawa E, Brown DW, Powell AJ, Nedder A, Engelmayr GC, Jr., Melero-Martin JM, Sacks MS, Mayer JE, Jr. In vivo monitoring of function of autologous engineered pulmonary valve. *The Journal of thoracic and cardiovascular surgery*. 2010;139:723-731
14. Hibino N, McGillicuddy E, Matsumura G, Ichihara Y, Naito Y, Breuer C, Shinoka T. Late-term results of tissue-engineered vascular grafts in humans. *The Journal of thoracic and cardiovascular surgery*. 2010;139:431-436, 436 e431-432
15. Dohmen PM, Lembcke A, Holinski S, Kivelitz D, Braun JP, Pruss A, Konertz W. Mid-term clinical results using a tissue-engineered pulmonary valve to reconstruct the right ventricular outflow tract during the ross procedure. *The Annals of thoracic surgery*. 2007;84:729-736
16. Simon P, Kasimir MT, Seebacher G, Weigel G, Ullrich R, Salzer-Muhar U, Rieder E, Wolner E. Early failure of the tissue engineered porcine heart valve synergraft in pediatric patients. *European journal of cardio-thoracic surgery: official journal of the European Association for Cardio-thoracic Surgery*. 2003;23:1002-1006; discussion 1006
17. Tudorache I, Calistru A, Baraki H, Meyer T, Hoffler K, Sarikouch S, Bara C, Gorler A, Hartung D, Hilfiker A, Haverich A, Cebotari S. Orthotopic replacement of aortic heart valves with tissue-engineered grafts. *Tissue engineering. Part A*. 2013;19:1686-1694

18. Hjortnaes J, Bouten CV, Van Herwerden LA, Grundeman PF, Kluin J. Translating autologous heart valve tissue engineering from bench to bed. *Tissue engineering. Part B, Reviews*. 2009;15:307-317
19. Sewell-Loftin MK, Chun YW, Khademhosseini A, Merryman WD. Emt-inducing biomaterials for heart valve engineering: Taking cues from developmental biology. *Journal of cardiovascular translational research*. 2011;4:658-671
20. DeForest CA, Anseth KS. Advances in bioactive hydrogels to probe and direct cell fate. *Annual review of chemical and biomolecular engineering*. 2012;3:421-444
21. Schoen FJ. Evolving concepts of cardiac valve dynamics: The continuum of development, functional structure, pathobiology, and tissue engineering. *Circulation*. 2008;118:1864-1880
22. Joyce EM, Liao J, Schoen FJ, Mayer JE, Jr., Sacks MS. Functional collagen fiber architecture of the pulmonary heart valve cusp. *The Annals of thoracic surgery*. 2009;87:1240-1249
23. Paranya G, Vineberg S, Dvorin E, Kaushal S, Roth SJ, Rabkin E, Schoen FJ, Bischoff J. Aortic valve endothelial cells undergo transforming growth factor-beta-mediated and non-transforming growth factor-beta-mediated transdifferentiation in vitro. *The American journal of pathology*. 2001;159:1335-1343
24. Bischoff J, Aikawa E. Progenitor cells confer plasticity to cardiac valve endothelium. *Journal of cardiovascular translational research*. 2011;4:710-719
25. Rabkin E, Aikawa M, Stone JR, Fukumoto Y, Libby P, Schoen FJ. Activated interstitial myofibroblasts express catabolic enzymes and mediate matrix remodeling in myxomatous heart valves. *Circulation*. 2001;104:2525-2532
26. Aikawa E, Whittaker P, Farber M, Mendelson K, Padera RF, Aikawa M, Schoen FJ. Human semilunar cardiac valve remodeling by activated cells from fetus to adult: Implications for postnatal adaptation, pathology, and tissue engineering. *Circulation*. 2006;113:1344-1352
27. Liu AC, Joag VR, Gotlieb AI. The emerging role of valve interstitial cell phenotypes in regulating heart valve pathobiology. *The American journal of pathology*. 2007;171:1407-1418
28. Walker GA, Masters KS, Shah DN, Anseth KS, Leinwand LA. Valvular myofibroblast activation by transforming growth factor-beta: Implications for pathological extracellular matrix remodeling in heart valve disease. *Circulation research*. 2004;95:253-260
29. Cushing MC, Liao JT, Anseth KS. Activation of valvular interstitial cells is mediated by transforming growth factor-beta1 interactions with matrix molecules. *Matrix biology: journal of the International Society for Matrix Biology*. 2005;24:428-437
30. Liu AC, Gotlieb AI. Transforming growth factor-beta regulates in vitro heart valve repair by activated valve interstitial cells. *The American journal of pathology*. 2008;173:1275-1285
31. Merryman WD, Lukoff HD, Long RA, Engelmayr GC, Jr., Hopkins RA, Sacks MS. Synergistic effects of cyclic tension and transforming growth factor-beta1 on the aortic valve myofibroblast. *Cardiovascular pathology: the official journal of the Society for Cardiovascular Pathology*. 2007;16:268-276
32. Thayer P, Balachandran K, Rathan S, Yap CH, Arjunon S, Jo H, Yoganathan AP. The effects of combined cyclic stretch and pressure on the aortic valve interstitial cell phenotype. *Annals of biomedical engineering*. 2011;39:1654-1667
33. Combs MD, Yutzey KE. Heart valve development: Regulatory networks in development and disease. *Circulation research*. 2009;105:408-421
34. Riem Vis PW, Kluin J, Sluijter JP, van Herwerden LA, Bouten CV. Environmental regulation of valvulogenesis: Implications for tissue engineering. *European journal of cardio-thoracic surgery: official journal of the European Association for Cardio-thoracic Surgery*. 2011;39:8-17
35. Armstrong EJ, Bischoff J. Heart valve development: Endothelial cell signaling and differentiation. *Circulation research*. 2004;95:459-470

36. Visconti RP, Ebihara Y, LaRue AC, Fleming PA, McQuinn TC, Masuya M, Minamiguchi H, Markwald RR, Ogawa M, Drake CJ. An in vivo analysis of hematopoietic stem cell potential: Hematopoietic origin of cardiac valve interstitial cells. *Circulation research*. 2006;98:690-696
37. Kumar AH, Metharom P, Schmeckpeper J, Weiss S, Martin K, Caplice NM. Bone marrow-derived cx3cr1 progenitors contribute to neointimal smooth muscle cells via fractalkine cx3cr1 interaction. *FASEB journal: official publication of the Federation of American Societies for Experimental Biology*. 2010;24:81-92
38. Peacock JD, Lu Y, Koch M, Kadler KE, Lincoln J. Temporal and spatial expression of collagens during murine atrioventricular heart valve development and maintenance. *Developmental dynamics: an official publication of the American Association of Anatomists*. 2008;237:3051-3058
39. Camenisch TD, Schroeder JA, Bradley J, Klewer SE, McDonald JA. Heart-valve mesenchyme formation is dependent on hyaluronan-augmented activation of erbb2-erbb3 receptors. *Nature medicine*. 2002;8:850-855
40. Langer R, Vacanti JP. Tissue engineering. *Science*. 1993;260:920-926
41. Hoerstrup SP, Sodian R, Daebritz S, Wang J, Bacha EA, Martin DP, Moran AM, Guleserian KJ, Sperling JS, Kaushal S, Vacanti JP, Schoen FJ, Mayer JE, Jr. Functional living trileaflet heart valves grown in vitro. *Circulation*. 2000;102:III44-49
42. Shinoka T, Breuer CK, Tanel RE, Zund G, Miura T, Ma PX, Langer R, Vacanti JP, Mayer JE, Jr. Tissue engineering heart valves: Valve leaflet replacement study in a lamb model. *The Annals of thoracic surgery*. 1995;60:S513-516
43. Zund G, Breuer CK, Shinoka T, Ma PX, Langer R, Mayer JE, Vacanti JP. The in vitro construction of a tissue engineered bioprosthetic heart valve. *European journal of cardio-thoracic surgery: official journal of the European Association for Cardio-thoracic Surgery*. 1997;11:493-497
44. Sodian R, Hoerstrup SP, Sperling JS, Martin DP, Daebritz S, Mayer JE, Jr., Vacanti JP. Evaluation of biodegradable, three-dimensional matrices for tissue engineering of heart valves. *ASAIO journal*. 2000;46:107-110
45. Schmidt D, Achermann J, Odermatt B, Breymann C, Mol A, Genoni M, Zund G, Hoerstrup SP. Prenatally fabricated autologous human living heart valves based on amniotic fluid derived progenitor cells as single cell source. *Circulation*. 2007;116:I64-70
46. Engelmayr GC, Jr., Hildebrand DK, Sutherland FW, Mayer JE, Jr., Sacks MS. A novel bioreactor for the dynamic flexural stimulation of tissue engineered heart valve biomaterials. *Biomaterials*. 2003;24:2523-2532
47. Nemir S, Hayenga HN, West JL. Pegda hydrogels with patterned elasticity: Novel tools for the study of cell response to substrate rigidity. *Biotechnology and bioengineering*. 2010;105:636-644
48. Nemir S, West JL. Synthetic materials in the study of cell response to substrate rigidity. *Annals of biomedical engineering*. 2010;38:2-20
49. Cushing MC, Anseth KS. Materials science. Hydrogel cell cultures. *Science*. 2007;316:1133-1134
50. Benton JA, Fairbanks BD, Anseth KS. Characterization of valvular interstitial cell function in three dimensional matrix metalloproteinase degradable peg hydrogels. *Biomaterials*. 2009;30:6593-6603
51. Benton JA, Kern HB, Anseth KS. Substrate properties influence calcification in valvular interstitial cell culture. *J Heart Valve Dis*. 2008;17:689-699
52. Kloxin AM, Kasko AM, Salinas CN, Anseth KS. Photodegradable hydrogels for dynamic tuning of physical and chemical properties. *Science*. 2009;324:59-63
53. Weber LM, Anseth KS. Hydrogel encapsulation environments functionalized with extracellular matrix interactions increase islet insulin secretion. *Matrix biology: journal of the International Society for Matrix Biology*. 2008;27:667-673
54. Cuchiara MP, Allen AC, Chen TM, Miller JS, West JL. Multilayer microfluidic pegda hydrogels. *Biomaterials*. 2010;31:5491-5497

55. Temenoff JS, Athanasiou KA, LeBaron RG, Mikos AG. Effect of poly(ethylene glycol) molecular weight on tensile and swelling properties of oligo(poly(ethylene glycol) fumarate) hydrogels for cartilage tissue engineering. *Journal of biomedical materials research*. 2002;59:429-437
56. Cushing MC, Liao JT, Jaeggli MP, Anseth KS. Material-based regulation of the myofibroblast phenotype. *Biomaterials*. 2007;28:3378-3387
57. Kloxin AM, Benton JA, Anseth KS. In situ elasticity modulation with dynamic substrates to direct cell phenotype. *Biomaterials*. 2010;31:1-8
58. Kloxin AM, Tibbitt MW, Kasko AM, Fairbairn JA, Anseth KS. Tunable hydrogels for external manipulation of cellular microenvironments through controlled photodegradation. *Advanced materials*. 2010;22:61-66
59. Masters KS, Shah DN, Leinwand LA, Anseth KS. Crosslinked hyaluronan scaffolds as a biologically active carrier for valvular interstitial cells. *Biomaterials*. 2005;26:2517-2525
60. Ramamurthi A, Vesely I. Evaluation of the matrix-synthesis potential of crosslinked hyaluronan gels for tissue engineering of aortic heart valves. *Biomaterials*. 2005;26:999-1010
61. Flanagan TC, Wilkins B, Black A, Jockenhoevel S, Smith TJ, Pandit AS. A collagen-glycosaminoglycan co-culture model for heart valve tissue engineering applications. *Biomaterials*. 2006;27:2233-2246
62. Masters KS, Shah DN, Walker G, Leinwand LA, Anseth KS. Designing scaffolds for valvular interstitial cells: Cell adhesion and function on naturally derived materials. *Journal of biomedical materials research. Part A*. 2004;71:172-180
63. Suri S, Schmidt CE. Photopatterned collagen-hyaluronic acid interpenetrating polymer network hydrogels. *Acta biomaterialia*. 2009;5:2385-2397
64. Rodriguez KJ, Piechura LM, Masters KS. Regulation of valvular interstitial cell phenotype and function by hyaluronic acid in 2-d and 3-d culture environments. *Matrix biology: journal of the International Society for Matrix Biology*. 2011;30:70-82
65. Tedder ME, Liao J, Weed B, Stabler C, Zhang H, Simionescu A, Simionescu DT. Stabilized collagen scaffolds for heart valve tissue engineering. *Tissue engineering. Part A*. 2009;15:1257-1268
66. Brigham MD, Bick A, Lo E, Bendali A, Burdick JA, Khademhosseini A. Mechanically robust and bioadhesive collagen and photocrosslinkable hyaluronic acid semi-interpenetrating networks. *Tissue engineering. Part A*. 2009;15:1645-1653
67. Kreger ST, Voytik-Harbin SL. Hyaluronan concentration within a 3d collagen matrix modulates matrix viscoelasticity, but not fibroblast response. *Matrix biology: journal of the International Society for Matrix Biology*. 2009;28:336-346
68. Hayashida K, Kanda K, Yaku H, Ando J, Nakayama Y. Development of an in vivo tissue-engineered, autologous heart valve (the biovalve): Preparation of a prototype model. *The Journal of thoracic and cardiovascular surgery*. 2007;134:152-159
69. Yamanami M, Yahata Y, Uechi M, Fujiwara M, Ishibashi-Ueda H, Kanda K, Watanabe T, Tajikawa T, Ohba K, Yaku H, Nakayama Y. Development of a completely autologous valved conduit with the sinus of valsalva using in-body tissue architecture technology: A pilot study in pulmonary valve replacement in a beagle model. *Circulation*. 2010;122:S100-106
70. Benton JA, DeForest CA, Vivekanandan V, Anseth KS. Photocrosslinking of gelatin macromers to synthesize porous hydrogels that promote valvular interstitial cell function. *Tissue engineering. Part A*. 2009;15:3221-3230
71. Ye Q, Zund G, Benedikt P, Jockenhoevel S, Hoerstrup SP, Sakyama S, Hubbell JA, Turina M. Fibrin gel as a three dimensional matrix in cardiovascular tissue engineering. *European journal of cardio-thoracic surgery: official journal of the European Association for Cardio-thoracic Surgery*. 2000;17:587-591

72. Jockenhoevel S, Zund G, Hoerstrup SP, Chalabi K, Sachweh JS, Demircan L, Messmer BJ, Turina M. Fibrin gel -- advantages of a new scaffold in cardiovascular tissue engineering. *European journal of cardio-thoracic surgery: official journal of the European Association for Cardio-thoracic Surgery*. 2001;19:424-430
73. Syedain ZH, Weinberg JS, Tranquillo RT. Cyclic distension of fibrin-based tissue constructs: Evidence of adaptation during growth of engineered connective tissue. *Proceedings of the National Academy of Sciences of the United States of America*. 2008;105:6537-6542
74. Hollister SJ. Porous scaffold design for tissue engineering. *Nature materials*. 2005;4:518-524
75. Duan B, Hockaday LA, Kang KH, Butcher JT. 3d bioprinting of heterogeneous aortic valve conduits with alginate/gelatin hydrogels. *Journal of biomedical materials research. Part A*. 2013;101:1255-1264
76. Kolesky DB, Truby RL, Gladman AS, Busbee TA, Homan KA, Lewis JA. 3d bioprinting of vascularized, heterogeneous cell-laden tissue constructs. *Advanced materials*. 2014
77. Kirschner CM, Alge DL, Gould ST, Anseth KS. Clickable, photodegradable hydrogels to dynamically modulate valvular interstitial cell phenotype. *Advanced healthcare materials*. 2014
78. Quinlan AM, Billiar KL. Investigating the role of substrate stiffness in the persistence of valvular interstitial cell activation. *Journal of biomedical materials research. Part A*. 2012;100:2474-2482
79. Rajamannan NM, Evans FJ, Aikawa E, Grande-Allen KJ, Demer LL, Heistad DD, Simmons CA, Masters KS, Mathieu P, O'Brien KD, Schoen FJ, Towler DA, Yoganathan AP, Otto CM. Calcific aortic valve disease: Not simply a degenerative process: A review and agenda for research from the national heart and lung and blood institute aortic stenosis working group. Executive summary: Calcific aortic valve disease-2011 update. *Circulation*. 2011;124:1783-1791
80. Hutcheson JD, Aikawa E, Merryman WD. Potential drug targets for calcific aortic valve disease. *Nature reviews. Cardiology*. 2014;11:218-231
81. Merryman WD. What modulates the aortic valve interstitial cell phenotype? *Future cardiology*. 2008;4:247-252
82. Wang H, Tibbitt MW, Langer SJ, Leinwand LA, Anseth KS. Hydrogels preserve native phenotypes of valvular fibroblasts through an elasticity-regulated pi3k/akt pathway. *Proceedings of the National Academy of Sciences of the United States of America*. 2013;110:19336-19341
83. Gould ST, Anseth KS. Role of cell-matrix interactions on vic phenotype and tissue deposition in 3d peg hydrogels. *Journal of tissue engineering and regenerative medicine*. 2013

7

Hydrogel Composition directs Valvular Interstitial Cell fate

Jesper Hjortnaes, MD[1,2,3], Gulden Camci-Unal, PhD[2,4], Joshua D. Hutcheson, PhD[5], Sung Mi Jung, PhD[6], Frederick J. Schoen, MD, PhD[7], Jolanda Kluin, MD, PhD[3], Elena Aikawa, MD, PhD[1,5*] Ali Khademhosseini, PhD[2,4,8*]

Advanced Healthcare Materials 2014

[1]Center of Excellence in Vascular Biology, Department of Medicine, Brigham and Women's Hospital, Harvard Medical School, Boston, MA, USA; [2]Division of Biomedical Engineering, Department of Medicine, Brigham and Women's Hospital, Harvard Medical School, Boston, MA, USA; [3]Department of Cardiothoracic Surgery, University Medical Center Utrecht, Utrecht, The Netherlands; [4]Harvard-MIT Division of Health Sciences and Technology, Massachusetts Institute of Technology, Cambridge, MA, USA [5]Center for Interdisciplinary Cardiovascular Sciences, Brigham and Women's Hospital, Harvard Medical School, Boston, MA, USA;[6]Department of Electrical Engineering and Computer Science, Massachusetts Institute of Technology, Cambridge, MA, USA, [7]Department of Pathology, Brigham and Women's Hospital, Harvard Medical School, Boston, MA, USA; [8]Wyss Institute for Biologically Inspired Engineering, Harvard University, Boston, MA, USA

ABSTRACT

Three dimensional (3D) hydrogel platforms are powerful tools, providing controllable, physiologically relevant microenvironments that could aid in understanding the role of various environmental factors in directing valvular interstitial cell (VIC) phenotype. Continuous activation of VICs and their transformation from quiescent fibroblast to activated myofibroblast phenotype is considered to be an initiating event in the onset of valve disease. However, relative contribution of changes in VIC phenotype are poorly understood since most 2-dimensional (2D) culture systems lead to spontaneous VIC myofibroblastic activation. Here, a hydrogel platform composed of photocross-linkable versions of native valvular extracellular matrix components –methacrylated hyaluronic acid (HAMA) and methacrylated gelatin (GelMA) – is proposed as a 3D culture system to study VIC phenotypic changes. Our results showed that VIC myofibroblast-like differentiation, determined by α-SMA, MMP-9, and Collagen type I expression, and occurs spontaneously in mechanically soft GelMA hydrogels. In contrast, VICs encapsulated in HAMA-GelMA hybrid hydrogels, does not occur spontaneously and require exogenous delivery of TGFβ1, indicating that hybrid hydrogels can be used to study cytokine-dependent transition of encapsulated VICs. This study demonstrated that a hybrid hydrogel platform can be used to maintain a quiescent VIC phenotype and study the effect of pathological environmental cues on VIC activation, which will aid in understanding pathobiology of valvular disease.

INTRODUCTION

Heart valves contain valvular interstitial cells (VICs), a heterogeneous cell population that maintains tissue homeostasis and structural integrity of the heart valve leaflet extracellular matrix (ECM).[1, 2] In native healthy heart valves, VICs are mostly described as having a quiescent fibroblast-like phenotype; however, upon stimulation by environmental cues, VICs can differentiate into myofibroblast-like cells. Activated VICs, hallmarked by alpha smooth muscle actin (α-SMA) expression, play an important role in valve tissue remodeling that is characterized by increased deposition of ECM proteins such as collagen, elastin, and glycosaminoglycans (GAGs), and overexpression of matrix metalloproteinases (MMPs), cathepsins and tissue inhibitors.[1, 3, 4] Persistent activation of VICs results in pathological remodeling of the valve matrix, in part attributed to valvular fibrosis.[2] Moreover, activated VICs are believed to play an active role in calcific aortic valve disease, in which myofibroblast-like cells differentiate into osteoblast-like cells resulting in calcium deposition.[5-7] However, regulation of the phenotypic changes in VICs and the role of VICs in tissue homeostasis during healthy and pathological remodeling are poorly understood. One major problem that has hindered research into valvular homeostasis and remodeling is the lack of a suitable *in vitro* system to study VIC behavior. Culturing VICs on tissue culture polystyrene has been shown to promote myofibroblastic activation.

In addition, although animal models such as murine,[3] rabbit[8] and porcine[9] exist that simulate aortic valve disease, they often fail to develop significant stenosis which is characteristic of human aortic valve disease. Furthermore these models are mostly based on hypercholesterolemia and subsequent atherosclerosis, which currently is viewed as a different etiology to calcific aortic valve disease.[7]

In order to better understand pathologic changes in VIC phenotype several studies have utilized bio-mimetic *in vitro* model systems that support physiological quiescence of VICs and does not directly promote VIC differentiation to activated myofibroblast-like cells.[10-12] An appropriate model system would closely simulate tissue homeostasis in order to monitor changes in VIC phenotype as homeostasis is perturbed. Understanding the mechanisms involved in VIC regulation of tissue homeostasis may not only elucidate the mechanisms of valve disease but also aid in the engineering of tissue valve substitutes and development of drug screening tools.

Cell-ECM interactions are important components of VIC regulation, with biomechanical signaling from deformation or changes in mechanical stiffness of the ECM playing a key role in modulating VIC phenotype.[13] External mechanical forces such as shear stress, pressure, and stretch are transmitted through the ECM to the VICs likely elicit cellular responses that drive homeostasis and disease.[14] Similarly, the intrinsic stiffness of the ECM can regulate cell function and modulate the response of VICs to other environmental stimuli. Cells can sense the local stiffness of the ECM by pulling on the substrate at focal adhesions.[15, 16] Cells respond to stiffness of a substrate by altering integrin expression, focal adhesions and cytoskeletal organization to establish a force balance between the resistance provided by the substrate and the cell-generated traction force.[17] In turn these processes

regulate intracellular signaling pathways, making cells sensitive to the surrounding stiffness.[18] To this point, 2D *in vitro* studies with VICs cultured on tunable substrates have predominantly shown myofibroblast-like differentiation on stiffer substrates.[10, 13] However, VIC activation has recently also been shown to occur in on soft substrates, with a phenotypic change threshold value at ~15kPa.[10] Therefore, further characterization of VIC responses to substrate mechanics is needed to understand the process of myofibroblast differentiation. Most knowledge on this interaction is based on 2D-culture studies, which are not appropriate representations of the *in vivo* microenvironment.

Hydrogel-based 3D culture platforms can provide for a more tissue-like environment to study VIC behavior due to their potential to mimic the natural ECM of specific tissues. Previously, VICs have been cultured within 3D matrices derived from natural ECM polymers such as commonly used collagen and fibrin.[19, 20] Although these matrices are able to facilitate good viability, collagen and fibrin gels seeded with VICs are increasingly susceptible to degradation and compaction, due to the contractile nature and expression of remodeling enzymes by activated VICs.[21] In addition, natural protein-based gels may initiate various cell-signaling cascades and are associated with sequestering growth factors and cytokines from media, providing for added complexity in isolating specific material-guided effects on VIC function over time. To this end, photocrosslinking has been used to engineer controllable and tunable hydrogels from naturally derived ECM polymers.[22, 23] Using modified naturally derived polymers such as gelatin or hyaluronic acid, cells can be encapsulated under relatively mild conditions, limiting cell damage.[24-26] Methacrylated gelatin (GelMA)[23] has successfully been used as a platform to investigate VIC fate,[25] which suggests the potential of this material for development of heart valve-like culture models. However, GelMA alone is a relatively weak material that quickly degrades even without cells, and thus poses challenges to longer experimental times. Furthermore, GelMA is susceptible to contraction by myofibroblast-like cells, which warrants the addition of another polymer component to strengthen this hydrogel network. Methacrylated hyaluronic acid (HAMA) has similarly been explored as a photocrosslinkable material for VIC-laden hydrogels.[26, 27] Hyaluronic acid is an important ECM of the adult heart valve and is a vital component of the cardiac jelly during heart embryogenesis. Therefore, hyaluronic acid is a critical ECM component needed to create a physiological representative environment to study VIC behavior. However, HAMA-based hydrogels have demonstrated limited cell adhesiveness, which results in restricted cell spreading.[26, 28] Conversely it has been shown that by adding HAMA to collagen, the formation of a collagen fiber network is altered to such an extent that the compaction of gels is impaired, compared to collagen gels alone.[29] In addition due to the slow degradation of HAMA,[30] it may increase the structural integrity of the hydrogel for long experiments.

In this paper we aimed to combine the unique advantages of GelMA and HAMA, two naturally derived materials, into a hybrid hydrogel platform, which is more analogous to the native valve ECM environment. By changing the concentration of polymers in the hydrogels, we aimed to develop a platform that could be used to maintain quiescence of VICs and study the effect of various environmental cues on VIC differentiation into myofibroblast-like cells. Such a platform may be a

useful tool to understand valvular pathobiology, and importantly aid in the development of drug discovery platform.

METHODS

Synthesis of materials

HAMA was synthesized as described previously.[31] Briefly, methacrylic anhydride (Sigma-Aldrich, St. Louis, MO) was added to a solution of 1 wt% hyaluronic acid (53 kDA, Lifecore Biomedical, Chaska, MN) in distilled water. The pH was adjusted to 8 using 5M NaOH (Sigma-Aldrich, St. Louis, MO) and kept on ice during the reaction for 24 hours. The HAMA solution was dialyzed against deionized water for 72 hours after which lyophilization was performed, resulting in a solid white foam-like material that was stored at -80°C prior to experimental use. The methacrylation degree of ~20% was determined by ^{1}H NMR

The synthesis of GelMA has also been reported before.[23, 32] Powdered type A cell culture tested gelatin from porcine skin (Sigma-Aldrich, St. Louis, MO) was dissolved in phosphate buffered saline and heated at 60°C under continuous stirring for 20 minutes to obtain a 10 wt% gelatin solution. After dropwise addition of 8% (v/v) methacrylic anhydride under constant stirring for 3 hours at 50°C, GelMA solution was diluted and dialyzed against deionized water at 40°C for one week. This yielded a methacrylation degree of ~80% as determined by ^{1}H NMR. Finally, the solution was lyophilized for one week, yielding a white porous foam-like substance, which was stored at −80°C before experimental use.

Hydrogel fabrication

Hydrogels were fabricated from HAMA and GelMA using photocrosslinking (Figure 1A-C). First, a 0.5% photoinitiator (PI) solution was prepared by dissolving 5mg PI (Igracure 2595) in 1 mL of phosphate buffered saline (PBS; Gibco) at 80°C. Solutions of 1wt% HAMA, 2 wt% HAMA and 5wt% GelMA, 10wt% GelMA, 1wt% HAMA-5wt% GelMA, and 2wt% HAMA-10wt% GelMA with 1 mL PI solution were placed in an 80°C oven for 20 minutes to yield respective prepolymer solutions. Hydrogels were formed by pipetting 50 µl of prepolymer solution between two 450 µm spacers and exposed to 2.5 mW/cm^2 UV light (Omnicure S2000, EXFO Photonic Solutions Inc., Ontario, Canada; wavelength 320–480 nm) for 30 seconds. The exposure to light facilitates crosslinking of the polymers in the solution yielding a disc shaped hydrogel with a height of 450 µm (Figure 1A-C). Unreacted polymer was then rinsed away with PBS.

Hydrogel Characterization

The porosity of the hydrogel conditions was visualized using scanning electron microscopy (SEM) (Cold field-emission gun scanning electron microscope (FEG-SEM), JEOL 6700F)). Samples were prepared by freezing fully hydrated hydrogels in liquid nitrogen followed by lyophilization. The

samples were broken in half to allow for imaging of cross-sections. The lyophilized samples were then coated with Pt/Pd before imaging. Pore size was quantified by determining equivalent circle diameter (ECD) with Image J of at least fifty pores from five SEM images made from three hydrogels per condition. Porosity was also examined using swelling analysis. Photocrosslinked hydrogels were placed in Eppendorf tubes containing 1mL of PBS for 24 hours to reach equilibrium swelling. The wet weight of the swollen hydrogels was determined after gently blotting excess liquid with kimwipes. The hydrogels were frozen and lyophilized to enable the measurement of the dry weight. Swelling ratio was determined by calculating (wet weight – dry weight) / dry weight. Five replicates were made for each hydrogel composition. For mechanical testing, 100 µl prepolymer solution (0.5% PI) was added between 1mm spacers and exposed to 90 seconds of 2.5mW/cm^2 UV light. After rinsing with PBS, hydrogels were stored in PBS at 4°C for 24 hours. Prior to mechanical testing, hydrogels were punched with an 8mm biopsy punch and excess liquid was removed. A strain rate of 0.2 mm/min was applied using an Instron 5542. The compressive modulus (kPa) was determined by taking the slope in the linear section of stress-strain curve at 10-15% strain area. Five hydrogels were tested for each condition.

Valvular Interstitial Cell isolation and culture

Aortic valve leaflets were obtained from hearts of 10 month old pigs sacrificed at a USDA approved abattoir (THOMA Meat Market, Saxonburg, PA). Within 3 hours after dissection valve surfaces were scraped to remove endothelial cells. VICs were isolated from valve leaflets using collagenase A (Sigma, St. Louis, MO) digestion. Cells were cultured in normal growth medium containing Dulbecco's modified Eagle's medium (DMEM) with 10% fetal bovine serum and 1% penicillin/streptomycin (Invitrogen, Grand Island, NY). Cells between passage 3 and 6 were used for all experiments. After culture, VICs were encapsulated in microengineered hydrogel constructs and cultured for up to 21 days at 37°C, 5% CO_2.

VIC Encapsulation

Prepolymer solutions were prepared for each condition as described above. The solutions were vortexed regularly. The polymer solution was then allowed to cool to 37°C. VICs at 80% confluency were trypsinized and centrifugated at 1500 rpm for 5 minutes. The supernatant was aspirated and the remaining cell pellet was resuspended in the prepolymer solution at a density of 10 million cells/mL. Fifty µL of the cell-laden prepolymer solution was dropwise added to a petri-dish between two spacers with a height of 450 µm and covered with an autoclaved sterile glass slide. The cell-laden solution was then subjected to 2.5 mW/cm^2 UV light (Omnicure S2000, EXFO Photonic Solutions Inc., Ontario, Canada; wavelength 320–500 nm) for 30 seconds, resulting in photocrosslinked VIC-laden hydrogel (Figure 1 A-C). The hydrogel was removed from the glass slide and put into a well plate containing normal growth medium. For selected experiments, Transforming Growth Factor β1 (TGFβ1) (R&D systems, Minneapolis, MN) was added at a concentration of 5 ng/mL. Medium was changed every 48 hours.

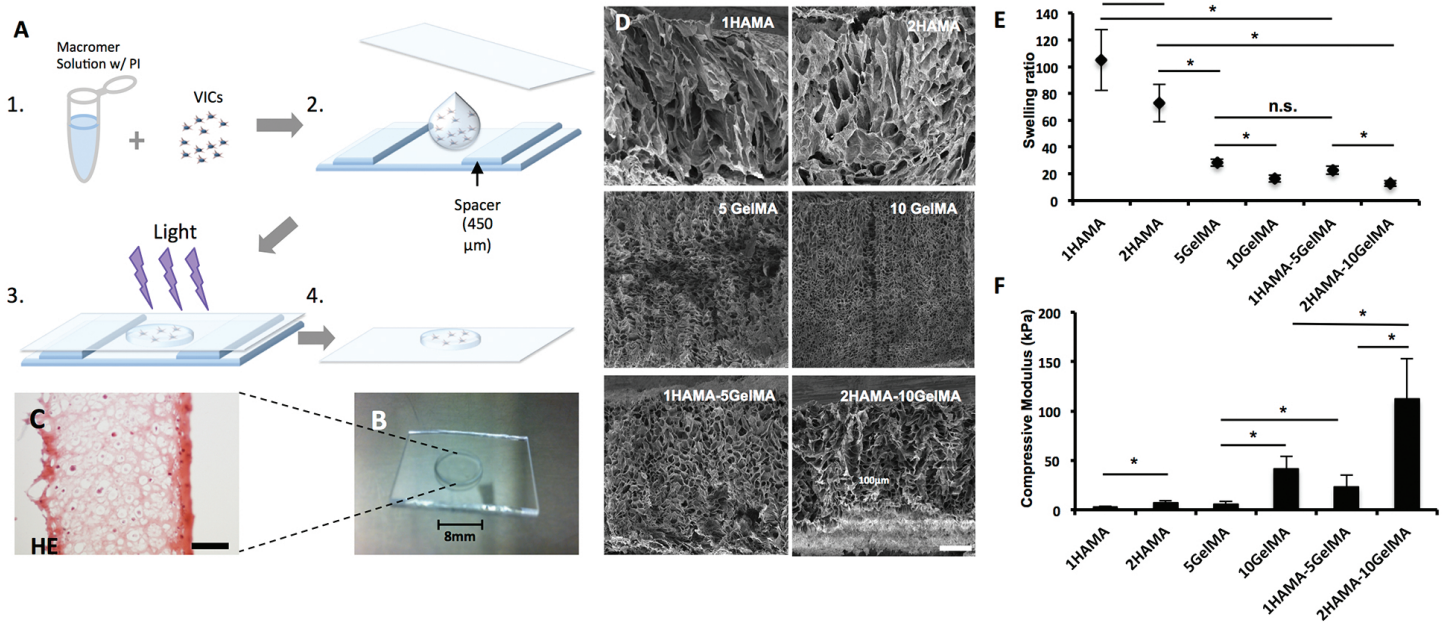

Figure 1. Microfabrication and characterization of VIC-laden hydrogels. (A) VICs are isolated and resuspended in macromer solution, which consists of HAMA and/or GelMA in 0.5% Photo-initiator (Igracure 2595) solution. Fifty µl pre-polymer solution is put onto a sterile mold between two spacers of 450 µm and covered with sterile glass slide, which is subsequently crosslinked by exposure to light (365nm) for 30 seconds at intensity of 2.5mW/cm^2. Cell-laden hydrogels are removed from the glass slide and cultured according to protocol. **(B)** Hematoxylin and Eosin stain of VIC-laden hydrogel. **(C)** Macroscopic image of VIC-laden hydrogel on glass slide. **(D)** Scanning Electron Microscopy (Ultra 55, Carl Zeiss, NY, USA, 5.0 kV) images of different hydrogel compositions. Bar: 100 µm. **(E)** Swelling ratio of hybrid hydrogels (Swelling Ratio = Wet Weight –Dry Weight/ Dry Weight). **(F)** Compressive modulus was calculated using compressive uniaxial test. 2% (w/v) HAMA-10% (w/v) GelMA demonstrated the highest modulus. Data is depicted as mean ± SD, *p <0.05.

Cell viability, proliferation and apoptosis

Cell viability was determined by fluorescent labeling with 4μM Calcein AM and 2μM Ethidium Homodimer-1 (LIVE/DEAD Viability kit for mammalian cells, Invitrogen). Cell-laden hydrogels were first washed with PBS for 5 minutes and then incubated with fluorescent dye for 20 minutes at room temperature. The cell-laden hydrogels were then washed with PBS and imaged using a confocal microscope (Nikon Instruments, Inc. A1/C1 Confocal Microscope). Three hydrogels were analyzed each time point for each condition. Of each hydrogel 3 z-stacks (10 μm per slice) were made of which a compressed image was formed. Viable cells were stained green and dead cells red, and the numbers of each type were manually counted using Image J Software. Data is depicted as percentage of live cells. To quantifiably analyze spreading of encapsulated VICs, mean cell surface area was determined from 3D reconstruction of the confocal z-stacks using MATLAB.

Proliferation of VICs encapsulated in the hydrogels, was assessed by EdU labeling. EdU binds to cell nuclei when they are in the S-phase of the cell cycle, making it highly specific assay for proliferation. First, VIC-laden hydrogels were incubated with 10 μM EdU for 12 hours on day 1, 7, 14 and 21. Samples were then fixed and permeabilized using a Fixation and Permeabilization kit (Invitrogen/ Life technologies) and subsequently washed with a 1% BSA solution in PBS, after which constructs were incubated with Click-iT solution (350 μl) from the Click-iT EdU Alexa Fluor 488 kit (Invitrogen/ Life technologies) for 30 minutes at room temperature. Cell nuclei were counterstained with DAPI. Cell-laden hydrogels were then analyzed by confocal microscopy. Three z-stacks were made per cell-laden hydrogel. Proliferation was assessed by Image J quantification of positively labeled cells of compressed images of the z-stacks. VICs in culture for 24 hours were stained at the same time using similar protocol for positive control. Three hydrogels were analyzed for each time point per using an EdU labeling kit (Invitrogen). Data is depicted as mean percentage of proliferating cells and mean cell number per high power field (HPF) magnification (x20).

Apoptosis was determined by TUNEL (terminal deoxynucleotidyl transferase mediated dUTP nick end labeling) staining (Millipore, Remecula, CA, USA), according to the manufacturer's protocol and quantified using fluorescence microscopy. Data are depicted as percentage of positively stained cells.

Histological evaluation of 3D cell-laden hydrogel constructs

Cell-laden hydrogels were washed with PBS for 5 minutes and then fixed in 4% paraformaldehyde for 20 minutes, followed by PBS wash. The hydrogels were kept in a 30 wt% sucrose solution overnight at 4°C, after which they were frozen in OCT compound (Sakura Finetech, Torrance, CA) and 10 μm sections were cut. For comparison, VICs cultured in 2D on TCPS were fixed after 24 hours in 4% paraformaldehyde for 15 minutes followed by PBS wash.

Immunofluorescence staining for alpha-smooth muscle actin (α-SMA), vimentin, matrix-metalloproteinase-9 (MMP-9) and Collagen type I (Col-I) was performed. VIC-laden hydrogel sections and VICs (2D) were permeabilized using 0.1% Triton-X. After blocking in 4% horse serum, sections were incubated with monoclonal mouse anti α-SMA primary antibody (Clone 1A4, Dako, Dako Denmark

A/S, Glostrup, Denmark), a monoclonal mouse anti-vimentin primary antibody (Abcam, Cambridge, USA), a monoclonal mouse anti-MMP9 (Santa Cruz), or a monoclonal mouse-anti COL-1 (Abcam, Cambridge, USA) for 90 minutes at room temperature (RT), followed by biotin labeled secondary antibody (Vector Labs, Burlingame, CA, USA) for 45 minutes at RT and streptavidin labeled AlexaFluor 488 (Invitrogen, Grand Island, NY, USA) for 20 minutes at RT. Sections were washed three times in PBS for 5 minutes and nuclei were counterstained with DAPI containing mounting medium (Vector Labs, Burlingame, CA, USA). Images were taken with an Eclipse 80i microscope (Nikon, Melville, NY, USA) and processed with Elements 3.20 software (Nikon, Melville, NY, USA). Positive staining was quantified by manually counting positively stained cells of the total cell number in five high power fields (HPF) per hydrogel. Three hydrogels were quantified per condition per time point.

Real Time Polymerase Chain Reaction for expression of cell markers

RNA from encapsulated VICs were isolated from cell-laden hydrogels by mechanical disruption of the hydrogels (TissueLyzer, Qiagen, Germany). Total RNA was isolated from using GE Healthcare RNAspin mini RNA Isolation kit. The amount of RNA in each sample was measured using NanoDrop 2000c (ThermoScientific). Total RNA was reverse transcribed with oligo-(dT)12-18 primers(Invitrogen/Life Technologies, Grand Island, NY, USA) and Superscript II reverse transcriptase (Invitrogen/Life Technologies, Grand Island, NY, USA) to obtain a target cDNA concentration of 0.335ug/mL followed by RT- PCR using SYBR Green (BioRad, Hercules, CA, USA), and annealing temperatures of 95 and 60 degrees Celsius for 35 cycles. Primer sequences were designed with Primer3 software and were as follows: α-SMA: F:5'-AGTGCGACATTGACATCAGG-'3 and R:5'-CTGGAAGGTGGACAGAGAGG-'3, Vimentin F:5'-AGCAGTATGAGAGTGTGGCC-'3 and R:5'-CTTCCATTTCCCGCATCTGG-'3, MMP-9 F:5'GGTGGACTATGTGGGCTACG-'3 and R:5'- AGTGCTGAAGCAGGACGAG-3', and Collagen type 1 F:5'CCAAGAGGAGGGCCAAGAAGAAGG-'3 and R:5'-GGGGCAGACGGGGCAGCACTC-'3. The housekeeping gene used was glyceraldehyde-3-phosphate dehydrogensase (GAPDH): F:5'-CCCAGAAGACTGTGGATGG-'3, R:5'- ACCTGGTCCTCAGTGTAGCC-'3. Expression was quantified using comparative Ct (Cycle threshold method $2^{-\Delta\Delta\ CT}$ method) with the following equations: (1) ΔCT =CT of target gene –CT of housekeeping gene, (2) ΔΔCT=ΔCT day x – ΔCT day 1; (3) Fold increase between groups = $2^{-\Delta\Delta Ct}$

Statistical Analysis

Results are presented as mean +/- standard deviation unless indicated otherwise. One- way ANOVA was used to evaluate statistical significant differences in multiple groups. $P < 0.05$ was considered significant.

RESULTS

Material characteristics of hydrogel compositions

Scanning electron microscopy (SEM) images of cross-sections of the various single component hydrogel conditions demonstrate different porosities characteristic of each hydrogel condition (Figure 1D). These images revealed that pore sizes decrease with increased hydrogel macromer concentrations. Significant differences are observed in the swelling ratio of each hydrogel condition, indicating that porosity is tunable by varying the concentration of polymer in the hydrogel (Figure 1E). Increasing the concentration of 1% (w/v) HAMA to 2% (w/v) HAMA resulted in a significant decrease in the swelling ratio of approximately 30%, ($p < 0.05$). A similar decrease of 30% ($p < 0.05$) occurred with an increased macromer concentration from 5% (w/v) GelMA to 10% (w/v) GelMA. In addition, GelMA hydrogels proved to be less porous than HAMA hydrogels ($p<0.05$).

The swelling ratios of the hybrid hydrogels 1% (w/v) HAMA – 5% (w/v) GelMA and 2% (w/v) HAMA – 10% (w/v) GelMA were 22±3 and 12±2, respectively. As such, when combining these HAMA and GelMA polymers together their swelling ratios are close to their separate GelMA counterparts 5% (w/v) (23±10) and 10% (w/v) GelMA (16±2). Notably, there is a significant difference in swelling ratio between 10% (w/v) GelMA and 2% (w/v) HAMA – 10% (w/v) GelMA; however, there is no significant difference ($p = 0.45$) in swelling ratio between the 1% (w/v) HAMA - 5% (w/v) GelMA hybrid and 5% (w/v) GelMA only. Pore sizes were also quantified using SEM images to determine equivalent circle diameter (ECD) (Supplemental Figure I), which also revealed no significant difference between 5% (w/v) GelMA hydrogels and 1% (w/v) HAMA - 5% (w/v) GelMA hydrogels.

An increase in HAMA or GelMA concentration facilitated an increase in compressive moduli. Similarly, we observed elevated hydrogel stiffness – described as compressive modulus - with increased total concentration of polymers in hybrid hydrogels (Figure 1F). As such, 2% (w/v) HAMA-10% (w/v) GelMA demonstrated the highest compressive modulus compared to all other conditions ($p<0.05$). All conditions were significantly different ($p < 0.05$). These results verify the inverse relationship of porosity and stiffness of the independent HAMA and GelMA-based hydrogels with increasing the polymer concentrations. However, although we observed a significant increase in stiffness when HAMA is added to GelMA, a relative small and non-significant change in porosity occurs.

VIC viability, spreading and proliferation in hydrogel composites

After 21 days of culture, VICs encapsulated in the various hydrogel conditions were evaluated for cell viability and compared to day 1. Figure 2A depicts representative cross-sections of the middle portion of the hydrogel from z-stacks obtained by confocal microscopy after live/dead staining. Overall, cell viability remained high (> 80%). However, VICs encapsulated in 2% (w/v) HAMA – 10% (w/v) GelMA hydrogels were less viable compared to 1% (w/v) HAMA – 5% (w/v) GelMA hydrogels (77.7±6.1 vs. 87.4±2.4, $p < 0.05$) (Figure 2B). In addition, TUNEL staining performed on sections of VIC-laden hydrogels at day 21 demonstrated no apoptotic cells compared to positive control (Supplemental Figure II). Notably, as visualized by live/dead staining, VICs seemed to spread more

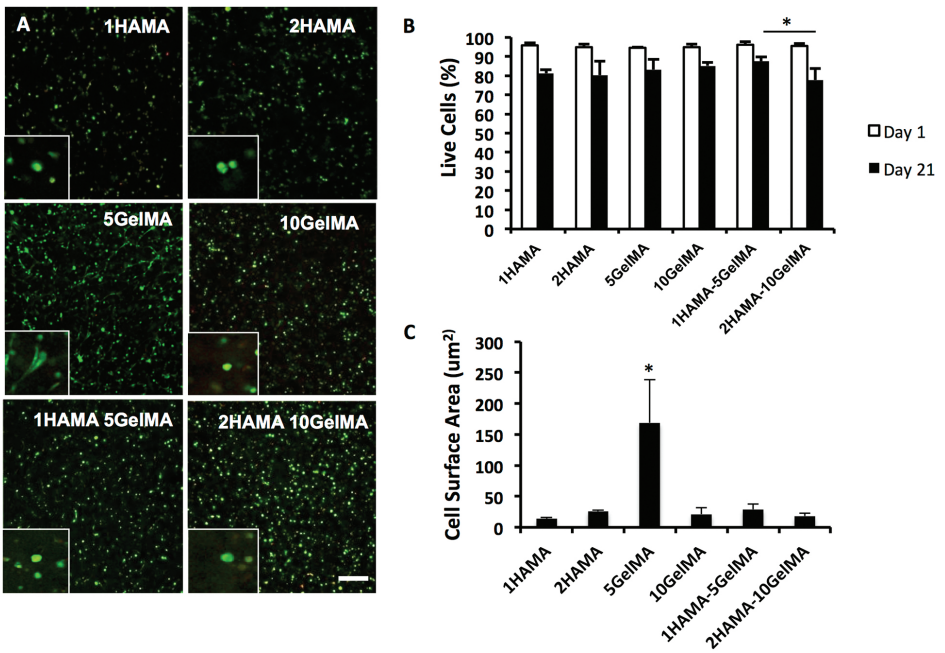

Figure 2. Hydrogel conditions maintain high viability and affects spreading. VIC-laden hydrogels were cultured up to 21 days. **(A)** Representative confocal images of live/dead stain of hydrogel conditions at day 21; bar: 50 µm. **(B)** Quantification of % live cells as determined from confocal z-stacks made from hydrogels (n=3). **(C)** Quantification of cell spreading per hydrogel condition (mean cell surface area). Data is depicted as mean ± SD. * $p < 0.05$.

when encapsulated in 5% (w/v) GelMA hydrogels (Figure 2A). This is confirmed by quantifying surface area as depicted in Figure 2C, demonstrating a significantly higher mean surface area in 5% (w/v) GelMA hydrogels (169.1±69.3 µm^2) compared to the other conditions (1% (w/v) HAMA; 13.8±2.2 µm^2, 2%(w/v) HAMA: 26.1±1.9 µm^2, 10% (w/v) GelMA: 21.4±10.4 µm^2, 1% (w/v) HAMA -5% (w/v) GelMA: 29.1±8.7 µm^2, and 2% (w/v) HAMA – 10% (w/v) GelMA: 18.3±5.0 µm^2, respectively).

Proliferation was assessed by EdU labeling. Figure 3A demonstrates representative cross-sections of the middle of the hydrogel as imaged by confocal microscopy. The bottom panels demonstrate control images of the cells populating the surface of 5% (w/v) GelMA and a positive control, which was obtained after 24 hours of culture in normal growth media after seeding. Using z-stack analysis of EdU labeled cells in hydrogels allows for evaluating proliferation of encapsulated cells.

The percentage of EdU expressing cells in 1% (w/v) HAMA was 61±13% after 1 day and 47±8% after 21 days of culture, but was not statistically significant. In 2% (w/v) HAMA hydrogels, VICs expressing EdU remained similar after 21 days of culture (day1:42±7%, day 21 46±9%). However in 5% (w/v) GelMA there was a significant decrease in EdU expression at day 7 (32±4%), day 14 (35±7%), day 21 (30±9%) compared to day 1 (47±8%), $p < 0.05$). In addition, the amount of VICS encapsulated in 5% (w/v) GelMA labeled with EdU were significantly lower at days 14 and day 21 compared to VICs encapsulated in all other hydrogel conditions ($p<0.05$). EdU expression in 10%

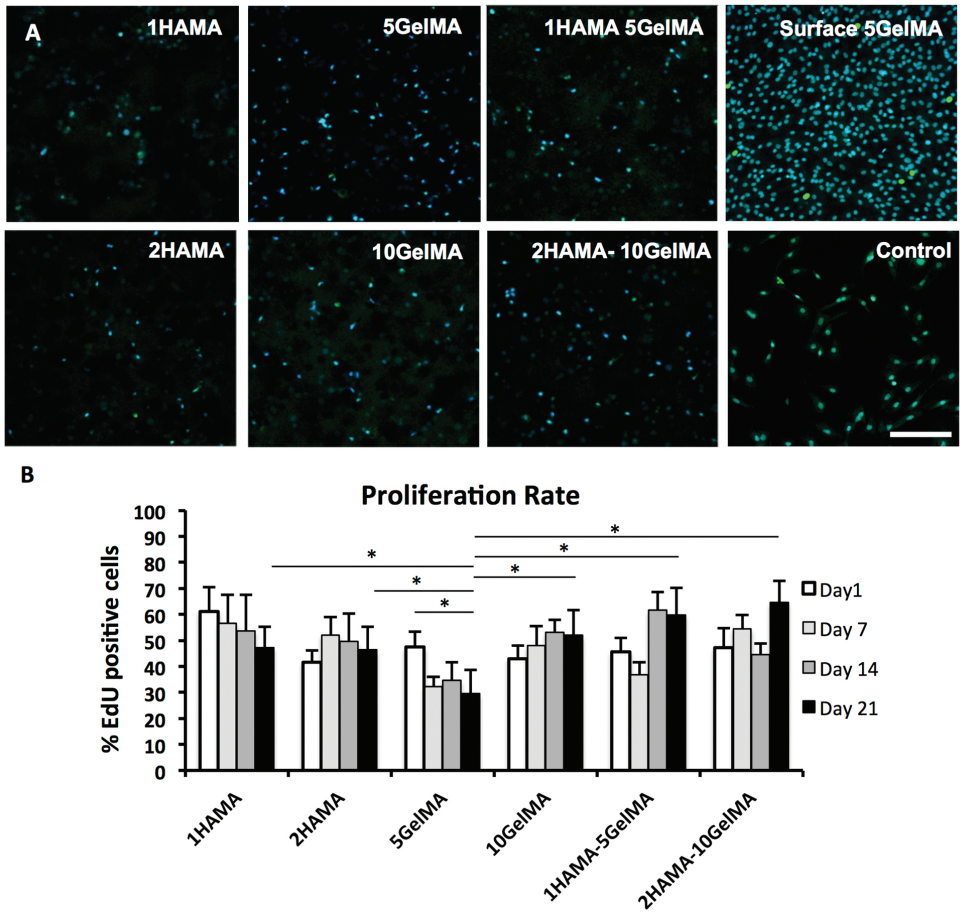

Figure 3. Proliferation of encapsulated VICs. VIC-laden hydrogels were cultured up to 21 days and analyzed for proliferation. **(A)** Representative confocal images of EdU click-it labelling of encapsulated VICs. Image of cells on surface of 5% (w/v) GelMA. Positive control was obtained by culturing VICs for 24 hours in medium containing 10% FBS. bar: 50 um **(B)** Quantification of encapsulated proliferating cells as determined by positive EdU labelling in different hydrogel conditions at day 1, day 7, day 14 and day 21, (n=3). **(C)** Amount of cells per high power field (HPF) as determined by positive DAPI staining. (N=3) Data is depicted as mean ± SD. *p<0.05.

(w/v) GelMA remained statistically similar after 21 days of culture. 1% (w/v) HAMA -5% (w/v) GelMA cell-laden hydrogels demonstrated EdU expressing VICs of day 1: 45±5%, day 7: 37±5%, day 14: 61±7% and day 21: 60±11%, where days 14 and 21 were significantly increased compared to days 1 and 7 ($p<0.05$).

Upon the number of cells stained for DAPI per high power field (x20), we observe a significant decrease of in 1% (w/v) HAMA hydrogels after 21 days (286±49) of culture compared to day 1 (120±10), ($p <0.05$). A similar trend is observed in 2% (w/v) HAMA hydrogels with a decrease of cell number after 21 days of culture (302±31 vs. 158±8, $p<0.05$). In 5% (w/v) GelMA hydrogels we observed an initial drop of cell number after day 1, but at day 21 the amount of cells is relatively similar (315±55 vs. 351±38, $p>0.05$). 10% (w/v) GelMA hydrogels demonstrated a decrease in cell

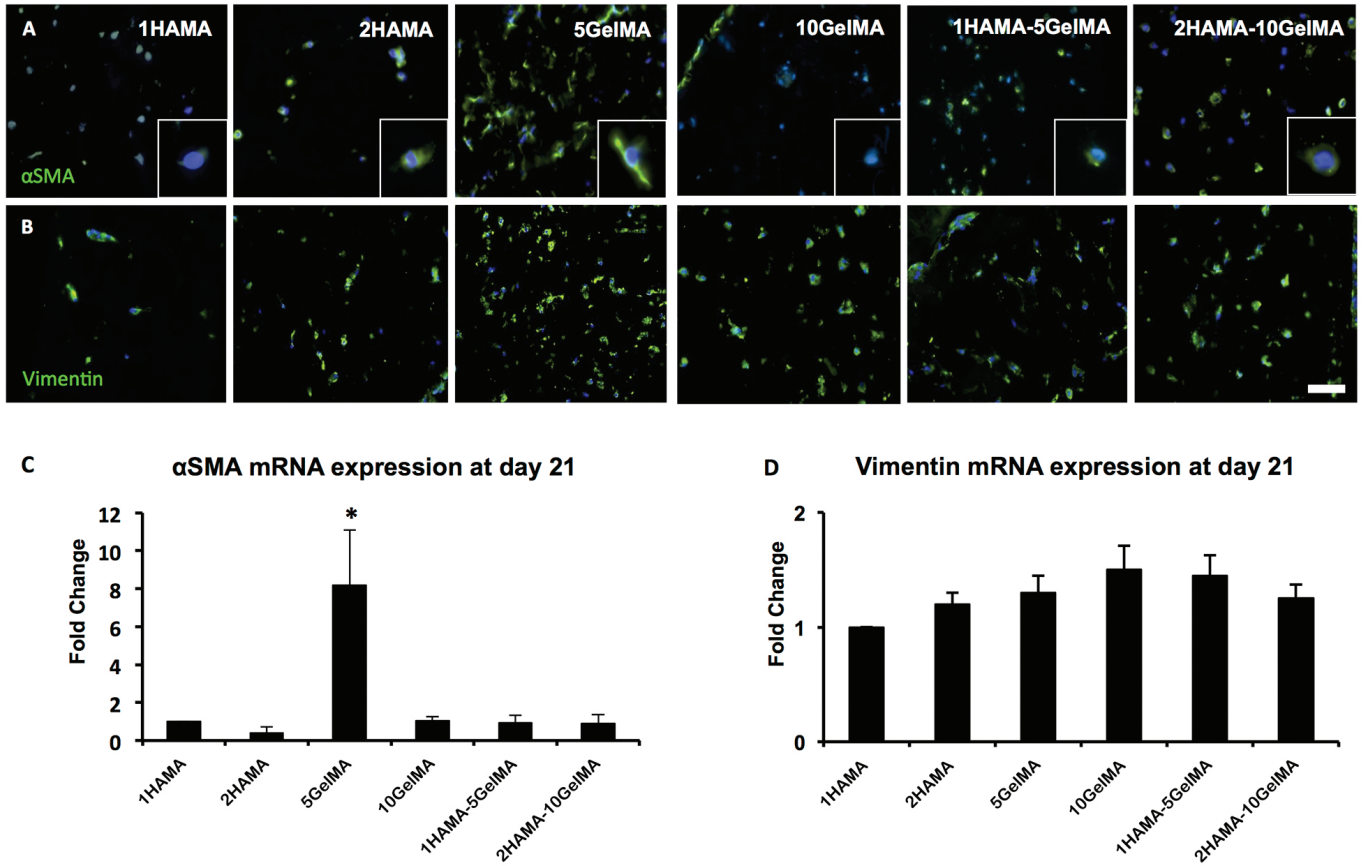

Figure 4. Hydrogel composition affects myofibroblast-like phenotype of VICs at day 21. (A) Immunofluorescence staining of alpha smooth muscle actin (α-SMA) in all VIC-laden hydrogel conditions. α-SMA: green, nuclei: blue, Inserts: 40x, **(B)** Immunofluorecence staining of vimentin; Vimentin: green, nuclei: blue, bar: 50μm **(C)** mRNA expression assessed by RT-PCR of αSMA and **(D)** vimentin. Expression is depicted as mean ± SD fold change to 1% (w/v) HAMA. *$p < 0.05$.

number after 21 days, p <0.05 similar to 1% (w/v) HAMA – 5% (w/v) GelMA where cell number decreased after 21 days of culture from 366±31 to 265±28, p<0.05). Cell number remained similar during culture in 2% (w/v) HAMA – 10% (w/v) GelMA: day 21: 332±31 vs. 372±36, p>0.05.

VIC cellular behavior in response to hydrogel composition

After 21 days of culture, encapsulated VICs were analyzed for their phenotypic responses to the hydrogel conditions. VICs demonstrated a myofibroblast-like phenotype characterized by positive immunofluorescence staining of α-SMA in 5% (w/v) GelMA hydrogels (Figure 4A). VICs in these gels exhibited a spread-like morphology (Figure 4A inserts) compared to VICs cultured in all other hydrogels. This phenotypic differentiation was confirmed by RT-PCR (Figure 4C) showing a significant increase in α-SMA mRNA expression of VICs in 5% (w/v) GelMA hydrogels (8.2±2.9, p < 0.05) relative to VICs encapsulated in 1% (w/v) HAMA. Vimentin, a general mesenchymal cell marker, was positively expressed by VICs in all hydrogel conditions (Figure 4B) and similarly confirmed by no significant change in mRNA expression across all groups (Figure 4D), indicating that VICs remain quiescent fibroblast-like cells in most hydrogel conditions when cultured in normal media. In contrast, VICs cultured on TCPS (2D) mostly exhibited myofibroblast-like differentiation indicated by positive α-SMA and Vimentin stain. (Supplemental Figure III)

However 5% (w/v) GelMA hydrogels seem to facilitate myofibroblast-like differentiation of VICs. In addition to elevated α-SMA, VICs in 5% GelMA exhibit an increased expression of MMP-9 as demonstrated by immunofluorescence (Figure 5A) and mRNA expression (fold change compared to 1% (w/v) HAMA: 4.4±0.7, p<0.05) (Figure 5C). Similarly VICs encapsulated in 5% (w/v) GelMA hydrogels exhibit increased expression of collagen type 1 (Figure 5B). RT-PCR quantification of collagen type 1 mRNA expression revealed (Figure 5D) a similar fold change compared to 1% (w/v) HAMA of all conditions containing GelMA (p > 0.05).

Quiescent VIC to activated VIC myofibroblast-like differentiation

After observing the quiescent nature of VICs in the hybrid hydrogels, we added TGFβ at 5ng/mL to the culture medium for 21 days to 1% (w/v) HAMA – 5% (w/v) GelMA hydrogels. We detected activated VICs encapsulated in 1% (w/v) HAMA – 5% (w/v) GelMA hydrogels as depicted by positive immunofluorescence staining of α-SMA, vimentin, MMP-9 and Col1A1 similar to results for 5% (w/v) GelMA alone (Figure 6A). In addition, mRNA expression levels of α-SMA (41.8±4.1) vimentin (4.5±0.3), MMP-9 (6.7±1.1) and COL1A1 (14.9±2.3) were increased compared to control medium, indicating a myofibroblast-like differentiation of encapsulated VICs in the 1% (w/v) HAMA – 5% (w/v) GelMA hydrogels when stimulated with TGFβ1 (Figure 6B).

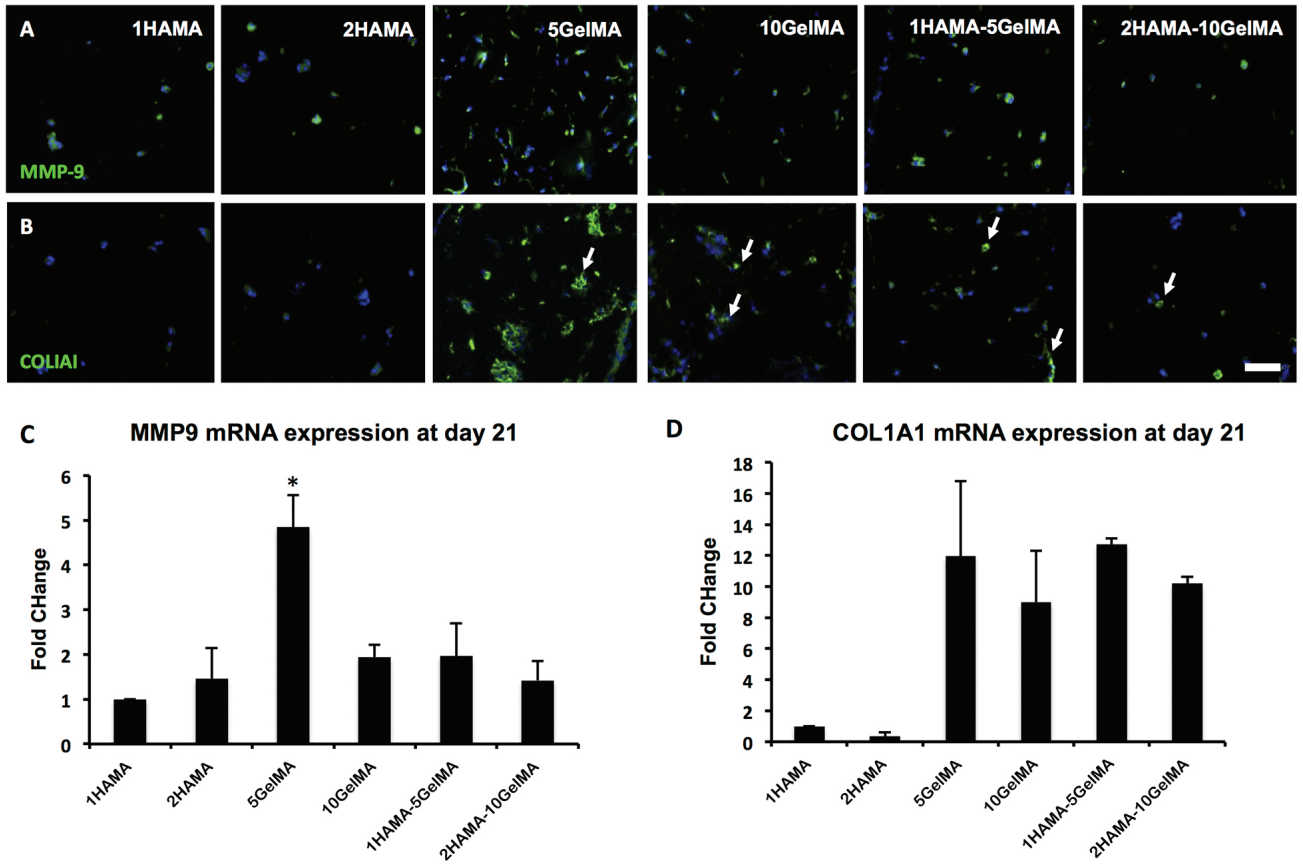

Figure 5. Hydrogel composition affects VIC behavior at day 21. (A) Immunofluorescence staining of metallomatrixproteinase-9 (MMP-9), MMP9: green, nuclei: blue **(B)** Immunofluorecence staining of collagen type 1 (COL1A1), COL1A1: green, nuclei: blue **(C)** mRNA expression assessed by RT-PCR of MMP-9. **(D)** Collagen type I (COL1A1). Expression is depicted as mean ± SD fold change to 1% (w/v) HAMA .* $p < 0.05$.

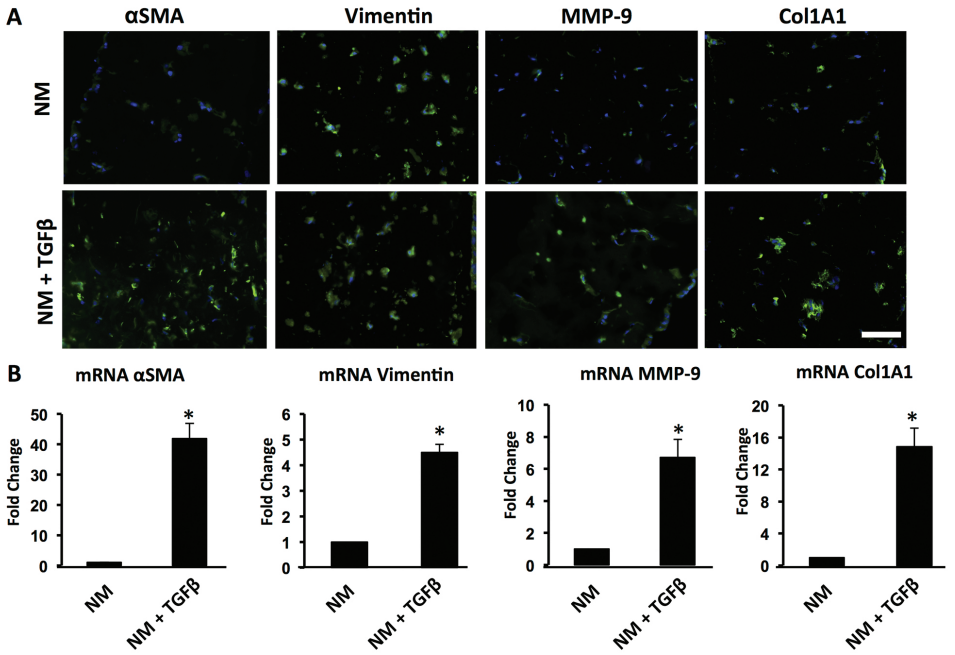

Figure 6. Activation of quiescent VICs by TGFβ. TGFβ1 was exogenously added to VICs cultured in 1% (w/v) HAMA – 5% (w/v) GelMA. **(A)** Immunofluorescence (αSMA, Vimentin MMP-9 COL1A1 = green, nuclei=blue) bar: 50 μm. **(B)** RT-PCR of mRNA expression of αSMA, Vimentin, MMP-9, COL1A1. Data is depicted as mean fold change ± SD compared to control (normal media), * $p < 0.05$.

DISCUSSION

Engineered 3D culture platforms, such as hydrogels have emerged as powerful tools to understand valvular biology, as they potentially provide physiologically relevant environments.[22] Hydrogel systems allow for the creation of tunable 3D environments, by changing their parameters to regulate cellular responses. This has become particularly important for studying valve biology *in vitro*, since VICs cultured on stiff tissue culture plates spontaneously develop an activated myofibroblast-like phenotype, characteristic of a 'disease'-like state.

By using naturally derived polymers, which are present in the native heart valve ECM, we aimed to develop a more physiologically relevant culture platform for VICs. In this study, we developed a tunable 3D hydrogel platform to analyze the phenotypic changes of VICs in response to hydrogel composition. We have demonstrated that by changing the relative concentrations of HAMA and GelMA separately within hybrid hydrogels, we can induce changes in hydrogel properties. Varying polymer concentrations in hydrogels demonstrated a consistently high viability of encapsulated VICs. However, proliferation rate was significantly decreased in 5% (w/v) GelMA hydrogels. VICs encapsulated in these hydrogels demonstrated a spread-like morphology, which was absent in other conditions that demonstrated a more rounded cell morphology. Our data indicated that VIC activation and subsequent myofibroblast-like differentiation only occurred in the relatively soft 5%

(w/v) GelMA hydrogel environment. When HAMA is added to the 5% (w/v) GelMA hydrogels, VICs remain quiescent. However, the addition of TGFβ1 to the VICs within 1% (w/v) HAMA-5% (w/v) GelMA hydrogels led to myofibroblast-like differentiation. These results indicate, that hybrid hydrogels can be used to maintain VICs in a quiescent phenotype, which can controllably be activated to undergo myofibroblast-like activation. Hence, hybrid hydrogels provide for a platform to study VIC phenotypic changes as they may occur in the heart valve.

The results of this study extend the evidence that VIC myofibroblast-like differentiation is not solely driven by increased stiffness as is observed in tissue culture,[11, 13, 33] but that also more compliant microenvironments can facilitate VIC activation. Interestingly, the aortic heart valve leaflet was initially considered to have a relatively stiff modulus of 1.74±0.29 MPa,[34] which seemed to increase while the valve becomes more fibrotic over time, driving observed myofibroblast-like differentiation of VICs *in vivo*. However, recent evidence has demonstrated that the modulus of the valve ECM may be layer specific, as the aortic valve leaflet consists of three distinct ECM layers characterized by specific ECM proteins; the *zona fibrosa*, which predominantly consists of collagen, *zona spongiosa*, mostly containing GAGs, and the *zona ventricularis*, characterized by elastin.[2] Micropipette aspiration indicated that the modulus of the *zona ventricularis* was ~ 3kPa and the *zona fibrosa* was ~ 5 kPa.[35] In our study, 5% (w/v) GelMA hydrogels demonstrated a modulus of 5.7±2.3 kPa corresponding to the modulus of the *zona fibrosa*. Considering that pathological changes, including calcification preceded by myofibroblast-like differentiation of VICs, most often occur in the *zona fibrosa*,[2] makes our 3D hydrogel platform clinically relevant.

Similar results were demonstrated by another recent study that explored the use of HAMA and GelMA as a composite hydrogel platform.[27] By altering the molecular weight of HA, Duan *et al.* varied the physical properties of their composite hydrogels. However, although an increased spread-like morphology was observed in their HAMA hydrogels containing GelMA, myofibroblast differentiation was only observed in hydrogels consisting of HAMA alone. We do not observe any myofibroblast differentiation in HAMA hydrogels. An explanation for this difference with our study might be that the difference in physical properties between our hydrogel conditions are more pronounced with moduli ranging from 5kPa to 120 kPA, leading to more apparent differences in VIC response. Further, our study indicates that quiescent VICs in hydrogels can be activated by the addition of TGFβ1. This observation is important because it indicates that these gels may be utilized as a model system to study known cytokine initiators of valve disease independently of VIC phenotypic changes caused by the culture environment.

Studies have shown that local mechanical properties of the ECM regulate cellular motility, proliferation and differentiation.[14] More specifically, cells intrinsically generate cytoskeletal tension as they exert tractional forces on the surrounding matrix; stiff matrices provide greater resistance to deformation, resulting in greater tractional forces.[14] Incorporation of α-SMA into the stress fibers aids in force generation[36] that becomes apparent when VICs are cultured on stiff tissue culture polystyrene plates. This suggests that VICs in our hydrogels would demonstrate increased α-SMA when faced with greater resistance due to stiffness.

The correlation between hydrogel stiffness and polymer crosslinking density[37] could explain the lack of myofibroblast-like differentiation in stiffer hydrogels. Decreasing polymer density and thus the number of peptides that must be cleaved to permit cell spreading and motility, could facilitate spreading and thus differentiation[23, 32] as there may be more space for VICs to extend outwards and exert tractional force. This may explain why VICs exhibit an activated phenotype in the 5% (w/v) GelMA hydrogels but are unable to spread and therefore, do not undergo the same phenotypic changes in the denser 10% (w/v) GelMA hydrogels. However, this phenomenon may also be aided by the increased degradation rate of softer, less dense 5% (w/v) GelMA hydrogels,[32] whereas 10% (w/v) GelMA hydrogels degrade slower and may thus hinder VIC myofibroblast-like differentiation and associated cell spreading. Hence, it remains to be elucidated to what extent material stiffness and degradation contribute to VIC phenotypical fate. An additional component to consider is the interaction of HA and VICs itself. Studies have shown that disruption of VIC-HA interaction may enhance myofibroblast-like differentiation of VICs, indicating HA could be crucial in maintaining a healthy quiescent VIC phenotype.[38]

After confirming a quiescent VIC phenotype in the hybrid 1% (w/v) HAMA - 5% (w/v) GelMA hydrogel, we further assessed the possibility of controllable VIC activation with biochemical cues. TGFβ1 is expressed in pathological aortic valves, and is a known potent inducer of myofibroblast differentiation of VICs both in 2D[21] and 3D cultures.[24] TGFβ1 is latent when secreted and stored in the valvular ECM. Matrix cues such as increased strain may result in the activation of TGFβ1 and subsequent myofibroblast activation of VICs. Moreover, TGFβ1 dependent induction of pathologic differentiation of VICs seems to be dependent on stretching the ECM.[39, 40] TGFβ1 is a relevant biochemical factor that may work alongside biomechanical forces in leading to VIC differentiation; however, utilizing a hybrid approach, encapsulating VICS in these hydrogels can allow for these biochemical affects to be studied specifically.

The approach to model VIC phenotypic transition in the present study is limited by the static nature of the hydrogel platform. Valves are dynamic organs exposed to repetitive strain and stress during the cardiac cycle.[2] Thus adding a dynamic component to a hydrogel platform would be warranted. In addition, a true *in vitro* valve model would also entail an endothelial monolayer as observed in the native valve. The advantage of including HAMA in a hybrid hydrogel platform is that although HA is void of cell adhesion motifs like collagen-like substrate, it is a glycosaminoglycan which is abundantly present in the *zona spongiosa* of the valve ECM,[35] which makes a hybrid hydrogel better suitable to mimic valve ECM to study VIC behavior in a 3D culture platform.

In conclusion, we have utilized the combination of naturally derived polymers HAMA and GelMA into a hybrid hydrogel platform, which can be used to study VIC phenotypic fate. By encapsulating VICs in a hybrid HAMA-GelMA hydrogel we could facilitate and maintain a quiescent VIC phenotype, which upon stimulation with TGFβ1, were able to differentiate into myofibroblast-like cells. Thus, we present here a 3D hybrid-hydrogel system that could serve as controllable model to study the transition from quiescent to activated myofibroblast-like VICs, in a more analogous *in vivo*

environment of native heart valve tissue. The results of this study may aid in the development of adequate valvular disease platforms or drug discovery tools.

ACKNOWLEDGEMENTS

The authors acknowledge the Dutch Heart Foundation (DHF) and Netherlands Scientific Council (NWO) to JH, and NIH R01HL114805 and NIH R01HL109506 to EA. AK acknowledges the Office of Naval Research Young National Investigator Award, the Presidential Early Career Award for Scientists and Engineers (PECASE), the National Science Foundation CAREER Award (DMR 0847287), and the National Institutes of Health (EB012597, HL092836, HL099073, EB008392).

REFERENCES

1. Rabkin E, Aikawa M, Stone JR, Fukumoto Y, Libby P, Schoen FJ. Activated interstitial myofibroblasts express catabolic enzymes and mediate matrix remodeling in myxomatous heart valves. *Circulation*. 2001;104:2525-2532
2. Schoen FJ. Evolving concepts of cardiac valve dynamics: The continuum of development, functional structure, pathobiology, and tissue engineering. *Circulation*. 2008;118:1864-1880
3. Aikawa E, Nahrendorf M, Sosnovik D, Lok VM, Jaffer FA, Aikawa M, Weissleder R. Multimodality molecular imaging identifies proteolytic and osteogenic activities in early aortic valve disease. *Circulation*. 2007;115:377-386
4. Aikawa E, Aikawa M, Libby P, Figueiredo JL, Rusanescu G, Iwamoto Y, Fukuda D, Kohler RH, Shi GP, Jaffer FA, Weissleder R. Arterial and aortic valve calcification abolished by elastolytic cathepsin s deficiency in chronic renal disease. *Circulation*. 2009;119:1785-1794
5. Mohler ER, 3rd, Gannon F, Reynolds C, Zimmerman R, Keane MG, Kaplan FS. Bone formation and inflammation in cardiac valves. *Circulation*. 2001;103:1522-1528
6. Otto CM. Calcific aortic stenosis--time to look more closely at the valve. *N Engl J Med*. 2008;359:1395-1398
7. Rajamannan NM, Evans FJ, Aikawa E, Grande-Allen KJ, Demer LL, Heistad DD, Simmons CA, Masters KS, Mathieu P, O'Brien KD, Schoen FJ, Towler DA, Yoganathan AP, Otto CM. Calcific aortic valve disease: Not simply a degenerative process: A review and agenda for research from the national heart and lung and blood institute aortic stenosis working group. Executive summary: Calcific aortic valve disease-2011 update. *Circulation*. 2011;124:1783-1791
8. Rajamannan NM, Subramaniam M, Stock SR, Stone NJ, Springett M, Ignatiev KI, McConnell JP, Singh RJ, Bonow RO, Spelsberg TC. Atorvastatin inhibits calcification and enhances nitric oxide synthase production in the hypercholesterolaemic aortic valve. *Heart*. 2005;91:806-810
9. Simmons CA, Grant GR, Manduchi E, Davies PF. Spatial heterogeneity of endothelial phenotypes correlates with side-specific vulnerability to calcification in normal porcine aortic valves. *Circulation research*. 2005;96:792-799
10. Kloxin AM, Benton JA, Anseth KS. In situ elasticity modulation with dynamic substrates to direct cell phenotype. *Biomaterials*. 2010;31:1-8
11. Quinlan AM, Billiar KL. Investigating the role of substrate stiffness in the persistence of valvular interstitial cell activation. *Journal of biomedical materials research. Part A*. 2012;100:2474-2482
12. Wyss K, Yip CY, Mirzaei Z, Jin X, Chen JH, Simmons CA. The elastic properties of valve interstitial cells undergoing pathological differentiation. *Journal of biomechanics*. 2012;45:882-887
13. Chen JH, Simmons CA. Cell-matrix interactions in the pathobiology of calcific aortic valve disease: Critical roles for matricellular, matricrine, and matrix mechanics cues. *Circulation research*. 2011;108:1510-1524
14. Discher DE, Janmey P, Wang YL. Tissue cells feel and respond to the stiffness of their substrate. *Science*. 2005;310:1139-1143
15. Choquet D, Felsenfeld DP, Sheetz MP. Extracellular matrix rigidity causes strengthening of integrin-cytoskeleton linkages. *Cell*. 1997;88:39-48
16. Wang HB, Dembo M, Hanks SK, Wang Y. Focal adhesion kinase is involved in mechanosensing during fibroblast migration. *Proceedings of the National Academy of Sciences of the United States of America*. 2001;98:11295-11300
17. Ingber DE. Cellular mechanotransduction: Putting all the pieces together again. *FASEB journal: official publication of the Federation of American Societies for Experimental Biology*. 2006;20:811-827
18. Tomasek JJ, Gabbiani G, Hinz B, Chaponnier C, Brown RA. Myofibroblasts and mechano-regulation of connective tissue remodelling. *Nature reviews. Molecular cell biology*. 2002;3:349-363

19. Taylor PM, Allen SP, Dreger SA, Yacoub MH. Human cardiac valve interstitial cells in collagen sponge: A biological three-dimensional matrix for tissue engineering. *The Journal of heart valve disease*. 2002;11:298-306; discussion 306-297
20. Ben-Dor I, Pichard AD, Gonzalez MA, Weissman G, Li Y, Goldstein SA, Okubagzi P, Syed AI, Maluenda G, Collins SD, Delhaye C, Wakabayashi K, Gaglia MA, Jr., Torguson R, Xue Z, Satler LF, Suddath WO, Kent KM, Lindsay J, Waksman R. Correlates and causes of death in patients with severe symptomatic aortic stenosis who are not eligible to participate in a clinical trial of transcatheter aortic valve implantation. *Circulation*. 2010;122:S37-42
21. Walker GA, Masters KS, Shah DN, Anseth KS, Leinwand LA. Valvular myofibroblast activation by transforming growth factor-beta: Implications for pathological extracellular matrix remodeling in heart valve disease. *Circulation research*. 2004;95:253-260
22. Slaughter BV, Khurshid SS, Fisher OZ, Khademhosseini A, Peppas NA. Hydrogels in regenerative medicine. *Adv Mater*. 2009;21:3307-3329
23. Nichol JW, Koshy ST, Bae H, Hwang CM, Yamanlar S, Khademhosseini A. Cell-laden microengineered gelatin methacrylate hydrogels. *Biomaterials*. 2010;31:5536-5544
24. Benton JA, Fairbanks BD, Anseth KS. Characterization of valvular interstitial cell function in three dimensional matrix metalloproteinase degradable peg hydrogels. *Biomaterials*. 2009;30:6593-6603
25. Benton JA, DeForest CA, Vivekanandan V, Anseth KS. Photocrosslinking of gelatin macromers to synthesize porous hydrogels that promote valvular interstitial cell function. *Tissue engineering. Part A*. 2009;15:3221-3230
26. Shah DN, Recktenwall-Work SM, Anseth KS. The effect of bioactive hydrogels on the secretion of extracellular matrix molecules by valvular interstitial cells. *Biomaterials*. 2008;29:2060-2072
27. Duan B, Hockaday LA, Kapetanovic E, Kang KH, Butcher JT. Stiffness and adhesivity control aortic valve interstitial cell behavior within hyaluronic acid based hydrogels. *Acta biomaterialia*. 2013;9:7640-7650
28. Masters KS, Shah DN, Leinwand LA, Anseth KS. Crosslinked hyaluronan scaffolds as a biologically active carrier for valvular interstitial cells. *Biomaterials*. 2005;26:2517-2525
29. Kreger ST, Voytik-Harbin SL. Hyaluronan concentration within a 3d collagen matrix modulates matrix viscoelasticity, but not fibroblast response. *Matrix biology: journal of the International Society for Matrix Biology*. 2009;28:336-346
30. Ifkovits JL, Tous E, Minakawa M, Morita M, Robb JD, Koomalsingh KJ, Gorman JH, 3rd, Gorman RC, Burdick JA. Injectable hydrogel properties influence infarct expansion and extent of postinfarction left ventricular remodeling in an ovine model. *Proceedings of the National Academy of Sciences of the United States of America*. 2010;107:11507-11512
31. Camci-Unal G, Aubin H, Ahari AF, Bae H, Nichol JW, Khademhosseini A. Surface-modified hyaluronic acid hydrogels to capture endothelial progenitor cells. *Soft matter*. 2010;6:5120-5126
32. Camci-Unal G, Cuttica D, Annabi N, Demarchi D, Khademhosseini A. Synthesis and characterization of hybrid hyaluronic acid-gelatin hydrogels. *Biomacromolecules*. 2013;14:1085-1092
33. Yip CY, Blaser MC, Mirzaei Z, Zhong X, Simmons CA. Inhibition of pathological differentiation of valvular interstitial cells by c-type natriuretic peptide. *Arteriosclerosis, thrombosis, and vascular biology*. 2011;31:1881-1889
34. Stradins P, Lacis R, Ozolanta I, Purina B, Ose V, Feldmane L, Kasyanov V. Comparison of biomechanical and structural properties between human aortic and pulmonary valve. *European journal of cardio-thoracic surgery: official journal of the European Association for Cardio-thoracic Surgery*. 2004;26:634-639
35. Zhao R, Sider KL, Simmons CA. Measurement of layer-specific mechanical properties in multilayered biomaterials by micropipette aspiration. *Acta biomaterialia*. 2011;7:1220-1227

36. Hinz B, Celetta G, Tomasek JJ, Gabbiani G, Chaponnier C. Alpha-smooth muscle actin expression upregulates fibroblast contractile activity. *Molecular biology of the cell*. 2001;12:2730-2741
37. Cha C, Liechty WB, Khademhosseini A, Peppas NA. Designing biomaterials to direct stem cell fate. *ACS nano*. 2012;6:9353-9358
38. Rodriguez KJ, Piechura LM, Masters KS. Regulation of valvular interstitial cell phenotype and function by hyaluronic acid in 2-d and 3-d culture environments. *Matrix biology: journal of the International Society for Matrix Biology*. 2011;30:70-82
39. Hutcheson JD, Setola V, Roth BL, Merryman WD. Serotonin receptors and heart valve disease--it was meant 2b. *Pharmacology & therapeutics*. 2011;132:146-157
40. Merryman WD, Lukoff HD, Long RA, Engelmayr GC, Jr., Hopkins RA, Sacks MS. Synergistic effects of cyclic tension and transforming growth factor-beta1 on the aortic valve myofibroblast. *Cardiovascular pathology: the official journal of the Society for Cardiovascular Pathology*. 2007;16:268-276

SUPPLEMENTAL FIGURES

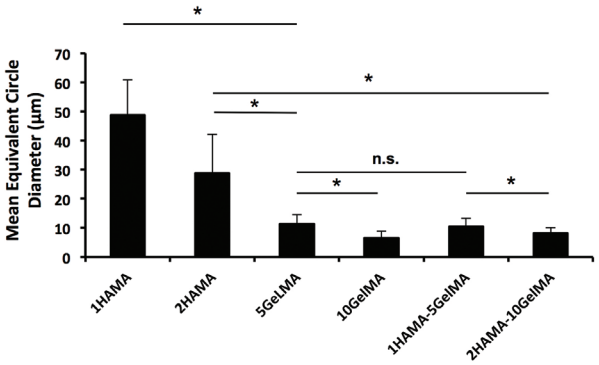

Supplemental Figure I. Pore size differed between each hydrogel condition. Porosity was quantified by measuring area size to determine ECD of at least 50 pores per SEM images using Image J Software. Three SEM images per sample were used for quantification. * p<0.05

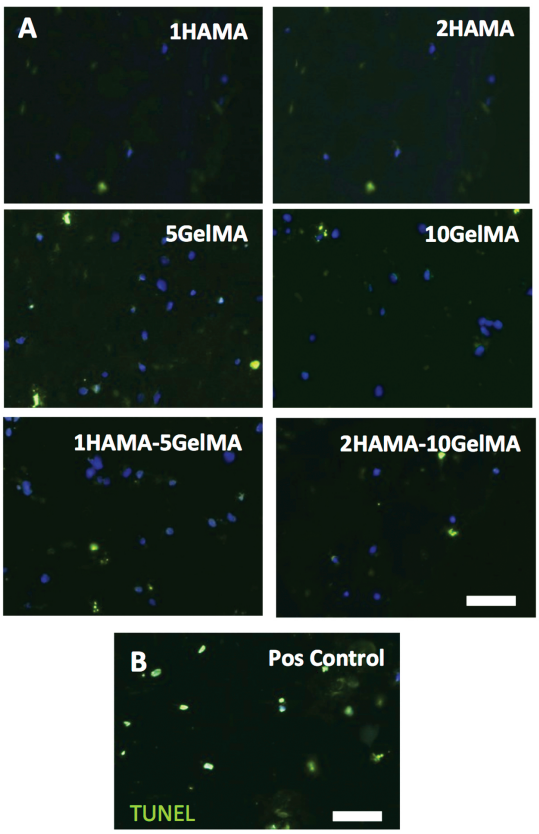

Supplemental Figure II. VICs did not undergo apoptosis when encapsulated in hydrogels. A TUNEL staining of VIC-laden hydrogel conditions at day 21. **B** Positive control by VICs plated on tissue culture plate treated with DNase.

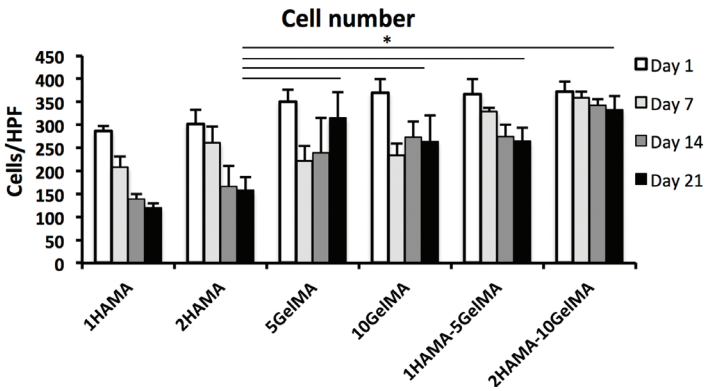

Supplemental Figure III. Phenotypic characterization of VICs in culture. Immunofluorescence staining of pVICs seeded in normal polystyrene tissue culture plate. αSMA, Vimentin, IgG: green, DAPI: blue, bar = 50 µm

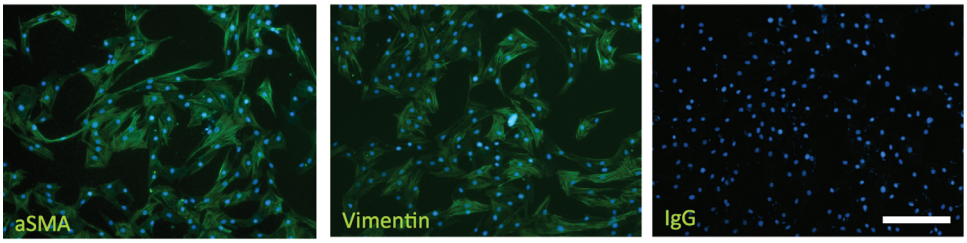

Supplemental Figure IV.

8

Simulation of Early Calcific Aortic Valve Disease in a 3D platform: a Role for Myofibroblast Differentiation

Jesper Hjortnaes, MD[1,2,3], Claudia Goettsch, PhD[4], Gulden Camci-Unal, PhD[2,5], Joshua D. Hutcheson[4] Lilian Lax, BSc[1], Katrin Scherer, BSc[1], Frederick J. Schoen, MD, PhD[6], Jolanda Kluin, MD, PhD[3], Ali Khademhosseini, PhD[2,5,7*], Elena Aikawa, MD, PhD[1,4*]

Under Revision

[1]Center of Excellence in Vascular Biology, Department of Medicine, Brigham and Women's Hospital, Harvard Medical School, Boston, MA, USA; [2]Center for Biomedical Engineering, Department of Medicine, Brigham and Women's Hospital, Harvard Medical School, Boston, MA, USA; [3]Department of Cardiothoracic Surgery, University Medical Center Utrecht, Utrecht, The Netherlands; [4]Center for Interdisciplinary Cardiovascular Sciences, Department of Medicine, Brigham and Women's Hospital, Boston, MA, USA; [5]Harvard-MIT Division of Health Sciences and Technology, Massachusetts Institute of Technology, Cambridge, MA, USA; [6]Department of Pathology, Brigham and Women's Hospital, Harvard Medical School, Boston, MA, USA; [7]Wyss Institute for Biologically Inspired Engineering, Harvard University, Boston, MA, USA

ABSTRACT

Introduction

Calcific aortic valve disease (CAVD) is the most prevalent valvular disease in the Western world. Recent difficulty in translating promising experimental results of statins to beneficial clinical effects warrants the need for understanding the role of valvular interstitial cells (VICs) in CAVD. In two-dimensional culture conditions, VICs undergo spontaneous activation similar to pathological differentiation, which intrinsically limits the use of *in vitro* models to study CAVD. Here, we hypothesized that a three-dimensional (3D) culture system based on naturally derived extracellular matrix polymers, mimicking the microenvironment of native valve tissue, could serve as a physiologically relevant platform to study the osteogenic differentiation of VICs.

Methods and Results

Aortic VICs were encapsulated in photocrosslinkable 3D hydrogels and cultured in control or osteogenic conditions for up to 21 days. VICs loaded into 3D constructs maintained a quiescent phenotype, similar to healthy human valves. In contrast, osteogenic environment induced an initial myofibroblast differentiation (hallmarked by increased alpha smooth muscle actin [αSMA] expression), followed by an osteoblastic differentiation, characterized by elevated Runx2 expression, and subsequent calcific nodule formation recapitulating CAVD conditions. Silencing of α-SMA under osteogenic conditions diminished VIC osteoblast-like differentiation and calcification, indicating that a VIC myofibroblast-like phenotype may precede osteogenic differentiation in CAVD.

Conclusions

Using a 3D hydrogel model, we simulated events occurring during early CAVD *in vivo* and provided a platform to investigate mechanisms of CAVD. This novel approach can provide important insight into valve pathobiology and serve as a promising tool for drug screening.

INTRODUCTION

Aortic valve stenosis due to calcific aortic valve disease (CAVD) is the most common heart valve disease in developed countries.[1] CAVD is a progressive disease characterized by a cascade of cellular events in the valve leaflets, followed by fibrotic thickening and calcification of the aortic valve that impairs functional leaflet movement and causes left ventricular outflow obstruction.[2] Although CAVD traditionally was viewed as a passive degenerative phenomenon resulting from years of mechanical stress, we now recognize it as an actively regulated disease, with evidence suggesting a process akin to bone formation.[3, 4] The disease progression is primarily regulated by valve interstitial cells (VICs), the most abundant cell type in the aortic valve. End-point analysis of calcified leaflets have identified various VIC phenotypes, including quiescent fibroblast-like VICs, which can differentiate into activated myofibroblast-like VICs during various pathological conditions, but also have revealed the presence of osteoblast-like cells which may be responsible for the deposition of calcium in CAVD.[3, 5-8]

VIC differentiation accelerates in response to pathophysiological cues caused by injury or disease,[9] which include inflammation,[10, 11] oxidized low-density lipoprotein (LDL) deposits,[12, 13] oxidative stress,[14] and extracellular matrix (ECM) disruption.[15, 16] No *in vitro* study, however, has identified all of the relevant VIC phenotypes and their respective contributions to CAVD.[15, 17] Moreover, understanding of pathological changes in VICs is hindered by a lack of *in vitro* model systems that maintain physiological VIC phenotypes without spontaneous VIC myofibroblast-like differentiation, as is observed when cultured on unnaturally stiff tissue culture plates. These myofibroblast-like VICs form dystrophic calcific nodules *in vitro*; however, these nodules do not display osteogenic attributes[15, 18] and osteoblast-like differentiation of VICs *in vitro* has proven difficult.[19] Given that both dystrophic and osteogenic calcification processes are observed in excised human CAVD leaflets[3] *in vitro* platforms that enable the study of both myofibroblast-like and osteoblast-like VICs are needed.

Three-dimensional (3D) culture platforms are emerging to provide a more tissue-like environment for studying valvular cell behavior.[17, 20] Such 3D cell culture systems could simulate the natural ECM of the valve and model an *in situ*-like environment of the *fibrosa* layer, where calcification is mainly observed.[21] Photocrosslinkable hydrogels used to engineer 3D culture platforms for VICs showed limited damage of encapsulated cells during fabrication[17, 20, 22] and preservation of cell–matrix interaction and matrix signaling.[23] Hyaluronic acid, an important glycosaminoglycan of the adult heart valve ECM, is a vital component of the cardiac jelly during heart embryogenesis. Gelatin — a denatured form of collagen — also is abundantly present in the heart valve ECM. By adding methacrylate groups to hyaluronic acid (HAMA) and gelatin (GelMA), these biopolymers can crosslink to each other in the presence of a photo-initiator and form 3D hydrogel platforms.[24, 25, 26] We have recently shown that combining HAMA and GelMA into a 3D hybrid hydrogel platform can maintain a quiescent VIC phenotype, while allowing VICs to undergo myofibroblast-like differentiation upon exogenous pathological stimulation.[29,30] This study provided us with an *in vitro* 3D platform that can be used to model VIC phenotype changes as thought to occur in early CAVD.

The present work uses a hydrogel culture platform composed of native valvular ECM molecules that simulates the *in situ*–like environment of the healthy heart valve. In this study, we will use this *in vitro* 3D model system to elucidate the role of VIC activation and calcification in mechanisms of CAVD.

METHODS

For detailed methods see supplemental material.

Valvular interstitial cell (VICs) isolation and culture

VICs were isolated from aortic heart valves as described previously[29] and cultured in DMEM with 10% fetal bovine serum and 1% penicillin/streptomycin (Invitrogen) at 37°C, 5% CO_2. Cells between passage 3 and 6 were used for all experiments.

Hydrogel fabrication

Hybrid hydrogels were fabricated from HAMA and GelMA, which were synthesized as reported previously[27,28] using photocrosslinking (Figure 1A).[25,29] Briefly, VICs were resuspended in the prepolymer solution consisting of 1wt% HAMA and 5wt% GelMA. 50 µL of the cell-laden polymer solution was added between two spacers each with a height of 450 µm and and subjected to light (wavelength 360 nm) with a light intensity of 2.5 mW/cm^2. VIC-laden hydrogels were cultured in either control medium (CM) or osteogenic medium (OM) (CM supplemented with 10 mM β-glycerophosphate, 10 ng/mL ascorbic acid, and 10 nM dexamethasone) or OM with tumor necrosis factor alpha (TNFα).

Silencing of alpha smooth muscle actin in VIC-laden hydrogels

To inhibit the expression of α-smooth muscle actin (α-SMA), ON-TARGET plus SMART-pool (L-003605-00-00100) and a negative control (scramble) from ThermoScientific was used. Transfection of 50 nmol/l siRNAs was performed using DharmaFECT 1 transfection reagent twice per week over the entire culture period.

Histological analysis and immunofluorescence staining of VIC-laden hydrogel constructs

Human calcified aortic valves were obtained from CAVD patients who underwent surgical valve replacement according to Brigham and Women's Hospital Institutional Review Board Protocol (IRB # 201-P-002567/2). VIC-laden hydrogels were frozen in optimal cutting temperature (OCT) compound, and 10-µm cross-sections were obtained. To detect calcium deposition, sections were stained with 0.02 mg/mL Alizarin Red S solution (Sigma). Von Kossa staining (American MasterTech) was used to visualize calcium-phosphate deposition.

Immunofluorescence staining for α-SMA and runt-related transcription factor 2 (Runx2) was performed using anti-human α-SMA antibody (Clone 1A4, Dako) or a anti-human Runx2 antibody

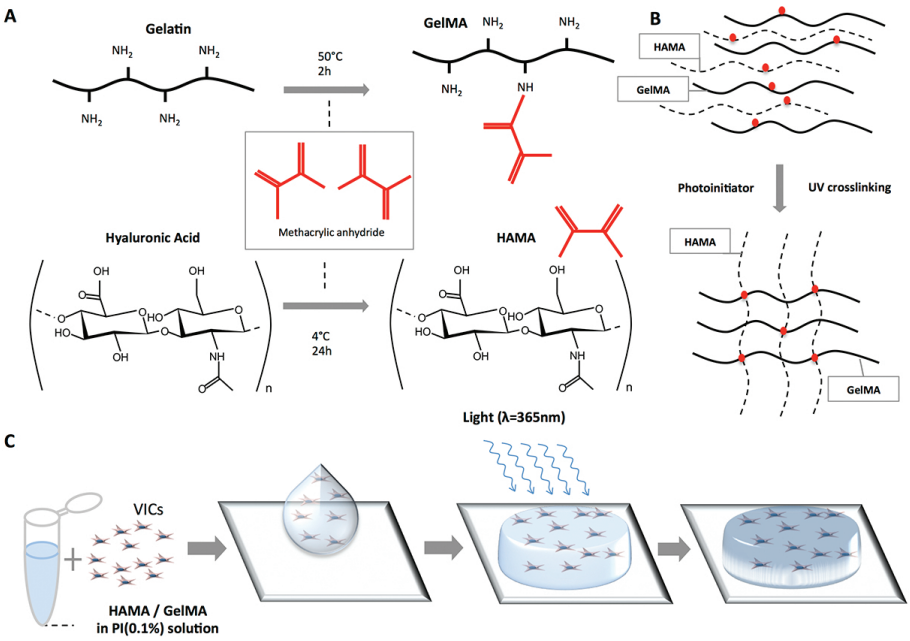

Figure 1. Fabrication of VIC-laden hydrogel platform. A Methacrylation of gelatin (GelMA) and hyaluronic acid (HAMA), respectively, occurs by the addition of methacrylic anhydride groups to dissolved gelatin and hyaluronic acid. **B** Schematic depiction of photocrosslinking GelMA and HAMA. By dissolving HAMA and GelMA into a solution containing a photoinitiator, when exposed to UV light, the polymers form crosslinks between the methacrylate groups, creating an ECM-like mesh. **C** Schematic depiction of fabricating VIC-laden hydrogels. (1) VICs are isolated from culture and resuspended into a photoinitiator solution containing dissolved 1%(w/v) HAMA and 5% (w/v) GelMA; (2) Cell-polymer suspension is pipetted on to a plate between two spacers (450 μm) and (3) exposed to light at an intensity of 2.5 mW/cm^2 for 30 seconds (λ=365 nm), which yields a (4) crosslinked VIC-laden hydrogel disc. VIC-laden hydrogels are then cultured for up to 21 days.

(Abcam), followed by biotin-labeled secondary antibody (Vector Labs) and streptavidin-labeled AlexaFluor 488 for α-SMA and AlexaFluor 594 for Runx2. Sections were counterstained with 4′,6-diamidino-2-phenylindole (DAPI). Images were taken with an Eclipse 80i microscope (Nikon) and processed with Elements 3.20 software (Nikon).

Quantification of alkaline phosphatase activity and calcium content in hydrogel constructs

Activity of alkaline phosphatase (ALP) and calcium content were measured using colorimetric assays (Biovision Lifesciences) and normalized to DNA content.

Real-Time Polymerase Chain Reaction for expression of cell markers

After mechanical disruption of the cell-laden hydrogels (TissueLyzer, Qiagen), total RNA was isolated using RNAspin mini RNA Isolation kit (GE Healthcare). Total RNA was reverse transcribed with oligo-(dT)12-18 primers and Superscript II reverse transcriptase (Life Technologies) followed by RT- PCR using SYBR Green (BioRad). Primer sequences were as follows: α-SMA: F:5′-AGTGCGACATTGACAT-

CAGG-'3 and R:5'-CTGGAAGGTGGACAGAGAGG-'3, Runx2 F:5'-ACCCAGAAGACTGTGGATGG-'3 and R:5'-ACCTGGTCCTCAGTGTAGCC-'3, GAPDH: F:5'-CCCAGAAGACTGTGGATGG-'3, R:5'-ACCTGGTCCTCAGTGTAGCC-'3. Expression was quantified using comparative $2^{-\Delta\Delta CT}$ method.

Cell viability and apoptosis

Cell viability was determined by LIVE/DEAD Viability kit (Life Technologies). Apoptosis was determined by TUNEL staining (Millipore). Cell-laden hydrogels were imaged using an A1/C1 confocal microscope (Nikon).

Statistical analysis

Results are presented as mean +/- standard deviation unless indicated otherwise. Unpaired student's t-test was used for comparisons between two groups. One-way ANOVA was used to evaluate statistical significant differences in multiple groups. $P < 0.05$ was considered statistically significant.

RESULTS

Osteogenic environment causes calcific nodule formation in 3D culture model

Osteogenic medium (OM) promoted calcific nodule formation in VIC-laden hydrogels, as demonstrated by Alizarin Red S staining. Calcific nodules localized throughout the VIC-laden hydrogel and were particularly increased at day 21 (Figure 2A).

To evaluate the potential of the hydrogel platform for studying specific pathophysiology related to early CAVD, such as inflammation, we used the pro-inflammatory cytokine TNF-α. TNF-α in OM promoted calcific nodule formation as visualized by Alizarin Red S staining (Figure 2B) and von Kossa (Figure 2C, Supplemental Figure I), while TNF-α supplementation to control media (CM) had negligible effect. Quantification of nodule formation revealed a 1.65 fold increase in VIC-laden hydrogels cultured in OM supplemented with 10 ng/ml TNF-α as compared to untreated cells ($p < 0.05$ Figure 2D). Further quantitative calcium analysis showed an OM-mediated induction of calcium deposition in a time-dependent manner that was further increase under TNF-α stimulation (Figure 2E, OM: 1.8±0.2 vs. OM+TNF-α: 1.0±0.1, $p < 0.05$). ALP activity, as marker of early calcification, peaked at day 10 (Supplemental Figure II). Addition of TNF-α to the OM significantly increased ALP activity (OM day 10:1.2±0.1 vs. OM+TNF-α day 10: 2.3±0.9, $p < 0.05$). No ALP activity was detected within cultures maintained in CM (data not shown).

To confirm the VIC-laden hydrogels demonstrated an active disease process of mineralization, contrary to being a consequence of apoptotic driven mineralization, we performed cell viability analysis and TUNEL staining. Cell viability when cultured in CM was 95±2% at day 1 and 90%±2 at day 21, compared to 91±2% at day 21 and 87±1% at day 21 when cultured in OM (Supplemental Figure III). TUNEL staining and quantification showed no apoptosis at 7, 14, and 21 days of culture in constructs cultured in OM and OM+TNF-α (Supplemental Figure IV, panels A and B). These results

suggest that the mineralization within VIC-laden hydrogels is primarily cellular driven, and that TNF-α primarily aggravates but not initiates mineralization in the 3D constructs.

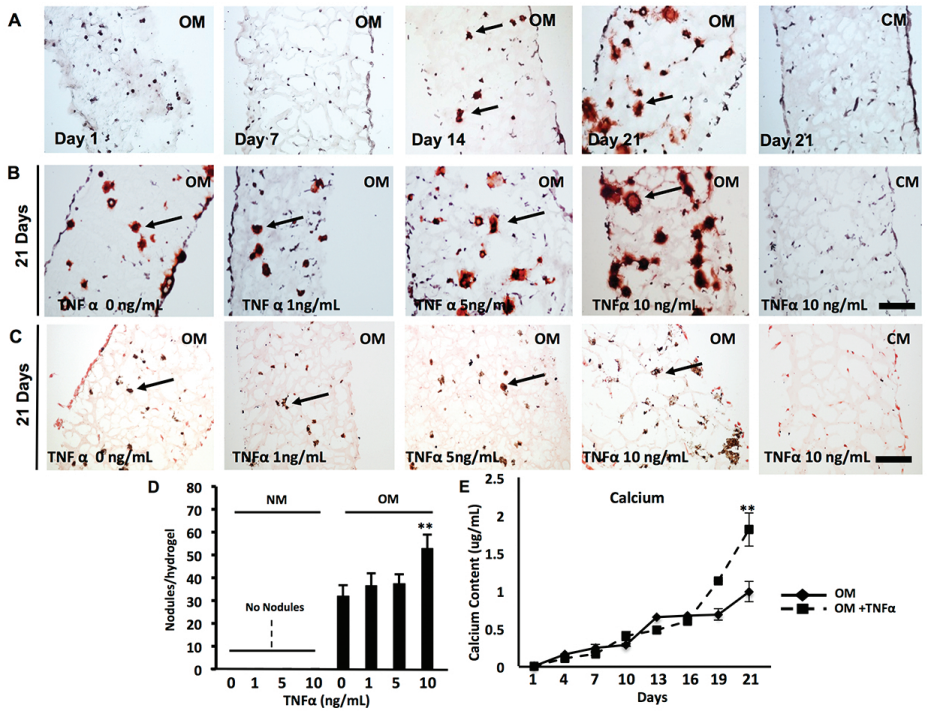

Figure 2. Calcification potential of 3D *in vitro* valve model. **A**, Alizarin red S staining of VIC-laden hydrogels cultured in control media (CM), osteogenic media (OM), or osteogenic media with TNFα (OM+TNFα) at day 1, 7, 14, and 21. **B**, Alizarin red S staining and **C**, Von Kossa staining of VIC-laden hydrogels cultured in CM or OM with TNFα (0,1,5 or 10 ng/mL) at day 21. Arrows indicate calcific noduli. Bar: 100 µm. **D,** Number of calcific noduli per hydrogel section (n=3). Data depicted as mean ± SD. **E,** Calcium measured every 3 days in hydrogel constructs cultured in OM or OM + TNFα (n=3 per time point). Data depicted as mean ± SD (**: $p < 0.05$).

Myofibroblast-like differentiation precedes osteoblastic VIC differentiation in 3D constructs

The mineralized VIC-laden hydrogels were analyzed for differentiation markers involved in the active disease process of CAVD. We stained VIC-laden hydrogels cultured in OM and OM+TNF-α for α-SMA, a marker for myofibroblast differentiation, and Runx2, a marker for osteoblast differentiation. At day 7, VIC-load in hydrogels and cultured in OM and OM+TNF-α had abundant positive immunofluorescence staining of α-SMA and no nuclear staining for Runx2 (Figure 3A). Conversely, at day 21, αSMA immunostaining decreased compared to day 7 (Supplemental Figure V), while nuclear Runx2-positive cells were detected (Figure 3B). Positive nuclear Runx2-stained cells were not identified at other time points (data not shown).

In addition, αSMA mRNA expression (Figure 3C) supported our findings and showed a significant increase at day 7 and decreases at days 14 and 21 (OM: day 1, 1±0; day 7, 5.1±1.1; day 14, 2.8±1.1; day

21, 1.8±0.8). 3D constructs treated with OM+TNF-α showed significantly reduced α-SMA expression at day 7 compared to OM alone (OM+TNF-α: 3.5±0.4 vs. OM 5.1±1.1, p <0.05).

Runx2 mRNA expression demonstrated a time-dependent increase (day 1 1±0; day 7 0.9±0.4; day 14 1.2±0.8; day 21 1.7±0.8). TNF-α caused an additional significant increase in Runx2 expression at day 21 (day 1;1±0; day 7 1.1±0.6; day 14 1.7±0.7; day 21 2±0.2), compared with constructs cultured in OM (Figure 3D). These results suggest an inverse relationship between myofibroblast-like differentiation and osteoblastic differentiation of quiescent VICs when cultured in an osteogenic environment.

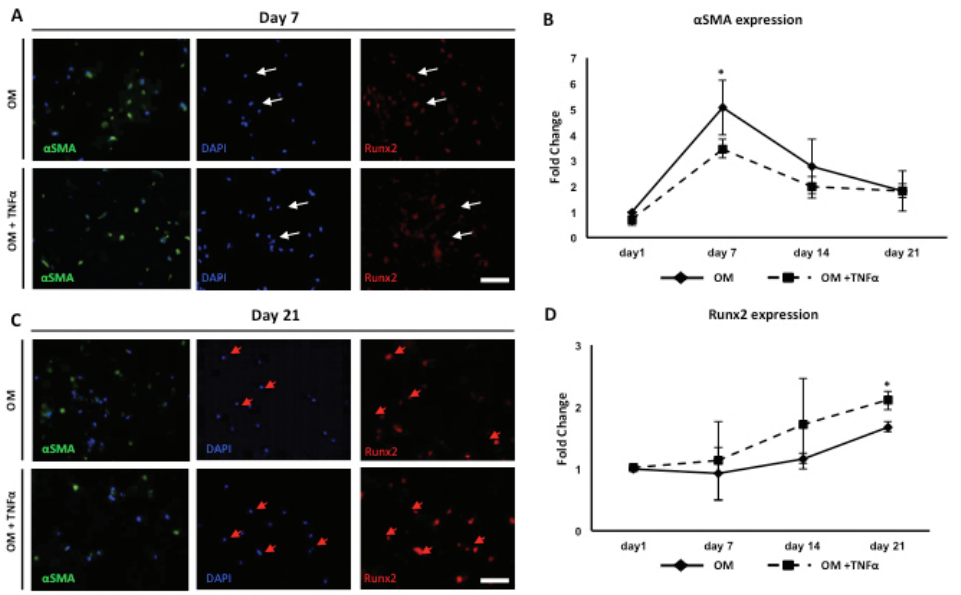

Figure 3. Inverse relationship between myofibroblast-like and osteoblast-like differentiation. VIC-laden hydrogels were cultured in osteogenic medium (OM) and osteogenic medium with TNFα (10ng/mL) (OM + TNFα) for 21 days. **A**, α-SMA and Runx2 immunofluorescence staining at day 7, red arrows indicate negative nuclear stain for Runx2. Bar: 50 μm. **B**, αSMA and Runx2 immunofluorescence staining at day 21. White arrows indicate positive nuclear Runx2 staining. Bar: 50 μm. **C**, mRNA expression of αSMA quantified by RT-PCR at day 1, 7, 14, and 21, (n=3, *: p < 0.05). **D**, mRNA expression of Runx2 quantified by RT-PCR at day 1, 7, 14, and 21 (n=3, * p < 0.05).

An osteogenic stimulus activates quiescent VICs in 3D culture constructs

To further understand myofibroblast-like differentiation of quiescent VICs, we compared α-SMA expression of VICs in human valves and VICs cultured in 2D and 3D models while cultured in CM, OM, or OM + TNF-α. Non-calcified areas of aortic valves express low levels of α-SMA (Figure 4A/B), similar to VICs laden in 3D hydrogels cultured in CM (Figure 4E).

Calcified areas of aortic valves showed increased α-SMA expression (Figure 4C/D), also observed in VIC-laden hydrogels cultured in OM (Figure 4F). Quantitative analysis supported a significant increase in α-SMA-positive cells within the VIC-laden hydrogels (17±5% vs. 40±10%, p<0.05) (Figure

4G), indicating an activated myofibroblast-like VIC phenotype. These observations were supported by RT-PCR, demonstrating a significant increase in α-SMA mRNA expression after culturing VICs for 21 days in OM, compared to CM (Figure 4H).

We next evaluated myofibroblast-like differentiation when VICs were seeded onto hydrogels and cultured in CM, OM, and OM+TNF-α for 1, 7, 14, and 21 days. Immunofluorescence staining revealed abundant numbers of α-SMA cells when cultured in CM (Figure 4I), similar to VICs seeded on to common tissue culture plates (Supplemental Figure VI). When 2D seeded VICs were cultured in OM or OM+TNF-α, α-SMA staining decreased at day 21 (Figure 4I).

Taken together our results demonstrate that VICs encapsulated in 3D hydrogels remain quiescent when cultured in CM; in OM, they become activated myofibroblast-like cells, thus simulating VIC behavior in physiological and diseased heart valves.

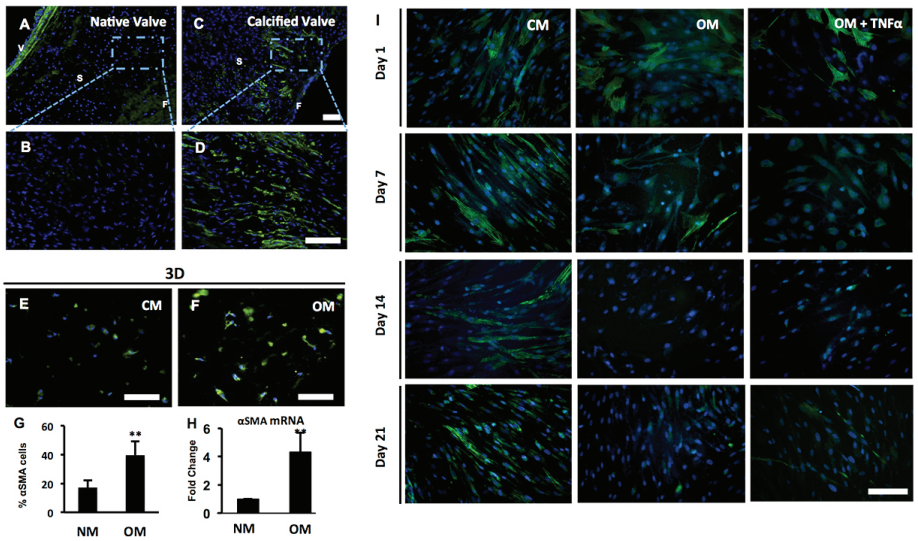

Figure 4. Osteogenic environment activates quiescent VICs in 3D hydrogels. A-D, Immunofluorescence αSMA staining (green), nuclei (blue) of a native aortic heart valve (normal valve), and calcified aortic valve of a patient with aortic stenosis. V: *Zona Ventricularis*, *S: Zona Spongiosa;* F: *Zona Fibrosa*. Bar: 50 μm. **C-D,** Higher magnification of **A/B**; Bar: 50μm. **E-F**, Immunofluorescence of αSMA staining in cell-laden hydrogels cultured for 21 days in control (CM) or osteogenic media (OM). Bar; 50μm. **G**, Quantification of αSMA-positive cells per high-power field (HPF), (n=3); **H**, mRNA expression of αSMA demonstrates increased myofibroblast phenotype (αSMA) when cultured in OM. Data depicted as mean ± SD (** $p < 0.01$) **I**, Immunofluorescent staining of αSMA expression of pVICs seeded onto hydrogels (2D) and cultured in CM, OM, or OM with TNFα. αSMA: green, DAPI: blue; bar = 50 μm

Reduction of α-SMA expression diminishes mineralization of VIC-laden hydrogels

We next investigated the impact of VIC myofibroblast-like differentiation and the role of α-SMA in calcification. VIC-laden hydrogels were cultured in CM, OM, and OM+TNF-α under the silencing of α-SMA by siRNA or scrambled non-targeted siRNA (SCR) as control. Immunofluoresce staining of α-SMA demonstrated positive α-SMA staining in VIC-laden hydrogels cultured in OM (SCR) with and

without TNF-α. Staining for α-SMA (Figure 5A) and analysis of mRNA expression levels (Figure 5B) verified silencing efficiency.

α-SMA silencing significantly decreased ALP activity in constructs cultured in OM and OM+TNF-α (OM: SCR 8.5±4.2 vs. Si-α-SMA 0.6±0.5, p<0.05, OM+TNFα: SCR 14.8±2.6 vs. Si-α-SMA 7.1±3.3, p<0.05) (Supplemental Figure VII). Further, α-SMA silencing caused a significant reduction in calcification, as detected by Alizarin Red S staining (Figure 5C) and von Kossa staining (Supplemental Figure VIII). Quantification of calcium content of VIC-laden hydrogels supported these findings and confirmed that silencing of α-SMA significantly decreases calcium content when cultured in OM and OM+TNF-α (Figure 5D). In addition, α-SMA silencing reduced Runx2 expression when cultured in OM (-76%, p<0.05) and OM+TNF-α (-49%, p=0.06) compared to control (Figure 5E), further suggesting that myofibroblast-like activation is an important step for VIC osteogenic transformation.

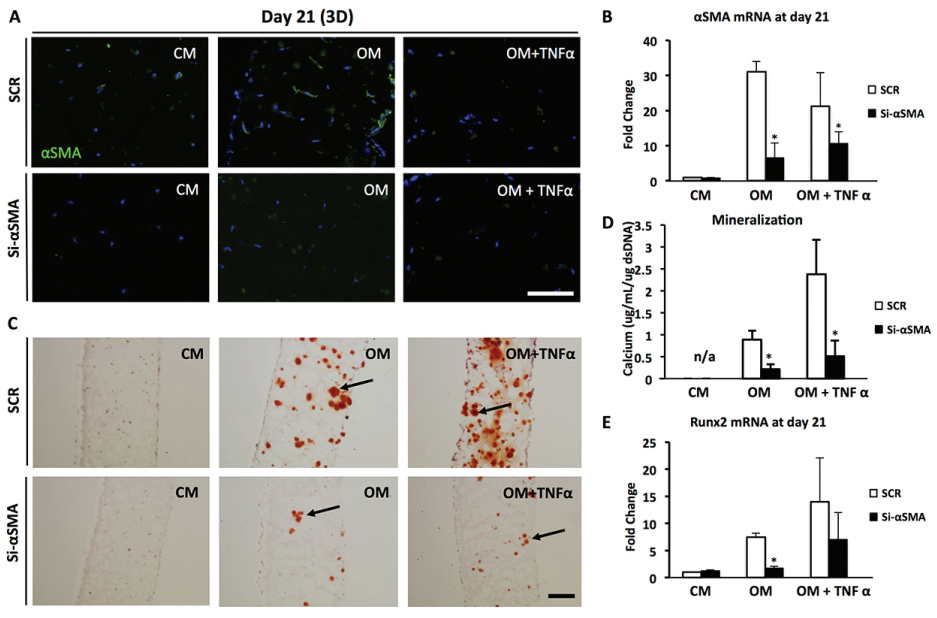

Figure 5. Silencing αSMA reduces osteogenesis. VIC-laden hydrogels were cultured up to 21 days in control (CM), osteogenic media (OM), or osteogenic media with TNFα (OM + TNFα). Silencing of αSMA (Si-αSMA) was performed twice per week. Scramble (SCR) SiRNA served as control. **A**, Immunofluorescent staining of αSMA expression, αSMA: green, DAPI: blue, bar = 50 μm. **B**, Alizarin red staining of VIC-laden hydrogels. **C,** RT-PCR of αSMA expression. **D**, RT-PCR of Runx2 mRNA expression. **E,** Calcium content normalized for DNA content at day 21. Data depicted as mean ± SD, *:p < 0.05.

DISCUSSION

This study establishes an *in vitro* 3D culture model to study early CAVD. It shows that a 3D hybrid hydrogel platform composed of hyaluronic acid and gelatin could maintain a quiescent VIC phenotype identified in healthy heart valves, thus providing a platform to study initial changes in CAVD.

We also demonstrated that quiescent VICs could be controllably activated by osteogenic stimuli to undergo myofibroblast-like differentiation and eventually differentiate into osteoblast-like cells, which actively deposit calcium. We provide a platform that allows observation of both osteoblast-like and myofibroblast-like VICs—the two pathologic phenotypes observed in CAVD. Furthermore, we established that myofibroblast-like differentiation, hallmarked by α-SMA expression, is necessary for osteoblast-like differentiation. We showed that this *in vitro* 3D model for calcification can be used to controllably study specific pathological mechanisms associated with CAVD, including inflammation and calcification (Figure 6).

Recent evidence suggests that early CAVD may be characterized as an active disease process, in which quiescent VICs become activated to undergo myofibroblast-like differentiation upon exposure to mechanical stress or inflammation, hallmarked by the presence of α-SMA stress-fibers within the cytoskeleton.[4] Activated VICs maintain valvular tissue integrity by pertinent remodeling of the valve ECM, by secreting cytokines,[8, 30] matrix metalloproteinases,[6, 31] and depositing ECM proteins.[30, 32] In addition, osteoblastic cells have been detected in *ex vivo* heart valves,[3, 5] characterized by Runx2 expression. Causal relationships between VIC phenotypes, however, have never been established. This work is the first, to our knowledge, to report that quiescent VICs differentiate into osteoblast-like VICs by first undergoing myofibroblast differentiation. This may explain the observation of both dystrophic and osteogenic calcific deposits *in vivo*. Dystrophic nodules may form by apoptotic myofibroblast-like VICs as demonstrated previously[30, 33] but a portion of these VICs may proceed to an osteoblast-like phenotype forming the observed osteogenic nodules.[3]

Growing evidence, supported by our data, suggests that VIC pathophysiology is highly dependent on the culture microenvironment.[15, 34, 29] More specifically, matrix elasticity and cell-matrix protein interactions play important roles in directing the pathological response of VICs.[15] VICs cultured on standard tissue culture polystyrene, an unnaturally stiff environment, undergo a complete phenotypic change into myofibroblast-like cells[35] — commonly considered a "diseased" state. Hence, numerous studies have focused on modulating 2D culture substrates, albeit by changing stiffness or by using various ECM proteins, to analyze their relationship to VIC behavior.[34-36] Initially, studies demonstrated that stiffer substrates elicit increased myofibroblast-like differentiation and even calcific nodule formation,[15, 35] but they were unable to identify osteoblastic markers. Indeed, when cultured on stiff gels (>25kPa), VICs seemed to form larger calcific nodules that also contained apoptotic cells,[15] much like that observed in dystrophic calcification.[9] The elastic modulus of the hybrid hydrogels used in this work was ~20kPA.[21,29] Similar to other recent studies,[15, 36] we showed that spontaneous myofibroblast-like differentiation can occur on more compliant substrates. This myofibroblast-like response of VICs encapsulated into 3D hydrogels only occurs, however, when exposed to exogenous environmental cues, and it is necessary to elicit an osteoblastic differentiation. The elastic modulus of 3D hydrogels used in our study corresponds to the perceived modulus of the *fibrosa* as measured by micropipette aspiration up to 21 kPA.[37] Notably, mineralization of the aortic valve by VICs predominantly occurs in the *fibrosa* of the heart valve ECM,[9] which recently was shown to have a relatively soft modulus.[37]

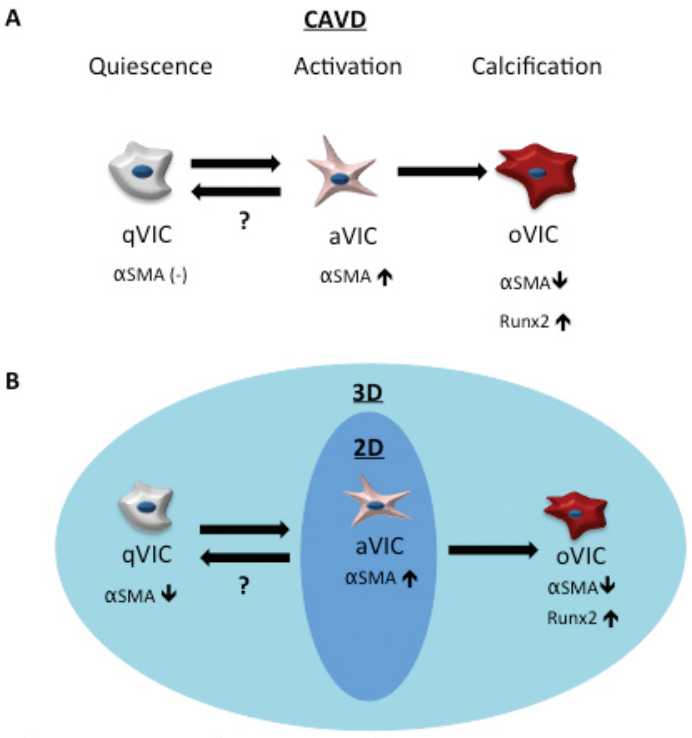

Figure 6. Schematic illustration of simulating early CAVD. A, Pathophysiological cellular concept of "active" mineralization in CAVD. Quiescent VICs (qVICs) become activated myofibroblast-like VICs (aVICs) hallmarked by increased α-SMA expression. In healthy valves, cells can return to a quiescent state, but in CAVD, aVICs can differentiate into osteoblast-like VICs (oVICs) characterized by decreased α-SMA expression and increased Runx2 expression. **B**, 3D versus 2D modeling of VIC-driven mineralization. Using a 3D culture platform, the entire cellular driven disease process of CAVD can be modeled.

In the present study, we did not observe apoptotic driven calcification in 3D VIC-laden hydrogels, but rather an "active" osteogenesis via the Runx2 pathway, in which calcific noduli, composed of calcium and phosphates, are formed throughout the construct. On a cellular level, we observed the ability of healthy quiescent VICs to differentiate eventually into osteoblast-like VICs — a process that, in the 3D environment, requires initial myofibroblast-like differentiation. Our observations offer insight into a lingering question in VIC biology: do osteoblast-like VICs solely derive from resident quiescent VICs or does a heterogeneous VIC population contain specific mesenchymal or osteogenic progenitor cells?[34] Considering that myofibroblast-like differentiation may be required for this transition, this could pose interesting pathways for possible therapeutic intervention. The potential of controllably investigating disease specific pathways in this 3D platform was tested by adding the pro-inflammatory stimulus TNF-α, a cytokine mainly secreted by macrophages and abundantly present in leukocyte infiltration areas in stenotic aortic valves.[10, 38] Studies suggest that inflammatory mechanisms play a regulatory role in the active development of CAVD.[38] We have demonstrated that the addition of TNF-α to osteogenic media increased osteoblastic differentia-

tion of VICs, but failed to affect calcific nodule formation when added to normal media. This may indicate that TNF-α may not participate in the initiation of osteoblast-like differentiation, but may have more of a catalyzing affect in an already present osteogenic milieu.

Our study is limited by the static nature of 3D hydrogel platform and the absence of an endothelial monolayer, both important components when modeling valvular biology. Blood flow–induced shear stress and hemodynamic forces are key in valve tissue development, structural integrity, and disease.[9] As is apparent from valve development and tissue engineering,[39, 40] biomechanical signals that are transduced to interaction between valvular endothelial cells, VICs, and the ECM are vital to understanding valvular biology and pathology.[41-43]

In conclusion, our study simulates events that occur in early CAVD using a 3D hydrogel culture platform, in which quiescent VICs differentiate to osteoblast-like cells through initial myofibroblast-like differentiation and subsequently mineralize. Moreover, this approach provides a robust platform to therapeutically target VIC calcification. The 3D approach presented in this work, which can maintain healthy quiescent VICs and thus can model the entire cellular process, suggests that this platform can be used as a tool for drug screening and for the validation of cellular and molecular mechanisms.

ACKNOWLEDGEMENTS

The authors acknowledge Sara Karwacki for her excellent editorial assistance.

FUNDING

This work was supported by the Dutch Heart Foundation (DHF) and Netherlands Scientific Council (NWO) (to J.H.), the Office of Naval Research Young National Investigator Award, the Presidential Early Career Award for Scientists and Engineers (PECASE), the National Science Foundation CAREER Award (DMR 0847287), and the National Institutes of Health (EB012597, HL092836, DE019024, HL099073, AR057837, EB008392, DE021468, to A.K.; NIH R01 114805 and NIH R01 109506, to E.A.).

CONFLICT OF INTEREST

None

REFERENCES

1. Stewart BF, Siscovick D, Lind BK, Gardin JM, Gottdiener JS, Smith VE, Kitzman DW, Otto CM. Clinical factors associated with calcific aortic valve disease. Cardiovascular health study. *J Am Coll Cardiol*. 1997;29:630-634
2. Otto CM. Calcific aortic stenosis--time to look more closely at the valve. *N Engl J Med*. 2008;359:1395-1398
3. Mohler ER, 3rd, Gannon F, Reynolds C, Zimmerman R, Keane MG, Kaplan FS. Bone formation and inflammation in cardiac valves. *Circulation*. 2001;103:1522-1528
4. Yutzey KE, Demer LL, Body SC, Huggins GS, Towler DA, Giachelli CM, Hofmann-Bowman MA, Mortlock DP, Rogers MB, Sadeghi MM, Aikawa E. Calcific aortic valve disease: A consensus summary from the alliance of investigators on calcific aortic valve disease. *Arteriosclerosis, thrombosis, and vascular biology*. 2014;34:2387-2393
5. Rajamannan NM, Subramaniam M, Rickard D, Stock SR, Donovan J, Springett M, Orszulak T, Fullerton DA, Tajik AJ, Bonow RO, Spelsberg T. Human aortic valve calcification is associated with an osteoblast phenotype. *Circulation*. 2003;107:2181-2184
6. Rabkin-Aikawa E, Farber M, Aikawa M, Schoen FJ. Dynamic and reversible changes of interstitial cell phenotype during remodeling of cardiac valves. *J Heart Valve Dis*. 2004;13:841-847
7. Mohler ER, 3rd, Chawla MK, Chang AW, Vyavahare N, Levy RJ, Graham L, Gannon FH. Identification and characterization of calcifying valve cells from human and canine aortic valves. *J Heart Valve Dis*. 1999;8:254-260
8. Chester AH, Taylor PM. Molecular and functional characteristics of heart-valve interstitial cells. *Philosophical transactions of the Royal Society of London. Series B, Biological sciences*. 2007;362:1437-1443
9. Schoen FJ. Evolving concepts of cardiac valve dynamics: The continuum of development, functional structure, pathobiology, and tissue engineering. *Circulation*. 2008;118:1864-1880
10. Hjortnaes J, Butcher J, Figueiredo JL, Riccio M, Kohler RH, Kozloff KM, Weissleder R, Aikawa E. Arterial and aortic valve calcification inversely correlates with osteoporotic bone remodelling: A role for inflammation. *European heart journal*. 2010;31:1975-1984
11. Aikawa E, Nahrendorf M, Sosnovik D, Lok VM, Jaffer FA, Aikawa M, Weissleder R. Multimodality molecular imaging identifies proteolytic and osteogenic activities in early aortic valve disease. *Circulation*. 2007;115:377-386
12. Rajamannan NM, Subramaniam M, Caira F, Stock SR, Spelsberg TC. Atorvastatin inhibits hypercholesterolemia-induced calcification in the aortic valves via the lrp5 receptor pathway. *Circulation*. 2005;112:I229-234
13. Rajamannan NM. The role of lrp5/6 in cardiac valve disease: Ldl-density-pressure theory. *Journal of cellular biochemistry*. 2011;112:2222-2229
14. Miller JD, Chu Y, Brooks RM, Richenbacher WE, Pena-Silva R, Heistad DD. Dysregulation of antioxidant mechanisms contributes to increased oxidative stress in calcific aortic valvular stenosis in humans. *J Am Coll Cardiol*. 2008;52:843-850
15. Yip CY, Chen JH, Zhao R, Simmons CA. Calcification by valve interstitial cells is regulated by the stiffness of the extracellular matrix. *Arteriosclerosis, thrombosis, and vascular biology*. 2009;29:936-942
16. Schoen FJ, Tsao JW, Levy RJ. Calcification of bovine pericardium used in cardiac valve bioprostheses. Implications for the mechanisms of bioprosthetic tissue mineralization. *The American journal of pathology*. 1986;123:134-145
17. Benton JA, Fairbanks BD, Anseth KS. Characterization of valvular interstitial cell function in three dimensional matrix metalloproteinase degradable peg hydrogels. *Biomaterials*. 2009;30:6593-6603
18. Hutcheson JD, Aikawa E, Merryman WD. Potential drug targets for calcific aortic valve disease. *Nature reviews. Cardiology*. 2014;11:218-231

19. Monzack EL, Masters KS. Can valvular interstitial cells become true osteoblasts? A side-by-side comparison. *J Heart Valve Dis*. 2011;20:449-463
20. Masters KS, Shah DN, Walker G, Leinwand LA, Anseth KS. Designing scaffolds for valvular interstitial cells: Cell adhesion and function on naturally derived materials. *Journal of biomedical materials research. Part A*. 2004;71:172-180
21. Otto CM, Kuusisto J, Reichenbach DD, Gown AM, O'Brien KD. Characterization of the early lesion of 'degenerative' valvular aortic stenosis. Histological and immunohistochemical studies. *Circulation*. 1994;90:844-853
22. Masters KS, Shah DN, Leinwand LA, Anseth KS. Crosslinked hyaluronan scaffolds as a biologically active carrier for valvular interstitial cells. *Biomaterials*. 2005;26:2517-2525
23. Slaughter BV, Khurshid SS, Fisher OZ, Khademhosseini A, Peppas NA. Hydrogels in regenerative medicine. *Adv Mater*. 2009;21:3307-3329
24. Nichol JW, Koshy ST, Bae H, Hwang CM, Yamanlar S, Khademhosseini A. Cell-laden microengineered gelatin methacrylate hydrogels. *Biomaterials*. 2010;31:5536-5544
25. Camci-Unal G, Cuttica D, Annabi N, Demarchi D, Khademhosseini A. Synthesis and characterization of hybrid hyaluronic acid-gelatin hydrogels. *Biomacromolecules*. 2013;14:1085-1092
26. Shah DN, Recktenwall-Work SM, Anseth KS. The effect of bioactive hydrogels on the secretion of extracellular matrix molecules by valvular interstitial cells. *Biomaterials*. 2008;29:2060-2072
27. Camci-Unal G, Nichol JW, Bae H, Tekin H, Bischoff J, Khademhosseini A. Hydrogel surfaces to promote attachment and spreading of endothelial progenitor cells. *Journal of tissue engineering and regenerative medicine*. 2012
28. Ramon-Azcon J, Ahadian S, Obregon R, Camci-Unal G, Ostrovidov S, Hosseini V, Kaji H, Ino K, Shiku H, Khademhosseini A, Matsue T. Gelatin methacrylate as a promising hydrogel for 3d microscale organization and proliferation of dielectrophoretically patterned cells. *Lab on a chip*. 2012;12:2959-2969
29. Hjortnaes J, Camci-Unal G, Hutcheson JD, Jung SM, Schoen FJ, Kluin J, Aikawa E, Khademhosseini A. Directing valvular interstitial cell myofibroblast-like differentiation in a hybrid hydrogel platform. *Advanced healthcare materials*. 2015;4:121-130
30. Walker GA, Masters KS, Shah DN, Anseth KS, Leinwand LA. Valvular myofibroblast activation by transforming growth factor-beta: Implications for pathological extracellular matrix remodeling in heart valve disease. *Circulation research*. 2004;95:253-260
31. Rabkin E, Aikawa M, Stone JR, Fukumoto Y, Libby P, Schoen FJ. Activated interstitial myofibroblasts express catabolic enzymes and mediate matrix remodeling in myxomatous heart valves. *Circulation*. 2001;104:2525-2532
32. Cushing MC, Liao JT, Anseth KS. Activation of valvular interstitial cells is mediated by transforming growth factor-beta1 interactions with matrix molecules. *Matrix biology: journal of the International Society for Matrix Biology*. 2005;24:428-437
33. Hutcheson JD, Chen J, Sewell-Loftin MK, Ryzhova LM, Fisher CI, Su YR, Merryman WD. Cadherin-11 regulates cell-cell tension necessary for calcific nodule formation by valvular myofibroblasts. *Arteriosclerosis, thrombosis, and vascular biology*. 2013;33:114-120
34. Chen JH, Simmons CA. Cell-matrix interactions in the pathobiology of calcific aortic valve disease: Critical roles for matricellular, matricrine, and matrix mechanics cues. *Circulation research*. 2011;108:1510-1524
35. Benton JA, Kern HB, Anseth KS. Substrate properties influence calcification in valvular interstitial cell culture. *J Heart Valve Dis*. 2008;17:689-699
36. Kloxin AM, Benton JA, Anseth KS. In situ elasticity modulation with dynamic substrates to direct cell phenotype. *Biomaterials*. 2010;31:1-8

37. Zhao R, Sider KL, Simmons CA. Measurement of layer-specific mechanical properties in multilayered biomaterials by micropipette aspiration. *Acta biomaterialia*. 2011;7:1220-1227
38. New SE, Aikawa E. Molecular imaging insights into early inflammatory stages of arterial and aortic valve calcification. *Circulation research*. 2011;108:1381-1391
39. Rabkin E, Hoerstrup SP, Aikawa M, Mayer JE, Jr., Schoen FJ. Evolution of cell phenotype and extracellular matrix in tissue-engineered heart valves during in-vitro maturation and in-vivo remodeling. *J Heart Valve Dis*. 2002;11:308-314; discussion 314
40. Hoerstrup SP, Sodian R, Daebritz S, Wang J, Bacha EA, Martin DP, Moran AM, Guleserian KJ, Sperling JS, Kaushal S, Vacanti JP, Schoen FJ, Mayer JE, Jr. Functional living trileaflet heart valves grown in vitro. *Circulation*. 2000;102:III44-49
41. Merryman WD, Lukoff HD, Long RA, Engelmayr GC, Jr., Hopkins RA, Sacks MS. Synergistic effects of cyclic tension and transforming growth factor-beta1 on the aortic valve myofibroblast. *Cardiovascular pathology: the official journal of the Society for Cardiovascular Pathology*. 2007;16:268-276
42. Thayer P, Balachandran K, Rathan S, Yap CH, Arjunon S, Jo H, Yoganathan AP. The effects of combined cyclic stretch and pressure on the aortic valve interstitial cell phenotype. *Annals of biomedical engineering*. 2011;39:1654-1667
43. Balachandran K, Alford PW, Wylie-Sears J, Goss JA, Grosberg A, Bischoff J, Aikawa E, Levine RA, Parker KK. Cyclic strain induces dual-mode endothelial-mesenchymal transformation of the cardiac valve. *Proceedings of the National Academy of Sciences of the United States of America*. 2011;108:19943-19948

SUPPLEMENTAL EXPANDED METHODS

Valvular interstitial cell (VIC) isolation and culture

Primary porcine valvular interstitial cells (VICs) isolated from aortic heart valves as described previously.(1) Briefly, hearts were acquired from pig (10 months), which were sacrificed at an USDA approved abattoir (THOMA Meat Market, Saxonburg, PA). To remove endothelial cells valve surfaces were scraped three hours after dissection. VIC isolation was performed using collagenase A (Sigma, St. Louis, MO) digestion. Cells were cultured in normal growth medium containing Dulbecco's modified Eagle's medium (DMEM) with 10% fetal bovine serum and 1% penicillin/streptomycin (control medium) (Invitrogen, Grand Island, NY) at 37°C, 5% CO2. Cells between passage 3 and 6 were used for all experiments.

Synthesis of materials

HAMA was synthesized as reported previously.(2) Briefly, after making a solution of 1wt% hyaluronic acid (Lifecore Biomedical, Chaska, MN) in deionized water, methacrylic anhydride (Sigma-Aldrich, St. Louis, MO) was added. By adding 5M NaOH (Sigma-Aldrich, St. Louis, MO), the pH was adjusted to 8, during which the solution was kept on ice for 24 hours. After metacrylation the HAMA solution was dialyzed against deionized water for 72 hours, which was followed by lyophilization. This resulted in solid white foam like material, which was stored at -80°C before using it for experiments.

The synthesis of GelMA has also been described before.(3) In brief, powdered type A cell culture tested gelatin from porcine skin (Sigma-Aldrich, St. Louis, MO) was dissolved in phosphate buffered saline (PBS), and then heated to 60°C under continuous stirring for 20 minutes to obtain a 10 wt% gelatin solution. Metacrylated gelatin (GelMA) solution was formed by drop wise adding of 8% (v/v) methacrylic anhydride under constant stirring for 3 hours at 50°C. The GelMA solution was then diluted and dialyzed against deionized water at 40°C for one week. Subsequently, the solution was lyophilized for 96 hours which yielded a white porous foam-like material, which was stored at –80°C before experimental use.

Hydrogel fabrication

Hybrid hydrogels were fabricated from HAMA and GelMA using photocrosslinking as previously reported.(1, 4) Briefly, 1mg photinitatior (PI) (Igracure 2595) was dissolved in 1 mL of phosphate buffered saline (PBS; Gibco) at 80°C. To achieve a concentration of 1wt% HAMA and 5wt% GelMA, we added 1 mL PI solution to 10 mg HA and 50 mg GelMA and put this into an 80°C oven for 20 minutes. The solutions were vortexed regularly. The polymer solution was then allowed to cool off to 37°C. VICs at 80% confluency were trypsinized and centrifugated at 1500 rpm for 5 minutes. The supernatant was aspirated and the remaining cell pellet resuspended in the prepolymer solution. We used a cell density of 10 million cells/mL. 50 µL of the cell-laden prepolymer solution was drop-wise added to a petri dish between two spacers with a height of 450 µm and covered with an autoclaved sterile glass slide. The cell-laden solution was then subjected to light (wavelength 360 nm) for 30

seconds with an intensity of 450 mW at a 10 cm height yielding a light intensity of 2.5 mW/cm^2. The exposure to light facilitated photoinitiator dependent crosslinking of the polymers in the solution yielding a disc shaped hydrogel with a height of 450 µm. The VIC-laden hydrogel was removed from the glass slide and placed into a well plate containing either control medium (CM) or osteogenic medium (OM) (control growth medium supplemented with 10 mM β-glycerophosphate, 10 ng/mL ascorbic acid, and 10^{-8} M dexamethasone) or OM with tumor necrosis factor alpha (TNF-α). The VIC-laden hydrogels were cultured for up to 21 days.

Silencing of alpha Smooth Muscle Actin in VIC-laden hydrogels

To inhibit the expression of α-smooth muscle actin (α-SMA), ON-TARGET plus SMART-pool (L-003605-00-00100) and a negative control (scramble (SCR)) from Dharmacon RNAi Technologies/ ThermoScientific (Chicago, IL, USA) was used. Transfection of 50 nmol/l siRNAs was performed using DharmaFECT 1 transfection reagent twice per week over the entire culture period. Samples were analyzed at day 14 and day 21 of culture.

Histological analysis and immunofluorescence staining of VIC-laden hydrogel constructs

Human calcified aortic valves were obtained from CAVD patients that underwent surgical valve replacement surgeries according to Brigham and Women's Hospital IRB protocol (#201-P-002567/2; BWH). Tissue was frozen in optimal cutting temperature (OCT) compound (Sakura Finetech, Torrance, CA), of which 7 µm sections were cut. The VIC-laden hydrogels were washed with PBS for 5 minutes and then fixed in 4% paraformaldehyde for 20 minutes, followed by PBS wash. The hydrogels were placed into a 30% (w/v) sucrose solution overnight at 4°C, after which they were frozen in OCT compound and 10µm sections were cut. To detect calcium deposition, sections were stained with 0.02 mg/mL Alizarin Red S (ARS) solution (Sigma, St. Louis, MO). Von Kossa staining (American MasterTech) was used to visualize phosphate deposition in the VIC-laden hydrogel cross sections. Images were obtained using Nikon Elipse microscope (Nikon Instruments). Calcific nodules/ positively stained cells were quantified by manually counting noduli per high power field (HPF) using five fields per hydrogel, and three hydrogels per time point for each condition.

Immunofluorescence staining for αSMA and runt-related transcription factor 2 (Runx2) was performed. Hydrogel sections were permeabilized using 0.1% Triton-X. After blocking in 4% horse serum, sections were incubated with monoclonal mouse anti-human α-SMA primary antibody (Clone 1A4, Dako, Dako Denmark A/S, Glostrup, Denmark) or a monoclonal mouse anti-Runx2 primary antibody (Abcam, Cambridge, USA) for 90 minutes at room temperature (RT), followed by biotin labeled secondary antibody (Vector Labs, Burlingame, CA, USA) for 45 minutes at RT and streptavidin labeled AlexaFluor 488 (Invitrogen, Grand Island, NY) for α-SMA and AlexaFluor 594 (Invitrogen, Grand Island, NY) for Runx2. Sections were washed three times in PBS for 5 minutes and nuclei were counterstained with 4',6-diamidino-2-phenylindole (DAPI) containing mounting medium (Vector Labs, Burlingame, CA, USA). Images were taken with an Eclipse 80i microscope (Nikon, Melville, NY, USA) and processed with Elements 3.20 software (Nikon, Melville, NY, USA). Positive

staining was quantified by manually counting positively stained cells of the total cell number in five HPF per hydrogel. Three hydrogels were quantified per condition for each time point.

Quantification of alkaline phosphatase and calcium in engineered hydrogel constructs

Alkaline phosphatase (ALP) activity was measured using a colorimetric kit (Biovision Lifesciences, Milpitas, CA, USA). Samples were washed in PBS, and stored in ultrapure water at -80°C before use. Three hydrogels per time point per experiment were pooled together. Upon analysis, samples were thawed and homogenized using a tissue lyzer (Qiagen, Venlo, The Netherlands). The homogenized hydrogels were centrifuged at 13.000 rpm for 3 minutes. The supernatant containing ALP was transferred to new tubes. To measure ALP activity we followed the manufacturer's protocol. Briefly, 16 µL of supernatant was added to 64 µL of ALP assay buffer and 50 uL of PnPP solution was added and incubated for 1 hour at room temperature. The absorbance was read at a wavelength of 405 nm. Values were normalized to the standard curve. Calcium content was quantified using a colorimetric kit (Biovision Lifesciences, Milpitas, CA, USA), using the manufacturer's protocol. Briefly, 50 µL of sample was added to 60 µL of calcium assay buffer, followed by 90 µL chromogenic reagent is added and incubation for 10 minutes at room temperature in the dark. Absorbance was read at a wavelength of 575nm with a plate reader. Values were normalized to the standard curve. Calcium content and ALP activity were normalized to DNA content. Double stranded DNA (dsDNA) was measured with a Quanti-it PicoGreen dsDNA Quantification Kit (Invitrogen, Grand Island, NY, USA).

Real Time Polymerase Chain Reaction for expression of cell markers

VICs were isolated from cell-laden hydrogels using a mechanical disruption of the hydrogels (TissueLyzer, Qiagen, Venlo, The Netherlands). Total RNA was isolated from using GE Healthcare RNAspin mini RNA Isolation kit. The amount of RNA in each sample was measured using NanoDrop 2000c (ThermoScientific, Waltham, MA, USA). Total RNA was reverse transcribed with oligo-(dT)12-18 primers(Invitrogen/Life Technologies,Grand Island, NY, USA) and Superscript II reverse transcriptase (Invitrogen/Life Technologies,Grand Island, NY, USA) to obtain a target cDNA concentration of 0.335ug/mL followed by RT- PCR using SYBR Green (BioRad, Hercules, CA, USA), and annealing temperatures of 95 and 60 degrees Celsius for 35 cycles. Primer sequences were designed with Primer3 software and were as follows: α-SMA: F:5'-AGTGCGACATTGACATCAGG-'3 and R:5'-CTGGAAGGTGGACAGAGAGG-'3, Runx2 F:5'-ACCCAGAAGACTGTGGATGG-'3 and R:5'-ACCTGGTCCTCAGTGTAGCC-'3 The housekeeping gene used was Glyceraldehyde-3-phosphate dehydrogensase (GAPDH): F:5'-CCCAGAAGACTGTGGATGG-'3, R:5'- ACCTGGTCCTCAGTGTAGCC-'3. Expression was quantified using comparative Ct (Cycle threshold method) $2^{-\Delta\Delta CT}$ method) with the following equations: (1) ΔCT =CT of target gene –CT of housekeeping gene, (2) ΔΔCT=ΔCT day x – ΔCT day 1; (3) Fold increase between groups = $2^{-\Delta\Delta Ct}$

Cell viability and apoptosis

Cell viability was determined by fluorescent labeling with 4μM Calcein AM and 2μM Ethidium Homodimer-1 (LIVE/DEAD Viability kit for mammalian cells, Invitrogen, Grand Island, NY, USA). Cell-laden hydrogels were first washed with PBS for 5 minutes and then incubated with fluorescent dye for 20 minutes at room temperature. The cell-laden hydrogels were then washed with PBS again and imaged using an A1/C1 confocal microscope (Nikon Instruments, Inc. Melville, NY) Three hydrogels were analyzed per time point per condition. Of each hydrogel 3 z-stacks (10 μm per slice) were made of which a compressed image was formed. Amount of viable cells were stained green and dead cells red, and were manually counted using Image J Software. Data is depicted as percentage of live cells. Apoptosis was determined by TUNEL (terminal deoxynucleotidyl transferase mediated dUTP nick end labeling) staining (Millipore, Remecula, CA, USA), according to manufacturer's protocol and quantified using fluorescence microscopy. Data are depicted as percentage of positively stained cells.

Statistical Analysis

Results are presented as mean +/- standard deviation unless indicated otherwise. Unpaired student's t-test was used for comparisons between two groups. One-way ANOVA was used to evaluate statistical significant differences in multiple groups. $P < 0.05$ was considered significant.

REFERENCES

1. Hjortnaes J, Camci-Unal, G.; Hutcheson, J.D.;Jung, S.M, Schoen, F.J.; Kluin, J.; Aikawa, E; Khademhosseini, A. Hydrogel Composition directs Valvular Interstitial Fate. Advanced Healthcare Materials., 2014
2. Camci-Unal G, Nichol JW, Bae H, Tekin H, Bischoff J, Khademhosseini A. Hydrogel surfaces to promote attachment and spreading of endothelial progenitor cells. Journal of tissue engineering and regenerative medicine. 2012. Epub 2012/01/10.
3. Ramon-Azcon J, Ahadian S, Obregon R, Camci-Unal G, Ostrovidov S, Hosseini V, et al. Gelatin methacrylate as a promising hydrogel for 3D microscale organization and proliferation of dielectrophoretically patterned cells. Lab on a chip. 2012;12(16):2959-69. Epub 2012/07/10.
4. Camci-Unal G, Cuttica D, Annabi N, Demarchi D, Khademhosseini A. Synthesis and characterization of hybrid hyaluronic acid-gelatin hydrogels. Biomacromolecules. 2013;14(4):1085-92. Epub 2013/02/20.

SUPPLEMENTAL FIGURES

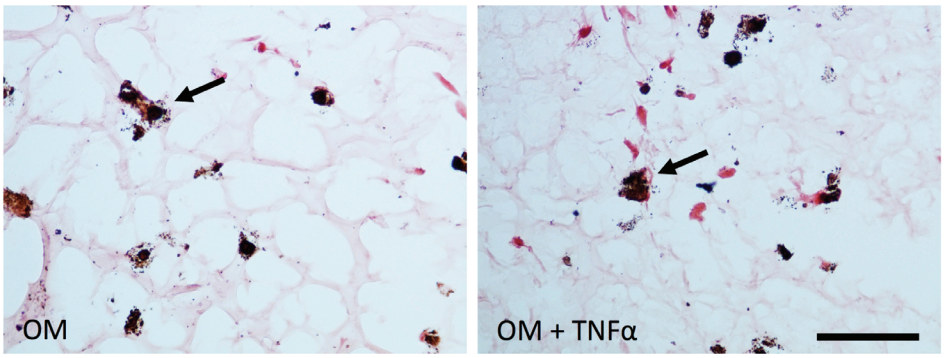

Supplemental Figure I. Calcification potential of 3D *in vitro* valve model.
40x magnification of Von Kossa staining of VIC laden hydrogels cultured in osteogenic media (OM) or osteogenic media with TNFα (OM + TNFα) at day 21. Arrows indicate brown/black positive staining. Bar: 50μm

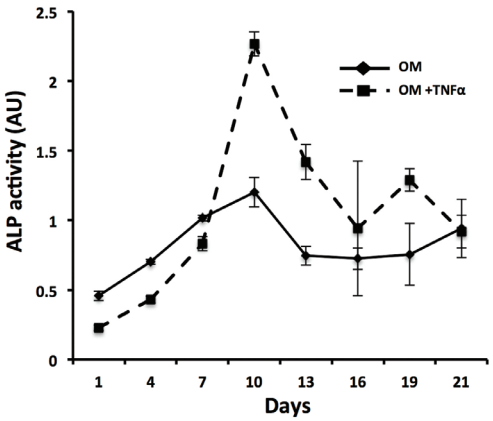

Supplemental Figure II. ALP Activity in 3D constructs.
ALP activity, a marker for early calcification was measured every 72 hours in VIC laden hydrogels cultured in osteogenic media (OM) and osteogenic media with TNFα. Data is depicted as mean ± SD (n=3)

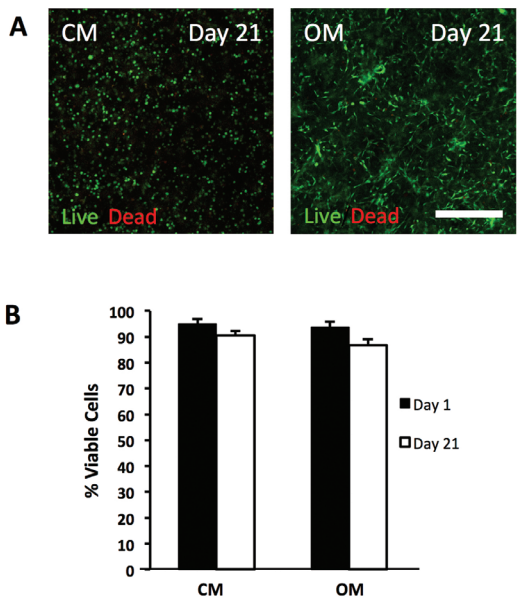

Supplemental Figure III. Cell viability after 21 days of culture. VIC-laden hydrogels were cultured in control media (CM) and osteogenic media (OM) for up to 21 days. **(A)** Representative confocal images of the middle of the VIC-laden hydrogel stained with Live/Dead assay. Live cells are green, dead cells red. **(B)** Quantification of cell viability. Data is depicted as mean percentage live cells ± SD (n=3). Bar: 100µm

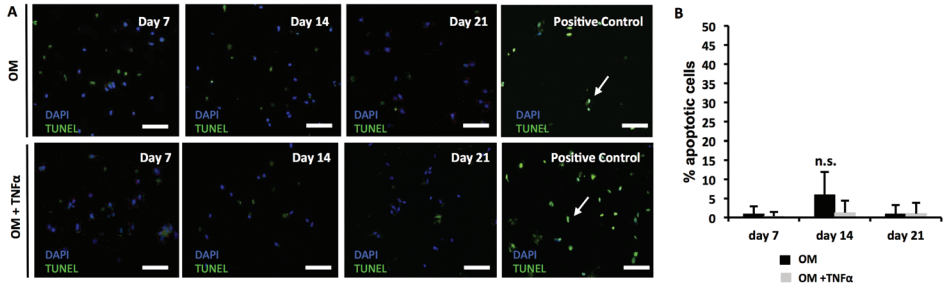

Supplemental Figure IV. Evaluation of apoptosis in VIC-laden hydrogels. **A** TUNEL staining of VIC laden hydrogels at day 7, 14 and 21 after culture in osteogenic media (OM) and osteogenic media with TNFα (OM + TNFα). Arrow indicates positive staining for apoptosis. Bar; 50 µm **B** Quantification of % negative apoptotic cells using Image J. (n=3) Data is depicted as mean±SD.

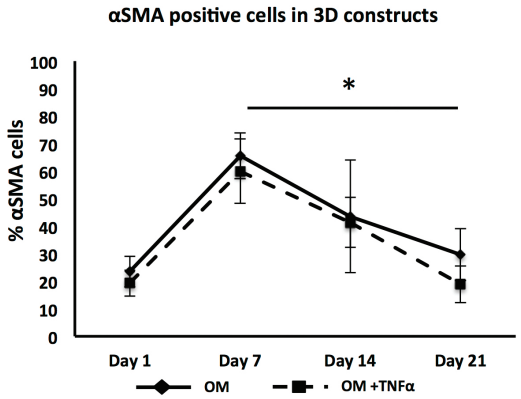

Supplemental Figure V. Quantification of αSMA positive cells . VIC-laden hydrogels were cultured osteogenic media (OM) and osteogenic media with TNFα (OM+TNFα) for up to 21 days. Quantification of positively stained cells for αSMA at each time point. Data is depicted as percentage of positive cells per high power field (HPF) (mean ± SD) (n=3) * p<0.05.

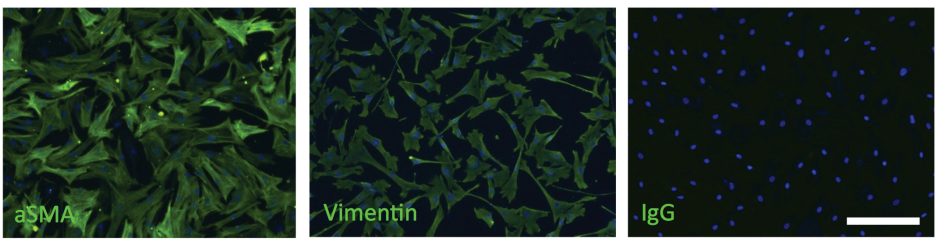

Supplemental Figure VI. Phenotypic characterization of VICs in culture. Immunofluorescence staining of pVICs seeded in normal polystyrene tissue culture plate. αSMA, Vimentin, IgG: green, DAPI: blue, bar = 50 µm

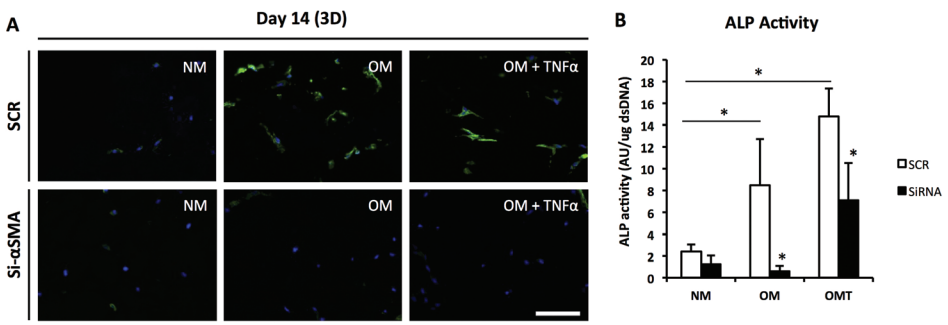

Supplemental Figure VII. Early marker for osteogenesis is reduced when by silencing of αSMA. VIC-laden hydrogels were cultured for up to 14 days in control media (CM), osteogenic media (OM) and osteogenic media with TNF-α (OM + TNFα) **A.** Immunofluorescent staining αSMA (green) at day 14, bar: 50µm **B** Alkaline phosphatase (ALP) activity normalized for DNA (ug/mL) content at day 14. Cell laden hydrogels were cultured for 14 days and either treated with SiRNA (SI-αSMA) against αSMA or scramble control (SCR) twice a week. (n=3) Data is depicted as mean ± SD. *p < 0.05,

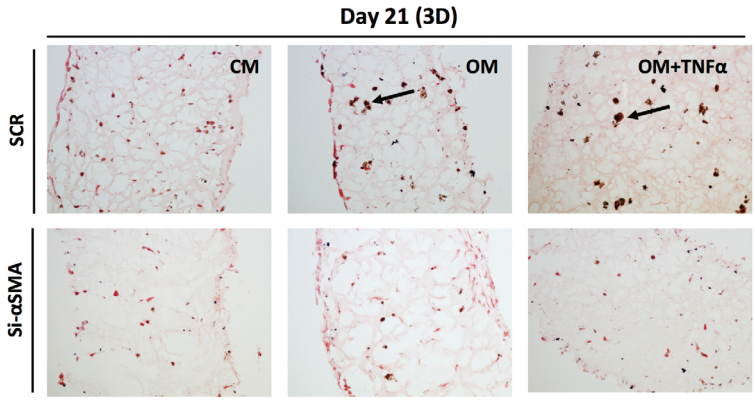

Supplemental Figure VIII. Silencing αSMA reduces osteogenesis. VIC-laden hydrogels were cultured up to 21 days in control media (CM), osteogenic media (OM) or osteogenic media with TNFα (OM + TNFα). Silencing of αSMA (Si-αSMA) was performed twice per week. Scramble (SCR) SiRNA served as control. Von Kossa staining with Nuclear Fast counterstain. Arrow indicates positive Von Kossa staining. Bar: 50 µm

9

Radiation-associated Calcific Aortic Valve Disease: Preliminary Insights

J. Hjortnaes[1,2], R. Driessen[1], J. W. van Rijswijck[1], D. Konozo[3], J. Kluin[1], E. Aikawa[2,4*], C. V. C. Bouten[5*]

In preparation

[1]Department of Cardiothoracic Surgery, Division of Heart and Lungs, University Medical Center Utrecht, Utrecht, the Netherlands. [2]Center of Excellence in Vascular Biology, Department of Medicine, Brigham and Women's Hospital, Harvard Medical School, Boston, USA; [3]Department of Oncological Radiotherapy, Dana Farber Institute, Brigham and Women's Hospital, Harvard Medical School, Boston, USA; [4] Center for Interdiscplinary Cardiovascular Sciences, Brigham and Women's Hosptial, Harvard Medical School, Boston, USA; [5]Department of Biomedical Engineering, Technical University Eindhoven, Eindhoven, The Netherlands

[*]equal contribution

ABSTRACT

Introduction

Mediastinal ionizing radiotherapy is associated with an increased risk of calcific aortic valve disease (CAVD). Due to an improved survival of patients with mediastinal tumors receiving mediastinal radiotherapy, prevalence of co-morbidities such as radiation-induced valve disease is increasing. However, the mechanism of radiation associated valvular disease is largely unknown. Aortic valve calcification is considered an actively regulated disease process by valvular interstitial cells (VICs). We hypothesize that ionizing radiation accelerates VIC-induced calcification.

Methods and Results

VICs were cultured in control medium (CM) or osteogenic medium (OM), and irradiated with 0, 2, 4, 8, and 16 Gy. Increase in radiation dosage demonstrated a decrease in amount of viable cells. Similarly, proliferation decreased in a dose-dependent manner after a culture period of 14 days. VICs cultured in OM demonstrated an increased loss of myofibroblast phenotype, when exposed to increased dose of irradiation, compared to VICs cultured in CM. Mineralization was mostly present in VICs exposed to 4 Gy Increase in irradiation dose showed VICs to develop into a quiescent giant-fibroblast like cell morphology.

Conclusion

This ongoing investigation demonstrated that radiation might accelerate loss of myofibroblast-like phenotype and mineralization by VICs. In addition, itradiation might induce differentiation of VICs into a terminally differentiated giant cell fibroblast. Further studies are needed to elucidate the mechanisms.

INTRODUCTION

Using radiotherapy for malignancies of the chest and the chest wall is associated with an increased risk for developing cardiomyopathy, pericarditis or valvular disease.[1-5] Moreover, this risk is elevated in patients receiving radiotherapy below the age of 21.[1] The majority of valvular disease includes aortic valve disease.[6] Within 20 years after mantle radiation for lymphoma, an incidence of aortic valve stenosis is 16%.[7] The only treatment for aortic valve stenosis is surgical replacement.[8] However, following chest radiotherapy, surgical risk is significantly increased.[9] Radiation-associated aortic valve disease demonstrates pathological hallmarks similar to calcific aortic valve disease (CAVD). Generally, CAVD is characterized by initial fibrotic thickening, mineralization, eventually leading to aortic valve leaflet dysfunction and subsequent aortic valve stenosis.[10]

Traditionally, CAVD is viewed as a passive disease, culminating from years of wear and tear. However, currently it is considered an active disease process, in which resident valvular interstitial cells (VICs) are considered to be key regulators. VICs exist in various phenotypes in the heart valve. Quiescent VICs are healthy fibroblast like cells, which upon exposure to environmental stimuli are able to differentiate into myofibroblast-like cells.[11] These activated VICs (aVICs) can remodel the extra cellular matrix (ECM) by expressing matrix metalloproteinases (MMPs) or depositing ECM proteins such as collagen.[11] The interplay between these phenotype changes is key to maintaining valve tissue homeostasis, and provides for the ability of heart valves to adapt to changes in functional demand. It is believed that the fibrotic response observed in early CAVD is a consequence of persistent activation of VICs. In addition, histological studies of end-stage stenotic valves have demonstrated the presence of osteoblast-like cells.[12] It is suggested that VICs can differentiate into osteoblast-like cells and actively deposit calcium in the valve interstitium. This osteoblast-like differentiation is characterized by loss of alpha smooth muscle actin phenotype and gaining bone markers such as the upregulation of the transcription factors runx2 and Osteocalcin, and increased ALP activity.[13] The temporal relationship of these VIC phenotypes and how they relate to disease onset or even disease progression in humans is unknown.

Radiation-associated disease cannot merely be considered similar to CAVD. Specific cellular and ECM responses to ionizing radiation have been well documented. Irradiation has shown to activate stromal fibroblasts.[14] In addition, increased activation and production of transforming growth factor – beta (TGFβ) has been reported as a result of irradiation to vessels and myocardium, which in turn leads to increased collagen deposition[15, 16] Explanted heart valves have shown the presence of terminally differentiated atypical giant-like fibroblasts, seen also in skin as a consequence of radiation.[17, 18]

Radiation-induced CAVD is a major burden in patients subjected to radiotherapy. Considering the increased survival of these patients, the incidence of radiation induced CAVD is expected to rise. The aim of this work is to investigate the relationship between radiation and using 2D and 3D in vitro models of CAVD. We hypothesize that radiation catalyzes the fibro-calcific response of VICs.

The work presented here is an initial step in the ongoing investigation to unravel the effects of irradiation on development of CAVD.

METHODS

Valvular interstitial cell isolation and culture

Porcine aortic valvular interstitial cells (pVICs) were obtained as described previously[19] and cultured in normal growth medium containing DMEM, high glucose, pyruvate (Gibco, Life Technologies, Grand Island, NY, USA) supplemented with 10% fetal bovine serum and 1% penicillin/streptomycin (Gibco) at 37°C and 5% CO2 in T150 flasks. This medium condition was also used as control (CM). The cells were subcultured at 70-80% confluency. For all experiments, cells between passage three and six were used. For immunofluorescence, cells were seeded on gelatin-coated coverslips. Cells from three different donors were used for all experiments.

Irradiation

For irradiation experiments, cells were plated at a seeding density of 10.000/cm^2, 24 hours before irradiating. Prior to irradiating, medium was changed to normal or osteogenic medium (control medium supplemented with 10 mM β-glycerophosphate, 10 nM dexamethasone and 0.5 mg/ml L-ascorbic acid (Sigma-Aldrich, St. Louis, MO, USA)). The cells were irradiated with 0, 2, 4, 8 and 16 Gy (0.90 Gy/min) with a Gammacell 40 Exactor Cs-137 irradiator (Best Therotronics, Ottawa, Ontario, Canada). The control group (0 Gy) was transported to the irradiator together with the treated groups. After radiation cells were kept in culture, depending on the analysis, for 1, 2, 7 or 14 days.

Hydrogel fabrication

Hybrid hydrogels were fabricated from HAMA and GelMA, which were synthesized as reported previously,[19] using photocrosslinking Briefly, VICs were resuspended in the prepolymer solution consisting of 1wt% HAMA and 5wt% GelMA. 50 µL of the cell-laden polymer solution was added between two spacers each with a height of 450 µm and and subjected to light (wavelength 360 nm) with a light intensity of 2.5 mW/cm^2. VIC-laden hydrogels were cultured in either control medium (CM) or osteogenic medium (OM) (CM supplemented with 10 mM β-glycerophosphate, 10 ng/mL ascorbic acid, and 10 nM dexamethasone). Hydrogels were irradiated with 0, 4 and 16 Gy. The effect of radiation on hydrogel composition was evaluated by performing a compaction assay.

Cell viability and proliferation

To assess the cell viability after radiation, the ATP content of the cells was measured at day 2. For this analysis a luminescent cell viability assay (Progema, Madison, WI) was used. The DNA content was measured with Quant-iT PicoGreen kit (Life Technologies).

Osteogenesis

The activity of ALP was quantified with a colorimetric assay kit (Biovision, Milpitas, CA) on day 1, 7 and 14. The ALP activity was normalized to DNA content. Calcium content in hydrogels was quantified using a colorimetric assay (Biovision, Milpitas, CA) normalized for DNA content.

Immunofluorescence and Histological Analysis

At day 14, VICs were fixed with ice-cold methanol for 30 minutes. Cells were stained for ALP activity with eosin counterstaining and for αSMA, collagen and the nucleus. αSMA was stained with an anti-human αSMA antibody (Clone 1A4, Dako, Carpinteria, CA, USA). For nuclear staining, DAPI (Life Technologies) was used and to visualize collagen we used an in-house developed probe CNA35. ALP activity was visualized with a 5-bromo-4-chloro-3-indolyl phosphate /nitroblue tetrazolium (BCIP/NBT) solution (Amresco, Kaysville, UT, USA) and an eosin counterstaining (Sigma-Aldrich).

Real-Time Polymerase Chain Reaction

To quantify mRNA expression of irradiated VICs, we performed RT- PC. RNA was isolated with an RNeasy kit (Qiagen, Valencia, CA, USA) on day 1, 7 and 14. From the extracted RNA, complementary DNA was made with oligo-(dT)12-18 primers and SuperScript II reverse transcriptase (Life Technologies). Real-Time Polymerase Chain Reaction (RT-PCR) was performed using SYBR Green (BioRad, Hercules, CA, USA) for αSMA (cell activation), collagen type I (functionality), vimentin (osteoblast differentiation), Runx2 (calcification), and housekeeping gene glyceraldehyde 3-phosphate dehydrogenase (GAPDH). The following primer sequences were used: αSMA: F:5'-AGTGCGACATTGACATCAGG-'3 and R:5'-CTGGAAGGTGGACAGAGAGG-'3, collagen type I F:5'CCAAGAGGAGGGCCAAGAAGAAGG-'3 and R:5'-GGGGCAGACGGGGCAGCACTC-'3, vimentin F:5'-AGCAGTATGAGAGTGTGGCC-'3 and R:5'- CTTC-CATTTCCCGCATCTGG-'3, Runx2 F:5'-ACCCAGAAGACTGTGGATGG-'3 and R:5'-ACCTGGTCCTCAGTG-TAGCC-'3 and GAPDH: F:5'-CCCAGAAGACTGTGGATGG-'3, R:5'- ACCTGGTCCTCAGTGTAGCC-'3. The mRNA expression was quantified using the comparative Ct method.

Statistics

Data is presented as the mean +/- standard deviation. To evaluate significant differences one-way ANOVA was performed using SPSS software. $P < 0.05$ was considered significant. For posthoc testing, the Bonferroni test was used.

RESULTS

Cell Viability and Proliferation

VICs were exposed to 0, 2, 4, 8, and 16 Gy of radiation. To evaluate cell viability after 48 hours we performed an ATP activity assay, demonstrating a dose response curve. (Figure 1)

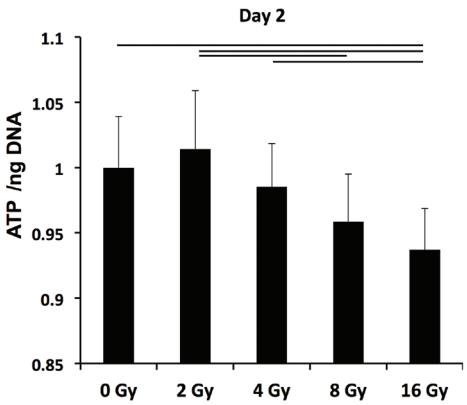

Figure 1. Cell viability decreases when radiation dose increases. ATP content was measured in VICs exposed to 0, 2, 4, 8, and16 Gy after 48 hours and normalized for DNA content, demonstrating a significant decrease in viability in 8 and 16 Gy exposed VICs. ($p < 0.05$)

ATP content of VICs decreased upon exposure to increased radiation doses. We observed a 7% decrease in cell viability compared to the control group (0 Gy). Next, we determined the proliferation response of irradiated VICs by quantifying DNA content at several time points (Figure 2). Proliferation also decreased upon increase in radiation dose, following a similar trend to cellular viability, establishing a dose-dependent response of VICs to radiation.

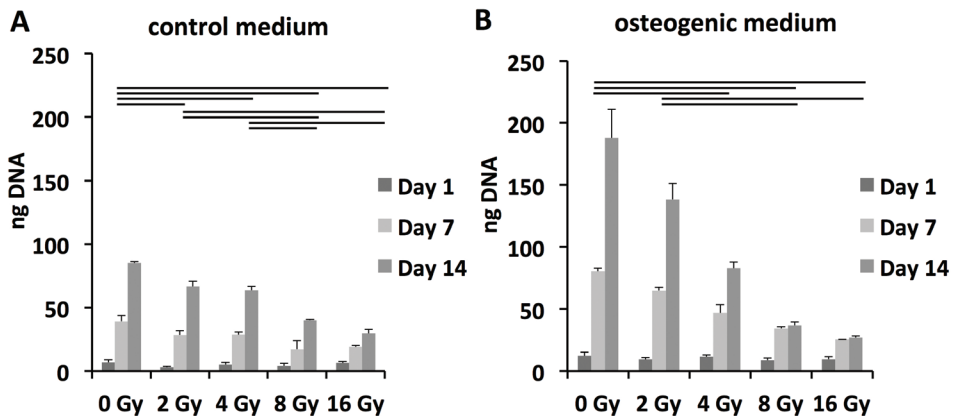

Figure 2. Cell proliferation decreases along radiation dose increase. DNA content was measured in VICs exposed to 0, 2, 4, 8, and 16 Gy at day 1, 7 and 14. An inverse relationship between radiation dose and proliferation is observed. Data is presented as mean±SD, $p < 0.05$.

VIC morphology, differentiation and functionality

VICs demonstrated a myofibroblast-like phenotype, hallmarked by αSMA expression, when cultured in control medium and osteogenic medium (Figure 3A). Notably, the amount of cells observed in each well decreased when exposed to increased radiation dose.

Conversely, the cellular size of VICs exposed to radiation increased. In addition, a decrease in αSMA-positive cells was observed when exposed to increased dose of radiation, in comparison to our control group (0 Gy), to be αSMA positive. This result was confirmed by RT-PCR, where αSMA expression follows a similar trend. (Figure 3B). No difference between groups was observed at day 1 after radiation, but at day 7 a clear decrease in αSMA expression is seen.

We also observed an increase in collagen staining at day 14 of culture in OM compared to CM, which remains present in lesser amount at 2Gy irradiation, but was obsolete at 4Gy and higher dosage. At 14 days, VICs cultured in control medium showed little collagen staining at 0Gy, but similarly to OM is absent at higher radiation dosages. This was confirmed by mRNA expression of collagen type 1, showing a decline in collage type I expression alongside radiation dosage increase. No difference between groups in αSMA and collagen mRNA expression was found in control media. Vimentin expression remained similar in all groups (data not shown).

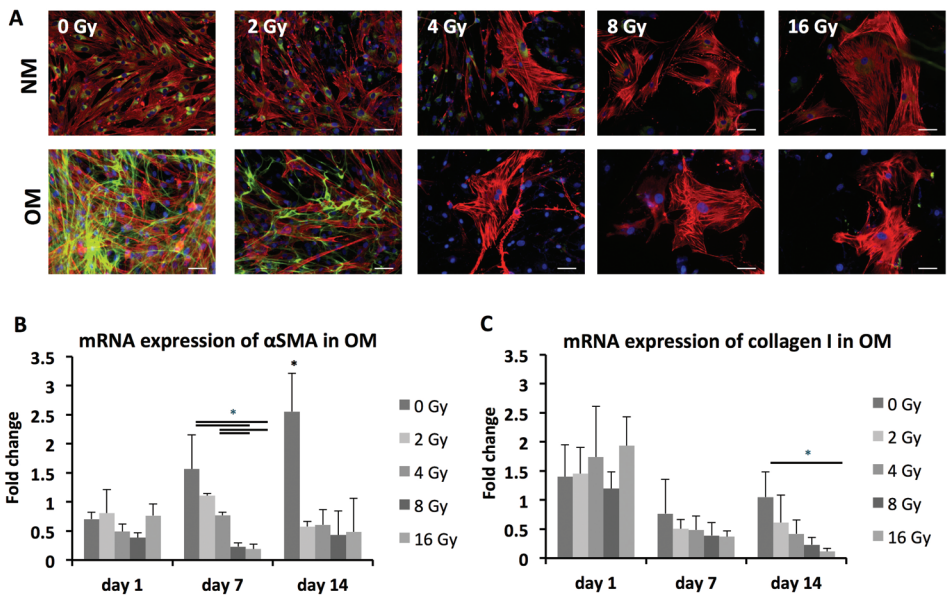

Figure 3. Myofibroblast-like differentiation of VICs changes in a dose dependent manner. A VICs were cultured in normal media (NM) and osteogenic media (OM) for up to 14 days after being irradiated with 0, 2, 4, 8, and 16 Gy. At day 14 VICs were double stained for αSMA (red), collagen (green), and cell nuclei (DAPI/blue) bar: 50 μm. **B** RT-PCR of mRNA expression of αSMA in OM **C** RT-PCR of mRNA expression of Collagen in OM. Data is depicted as mean +/- SD. $p < 0.05$

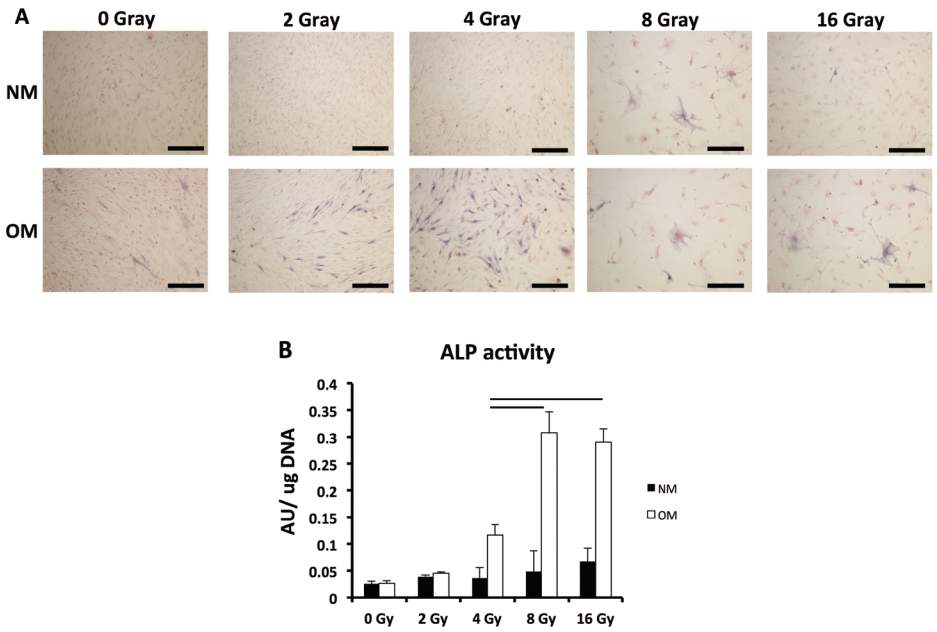

Figure 4. Radiation is associated with VIC-driven osteogenesis. A ALP staining (BCIP/NTP) of VICs cultured in control media (CM) and osteogenic media (OM). VICs exposed to 4Gy radiation demonstrate increased ALP activity compared to 2Gy and control. At 8 and 16 Gy, cellular density seems to have declined and morphology changed. bar: 50 µm. **B** ALP activity was quantified and normalized to DNA content demonstrating an increase in osteogenesis upon increase of radiation dose. Data is depicted as mean ± SD, $p < 0.05$

9

Osteogenesis and Radiation of VICs

The activity of the early osteogenic marker ALP was measured at day 1, 7 and 14 of culture. We demonstrated ALP activity to be present in high dose groups at day 14 of culture. To visualize ALP activity, cells were stained with BCIP/NBT, resulting in a dark blue staining upon ALP hydrolyzing BCIP. (Figure 4) No ALP staining was observed in the CM groups, apart from high radiation doses, showing some positive ALP cells. When cultured in OM, VICs show ALP staining predominantly in the 0,2 and 4 Gy groups. Upon exposure to 8 or 16Gy and cultured in OM, there were less ALP positive cells.

Preliminary data of VIC-laden hydrogels exposed to radiation

Cell-free hydrogels exposed to radiation demonstrated no difference in compaction (Figure 5A), indicating that radiation did not affect crosslinking or composition of the hydrogels. There was no significant difference observed in proliferation of VICs encapsulated in hydrogels, exposed to radiation and cultured in either control or osteogenic media. (Figure 5B) In an early pilot experiment, we observed an increase in calcium content in VIC-laden hydrogels cultured in OM when exposed to 4Gy of radiation compared to the control group. (Figure 5C) However, a decrease in calcium content was seen in 16Gy irradiated VIC-laden hydrogels.

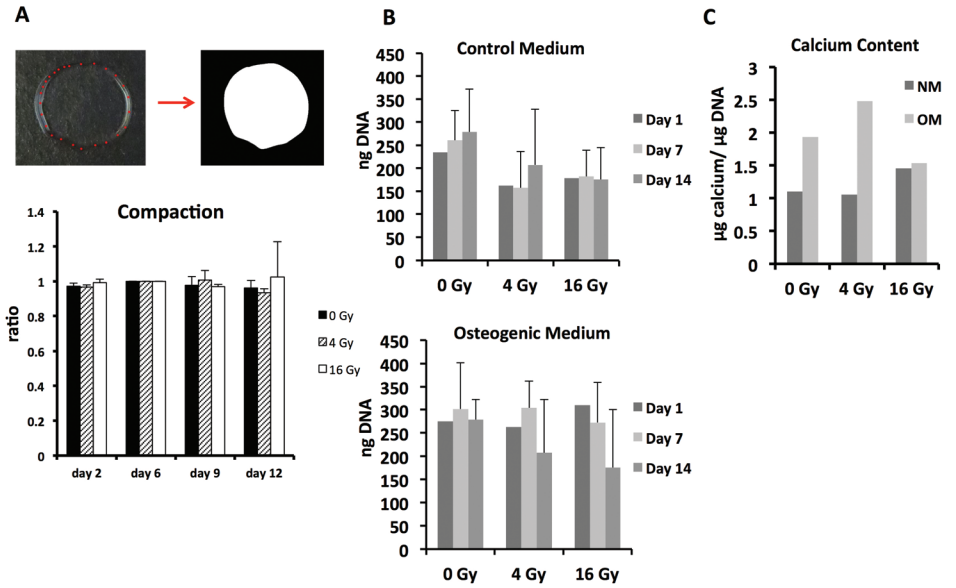

Figure 5. Preliminary results of irradiation of VIC-laden hydrogels. A Hydrogels without cells were exposed to 0, 4, and 16 Gy irradiation (n=6). A gel-compaction assay demonstrated no change over time, indicating no effect of radiation on the crosslinking or stability of the hydrogel. **B** VIC-laden hydrogels were exposed to 0, 4, and 16 Gy before cultured in CM or OM. No significant difference in proliferation was demonstrated in either group. **C** Calcium content was quantified after VIC-laden hydrogels were irradiated and cultured for 14 days. An increase in calcium content was observed at 4 Gy in OM, whereas a decrease was observed in 16 Gy radiated VIC-laden hydrogels. One donor was used for this pilot experiment. Data is depicted as mean ± SD. $p < 0.05$.

DISCUSSION

This study is ongoing work, in which we aim to unravel radiation-associated CAVD. We demonstrate that radiation induces a decrease in cell viability and proliferation of VICs in culture in a dose dependent manner. In addition, we observe an increase in cell size of VICs *in vitro* exposed to higher doses of radiation. Moreover, we show a decrease in both myofibroblast-like differentiation of VICs when exposed to increasing radiation doses both in control and osteogenic media. However, an increase in early osteogenic activity is observed upon increasing radiation dose. Finally, we observe differentiation of VICs into a giant-cell fibroblast phenotype at high dose of irradiation.

However, caution is warranted when interpreting these results. When VICs are exposed to 8Gy and 16Gy, next to a lower viability and proliferation, we observe a marked change in cell shape. It is clear that these radiation dosages alter cellular function drastically; by the almost giant fibroblast-like aspect they obtain after 14 days of culture. Previous studies have reported on these atypical giant sized fibroblasts in skin, indicating terminal differentiation.[17] This arrested state may eventually result in excessive growth of the cell, which could explain why we observe a metabolic active cell. Although we have not looked at DNA damage at this stage, other work has demonstrated that these doses of radiation are associated with increased cellular damage.[20] It might explain the

deviant shape VICs demonstrate. Curiously, these cells do exhibit ALP activity, a marker for early osteogenesis. More accurate analysis of the mineralization potential of these cells is warranted, but these results indicate that radiation may induce an osteogenic active phenotype of VICs *in vitro*.

VICs have a higher radio-resistance than most cancer cell lines.[21] Nevertheless, they do follow a similar dose-dependent pattern to other cancer cell line studies.[21] Osteogenic activity was also observed in VICs in control media exposed to high dosages of radiation, supporting the hypothesis that radiation somehow can accelerate the osteoblast-like differentiation of VICs even if not in an osteogenic environment.

Few studies have researched radiation-associated CAVD. Studying VIC response in vitro is not sufficient to recapitulate the events that may occur in vivo. To overcome this challenge, hydrogel micro engineering has emerged as a powerful tool to create three dimensional (3D) tissue models able to simulate the VIC micro-environment *in vitro*. We have recently demonstrated that combining hyaluronic acid and collagen by photo-crosslinking, a three dimensional environment can be fabricated that simulates the valvular micro- environment. Since this environment facilitates the quiescence of VICs,[19] it is a potentially valuable approach to study the effect of radiation, as it may occur in vivo, in which quiescent VICs are exposed to radiation. Our preliminary results demonstrate that hydrogel composition seems unaffected by radiation, as measured by compaction. Arguably, elasticity and porosity must also be evaluated.

Due to our observation that VICs in culture form into atypical giant-like fibroblasts when exposed to 8 and 16 Gy, but retain their native morphology at 4 Gy, we chose to expose VIC-laden hydrogels to 0, 4, and 16 Gy. In addition, 16 Gy demonstrate osteogenic activity of VICs even in normal growth media, potentially accentuating the accelerated mineralization observed in patients. Although currently radiotherapy is mostly conducted in a fractioned from, 4 Gy is similar to the therapeutic range subjected to patients.

In non-radiation associated CAVD mechanical stress is thought to be one of the initiators of calcification of the valve.[22] This stress can induce lesions in the *fibrosa* layer, eventually perpetuating CAVD. Radiation also creates micro fractures in collagen.[23] Therefore, the micro lesions in irradiated heart valves can be one of the key mechanisms of valvular heart disease in irradiated patients. Although compaction analysis shows little difference, it doesn't rule out damage to the ECM proteins in the hydrogel. Structural analysis is needed to investigate this mechanism.

To date little is known about the relationship between VICs and radiotherapy. One other study has demonstrated an increase in osteoblast-like differentiation of VICs in vitro when exposed to radiation.[24] However, only one dosage was used. It is paramount in the pursuit of potentially adjusting dosage regimens of radiotherapy to investigate various dosages of radiation, considering the variation of effects it may inflict on tissue. Great development has already been made in radiotherapy. With current standards gamma radiation can better focus on targeted tissue and shield surrounding tissues as much as possible. This has lead to the ability of using a higher dose of radiation to target a smaller area. To this end, it is believed that the amount of patients developing cardiovascular disease would diminish. However, the aortic valve area remains unshielded in

mantle field radiation for Hodgkin's lymphoma.[25] In addition, indirect damage by reactive oxygen species (ROS) as a consequence of radiation may occur in otherwise shielded areas.[26]

In summary, this preliminary work demonstrates that radiation might accelerate loss of myofibroblast-like phenotype and mineralization by VICs. In addition, we demonstrate how a tissue engineered three-dimensional model for the valvular microenvironment is necessary to understand key processes of radiation associated CAVD as it may occur in vivo. However, further work on this research is required to draw clinically relevant conclusions.

REFERENCES

1. Aleman BM, van den Belt-Dusebout AW, Klokman WJ, Van't Veer MB, Bartelink H, van Leeuwen FE. Long-term cause-specific mortality of patients treated for hodgkin's disease. *Journal of clinical oncology: official journal of the American Society of Clinical Oncology*. 2003;21:3431-3439
2. Adams MJ, Lipshultz SE, Schwartz C, Fajardo LF, Coen V, Constine LS. Radiation-associated cardiovascular disease: Manifestations and management. *Seminars in radiation oncology*. 2003;13:346-356
3. Hancock SL, Tucker MA, Hoppe RT. Factors affecting late mortality from heart disease after treatment of hodgkin's disease. *Jama*. 1993;270:1949-1955
4. McGale P, Darby SC, Hall P, Adolfsson J, Bengtsson NO, Bennet AM, Fornander T, Gigante B, Jensen MB, Peto R, Rahimi K, Taylor CW, Ewertz M. Incidence of heart disease in 35,000 women treated with radiotherapy for breast cancer in denmark and sweden. *Radiotherapy and oncology: journal of the European Society for Therapeutic Radiology and Oncology*. 2011;100:167-175
5. Cella L, Liuzzi R, Conson M, Torre G, Caterino M, De Rosa N, Picardi M, Camera L, Solla R, Farella A, Salvatore M, Pacelli R. Dosimetric predictors of asymptomatic heart valvular dysfunction following mediastinal irradiation for hodgkin's lymphoma. *Radiotherapy and oncology: journal of the European Society for Therapeutic Radiology and Oncology*. 2011;101:316-321
6. Heidenreich PA, Hancock SL, Lee BK, Mariscal CS, Schnittger I. Asymptomatic cardiac disease following mediastinal irradiation. *Journal of the American College of Cardiology*. 2003;42:743-749
7. Hull MC, Morris CG, Pepine CJ, Mendenhall NP. Valvular dysfunction and carotid, subclavian, and coronary artery disease in survivors of hodgkin lymphoma treated with radiation therapy. *Jama*. 2003;290:2831-2837
8. Hammermeister KE, Sethi GK, Henderson WG, Oprian C, Kim T, Rahimtoola S. A comparison of outcomes in men 11 years after heart-valve replacement with a mechanical valve or bioprosthesis. Veterans affairs cooperative study on valvular heart disease. *The New England journal of medicine*. 1993;328:1289-1296
9. Crestanello JA, McGregor CG, Danielson GK, Daly RC, Dearani JA, Orszulak TA, Mullany CJ, Puga FJ, Zehr KJ, Schleck C, Schaff HV. Mitral and tricuspid valve repair in patients with previous mediastinal radiation therapy. *The Annals of thoracic surgery*. 2004;78:826-831; discussion 826-831
10. Yutzey KE, Demer LL, Body SC, Huggins GS, Towler DA, Giachelli CM, Hofmann-Bowman MA, Mortlock DP, Rogers MB, Sadeghi MM, Aikawa E. Calcific aortic valve disease: A consensus summary from the alliance of investigators on calcific aortic valve disease. *Arteriosclerosis, thrombosis, and vascular biology*. 2014;34:2387-2393
11. Rabkin E, Hoerstrup SP, Aikawa M, Mayer JE, Jr., Schoen FJ. Evolution of cell phenotype and extracellular matrix in tissue-engineered heart valves during in-vitro maturation and in-vivo remodeling. *The Journal of heart valve disease*. 2002;11:308-314; discussion 314
12. Otto CM, Kuusisto J, Reichenbach DD, Gown AM, O'Brien KD. Characterization of the early lesion of 'degenerative' valvular aortic stenosis. Histological and immunohistochemical studies. *Circulation*. 1994;90:844-853
13. Mohler ER, 3rd, Gannon F, Reynolds C, Zimmerman R, Keane MG, Kaplan FS. Bone formation and inflammation in cardiac valves. *Circulation*. 2001;103:1522-1528
14. Qayyum MA, Insana MF. Stromal responses to fractionated radiotherapy. *International journal of radiation biology*. 2012;88:383-392
15. de Cortie K, Russell NS, Coppes RP, Stewart FA, Scharpfenecker M. Bone marrow-derived macrophages incorporate into the endothelium and influence vascular and renal function after irradiation. *International journal of radiation biology*. 2014;90:769-777
16. Herskind C, Rodemann HP. Spontaneous and radiation-induced differentiationof fibroblasts. *Experimental gerontology*. 2000;35:747-755

17. Lara PC, Russell NS, Smolders IJ, Bartelink H, Begg AC, Coco-Martin JM. Radiation-induced differentiation of human skin fibroblasts: Relationship with cell survival and collagen production. *International journal of radiation biology*. 1996;70:683-692
18. Russell NS, Lara PC, Grummels A, Hart AA, Coco-Martin JM, Bartelink H, Begg AC. In vitro differentiation characteristics of human skin fibroblasts: Correlations with radiotherapy-induced breast fibrosis in patients. *International journal of radiation biology*. 2000;76:231-240
19. Hjortnaes J, Camci-Unal G, Hutcheson JD, Jung SM, Schoen FJ, Kluin J, Aikawa E, Khademhosseini A. Directing valvular interstitial cell myofibroblast-like differentiation in a hybrid hydrogel platform. *Advanced healthcare materials*. 2015;4:121-130
20. Offit K, Gilad S, Paglin S, Kolachana P, Roisman LC, Nafa K, Yeugelewitz V, Gonzales M, Robson M, McDermott D, Pierce HH, Kauff ND, Einat P, Jhanwar S, Satagopan JM, Oddoux C, Ellis N, Skaliter R, Yahalom J. Rare variants of atm and risk for hodgkin's disease and radiation-associated breast cancers. *Clinical cancer research: an official journal of the American Association for Cancer Research*. 2002;8:3813-3819
21. Concin N, Zeillinger C, Stimpfel M, Schiebel I, Tong D, Wolff U, Reiner A, Leodolter S, Zeillinger R. P53-dependent radioresistance in ovarian carcinoma cell lines. *Cancer letters*. 2000;150:191-199
22. Butcher JT, Simmons CA, Warnock JN. Mechanobiology of the aortic heart valve. *The Journal of heart valve disease*. 2008;17:62-73
23. Sarathchandra P, Smolenski RT, Yuen AH, Chester AH, Goldstein S, Heacox AE, Yacoub MH, Taylor PM. Impact of gamma-irradiation on extracellular matrix of porcine pulmonary valves. *The Journal of surgical research*. 2012;176:376-385
24. Nadlonek NA, Weyant MJ, Yu JA, Cleveland JC, Jr., Reece TB, Meng X, Fullerton DA. Radiation induces osteogenesis in human aortic valve interstitial cells. *The Journal of thoracic and cardiovascular surgery*. 2012;144:1466-1470
25. Yahalom J. Changing role and decreasing size: Current trends in radiotherapy for hodgkin's disease. *Current oncology reports*. 2002;4:415-423
26. Yahalom J, Mauch P. The involved field is back: Issues in delineating the radiation field in hodgkin's disease. *Annals of oncology: official journal of the European Society for Medical Oncology / ESMO*. 2002;13 Suppl 1:79-83

10

Valvular Interstitial Cells Suppress Calcification by Valvular Endothelial Cells

Jesper Hjortnaes[1,4*], Kayle Shapero[2*], Claudia Goettsch[3], Joshua D. Hutcheson[3], Joshua Keegan[1], Jolanda Kluin[4], John E. Mayer[5], Joyce Bischoff [2], Elena Aikawa[1,3]

Atherosclerosis 2015

[1]Center of Excellence in Vascular Biology, Cardiovascular Medicine, Brigham and Women's Hospital, Harvard Medical School, Boston, MA, USA; [2]Vascular Biology Program and Department of Surgery, Boston, MA, USA Children's Hospital, Harvard Medical School, Boston, MA, USA; [3]Center for Interdisciplinary Cardiovascular Sciences, Brigham and Women's Hospital, Harvard Medical School, Boston, MA, USA; [4]Department of Cardiothoracic Surgery, University Medical Center Utrecht, Utrecht, The Netherlands; [5]Department of Cardiothoracic Surgery, Boston, MA, USA Children's Hospital, Harvard Medical School, Boston, MA, USA.

ABSTRACT

Introduction

Calcific aortic valve disease (CAVD) is the most common heart valve disease in the Western world. We previously proposed that valvular endothelial cells (VECs) replenish injured adult valve leaflets via endothelial-to-mesenchymal transformation (EndMT); however, whether EndMT contributes to valvular calcification is unknown. We hypothesized that aortic VECs undergo osteogenic differentiation via an EndMT process that can be inhibited by valvular interstitial cells (VICs).

Methods and Results

VEC clones underwent TGF-β_1-mediated EndMT, shown by significantly increased mRNA expression of the EndMT markers α-SMA (5.3±1.2), MMP-2 (13.5±0.6) and Slug (12±2.1) ($p<0.05$), (compared to unstimulated controls). To study the effects of VIC on VEC EndMT, clonal populations of VICs were derived from the same valve leaflets, placed in co-culture with VECs, and grown in control/TGF-β_1 supplemented media. In the presence of VICs, EndMT was inhibited, shown by decreased mRNA expression of α-SMA (0.1±0.5), MMP-2 (0.1±0.1), and Slug (0.2±0.2) ($p<0.05$). When cultured in osteogenic media, VECs demonstrated osteogenic changes confirmed by increase in mRNA expression of osteocalcin (8.6±1.3), osteopontin (3.7±0.3), and Runx2 (5.5±1.5). The VIC presence inhibited VEC osteogenesis, demonstrated by decreased expression of osteocalcin (0.4±0.1) and osteopontin (0.2±0.1) ($p<0.05$). Time course analysis suggested that EndMT precedes osteogenesis, shown by an initial increase of α-SMA and MMP-2 (day 7), followed by an increase of osteopontin and osteocalcin (day 14).

Conclusions

The data indicate that EndMT may precede VEC osteogenesis. This study shows that VICs inhibit VEC EndMT and osteogenesis, indicating the importance of VEC–VIC interactions in valve homeostasis.

INTRODUCTION

Calcific aortic valve disease (CAVD) and subsequent aortic valve stenosis is the most common heart valve disease in the Western world.[1, 2] CAVD is currently considered an actively regulated and progressive disease, characterized by a cascade of cellular changes that initially cause fibrotic thickening, followed by extensive calcification of the aortic valve leaflets. This in turn leads to significant aortic valve stenosis and eventual left ventricular outflow obstruction,[3, 4] for which surgical replacement remains the only viable treatment option.

Heart valves contain a heterogeneous population of valvular endothelial cells (VECs) and valvular interstitial cells (VICs), which maintain valve homeostasis and structural leaflet integrity. VICs, the most abundant cell type in the heart valve, play a key role in CAVD progression. Various VIC phenotypes have been identified in diseased human heart valves,[5] including quiescent fibroblast-like VICs (qVICs), which upon pathological cues can differentiate into activated myofibroblast-like VICs (aVICs); and osteoblast-like VICs (oVICs), which are responsible for the active deposition of calcium in CAVD.[6-8] Additionally, numerous studies have demonstrated the ability of VICs to undergo osteogenic differentiation.[9-11] Relatively little is known about the role of VECs in CAVD. VECs cover the surface of the heart valve to form an endothelial monolayer, and are unique in that they can undergo endothelial-to-mesenchymal transformation (EndMT) — a critical process in developmental valvulogenesis.[12-15] During development, EndMT occurs in the endocardial cushions, where a subset of endothelial cells detach from the endothelium, transiently enhance the contractile protein α-SMA, and migrate into the interstitium of the embryonic valve to become VICs.[13, 16, 17] EndMT also occurs in adult valves, where cells co-expressing endothelial markers and α-SMA have been detected along the valve endothelium and in subendothelial locations.[18] These observations prompted the hypothesis that low or basal levels of EndMT contribute to the replenishment of VICs as part of physiologic valve remodeling that is required throughout postnatal life.[19] We recently demonstrated that EndMT plays a role in the adaptive pathologic remodeling of mitral valve leaflets in an ovine model of functional mitral regurgitation.[20] In addition, EndMT has shown to be potentiated by exposure to cyclic mechanical strain.[21] Additionally we showed that mitral VECs are able to differentiate *in vitro* into mesenchymal lineages, including osteogenic cells.[14]

VECs have been indicated as key regulators in early CAVD via recruitment of immune cells,[22] dysregulation of protective nitric oxide (NO) signaling,[23, 24] and phenotypic plasticity through the expression of procalcific proteins.[14] Collectively, these studies indicate a potential role for dysregulated VECs in valvular disease, but the role of EndMT in aortic valve leaflet calcification in CAVD is yet unknown. Furthermore, factors that regulate EndMT-associated VEC differentiation into osteogenic cells remain unclear. Based on our previous investigations, we hypothesized that VEC–VIC interaction serves as a native barrier to prevent excessive VEC EndMT and subsequent osteogenic differentiation.

METHODS

Aortic valve cell isolation

Ovine tissues from animals 8-10 months of age, weighing 20–25 kg, were obtained under approved NIH guidelines for animal experimentation as performed at Children's Hospital Boston. Valve leaflets were incubated in endothelial basal medium (EBM-2) (CC- 3156, Cambrex Bio Science, Walkersville, MD) with 5% fetal bovine serum (FBS) (Hyclone, Logan, UT), 1% GPS (Invitrogen, Carlsbad, California), 2 mmol/L L-glutamine, and 100 µg/ml gentamicin sulfate for 1–4 hours. They were then minced into 2-mm pieces and incubated with 0.2% collagenase A (Roche Diagnostics, Indianapolis, IN) in EBM-2 for 5 minutes at 37°C, and diluted with Hanks' balanced salt solution containing 5% FBS, 1.26 mmol/L $CaCl_2$, 0.8 mmol/L $MgSO_4$, and 1% GPS (wash buffer). The supernatant was sedimented at 200× g, resuspended in VEC medium (EBM-2 medium, 10% heat-inactivated FBS, 1% GPS, and 2 ng/mL basic fibroblast growth factor [bFGF]; Roche Diagnostics, Indianapolis, IN) and plated. The following day, primary cultures were washed to remove unattached cells. Primary cultures were trypsinized, resuspended in growth medium at 3.3 cells/ml, and 100 µl were plated in each well of a 96-well plate, at a concentration of approximately one cell to every third well; visual inspection was performed to assess that single colonies appeared in a subset of wells. When the colonies covered two-thirds of the well, cells were split into 24-well dishes. Based on morphology, these clones were initially visually identified as either endothelial or interstitial. These observations were confirmed with phenotypic characterization and designated as either endothelial (VEC)[25, 26] or interstitial (VIC-K3, VIC-K5, VIC-K6), and expanded on 1% gelatin-coated dishes in VEC media. Cells were passaged 1:3 or 1:4 every 6 to 14 days, and experiments were performed using VEC and VIC clones between passages 8 and 14. VECs were grown in VEC media, and VICs were cultured in VIC media (DMEM, 10% FBS, 1% GPS).

10

Human calcified aortic valves

Aortic valve leaflets (n=5) were harvested from patients undergoing aortic valve replacement for aortic valve stenosis and a healthy valve was obtained from autopsy, performed using criteria established by the declaration of Helsinki. Tissue samples were frozen in optimal cutting temperature compound (OCT, Sakura Finetech, Torrance, CA) and 7 µm serial sections were cut and stained. Tissue was collected according to Brigham and Women's Hospital IRB Protocols.

Mouse model of CAVD

Male apolipoprotein E-deficient mice ($apoE^{-/-}$ mice; 10 weeks old) were purchased from Jackson Laboratory (Bar Harbor, ME). High-fat diet (21% fat and 0.21% cholesterol) was obtained from Research Diets (D12079B, New Brunswick, NJ). Mice were fed with an atherogenic diet for a total of 22 weeks. Mice were euthanized for tissue collection and histopathology at 32 weeks. The animal procedures were performed conform the NIH guidelines and approved by the Brigham and

Women's Hospital Animal Care and Use Committee. This model is characterized by the presence of functional and histopathological changes found in human CAVD.[33]

Endothelial-to-Mesenchymal Transformation (EndMT)

EndMT was induced as described previously.[26] The assay was also performed in the presence of VICs in an indirect co-culture system, using a Transwell system (12-mm Transwells with 0.4-µm pore polycarbonate membrane inserts; Corning Life Sciences, Acton, MA) (Supplemental Figure I). Briefly, VECs were grown alone or in co-culture with VICs in VEC media, or VEC media supplemented with 2 ng/mL TGF-β_1 (R&D Systems, Minneapolis, MN), for up to 14 days. Media was changed every 2–3 days.

VEC and VIC osteogenic potential

The osteogenic potential of VEC and VIC clones was tested both separately and in co-culture for up to 21 days via treatment with osteogenic media (OM) (DMEM with 10% FBS, 1% GPS with 10 nmol/L beta-glycerolphosphate, 50 µmol/L ascorbic acid, 10 µmol/L dexamethasone). DMEM with 10% FBS, 1% GPS was used as control medium (NM). Media was changed every 2–3 days.

VEC-VIC indirect co-culture

Co-culture experiments were performed using Transwell plates (Corning, Tewksbury, MA) (Supplemental Figure I). Cells were plated either in the Transwell inserts or on the bottom of 6-well plates at a density of 1 x 10^5 cells/cm^2 and allowed to adhere overnight. After 24 hours, the two cell types were combined to begin the co-culture by placing the inserts into the corresponding well of the 6 well plate. For the conditioned media experiments, cells were treated with media that had been conditioned by the specific cell type for 24 hours. Conditioned media was sterile-filtered and added in a 1:1 ratio with fresh media to treated cells. Media was changed every 2–3 days.

Histological detection of VEC and VIC mineralization

Upon completion of experiments, cells were washed with PBS and fixed using 4% paraformaldehyde for 15 minutes. Cells were subsequently washed with PBS. Mineralization was analyzed by staining with 0.02 mg/L of Alizarin Red S (Sigma-Aldrich). The area of positive Alizarin Red S staining was normalized to cell number. To detect the expression of alkaline phosphatase (ALP), nitro-blue tetrazolium/indolylphosphate (NBT/BCIP) staining was performed. Before staining, the cells were washed with PBS, 0.5 ml of NBT/BCIP was added, and the samples were then incubated at 37°C in a humidified chamber containing 5% CO_2 for 30 minutes. Samples were then washed with PBS and fixed with 4% PFA, after which they underwent a counter stain with 0.1% eosin for 5 minutes. Images were taken with an Eclipse 80i microscope (Nikon) and processed with Elements 3.20 software (Nikon).

Alkaline phosphatase activity and calcium measurements

A colorimetric kit was used to measure ALP activity (BioVision, Milpitas, CA) according to the manufacturer's instructions. 16 µl of supernatant from 12-well plates was added to 64 µl of ALP assay buffer and 50 µl of PnPP solution was added and incubated for 1 hour at room temperature. The absorbance was read at a wavelength of 405 nm. Values were normalized to the standard curve. Calcium content was quantified using a colorimetric kit (BioVision) according to the manufacturer's protocol. Briefly, 50 µL of sample was added to 60 µL of calcium assay buffer, after which 90 µL of chromogenic reagent was added and incubated for 10 minutes at room temperature in the dark. Absorbance was read at a wavelength of 575 nm with a plate reader. Values were normalized to the standard curve.

Immunofluorescence and western blotting

Immunofluorescence staining was performed on methanol-fixed cells and human and mouse aortic valve leaflets using anti-human VE-cadherin (Santa Cruz) or CD31 (Cell Signaling), anti-human α-SMA (clone 1A4, Sigma-Aldrich), anti-vimentin antibody (Abcam, Cambridge, MA) and anti-osteocalcin (Abcam). Secondary antibodies conjugated with AlexaFluor 488 (Invitrogen) were used. Images were taken with an Eclipse 80i microscope (Nikon) and processed with Elements 3.20 software (Nikon). For western blotting, cells were lysed as previously described.[14] Briefly, cells were lysed with 4 mol/L urea, 0.5% SDS, 0.5% NP-40, 100 mmol/L Tris, and 5 mmol/L EDTA, pH 7.4, containing 100 µmol/L leupeptin 10 mmol/L benazmidine, 1 mmol/L PMSF, and 12.5 µg/mL aprotinin. Lysates were subjected to 10% SDS-PAGE (13 µg of protein per lane) and transferred to Immobilon-P membrane (Millipore, Bedford, MA). Membranes were incubated with murine anti-human α-SMA, goat anti-human CD31, and goat anti-human VE-Cadherin diluted in 5% dry milk in 1x PBS-T (0.1% Tween-20, 25 µM Tris-HCL, 0.15 M NaCl in PBS), and then with secondary antibody (peroxidase-conjugated anti-mouse or anti-goat). Antigen-Ab complexes were visualized using chemiluminescent sensitive film. Equal protein amounts (12-15 µg) were loaded in each lane (determined by u-BCA assay, Pierce), and expression was quantified via densitometry analysis and normalized to that of β-actin (Sigma). All antibodies were shown to cross-react with their ovine homologs.

Real-time Polymerase Chain Reaction

Total RNA was isolated using RNeasy Mini Kit (Qiagen), supplemented with DNase I treatment (Qiagen). Reverse transcription was performed with Superscript II cDNA synthesis kit (Invitrogen/Life Technologies, Grand Island, NY) to obtain a target cDNA concentration of 0.335 µg/mL, followed by RT- PCR using SYBR Green (BioRad, Hercules, CA), and annealing temperatures of 95º C and 60º C for 35 cycles. Oligonucleotide primer sequences are presented in Table 1. All PCR products were sequenced using ABi DNA sequences (Children's Hospital Boston core facility) to verify the sequence corresponding to the gene of interest (Suppl.Table 1).

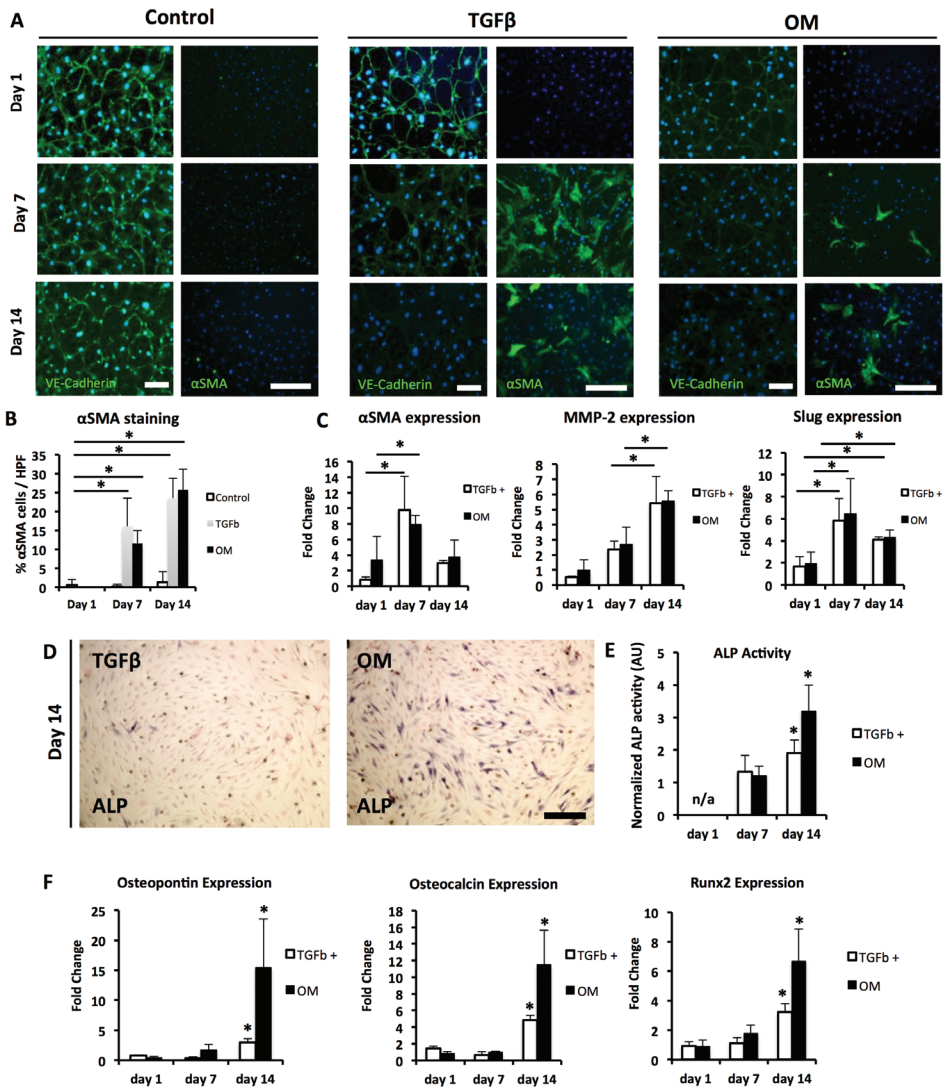

Figure 1. EndMT may precede VEC osteoblastic differentiation. VECs were treated with normal media (NM) or osteogenic media (OM) ± TGF-β_1 for 1, 7, or 14 days. **(A)** Immunofluorescent staining of VE-Cadherin and α-SMA (green), cell nuclei (DAPI/blue). Bar: 50 μm. **(B)** Quantification of α-SMA staining. **(C)** mRNA expression α-SMA, MMP-2, and Slug. **(D)** ALP staining of VECs in media + TGF-β_1 or OM at day 14. Bar: 50 μm. **(E)** ALP activity of VECs in media + TGF-β_1 or OM at day 1. Data is depicted as mean ± SD/ normalized to NM conditions, *p<0.05. **(F)** mRNA expression of osteopontin, osteocalcin and Runx2. Data is depicted as mean ± SD fold change, *p<0.05.

Migration assay

100 μg/mL rat tail collagen type I (0.02 N acetic acid) was used to coat 6.5-mm Transwells with 8.0-μm pore polycarbonate membrane inserts for 1 hour at 37°C, followed by one wash with PBS. Cells were treated as specified, trypsinized, and seeded in the upper chamber of the transwell plate at a

density of $1x10^4$ cells/well (100 µl volume). 300 µL of control media (EBM-2 / serum-free and growth factor-free) or VEC media supplemented with 20% FBS was added to the lower chamber. Cells were then allowed to migrate for 4 hours at 37º C. The cells in the upper chamber were gently removed using a cotton swab, and the lower surface was fixed with ice-cold methanol and mounted on glass slides in mounting media containing DAPI. Cells were counted using a fluorescent microscope.

Statistical analysis

Results are presented as mean +/- standard deviation (SD) unless indicated otherwise. Unpaired Student's t-test was used for comparisons between two groups. One-way ANOVA was used to evaluate statistical significant differences in multiple groups. $P < 0.05$ was considered statistically significant.

RESULTS

TGF-β1 and osteogenic media induce VEC EndMT

Clonal populations from ovine aortic valve leaflets were isolated using a brief collagenase-A procedure, which has been described previously.[12] The VEC clone demonstrated cobblestone endothelial morphology and stained positively for VE-Cadherin and negatively for α-SMA (Supplementary Figure II). VIC clonal populations from the same valve were isolated and characterized. Immunofluorescence staining of the aortic VIC clones (VIC-K3, VIC-K5, and VIC-K6) confirmed the characteristic myofibroblastic phenotype of VICs grown in culture, with positive staining for α-SMA and vimentin and negative staining for the endothelial cell marker VE-Cadherin (Supplementary Figure III).

In accordance with our earlier work,[12] this VEC clone was able to undergo TGF-β_1–induced EndMT, as visualized by anti-α-SMA immunofluorescence after 8 days of TGF-β_1 stimulation (Supplementary Figure IVA). Western blot analysis confirmed the changes in protein expression (Supplemental Figure IVB). Significant increases in mRNA expression of the EndMT markers α-SMA (5.3±1.2), MMP-2 (13.5±0.6) and Slug (12±2.1), as well as a decrease of the endothelial marker VE-Cadherin (0.2±0.1) ($p<0.05$) confirmed TGF-β_1–induced EndMT of the VECs (n=3, Supplementary Figures IVC-F).

We performed a time-course analysis of EndMT-associated proteins in VECs treated with either TGF-β_1 or osteogenic media (OM) for up to 14 days. VECs were stained for VE-cadherin and α-SMA at days 1, 7, and 14 of culture (Figure 1A).

Both TGF-β_1 and OM induced a progressive loss of VE-cadherin compared to NM in the VECs. Quantification of α-SMA–positive cells confirmed the increase of myofibroblast-like differentiation of VECs after day 7 and day 14, as compared to day 1 ($p<0.05$). When VECs were cultured in OM, a higher percentage of α-SMA–positive cells were present on day 14, as compared to day 7 (Figure 1B). RT-PCR analysis of EndMT markers revealed a significant increase in mRNA expression of α-SMA at day 7 relative to day 1 when cultured with TGF-β_1 (9.8±4.3) and OM (7.9±1.1), but α-SMA expression decreased at day 14 as compared to day 7 (Figure 1C). In cells stimulated with TGF-β_1 or

OM, MMP-2 expression increased significantly from day 7 (TGF-β_1: 2.3±0.5; OM: 2.7±1.1) to day 14 (TGF-β_1: 5.4±1.8; OM: 5.6±0.7). Slug expression follows a similar pattern to α-SMA, demonstrating a significant increase at day 7 (TGFβ_1: 5.8±1.9; OM: 6.4±2.2) compared to day 1 ($p<0.05$). While day 14 for Slug was not significantly different from day 7, it remained significantly increased as compared to day 1 (TGF-β_1: 4.1±0.3; OM: 2.6±0.7) (Figure 1C). The increase in expression of these EndMT markers between days 1 and 7 suggests that a process of EndMT occurs in both the VECs treated with TGF-β_1 and those treated with OM.

Osteogenic differentiation follows EndMT in VECs

We next evaluated osteogenic differentiation over time. We detected a small number of ALP-positive cells following 14 days of stimulation with TGF-β_1, but when VECs were cultured in OM, a more pronounced ALP staining was observed (Figure 1D). This observation was confirmed by quantification of the ALP activity (OM: 3.2±0,8 vs. TGF β_1: 1.9 ±0.4 (Figure 1E). TGF-β_1 significantly increased osteopontin (2.9±0.6) osteocalcin (4.8±0.5), and Runx2 (3.2±0.5) mRNA expression ($p<0.05$) at day 14 (Figure 1F). In addition, when we cultured VECs in OM, we found a significant increase in osteopontin (15.5±8.1), osteocalcin (11.5±4.3), and Runx2 (6.7±2.1) expression at day 14, as compared with earlier time points ($p <0.05$) (Figure 1F).

VICs suppress TGFβ_1–induced EndMT of VECs

The presence of VICs (in co-culture) attenuated TGF-β_1–induced EndMT. VICs suppressed TGF-β_1–induced expression of α-SMA in VECs, as demonstrated by immunofluorescence staining (Figure 2A) and confirmed by Western blot. Three different VIC clones suppressed the EndMT marker α-SMA when the VECs were stimulated with TGF-β_1 (Figure 2B, Supplementary Figure V). VICs significantly suppressed the expression of three EndMT markers in TGF-β1 treated VECs: α-SMA (0.1±0.5), MMP-2 (0.1±0.1) and Slug (0.2±0.2) (three different VIC clones, $p<0.05$; Figures 2C, 2D, 2E). A similar inhibition of EndMT markers was observed when using VIC conditioned media at a 1:1 ratio (Supplementary Figure VI). The presence of VICs also inhibited TGF-β1-induced migration potential of VECs that were first co-cultured with VICs and TGF-β_1, as compared to VECs treated with TGF-β_1 alone (Supplementary Figure VII).

VICs inhibit osteogenic differentiation of VECs

VECs were cultured in OM to evaluate their osteogenic differentiation capacity, using DMEM-based normal growth media (NM) as a control. VECs cultured in OM for 21 days demonstrated a loss of VE-Cadherin, compared with VECs cultured in NM (Figure 3A). Mineralized matrix, visualized using Alizarin Red S staining, was observed after culturing VECs for 21 days in OM, but was not detected in VECs cultured in NM (Figure 3A). The presence of VICs (in co-culture) prevented both the OM-mediated decrease in VE-Cadherin and the increase in mineralized matrix (Figure 3B). There was no difference in cell number between groups (Supplementary Figure VIII). Analyses of mRNA expression at day 21 confirmed the inhibitory effect of VICs on the osteogenic differentiation of VECs.

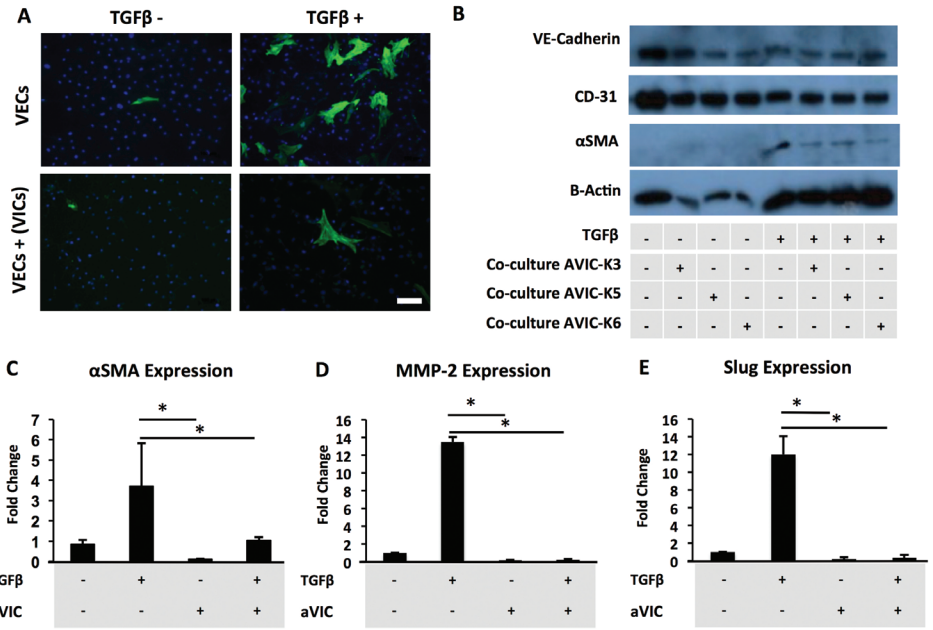

Figure 2. VICs suppress TGF-β_1–induced VEC EndMT. VECs were co-cultured with VICs in a transwell culture system and treated with TGF-β_1 for 8 days. **A** Immunofluorescence staining of α-SMA (green), cell nuclei (DAPI/blue). Bar: 50 μm**. B** Western blot for endothelial markers (VE-Cadherin, CD31) and myofibroblastic marker (α-SMA). **C** mRNA expression of EndMT markers α-SMA, MMP-2, and Slug. Data is depicted as mean ± SD fold change, *p<0.05.

VE-Cadherin expression decreased significantly in VECs in OM compared to NM (0.3±0.2 p<0.05). This decrease was inhibited by the presence of VICs in co-culture (0.8±0.5) (Figure 3C). Expression of α-SMA increased when VECs were cultured in OM (17.3±7.5, p<0.05), and this increase was mitigated by the presence of VICs in co-culture (1.3±0.7) (Figure 3D). VEC cultured in OM showed increased expression of osteocalcin (8.6±1.3, p<0.05), osteopontin (3.7±0.3, p<0.05) and Runx2 (5.5±1.5, p<0.05), compared with cells cultured in NM (Figures 3E, 3F, and 3G). The co-culture of VECs with VICs in OM abolished the induction of osteogenic differentiation markers. A functional consequence of osteogenic differentiation, calcium deposition, increased when VECs were cultured in OM alone, but was significantly impaired when VECs were co-cultured with VICs (OM: 4.2±1.7 μg/mL, OM+VICs: 1.9±0.8 μg/mL, n=3, p<0.05) (Figure 3H).

VECs do not suppress osteogenic differentiation of VICs

We evaluated whether VECs have a similar inhibitory effect on the osteogenic differentiation of VICs. VICs cultured in OM for 21 days demonstrated mineralized matrix by Alizarin Red S staining (Figure 4A). When VICs were co-cultured with VECs in NM or OM, VICs also stained positively for both α-SMA and calcium (Figure 4B). Expression of α-SMA increased in VICs cultured for 21 days in OM (1.4±0.3, p<0.05) (Figure 4C). VICs cultured in OM with VECs demonstrated a significant decrease in α-SMA expression (0.2±0.1 p<0.05). The mRNA expression of osteogenic differentiation markers osteocal-

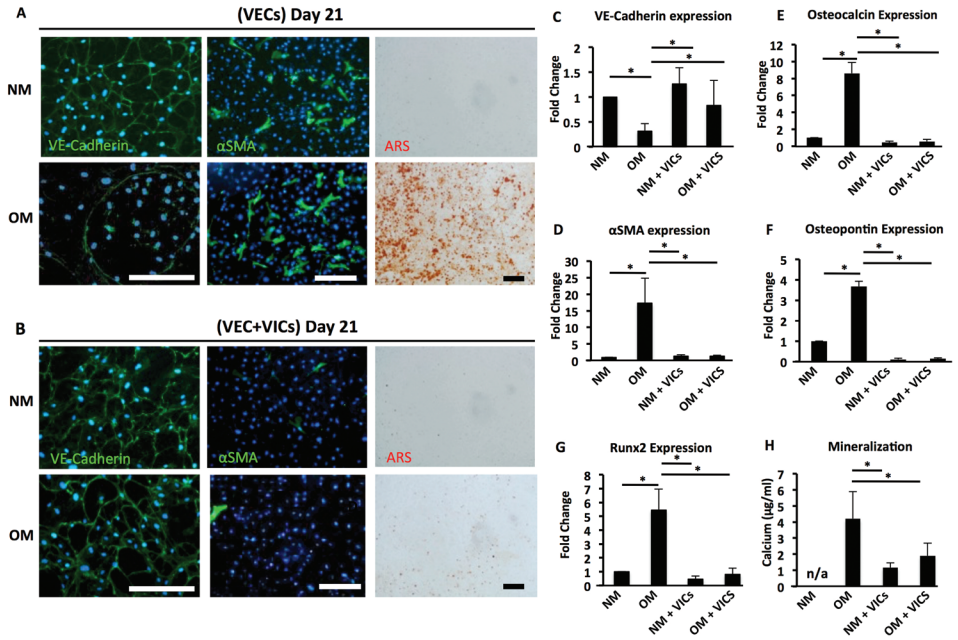

Figure 3. VICs suppress OM-induced VEC osteogenesis. VECs were co-cultured with VICs in a transwell culture system in osteogenic media (OM) for 21 days. **A-B** Immunofluorescent staining of VE-Cadherin (green), α-SMA (green), cell nuclei (DAPI/blue), and Alizarin Red S (ARS) (red/orange). Bar: 50µm. **C** mRNA expression of VE-Cadherin, **D** α-SMA, **E** Osteocalcin, **F** Osteopontin, **G** Runx2. **H** Calcium content. Data is depicted as mean ± SD fold change, *p<0.05.

cin, osteopontin, and Runx2 and the activity of ALP further revealed that VECs do not exhibit an inhibitory effect on VIC osteogenic differentiation (Figures 4D, 4E, and 4F, Supplementary Figure IX). Functionally, we observed a significant increase in VIC calcium deposition in the co-culture samples (Figure 4G).

Human and mouse calcified aortic valves leaflets demonstrate EndMT

After observing EndMT in isolated aortic VECs, we evaluated the presence of EndMT in human calcified aortic valve leaflets. Using immunofluorescence we demonstrate co-expression of α-SMA and CD31 (Figure 5), confirming the presence of EndMT in calcific valves. In addition, both α-SMA and CD31 co-expressed with osteocalcin, indicating a potential role for EndMT in human calcific aortic valve disease. Further, α-SMA was not observed in the endothelium of a non-calcified human aortic valve leaflets. To further evaluate the *in vivo* relevance of EndMT in CAVD we assessed α-SMA expression in the aortic valve of wild type and *Apoe* -/- mice, a common mouse model of cardiovascular calcification.[33] Increased expression of a-SMA was observed in the endothelium of the *Apoe* -/- mice.

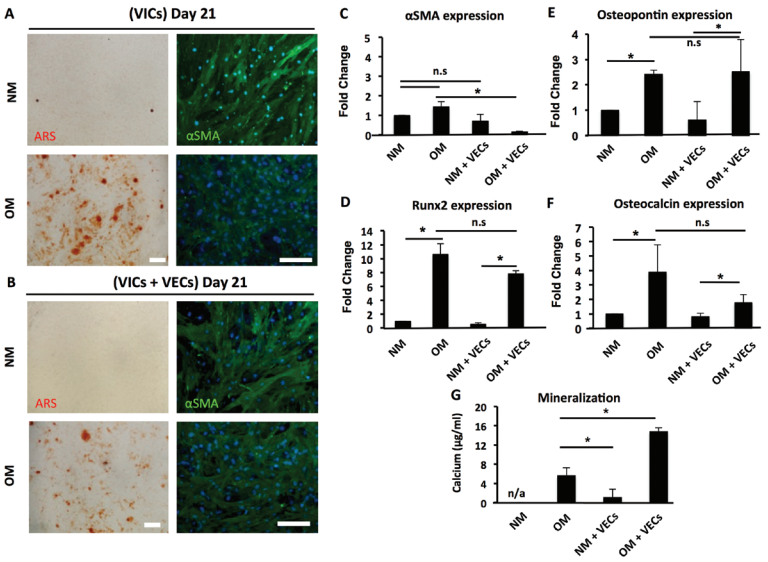

Figure 4. VECs do not suppress OM-induced VIC osteogenesis. VICs were co-cultured with VECs in a transwell culture system in osteogenic media (OM) for 21 days. **A-B** Immunofluorescent staining of Alizarin Red S (red/orange), α-SMA (green), cell nuclei (DAPI/blue). Bar: 50 μm. **C** mRNA expression of α-SMA, **D** Osteocalcin, **E** Osteopontin, **F** Runx2. **G** Calcium content. Data is depicted as mean ± SD fold change, *p<0.05.

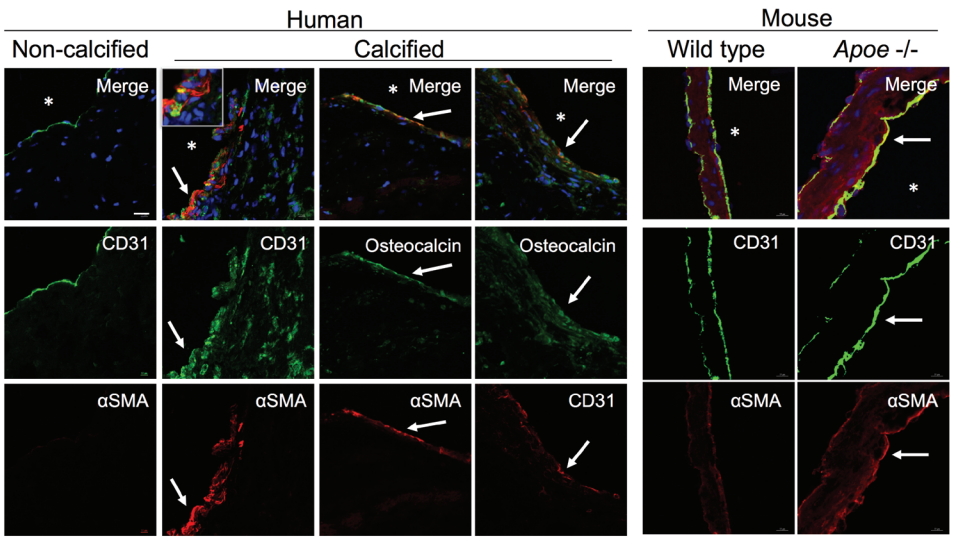

Figure 5. Human and mouse aortic valves demonstrate EndMT. Human non-calcified (n=1) and calcified (n=5) aortic valves were stained for CD31, aSMA and Osteocalcin. Aortic root sections from wild type (n=2) and *Apoe* -/- (n=3) mice were stained for CD31 and aSMA. Images of the leaflets are shown. * = aortic side. (bar: 20 μm)

DISCUSSION

We report that VICs can inhibit EndMT of VECs even when stimulated with TGF-β_1, a well-established inducer of EndMT.[12, 13, 19, 27] We have also demonstrated that VEC osteogenic differentiation is inhibited by VICs when cultured in an osteogenic environment. Conversely, in our study, VECs did not inhibit VIC mineralization. In addition, we have shown that EndMT may precede VEC osteogenesis. Finally, EndMT was observed to co-express with osteogenic markers in a mouse model of aortic valve calcification and human aortic valves obtained from patients with calcific aortic valve disease. We thus propose that VECs contain the capacity to differentiate into endothelial-derived VICs (eVICs) through an EndMT process. In certain disease conditions where communication between VICs and VECs is disrupted, EndMT may be promoted. EndMT-derived eVICs may populate the valve leaflet and differentiate into osteoblastic cells (oVICs), contributing to the pathological remodeling observed in CAVD (Figure 6).

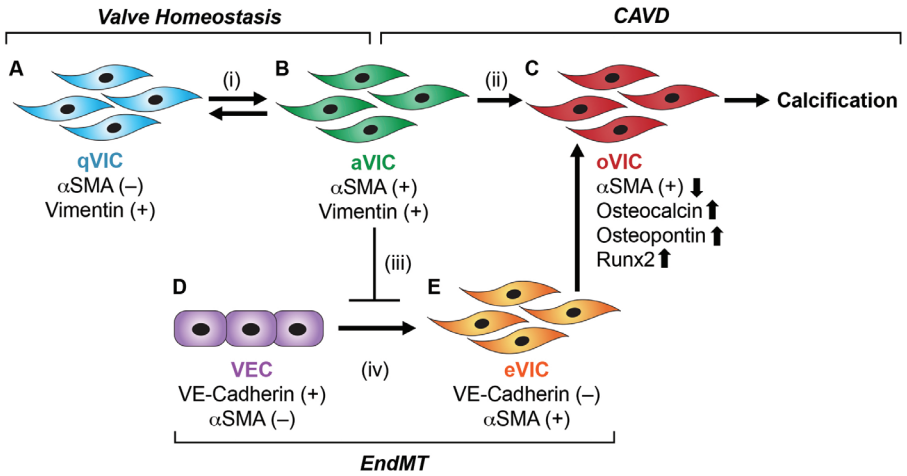

Figure 6. Schematic depiction of cellular mechanism of the role of VECs in valvular osteogenesis. Quiescent VICs (qVICs) may differentiate into activated myofibroblast-like VICs (aVICs), responsible for functional remodeling of the heart valve ECM (i). The interplay between qVICs and aVICs is thought to be the cornerstone of valve homeostasis. Upon pathological stimulation, aVICs can further differentiate into osteoblastic VICS (oVICs), which may be responsible for calcium deposition in CAVD. Valvular endothelial cells (VECs) can differentiate into endothelial-derived VICs (eVICs) via the EndMT process. In turn, eVEC may also differentiate into oVICs and contribute to calcification of the valve. VIC interaction with VEC may further inhibit EndMT-induced osteogenic eVIC differentiation (ii).

This study builds on our previous work, in which we demonstrated that VEC clones from ovine mitral valve leaflets might be a source for osteoblastic VICs.[14] Endothelial osteoblastic differentiation potential has been proposed in VECs,[14] prostate tumor EC,[28] mutant ECs with constitutively active ALK2[29] and in arterial endothelial cells in matrix Gla protein-deficient mice.[30] We previously showed that the *in vitro* osteogenic differentiation potential of mitral VEC corresponded with focal regions of osteogenic endothelium in tethered mitral valves *in vivo*.[20] The role of the endothelium in valve

calcification was also suggested by the finding that the endothelial activation marker VCAM-1 expression correlated with VIC osteoblastic differentiation in a model of aortic valve stenosis.[31] This work also underscores the unique plasticity within subsets of VECs, which is reflected not only in diseased states but also in normal valve physiology, as evident by the co-expression of CD31 and α-SMA in human fetal and postnatal semilunar valves.[19]

These findings have prompted our hypothesis that — when needed — a progenitor-like subset of VECs can replenish the VIC population via EndMT.[14] In turn, this transdifferentiation could contribute to maintaining structural integrity and function of the heart valve (Figure 6). In normal valves, qVICs are activated by environmental cues and can differentiate into myofibroblast-like VICs (aVICs; α-SMA-positive), which maintain tissue integrity by adaptive remodeling of the valve ECM through the secretion of various cytokines,[32, 33] matrix metalloproteinases,[34, 35] and deposition of ECM proteins.[33, 36] But when persistent activation of VICs occurs, an excessive, lasting remodeling of the valve ECM may also take place. Such a maladaptive process may lead to a pathological disruption of the valve's normal connective tissue homeostasis, leading to fibrosis and eventual calcification by differentiation of oVICs.[37] Although the role of VECs in CAVD remains to be elucidated, mounting evidence indicates that endothelial dysfunction correlates with such continuous maladaptive VIC activation.[37] To our knowledge, the present work is the first to investigate VEC–VIC direct interaction in relation to osteogenesis in an *in vitro* culture model system. VICs in culture mostly demonstrate a myofibroblast-like phenotype attributed to the unnatural stiff substrate of the tissue culture plates.[38] To what extent qVICs affect VEC phenotype in co-culture remains to be elucidated. In the current experimental setup, we cannot separate the culture conditions to modulate VIC and VEC phenotypes independently. Therefore, both VICs and VECs were cultured in an osteogenic environment. This may be similar to the tissue, wherein both cell types are likely exposed to pathologic stimuli simultaneously, but it is possible that certain cues lead to phenotypic changes in only one cell type (e.g., hemodynamic changes that affect VECs only). Future studies may try to build on the current work to isolate changes in each cell type.

It remains unclear how closely the EndMT we have observed in VECs *in vitro* reflects the EndMT that occurs *in vivo,* either during valve development or disease. As such, it is important to note that although we demonstrate a correlation of EndMT and osteogenesis, our *in vivo* results cannot offer a causal role for VEC EndMT in CAVD. Our *in vivo* knowledge of valve EndMT mostly stems from end-point analyses of human postnatal pulmonary valve specimens or studies of the murine endocardial cushion[19], where hallmarks of EndMT consist of a loss of cell–cell contact in the EC monolayer; increased expression of α-SMA, MMP-2, and Slug; and increased cellular invasion. The present study confirms our earlier work that EndMT — as determined by these hallmarks — can be simulated *in vitro.*[12] Therefore, our current results build upon previous work suggesting that EndMT plays an important role in the onset of CAVD. Aortic VECs represent a cell population with the intrinsic plasticity to differentiate into myofibroblast-like aVICs, and further into osteoblast-like oVICs. That both phenotypes have been shown to possess the potential to contribute to the development of CAVD underscores the importance of understanding the role of the valvular endothelium in the

disease process. Future works may use cell lineage tracing and cell fate models to determine the source of cells that populate the aortic valve leaflet during tissue remodeling and pathogenesis.[39] By building a better understanding the cellular contributions valve remodeling, specific populations of cells may be targeted to control valvular homeostasis and develop therapeutics for CAVD.

Acknowledgments

The authors would like to thank Sara Karwacki for excellent editorial assistance.

Sources of Funding

This study was supported by grants from the Netherlands Heart Foundation (NHS-2011T024), Netherlands Scientific Council (NWO) to J.H., the Tommy Kaplan Discretionary Fund to J.E.M., and National Institutes of Health R01HL114805, to E.A.; and R01HL109506, to E.A. and J.B.

Disclosures

None.

REFERENCES

1. Stewart BF, Siscovick D, Lind BK, Gardin JM, Gottdiener JS, Smith VE, Kitzman DW, Otto CM. Clinical factors associated with calcific aortic valve disease. Cardiovascular health study. *J Am Coll Cardiol*. 1997;29:630-634
2. Takkenberg JJ, Rajamannan NM, Rosenhek R, Kumar AS, Carapetis JR, Yacoub MH. The need for a global perspective on heart valve disease epidemiology. The shvd working group on epidemiology of heart valve disease founding statement. *J Heart Valve Dis*. 2008;17:135-139
3. Rajamannan NM, Evans FJ, Aikawa E, Grande-Allen KJ, Demer LL, Heistad DD, Simmons CA, Masters KS, Mathieu P, O'Brien KD, Schoen FJ, Towler DA, Yoganathan AP, Otto CM. Calcific aortic valve disease: Not simply a degenerative process: A review and agenda for research from the national heart and lung and blood institute aortic stenosis working group. Executive summary: Calcific aortic valve disease-2011 update. *Circulation*. 2011;124:1783-1791
4. Otto CM. Calcific aortic stenosis--time to look more closely at the valve. *N Engl J Med*. 2008;359:1395-1398
5. Liu AC, Joag VR, Gotlieb AI. The emerging role of valve interstitial cell phenotypes in regulating heart valve pathobiology. *The American journal of pathology*. 2007;171:1407-1418
6. Otto CM, Kuusisto J, Reichenbach DD, Gown AM, O'Brien KD. Characterization of the early lesion of 'degenerative' valvular aortic stenosis. Histological and immunohistochemical studies. *Circulation*. 1994;90:844-853
7. Mohler ER, 3rd, Gannon F, Reynolds C, Zimmerman R, Keane MG, Kaplan FS. Bone formation and inflammation in cardiac valves. *Circulation*. 2001;103:1522-1528
8. Aikawa E, Whittaker P, Farber M, Mendelson K, Padera RF, Aikawa M, Schoen FJ. Human semilunar cardiac valve remodeling by activated cells from fetus to adult: Implications for postnatal adaptation, pathology, and tissue engineering. *Circulation*. 2006;113:1344-1352
9. Peacock JD, Levay AK, Gillaspie DB, Tao G, Lincoln J. Reduced sox9 function promotes heart valve calcification phenotypes in vivo. *Circ Res*. 2010;106:712-719
10. Osman L, Yacoub MH, Latif N, Amrani M, Chester AH. Role of human valve interstitial cells in valve calcification and their response to atorvastatin. *Circulation*. 2006;114:I547-552
11. Rajamannan NM, Subramaniam M, Rickard D, Stock SR, Donovan J, Springett M, Orszulak T, Fullerton DA, Tajik AJ, Bonow RO, Spelsberg T. Human aortic valve calcification is associated with an osteoblast phenotype. *Circulation*. 2003;107:2181-2184
12. Paranya G, Vineberg S, Dvorin E, Kaushal S, Roth SJ, Rabkin E, Schoen FJ, Bischoff J. Aortic valve endothelial cells undergo transforming growth factor-beta-mediated and non-transforming growth factor-beta-mediated transdifferentiation in vitro. *The American journal of pathology*. 2001;159:1335-1343
13. Armstrong EJ, Bischoff J. Heart valve development: Endothelial cell signaling and differentiation. *Circ Res*. 2004;95:459-470
14. Wylie-Sears J, Aikawa E, Levine RA, Yang JH, Bischoff J. Mitral valve endothelial cells with osteogenic differentiation potential. *Arterioscler Thromb Vasc Biol*. 2011;31:598-607
15. Madri JA, Pratt BM, Tucker AM. Phenotypic modulation of endothelial cells by transforming growth factor-beta depends upon the composition and organization of the extracellular matrix. *The Journal of cell biology*. 1988;106:1375-1384
16. Combs MD, Yutzey KE. Heart valve development: Regulatory networks in development and disease. *Circ Res*. 2009;105:408-421
17. Person AD, Klewer SE, Runyan RB. Cell biology of cardiac cushion development. *International review of cytology*. 2005;243:287-335
18. Frid MG, Kale VA, Stenmark KR. Mature vascular endothelium can give rise to smooth muscle cells via endothelial-mesenchymal transdifferentiation: In vitro analysis. *Circ Res*. 2002;90:1189-1196

19. Paruchuri S, Yang JH, Aikawa E, Melero-Martin JM, Khan ZA, Loukogeorgakis S, Schoen FJ, Bischoff J. Human pulmonary valve progenitor cells exhibit endothelial/mesenchymal plasticity in response to vascular endothelial growth factor-a and transforming growth factor-beta2. *Circ Res*. 2006;99:861-869
20. Chaput M, Handschumacher MD, Guerrero JL, Holmvang G, Dal-Bianco JP, Sullivan S, Vlahakes GJ, Hung J, Levine RA, Leducq Foundation MTN. Mitral leaflet adaptation to ventricular remodeling: Prospective changes in a model of ischemic mitral regurgitation. *Circulation*. 2009;120:S99-103
21. Balachandran K, Alford PW, Wylie-Sears J, Goss JA, Grosberg A, Bischoff J, Aikawa E, Levine RA, Parker KK. Cyclic strain induces dual-mode endothelial-mesenchymal transformation of the cardiac valve. *Proc Natl Acad Sci U S A*. 2011;108:19943-19948
22. Skowasch D, Schrempf S, Wernert N, Steinmetz M, Jabs A, Tuleta I, Welsch U, Preusse CJ, Likungu JA, Welz A, Luderitz B, Bauriedel G. Cells of primarily extra-valvular origin in degenerative aortic valves and bioprostheses. *European heart journal*. 2005;26:2576-2580
23. Bosse K, Hans CP, Zhao N, Koenig SN, Huang N, Guggilam A, LaHaye S, Tao G, Lucchesi PA, Lincoln J, Lilly B, Garg V. Endothelial nitric oxide signaling regulates notch1 in aortic valve disease. *Journal of molecular and cellular cardiology*. 2013;60:27-35
24. Richards J, El-Hamamsy I, Chen S, Sarang Z, Sarathchandra P, Yacoub MH, Chester AH, Butcher JT. Side-specific endothelial-dependent regulation of aortic valve calcification: Interplay of hemodynamics and nitric oxide signaling. *The American journal of pathology*. 2013;182:1922-1931
25. Melero-Martin JM, De Obaldia ME, Kang SY, Khan ZA, Yuan L, Oettgen P, Bischoff J. Engineering robust and functional vascular networks in vivo with human adult and cord blood-derived progenitor cells. *Circ Res*. 2008;103:194-202
26. Yang JH, Wylie-Sears J, Bischoff J. Opposing actions of notch1 and vegf in post-natal cardiac valve endothelial cells. *Biochem Biophys Res Commun*. 2008;374:512-516
27. Dvorin EL, Jacobson J, Roth SJ, Bischoff J. Human pulmonary valve endothelial cells express functional adhesion molecules for leukocytes. *J Heart Valve Dis*. 2003;12:617-624
28. Dudley AC, Khan ZA, Shih SC, Kang SY, Zwaans BM, Bischoff J, Klagsbrun M. Calcification of multipotent prostate tumor endothelium. *Cancer cell*. 2008;14:201-211
29. Medici D, Shore EM, Lounev VY, Kaplan FS, Kalluri R, Olsen BR. Conversion of vascular endothelial cells into multipotent stem-like cells. *Nat Med*. 2010;16:1400-1406
30. Yao Y, Jumabay M, Ly A, Radparvar M, Cubberly MR, Bostrom KI. A role for the endothelium in vascular calcification. *Circ Res*. 2013;113:495-504
31. Aikawa E, Nahrendorf M, Sosnovik D, Lok VM, Jaffer FA, Aikawa M, Weissleder R. Multimodality molecular imaging identifies proteolytic and osteogenic activities in early aortic valve disease. *Circulation*. 2007;115:377-386
32. Chester AH, Taylor PM. Molecular and functional characteristics of heart-valve interstitial cells. *Philosophical transactions of the Royal Society of London. Series B, Biological sciences*. 2007;362:1437-1443
33. Walker GA, Masters KS, Shah DN, Anseth KS, Leinwand LA. Valvular myofibroblast activation by transforming growth factor-beta: Implications for pathological extracellular matrix remodeling in heart valve disease. *Circ Res*. 2004;95:253-260
34. Rabkin E, Aikawa M, Stone JR, Fukumoto Y, Libby P, Schoen FJ. Activated interstitial myofibroblasts express catabolic enzymes and mediate matrix remodeling in myxomatous heart valves. *Circulation*. 2001;104:2525-2532
35. Rabkin-Aikawa E, Farber M, Aikawa M, Schoen FJ. Dynamic and reversible changes of interstitial cell phenotype during remodeling of cardiac valves. *J Heart Valve Dis*. 2004;13:841-847

36. Cushing MC, Liao JT, Anseth KS. Activation of valvular interstitial cells is mediated by transforming growth factor-beta1 interactions with matrix molecules. *Matrix biology: journal of the International Society for Matrix Biology*. 2005;24:428-437
37. Hinton RB, Jr., Lincoln J, Deutsch GH, Osinska H, Manning PB, Benson DW, Yutzey KE. Extracellular matrix remodeling and organization in developing and diseased aortic valves. *Circ Res*. 2006;98:1431-1438
38. Wang H, Tibbitt MW, Langer SJ, Leinwand LA, Anseth KS. Hydrogels preserve native phenotypes of valvular fibroblasts through an elasticity-regulated pi3k/akt pathway. *Proc Natl Acad Sci U S A*. 2013;110:19336-19341
39. Visconti RP, Ebihara Y, LaRue AC, Fleming PA, McQuinn TC, Masuya M, Minamiguchi H, Markwald RR, Ogawa M, Drake CJ. An in vivo analysis of hematopoietic stem cell potential: Hematopoietic origin of cardiac valve interstitial cells. *Circ Res*. 2006;98:690-696

SUPPLEMENTAL FIGURES

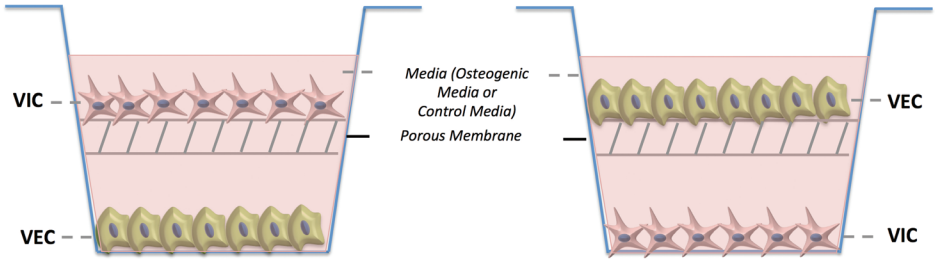

Supplemental Figure I. Schematic depiction of experimental setup. Transwell plates were used to setup a co-culture experiments with Valvular interstitial cells (VICs) and (VECs). These were cultured in either osteogenic media or control media with or without TGF-beta. Cells at the bottom of the well were used for analysis.

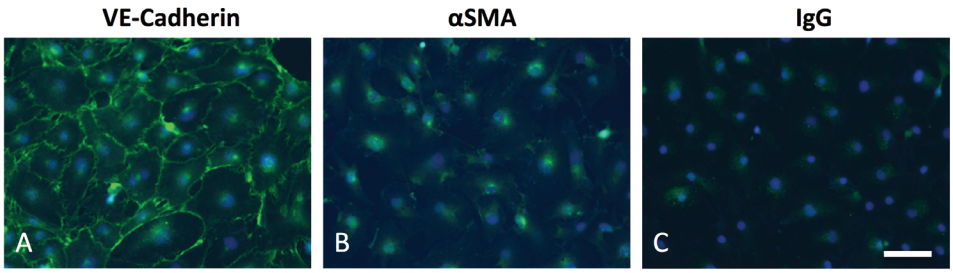

Supplemental Figure II. Valvular Endothelial Cell Phenotype VEC (Wav-1) were cultured 5 days in VEC media. Immunofluorescent staining of VEC phenotype for VE-Cadherin **(A)**, αSMA **(B).** Primary antibody was left out and substituted for IgG negative control (**C).** Bar: 50 um

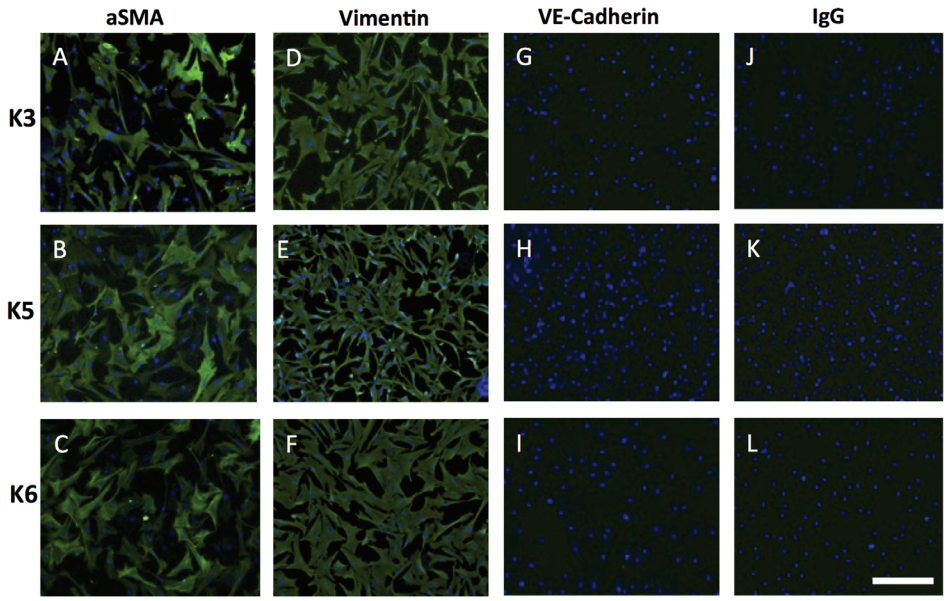

Supplemental Figure III. VIC clones were cultured 5 days in VIC media. Immunofluorescent staining of aVIC clones phenotype. K3, K5, K6 were stained for aSMA **(A-C)**, Vimentin **(D-F)**, VE-Cadherin **(G-I)**. Primary antibody was left out and substituted for IgG negative control **(J-L)**. Bar: 100um

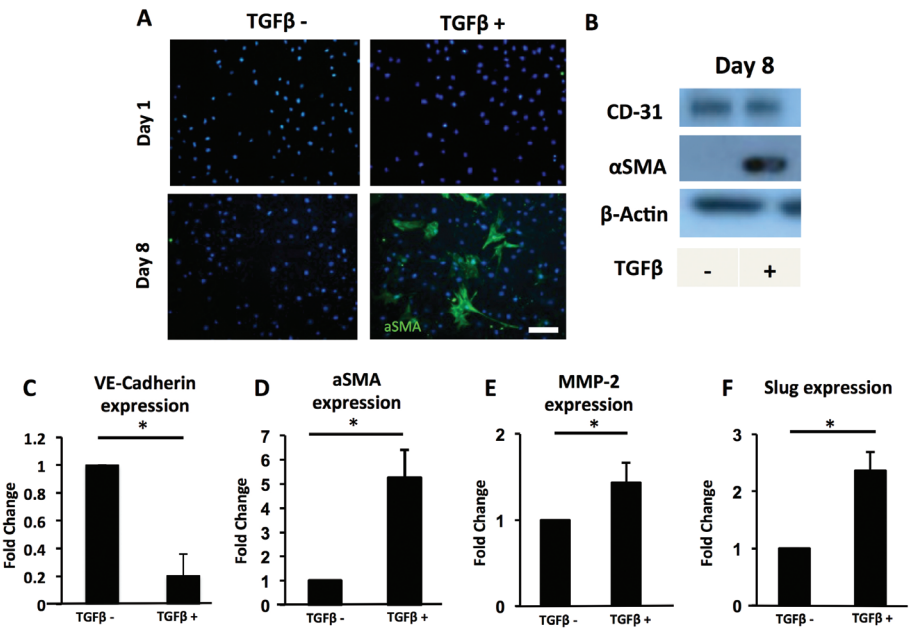

Supplemental Figure IV. VECs undergo TGFβ-induced EndMT. VECs were with TGFβ for 8 days**. A** Immunofluorescent staining of α-SMA (green), cell nuclei (DAPI/blue) at day 1 and 8. bar: 50μm. **B** Western blot displaying expression of endothelial markers (CD31) and myofibroblastic marker (α-SMA). **C** mRNA expresssion of EndMT markers VE-Cadherin, α-SMA, MMP-2 and Slug. Data is depicted as mean±SD fold change, *p<0.05

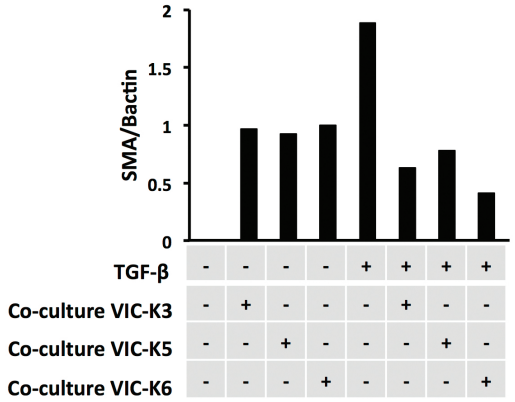

Supplemental Figure V. Densitrometry data VECs were treated with VIC conditioned media, TGF-β, or VIC-conditioned media and TGF-β for 8 days. Densitometry quantification of Western blot for αSMA expression

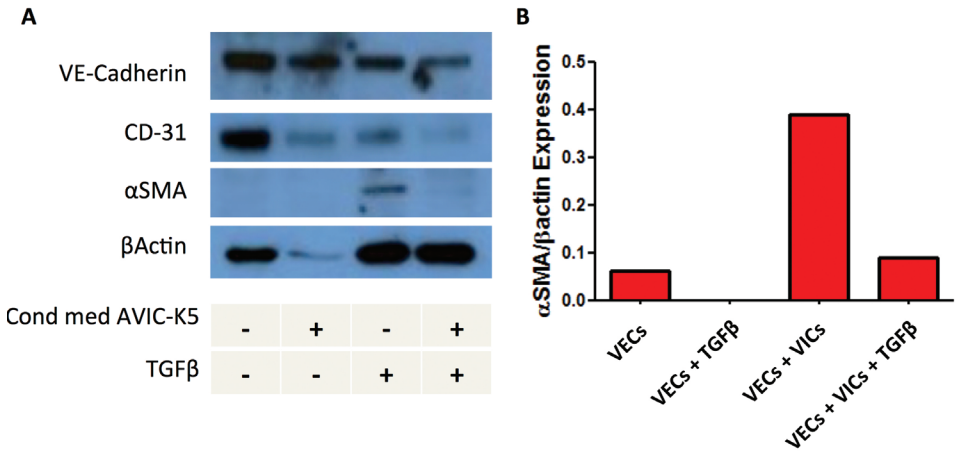

Supplemental Figure VI. Conditioned media from VICs inhibit TGFβ-induced EndMT. VECs were treated with VIC conditioned media, TGFβ, or VIC conditioned media and TGFβ for 8 days. **A** Western blot displaying expression of endothelial markers (VE-Cadherin, CD31) and myofibroblastic marker (α-SMA). **B** Densitometry quantification of western blot

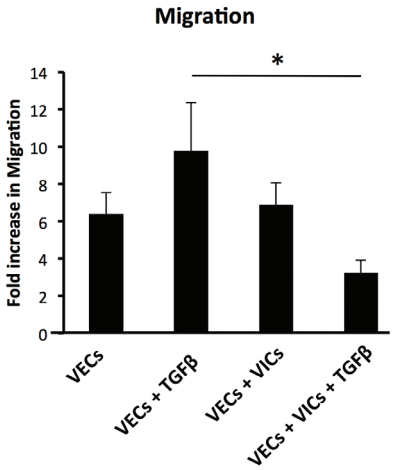

Supplemental Figure VII. VICs supress migration potential of VECs. VECs were cultured in transwell system with VIC and treated with TGFβ for 8 days, after which a migration assay on the VECs was performed. Data is depicted as mean ± SD fold change. *p < 0.05

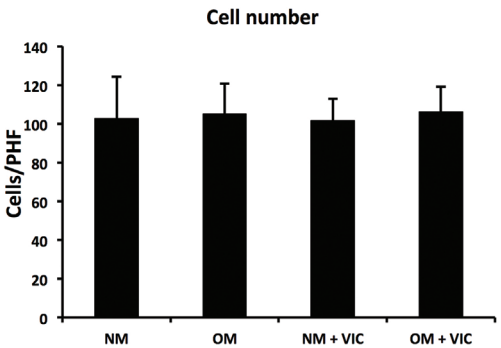

Supplemental Figure VIII. VEC cell number remains similar when cultured in NM, OM and in co-culture with VICs. . VECs were cultured in NM, OM, and in co-culture with VICs, and counted for positive DAPI staining. (n=5), *p < 0.05

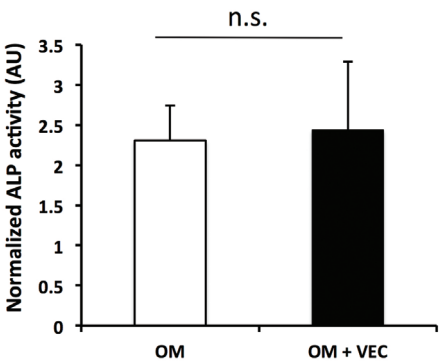

Supplemental Figure IX. ALP activity day 14. aVICs were cultured for 14 days in OM and in OM with aVECs. (n=3) Data is depicted as mean ± SD/normalized to NM conditions. * p < 0.05,

Final Thoughts

11

Summary and Conclusions

INTRODUCTION

Calcific aortic valve disease (CAVD) is the most common valve disease in the Western world. There is no therapeutic medication that can prevent or halt the progression of disease. As such, surgical or trans-catheter valve replacement remain the only treatment options to date. Considering that the burden of this disease is expected to triple in the next decades, improved understanding of CAVD and in particular its onset is warranted. The objective of this thesis was to address this challenge and use new means of elucidating mechanisms of early CAVD. The specific aims pursued in this these were defined as follows:

I Using molecular imaging as a tool to study early onset CAVD and identify hallmarks of disease progression

II Developing an *in vitro* model that can recapitulate the process of early CAVD as it may occur in situ.

VISUALIZING EARLY CALCIFIC AORTIC VALVE DISEASE

Patients often do not present with symptoms of CAVD until it has developed into significant aortic stenosis. This observation inherently means that mechanisms of disease progression and disease onset in humans remain relatively unknown. As such, we have based most of our understanding on either in vitro cellular experiments or in vivo animal models. However, albeit both of vital importance to study various aspects of disease, both approaches have been unable to recapitulate disease progression or even disease onset as it may occur in situ. An important and also clinically relevant challenge lies in visualizing the entire disease process. To this end, molecular imaging has emerged as a new and powerful tool to visualize cellular processes of disease *in situ*.

Part I of this thesis describes and explores the use of molecular imaging in studying CAVD. Currently both vascular and valvular calcifications are visualized by non-invasive imaging modalities such as echocardiography, computed tomography (CT) and magnetic resonance imaging (MRI). Even though CT and echocardiography are vital diagnostic tools, clinical imaging is only performed when patients are becoming symptomatic. Early detection methods are not only needed to elucidate early mechanism of cardiovascular calcification, but also to establish potential reversibility of disease.

Chapter 3 elaborates on how molecular imaging has been able to visualize novel concepts of both vascular as valvular calcification. In **Chapter 4** we use molecular imaging to visualize mechanism of disease in an established model of cardiovascular calcification. We demonstrate *in vivo* evidence for a potential inverse relationship between cardiovascular calcification and bone mineral density in mouse models of atherosclerosis and chronic renal disease. In addition, this work reveals

an association between aortic valve calcification and arterial calcification in these mouse models. Notably, we observe increased inflammatory activity in arteries, aortic valves and long bones in atherosclerosis and renal failure, demonstrating that systemic inflammatory disease could possible connect loss of bone mineral density and ectopic calcification. It validates the enormous potential molecular imaging holds in visualizing disease progression on a cellular and molecular level.

Clinically, an association exists between coronary artery disease and aortic valve stenosis, linking atherosclerosis to calcific aortic valve disease. In addition, both mouse and rabbit models demonstrate that aortic valve calcification can be treated by lipid-lowering therapies such as statins, considering it has been proven successful in treating atherosclerosis. In hallmark histological work atherosclerotic-like plaques have been identified in calcified aortic heart valves. However, randomized clinical trials have failed to show a beneficial effect. It is left to question whether atherosclerosis and associated vascular calcification should even be considered a similar disease to aortic valve calcification. In any event it is clear, that we still were unable to grasp the mechanisms of disease of CAVD, particularly relating to its onset and progression.

MODELING EARLY CALCIFIC AORTIC VALVE DISEASE

In pursuit of understanding CAVD disease onset, it became clear that we needed a new approach that could not only mimic aortic valve biology but also simulate aortic valve disease as it might occur in humans. In **Part II** we approach this challenge by looking towards tissue engineering. Tissue engineering pursues the development of organs or tissue suitable to replace or improve biological functions. In this thesis we used hydrogel micro engineering to develop a model of valve tissue able to recapitulate valve (patho) biology as it may occur in situ. Hydrogels resemble native extracellular matrix, and can be fabricated using natural extracellular matrix components, making it a potentially important tool in controllably re-creating the micro-environment of the heart valve. **Chapter 5** elaborates on the application of hydrogels in tissue engineering, in addition to **Chapter 6**, which focuses on discussing the application of hydrogels to heart valve tissue engineering.

In pursuit of fabricating an *in vitro* model for CAVD, we use hydrogel micro engineering to first create a micro-environment that is similar to that in the aortic valve. **Chapter 7** describes how we used hyaluronic acid and collagen, vital components of the valve ECM, to fabricate three-dimensional heart-valve like structures. We demonstrate that this approach allows for studying phenotypic changes of valvular interstitial cells (VICs). By varying collagen and hyaluronic acid content, we first fabricate a hydrogel with similar characteristics to the *zona fibrosa* of the heart valve. This is the layer of the valve where calcification solely occurs. Establishing the ability to harness quiescent healthy VICs within a three dimensional valve like construct, we next show that we can controllably direct VICs into a myofibroblast-like differentiation. This process is considered the hallmark of valve fibrosis, and potentially the onset of CAVD.

Chapter 8 describes how we use these micro-engineered valve-like constructs to study CAVD onset and mineralization. It shows how our hydrogel platform can maintain a quiescent VIC phenotype similar to healthy heart valves, and thus providing for a platform that can study disease onset. By exposing these VIC-laden hydrogels to osteogenic and inflammatory stimuli, VICs undergo myofibroblast-like differentiation and eventually differentiate into osteoblast-like cells, which actively deposit calcium. To our knowledge, this is the first study demonstrating all phenotypes of VICs involved in CAVD in one model. We also establish that myofibroblast-like differentiation is required for osteoblast-like differentiation, potentially opening up a window for therapeutic targeting. We show that this 3D *in vitro* model for calcification can be used to controllably study specific pathological mechanisms associated with CAVD, including inflammation.

Furthermore, this model can be used to study relationships within other disease etiologies. In **Chapter 9** we apply our 3D model valve-like model to study the relationship between radiation therapy - in for instance lymphoma or breast cancer - and accelerated calcification of the aortic valve, as is often observed in the clinic. This preliminary work demonstrates an accelerated loss of myofibroblast-like phenotype and mineralization by VICs when exposed to irradiation. We demonstrate the potential of our 3D model to be used as a testing platform for environmental stimuli such as radiation associated with CAVD.

In pursuit of fabricating an *in vitro* model for valve disease, the endothelium cannot be overlooked. Mounting evidence indicates that valvular endothelial cells may hold a reciprocal relationship with valvular interstitial cells both in maintaining a healthy valve homeostasis as well as in valve disease. **Chapter 10** examines the relationship between valvular interstitial cells and valvular endothelial cells in both a healthy and osteogenic environment, with the purpose of improving our understanding of valvular endothelial cells in calcific aortic valve disease. We demonstrate that VECS are able to differentiate into osteoblastic cells and deposit calcium. Moreover, this is a process that is driven by endothelial to mesenchymal transition. More importantly, we observe that activated VICs can inhibit mineralization by VECS, by inhibiting the mesenchymal differentiation process of VECs. We corroborate these findings in both mouse models of valve disease and human calcified valve specimens. Based on this work, we propose that VECs may differentiate into endothelial-derived VICs and contribute to the onset of CAVD.

In this thesis, we set out to overcome important challenges in CAVD research. First, we use molecular imaging to visualize disease progression in vivo and identified important hallmarks for disease propagation. Second, we develop a three-dimensional in vitro valve-like model of CAVD and used it to study the onset and progression of CAVD as it may occur in humans. We believe that results of this work may aid in the development of targets for therapeutic strategies that can possibly prevent, diagnose, or treat CAVD, broaden our data to other disease processes and further the progress in engineering valve substitutes.

12

General Discussion

CALCIFIC AORTIC VALVE DISEASE: SHEDDING LIGHT ON ITS ONSET

Research into calcific aortic valve disease (CAVD) has received renewed impulse and attention in the field. An important reason is that successful translation of experimental and pre-clinical research to clinical practice remains wanting. Without intervention, upon diagnosis of symptomatic aortic valve stenosis, death follows within months to a few years.[1, 2] The main treatment for CAVD is surgical valve replacement, where trans-catheter valve replacement is reserved for patients with excess operative risk.[3] Tissue engineered valve replacements also holds great promise, however remains to be successfully translated to the patient.[4] Currently, there are just no medical therapies for CAVD as an alternative to surgery.

This observation means that we do not fully understand the mechanisms involved in CAVD; or valvular biology for that matter. Although great progress has been made, elucidating disease onset and its seemingly inevitable progression to significant aortic valve stenosis remains challenging. Considering the exponential increase of disease burden that is bound to follow an ageing world population, strong motivation exists to overcome this challenge.

The objective of this thesis is to shed light on the onset of CAVD, by first visualizing cellular mechanisms *in vivo* and identifying hallmarks of disease progression and secondly developing a new *in vitro* model for CAVD able to simulate events that may occur in early CAVD in situ. In this general discussion we will elaborate on how our work relates to the current status of CAVD research. In addition we will describe recommendations for future study.

LESSONS FROM HUMAN END-STAGE CALCIFIC AORTIC VALVE DISEASE

In brief, CAVD is currently considered a progressive disorder, ranging from mild valve thickening called sclerosis to severe calcification with impaired leaflet motion eventually causing aortic valve stenosis. Due to a persistent fibrotic collagen accumulation in the valve leaflet, which seemingly precedes calcific nodule formation,[5] CAVD can also be labelled as a fibro-calcific disease.[6] However, whether calcific nodule formation may occur simultaneous to the persistent fibrotic response is unknown.

The fibro-calcific process is actively regulated by valvular interstitial cells (VICs), which reside in the valve interstitium and are responsible for structurally maintaining the valve extracellular matrix. (Chapter 1) More specifically, quiescent VICs (qVICs) reside throughout healthy native valves and differentiate into activated myofibroblast-like VIC (aVICs) upon environmental cues[7, 8], subsequently leading to remodelling of the ECM.[9] Persistent activation of qVICs is considered the fundamental mechanism of the fibrotic response and related to the calcification process.[10]

CAVD is characterized by the deposition of calcium phosphate mineral within the extracellular matrix.[11] Two osteogenic processes may be considered as key mechanisms of CAVD. First, calcification may be present as dystrophic calcification, a disorganized crystal structure that is

associated with the precipitation of calcium phosphate on debris remaining after cell death. Secondly, calcification can be observed as a bone-like organized crystal lattice of hydroxyapatite, indicating an active osteogenic process.[12-14] Histological analyses delineate an estimate of up to 83% of dystrophic calcification and 13% bone-like structures present in calcified valve explants.[13] How these osteogenic processes relate to each other is unclear.[15] The bone-like calcification has been attributed to osteoblast-like cells that actively deposit calcium in the valve extracellular matrix.[12]

Notably, spherical particles containing calcium phosphate mineral have recently been identified in calcified aortic valves. The origin of these particles is uncertain, but may be considered cellular derived matrix vesicles, which are thought to contribute to the initiation of hydroxyapatite mineralization.[16] Evidence suggest that these vesicles are released by macrophages or valvular interstitial cells, enriched in calcium binding proteins which serve as nucleation sites for calcium phosphate.[17] Further investigation will elucidate how these vesicles play a role in CAVD.

THE POINT OF NO RETURN

An important discussion in the field of CAVD research involves whether the disease is reversible, whether there is a point of no return in the disease process, and where such a point may lie. Answers to these questions would have vital implications for therapeutic intervention, including determining the optimal timing of surgery. Developing imaging tools that can monitor events associated with the disease process in patients with risk factors is thus a vital goal. (Chapter 3) Traditional imaging modalities such as echocardiography and computerized tomography, albeit very suitable in identifying and quantifying calcification, are limited because they are unable to detect early CAVD lesions. Molecular imaging has emerged in the search for new technologies to allow early detection and offer insight into the mechanism of CAVD, as a successful tool that can detect pathobiological processes associated with inflammation and early stages of calcification *in vivo* at the cellular level.[18-21] Studies have successfully detected pro-inflammatory, pro-osteogenic, and proteolytic activity in cardiovascular calcification *in vivo*.[19, 22-24] Imaging agents use molecular processes to generate image contrast using high-resolution imaging technology. This approach has led to the discovery of imaging agents that chemically attach to an affinity ligand, such as a fluorochrome or magnetic compound (e.g., biphosphonate-conjugated fluorescent agents, cross-linked iron oxide fluorescent nanoparticles to detect macrophages). We can visualize enzyme activity in CAVD by employing molecular imaging agents to interact with enzymes that, when active, undergo a chemical change leading to signal amplification.[19, 24] Currently, only optical imaging modalities can be used to detect calcification and early stages of the disease, due to limited signal detection by conventional imaging techniques such as CT and MRI. Visualizing pathways involved in early stages of CAVD is warranted in the pursuit of new therapeutic targets. The work presented in this thesis (Chapter 4) utilized multimodal molecular imaging to detect and monitor over time

the dynamic changes in inflammation and ectopic calcification in mouse models of cardiovascular calcification[19, 22, 25] (Figure 1).

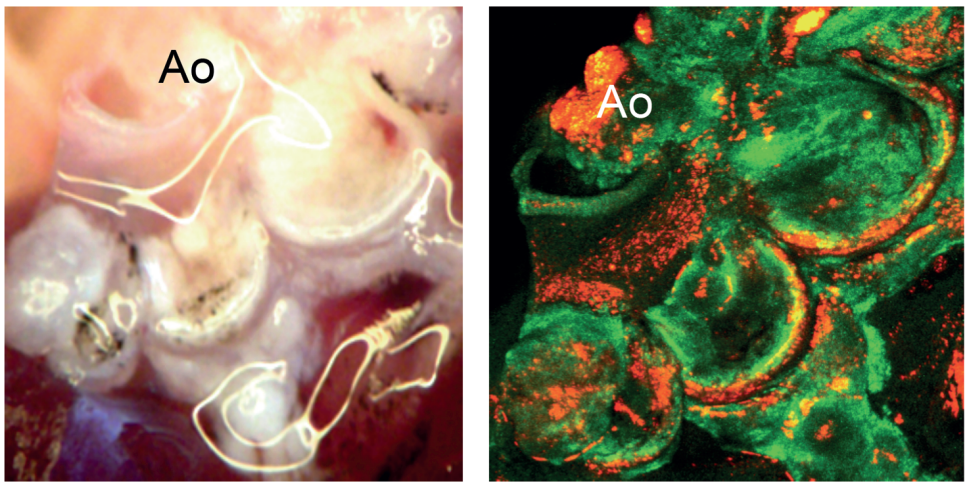

Figure 1. Inflamed aortic valves of apoE$^{-/-}$ mice had characteristics of early calcific disease. Gross morphology (left) and fluorescence microscopy (image stacks; right) of calcified aortic valves visualized osteogenic activity (OsteoSense-680, red) in the areas of leaflet attachment to the aortic wall in inflamed valves (CLIO-750, green)

These changes are undetectable by conventional imaging techniques. In addition, molecular imaging provides the opportunity to effectively visualize biological processes simultaneously using different imaging agents. This research demonstrates the importance of developing imaging techniques able to non-invasively characterize stages of disease progression, and thus detect early calcification before a "point of no return," and to establish the reversibility potential of CAVD. Great progress in translating molecular imaging to humans has recently been made, using radiotracers ^{18}F-fluorodeoxyglucose and ^{18}F sodium fluoride to visualize inflammatory activity and calcification using PET-CT scanning.[26, 27] This work underscores the ability for molecular imaging approaches to visualize key pathological processes. Conversely, molecular imaging can also be used to track effect of therapeutic intervention and facilitate the development and validation in individual subjects.

THE ATHEROSCLEROSIS PARADOX

A hallmark histological study by Otto et al, demonstrated that human calcified aortic valve leaflets harboured similar atherosclerotic lesions as found in coronary artery disease, including macrophages, foam cells, oxidized LDL, and lipid deposits.[28] In addition, pre-clinical studies have demonstrated atherosclerosis-like lesions in aortic valve leaflets both in rabbit and mouse models of atherosclerosis. Lowering cholesterol levels in mice even ceased progression of aortic valve

calcification.[29] Clinical studies also suggest that CAVD and coronary artery disease share similar epidemiologic risk factors, such as age, gender, hypercholesterolemia, and hypertension.[10, 30, 31]

Taken together, this has led to the hypothesis that CAVD shares similar mechanisms to atherosclerosis and could thus potentially be treated using similar therapeutic strategies.[5] However, randomized clinical trials treating patients with CAVD with statins showed no benefit of treatment. Conversely, it must be argued that patients included in these trials already had moderate to severe aortic valve stenosis, which means that disease could have passed ' the point of no return'. As such, whether statin therapy might benefit patients with early CAVD remains to be elucidated. Nevertheless, results from these trials spurred the discussion to what extent atherosclerosis and CAVD should be considered similar etiological entities.

A paradox exists between treating atherosclerosis and CAVD. Atherosclerosis is characterized by a collagen-rich fibrotic cap encapsulating an underlying calcification that forms within the plaque,[32] which is reminiscent of fibrosis and calcification observed in CAVD. Interestingly, from a therapeutic standpoint an important difference exists between the fibrotic response of atherosclerosis and CAVD. Collagen accumulation in an atherosclerotic lesion is desirable to stabilize the plaque and minimize the potential for rupture and thrombosis[33-35] Lesion stability has traditionally been determined by collagen thickness in the fibrotic cap.[36] Subsequent calcification then further stabilizes the plaque.[37] Patients treated with statins demonstrate heightened atherosclerotic plaque stability, attributed to increased collagen accumulation within the fibrous cap.[38] The desirability of atherosclerotic plaque growth is only limited by the ensuing stenosis of a vessel. Nevertheless, a heightened fibro-calcific response seems the aim of atherosclerosis management. Conversely, this completely contradicts treatment goals of CAVD, where added fibro-calcific response would only increase valvular dysfunction.

INFLAMMATION

A possible link between arterial calcification and CAVD could be the manifestation of inflammatory disease. Both CAVD and calcification in atherosclerotic plaques is associated with the presence of inflammatory cells, such as macrophages and T-cells.[25, 27] In established mouse models for atherosclerosis and chronic renal disease (CRD), we demonstrate in this thesis the correlation of macrophage activity in arteries and aortic valves. (Chapter 4) More specifically, we hypothesize that infiltration of inflammatory cells is an early event in aortic valve calcification and atherosclerotic lesions.[19, 39] Inflammatory cells actively release protease that degrade extracellular matrix proteins, and thus could indicate a role initiating the remodelling processes that lead to calcification. Particularly, persistent inflammation, attributed to for instance diabetes mellitus or the metabolic syndrome, has detrimental effects. Collagen degradation in atherosclerotic plaques leads to a decrease in plaque stability.[33] These cells also release pro-inflammatory cytokines, promoting pathological differentiation of VICs and VECs.

Osteogenic differentiation is for instance related to exposure to tumor necrosis factor-alpha (TNFα) (Chapter 8), and interleukin-6 (IL-6). We also observe this process that TNFα catalyzes mineralization of heart-valve like constructs *in vitro* (Chapter 8), by activating runt-related transcription factor 2 (runx2). In addition, Msx2/Wnt signalling cascades have also been shown to be upregulated to inflammatory cytokines, leading to mineralization and ectopic bone formation.[40] In addition, there is mounting evidence suggesting that the inflammatory milieu in CAVD actually favours inhibition of osteoclastogenesis, because osteoprotegerin is upregulated early in disease progression of valve tissue, and in serum OPG has shown to predict mortality in patients with symptomatic CAVD.[41]

Furthermore, a regulator of macrophage biology, NAD-dependent deacteylase sirtuin-1, has been shown to decrease resistin expression.[42] Resistin leads to the accumulation of LDL in arterial walls and is correlated with CAVD in patients over 70 years of age.[43] Therefore, inflammation might also be associated with lipid changes that influence valvular remodelling.

To this end, it would be of great interest to investigate the effect of anti-inflammatory agents and if they are able to prevent and reduce the extent of calcification and osteogenesis, which is known to be triggered by inflammatory mediators. As such, the on-going Cardiovascular Inflammation Reduction Trial (CIRT) is examining whether treatment with low-dose methotrexate, an effective anti inflammatory drug, may affect progression of CAVD.[44]

FROM *IN VIVO* TO *IN VITRO* MODELS

Because we are unable to adequately study disease onset in humans, the majority of experimental evidence relies on using *in vivo* animal models or *in vitro* models. *In vivo* models hold the advantage of modelling complex physiology akin to humans. In addition, animals can be genetically modified to express a specific pathology. Great strides have been made in understanding the functional consequences of various mediators in calcific aortic valve disease, however one must recognize the limitations of laboratory experiments on mice.[45] The inbred strains used in sterile environments in which we raise our mice, allow for well controlled experiments, but are unable to reflect the heterogeneity of humans, including human interaction with microbes. Laboratory experiments usually utilize mice by exaggerating disease. Research pertaining to mechanistic study of CAVD has mostly used rabbit or mice models. Rabbit models require very high cholesterol diets[46] to induce atherosclerotic disease also observed in patients, and the addition of Vitamine D to cause calcification.[47] Mouse models are genetically modified and require very high cholesterol addition to their diet to induce calcification. Both LDL receptor knockout and ApoE knockout mice, also utilized in this thesis (Chapter 4), must be fed a high cholesterol diet to develop hypercholesterolemia associated cardiovascular calcification over time.[6, 25] This exaggeration allows for an expedited experimental time of weeks to months, compared to the human disease process, which requires years if not decades. Although, these limitations should not cast any shadow on knowledge gained from this work, it does necessitate caution when extrapolating results to clinical disease.

As such, even though CAVD and atherosclerosis share risk factors in patients, one must question if disease simulated in these models progress through the same mechanisms as human disease,[48] particularly since translation of therapeutic targets in these animal models to patients remains elusive.

Conversely, *in vitro* models, which allow better isolation and manipulation of independent variables, offer a powerful window of opportunity to study CAVD, but not in its traditional form. **(Chapter 5)** *In vitro* systems have historically used Petri-dishes, to study the role the valvular cell population might have in valve calcification. However, therein lies its greatest limitation. *In vitro* models are intrinsically unnatural environments for cells, due to the unnaturally stiff substrate of plastic and the two-dimensional environment cells when in culture reside in.[49] In addition, VICs have demonstrated a high degree of mechanosensitivity, leading to uncontrollable phenotypic changes in 2D culture systems.[50] Therefore the development of a 3D *in vitro* system that allows for the independent modulation of the VIC phenotype with the purpose of modelling the entire cellular driven process of valve homeostasis and pathology would be a great leap forward.

ENGINEERING CALCIFIC AORTIC VALVE DISEASE: WHEN IS IT GOOD ENOUGH?

To overcome this challenge we developed an *in vitro* three-dimensional heart valve-like construct using hydrogel microengineering. (chapter 5,6,7) Hydrogels can be designed using natural proteins to recapitulate important environmental cues in native tissues, and have gained a great deal of interest also in valve tissue engineering due to their ability to be chemically and mechanically tailored to specific needs.[51] VICs have proven to be very sensitive to their micro-environment.[50] Thus, an important question to address in the discussion of work presented in this thesis is: First, what complex variables must be considered to appropriately simulate the valve micro-environment? Second, how does our model relate to the native aortic valve micro-environment? In short, is our model good enough? These questions will be addressed by discussing the following concepts: substrate stiffness and dimensions, substrate components, hemodynamics, and the role of VECs.

SUBSTRATE STIFFNESS AND DIMENSIONS

As described earlier, the native valve extracellular matrix is comprised of three layers, *the zona fibrosa, zona spongiosa and zona ventricularis*. CAVD predominantly occurs in the *zona fibrosa* of the aortic valve, which mainly consists of collagen and glycosaminoglycans (e.g. hyaluronic acid). We based our hydrogel model on using methacrylated gelatin, a denatured form of collagen, and hyaluronic acid to recapitulate the environment of the aortic valve in which CAVD occurs. By photo-

crosslinking GelMA and HAMA we engineered an *in vitro* 3D culture system to study VIC phenotype change. We show that VICs encapsulated in a combination of HAMA and GelMA preserve the quiescent fibroblast like phenotype in VICs, contrary to VICs cultured on plastic plates (Chapter 7). The modulus of our hydrogels maintaining VIC quiescence was measured to be around 25 kPa, corroborating earlier work demonstrating the native aortic valve *zona fibrosa* to posses similar modulus.[52]

In the pursuit of fabricating an in vitro model similar to the native micro-environment, the layered structure and its mechanics must be taken into account. The structural integrity of the aortic valve is mostly supplied by the collagen rich- *zona fibrosa*,[53] suggesting that the ECM layers have different elasticities. Studies used different testing methods to determine moduli of normal aortic valves, which may account for the relative large difference between reported moduli (8.5 kPa vs 2 mPA).[49] If only, these discrepancies underline the need to determine a unified method to spatially map the mechanical properties of valve tissue, particularly in relation to disease progression.

Previous work determined that a substrate modulus of E>15kPa would facilitate a threshold like myofibroblast response of VICs in vitro,[54] however this was shown in VICs seeded onto a substrate in two dimensions. Interestingly is that other work showed this substrate modulus to be associated with the formation of osteogenic calcific nodules in the presence of TGFβ1.[55] This observation underscores the notion that cells behave differently in a three-dimensional culture system. The threshold for pathological behaviour induced by relevant biochemical cues may vary greatly depending on the substrate environment.

Nevertheless, substrate modulus is also associated with calcification. For instance, VICs demonstrate an increase in calcific nodule formation when cultured on tissue culture-treated polysterene (TCPS) compared to VICs seeded on hydrogels functionalized with integrin binding small peptide RGD.[54] On soft, thick, type I collagen gels, VICs hardly showed any mineralization, compared to stiffer substrates. This work indicates that substrate elasticity can elicit different VIC responses, but also confirms the need to move away from traditional TCPS plates for to culture platforms in which matrix elasticity can be fine tuned to physiological relevance. To underscore this point, tractional forces by cells should be considered.[56] VICs apply tractional forces to the surrounding matrix, which is resisted in part by the elasticity of the ECM. VIC traction probably stiffens valve tissue during the relaxed state of systole.[57] However ECM tractional stress often exceeds external tractional stress applied to cells. Cells respond to changes in matrix elasticity by altering adhesion to the ECM and cytoskeletal organization.[58] Thus mechanical properties of the matrix can activate and modify intracellular signalling pathways an alter VIC function. Studies have shown that the preservation of native VIC phenotypes has recently been attributed to go through an elasticity regulated PI3K/AKT pathway. PI3K/AKT signalling antagonizes apoptosis and promotes cell survival and proliferation.[59] It is hypothesized that elevated AKT activity in myofibroblasts could be an important cause or persistent activation due to its sensitivity to mechanosensing.

Mechanosensing might also explain the difference in the nature of mineralization observed in stenotic valves. VICs cultured in osteogenic media on compliant and stiff collagen gels formed

calcific nodules, but they differed from one another.[50] On compliant substrates, similar to fibrosa elasticity (~25kPa), VICs formed small aggregates of viable cells expressing osteogenic genes and proteins leading to bone formation. However, VICs cultured on stiffer gels in osteogenic media, mimicking stiffness of stenotic tissue, VICs demonstrated a myofibroblast phenotype, formed larger calcific nodules with apopotic cells.[50] Perhaps this provides insight into osteogenic differentiation occurring predominantly in the *fibrosa*, and that this process may precede dystrophic calcification.

9. HYDROGEL SUBSTRATE COMPONENTS

Our model is in essence a relatively simple one, in which other ECM proteins have not been included. For instance, it is known that VICs cultured on fibrin exhibit more nodules than on collagen, fibronectin or laminin.[54] Fibronectin coated tissue culture polystyrene suppressed calcification.[60] However both fibronectin and fibrin coating soft hydrogels suppressed calcification,[61] indicating that perhaps substrate stiffness is more important than substrate composition. When VICs cultured on either collagen-I or fibronectin are exposed to strain, collagen showed less myofibroblast differentiation of VICs compared to fibronectin.[62] This indicates that interaction with collagen in the fibrosa layer might play part in maintaining tissue homeostasis. As such, substrate composition is an important concept in which to compare our model to that of the native valvular micro-environment.

A limitation to our work is that we only included a collagen-based material and a glycosaminoglycan. The important *zona ventricularis*, predominantly comprised of elastin, is not included in our hydrogel model. Elastin is a vital yet elusive extra-cellular matrix protein of the native heart valve. The *zona ventricularis* is responsible of the extension of the valve leaflet in diastole and recoil in systole during the cardiac cycle. It is an important component of valve durability, and has remained an elusive part of the extra cellular matrix to generate both in the setting of a laboratory or in efforts to create a functional tissue engineered heart valve. The importance of creating or maintaining a *zona ventricularis* is underscored by studies demonstrating the exacerbation of tissue calcification when exposed to elastin fragments.[22] In addition, in vivo mouse studies demonstrated inflammation might accelerate calcification by Cathepsin-S induced elastolsysis.[22]

The next step in our work is to include an elastin-based or elastomeric layer to the hydrogel to recapitulate the layered nature of the heart valve. Successful efforts have been underway to create an elastin-based hydrogel.[63] Notably, recombinant human tropo-elastin, a precursor to elastin, can be methacrylated and subsequently crosslinked to fabricate a elastomeric hydrogel.[64]

In our work we used a collagen-based material and a glycosaminoglycan, hyaluronic acid, to purposefully simulate the microenvironment of the *zona fibrosa*, with the eventual goal to study CAVD. Arguably, this does not comprise the intrinsic complex composition of the aortic valve, particularly considering the mechano-signalling transfer the *zona ventricularis* may have on *the zona fibrosa*. Combining elastomers to our hydrogel model, would be an important next step to make.

10. HEMODYNAMICS

Considering the entire ECM structure of the valve, one must also discuss the valvular hemodynamics and to what an extent it may influence disease onset and progression. Clearly, our model as studied in this thesis, does not take hemodynamics into account due to its intrinsic static nature. To claim the recapitulation of the valvular microenvironment, a strong case can be made for the inclusion of appropriate hemodynamics, which can have profound consequences on both macroscopic and microscopic scales. Hemodynamic forces exert shear stress on the surface of the valve leaflets, which are transduced to the valvular endothelial cells that line the leaflet surface and VICs in the valvular interstitium.[65] As described earlier, VIC phenotype and function is regulated by cues from the local environment, in which the mechanical environment can play a critical modulatory role. Shear stress can cause valvular dysfunction, and pathological stretching, causing activation of VICs, upregulated latent TGFβ signalling, promoting maladaptive tissue remodelling.[53] Notably, VICs in the *zona fibrosa* demonstrated an increased deformation upon tissue stretch compared to VICs in the zona ventricularis, contributing in part to the explanation as to why myofibroblast activation predominantly occurs in the zona fibrosa.[52]

Importantly, a synergistic effect of valve tissue stretching and TGFβ -1 treatment on VIC activation has been described.[66] VIC αSMA expression was similar when exposed to cyclical stretch or cultured with soluble TGFβ 1, however when both were exposed to VICs, αSMA expression increased synergistically. This link between mechanical stimulation and TGFβ 1 signalling was confirmed by observing mechanical activation of latent TGFβ 1.[67] As such, it is reasonable to believe that adding TGFβ in its soluble form to our hydrogel based valve-like in vitro system functionally could be considered a simulation of mechanical stretch. Nevertheless, combining our hydrogel based platform to a hemodynamic stretch component, such as a bioreactor or a pulsatile substrate (e.g. FlexCell) is an important next step.

11. THE CRUCIAL ROLE OF VALVULAR ENDOTHELIAL CELLS

Another important observation when evaluating our hydrogel system is that it solely looked at valvular interstitial cell behaviour. Although VICs are considered the key mediator of valve extracellular matrix integrity and tissue homeostasis, VECs also play an important role in valve biology or pathology. Recapitulating the interaction between VICs with VECs is paramount in modelling human valvular disease *in vitro*. As such, 3D culture systems have been engineered to simulate the spatial relationship observed between VICs and VECs in their native valve environment. Co-culture experiments using 3D hydrogels allow for a dynamic simulation of the valve microenvironment, allowing for *in vitro* study of the role of VECs on VIC behaviour and vice-versa.

The importance of VECs in valve homeostasis is apparent from the difference in gene expression of VECs located on opposite sides of the valve leaflet.[68] Results from shear stress studies confirm

differential gene expression between fibrosa and ventricularis VECS.[69] Leaflets exposed to change in shear stress ex vivo demonstrate increase expression of vascular cell adhesion molecule-1 (VCAM-1), intercellular adhesion moleculue-1 (ICAM-1), BMP-4, and TFGβ, but only on the *fibrosa* side, indicating side dependent shear sensitivity correlating with side-dependent disease development.[68, 69]

Furthermore, it is currently believed that VECs play a critical role in regulating VIC phenotype via paracrine signalling. Studies have demonstrated VECs able to influence pathological differentiation of VICs.[69] More specifically, VECS may be a key modulator of progression of CAVD by regulating VIC activation and calcification. The regulation of VIC phenotype has been correlated with nitric oxide (NO) secretion, as synthetically generated NO can decrease calcific nodule formation in VIC cultures in vitro.[70] Interestingly, other CAVD risk factors such as hypercholesterolemia or diabetes mellitus decrease in NO expression.[71] The exact mechanism of what paracrine factors drive or inhibit VIC phenotype change is unknown. Isolating the effect of the valvular endothelium is difficult to study in vivo because both biophysical and biochemical factors likely affect VIC function and phenotype. Developing an in vitro platform able to simulate events that may occur in vivo is the most successful course of action.

We sought to investigate this intracellular relationship by studying the interaction of VICs and VECs from the same species in an osteogenic environment. Our work (Chapter 10) adds to a growing body of evidence that a reciprocal bond exists between VICs and VECs, and that alteration in this relationship influences valve tissue homeostasis and disease. Our work utilized an indirect co-culture system to explore this relationship. However, this approach is intrinsically limited by not being able to take substrate stiffness or composition – as discussed previously – into account. The next step is to use our hydrogel system as a co-culture in vitro model for valve (patho) biology. Adding an endothelial layer to a cell-laden hydrogel is vital in the pursuit of accurately simulating the valvular micro-environment *in vitro*. Hydrogels have been used before to study this particular feature; by encapsulating VICs in collagen gels and seeding these with VECs. However, collagen gels are intrinsically soft and alone do not recapitulate the valvular substrate stiffness or even composition. Synthetic Poly(ethylene glycol) (PEG) hydrogels have also been explored as a co-culture modality. PEG based hydrogels are useful in their mechanical tunability, and able to provide for a range of elastic moduli. Using these PEG-hydrogels, recent work has shown that the inhibition of VIC activation by VECs is increased in stiffer hydrogels.[72]

VECs also play a key role in valve biology through a process called endothelial-to mesenchymal transition (EndMT).[73] Our work shows that ovine aortic valve VECs differentiate to myofibroblast like cells, when stimulated with TGFβ, corroborating previous work.[74] In addition, we show VECs to differentiate into osteoblast-like cells, a process inhibited by VICs. This means that VECs and VICs may exist in a reciprocal relationship. The exact relationship of EndMT and CAVD is unclear, but we add to the notion that VECs may replenish the cellular population of valves upon suffering injury contributing to maintaining valve homeostasis.[73] In turn endothelial dysfunction may inhibit this repairing mechanism.

12. FINAL THOUGHTS

Evidently, CAVD is a complex multifactorial disease. Although a great deal of improvement in our understanding of the pathobiology has been made over the last decades, we still lack vital diagnostic tools to detect CAVD, particularly its onset and progression. Although we know and are familiar with some risk factors, not everyone with CAVD progresses to end stage aortic stenosis. We cannot predict with any certainty who will or will not progress. Development of new non-invasive diagnostic tools to visualize early CAVD is a necessary strategy not only for understanding disease onset, but also provide for means to evaluate its progression and potential response to new therapeutic strategies. A point of no return needs to be determined to identify patients who may benefit from medical treatment. This would also aid in determining for which patients surgical valve replacement is inevitable, and may strengthen the argument to surgically treat a category of asymptomatic patients.

These challenges can be met if we learn to understand the entire process of CAVD, and in particular its onset and progression. Considering the fact that patients do not develop symptoms until end-stage CAVD in the form of aortic valve stenosis, new means of studying CAVD are warranted. Two main goals are defined in this thesis. One is to use molecular imaging as a novel tool to visualize key processes involved in CAVD progression. The second goal is to model CAVD in vitro as it may occur in humans.

Molecular imaging is a powerful tool to study the disease process. It allows for specific visualization of cellular mechanisms involved in cardiovascular calcification. We have shown inflammation to be a hallmark of disease progression in mouse models simulating cardiovascular calcification. Next to developing such tools, we must always be critical of the models used to study human disease. A strong case can be made that no animal models fully recapitulate CAVD as it may occur in situ. Thus we turn to in vitro studies, which offer much more control over variables involved. However, in vitro studies alone also represent a non-physiological environment. As such we look towards tissue engineering to re-create the valve microenvironment in the laboratory simulating events that occur in human CAVD. An important step has been made, by demonstrating that we can controllably differentiate healthy quiescent valve cells to a diseased state, making this the first to simulate all cellular phenotypes involved in CAVD in one model system. However, like we have discussed throughout this entire thesis. CAVD is a multifactorial complex disease. A leap forward has been made, and part of the CAVD process has successfully been simulated in the laboratory. But important components such as elasticity, hemodynamics, and an endothelial layer is required to claim we have re-created the aortic valve micro-environment outside of the human body.

In the end, once we can build it, we understand it *(Richard Feynmann)*.

REFERENCES

1. Hammermeister K, Sethi GK, Henderson WG, Grover FL, Oprian C, Rahimtoola SH. Outcomes 15 years after valve replacement with a mechanical versus a bioprosthetic valve: Final report of the veterans affairs randomized trial. *J Am Coll Cardiol*. 2000;36:1152-1158
2. Stewart BF, Siscovick D, Lind BK, Gardin JM, Gottdiener JS, Smith VE, Kitzman DW, Otto CM. Clinical factors associated with calcific aortic valve disease. Cardiovascular health study. *J Am Coll Cardiol*. 1997;29:630-634
3. Lindman BR, Bonow RO, Otto CM. Current management of calcific aortic stenosis. *Circulation research*. 2013;113:223-237
4. Cheung DY, Duan B, Butcher JT. Current progress in tissue engineering of heart valves: Multiscale problems, multiscale solutions. *Expert opinion on biological therapy*. 2015:1-18
5. Hutcheson JD, Aikawa E, Merryman WD. Potential drug targets for calcific aortic valve disease. *Nature reviews. Cardiology*. 2014;11:218-231
6. Weiss RM, Miller JD, Heistad DD. Fibrocalcific aortic valve disease: Opportunity to understand disease mechanisms using mouse models. *Circulation research*. 2013;113:209-222
7. Rabkin-Aikawa E, Farber M, Aikawa M, Schoen FJ. Dynamic and reversible changes of interstitial cell phenotype during remodeling of cardiac valves. *J Heart Valve Dis*. 2004;13:841-847
8. Mulholland DL, Gotlieb AI. Cell biology of valvular interstitial cells. *Can J Cardiol*. 1996;12:231-236
9. Chester AH, Taylor PM. Molecular and functional characteristics of heart-valve interstitial cells. *Philosophical transactions of the Royal Society of London*. 2007;362:1437-1443
10. Freeman RV, Otto CM. Spectrum of calcific aortic valve disease: Pathogenesis, disease progression, and treatment strategies. *Circulation*. 2005;111:3316-3326
11. Otto CM. Calcific aortic stenosis--time to look more closely at the valve. *N Engl J Med*. 2008;359:1395-1398
12. Mohler ER, 3rd, Chawla MK, Chang AW, Vyavahare N, Levy RJ, Graham L, Gannon FH. Identification and characterization of calcifying valve cells from human and canine aortic valves. *J Heart Valve Dis*. 1999;8:254-260
13. Mohler ER, 3rd, Gannon F, Reynolds C, Zimmerman R, Keane MG, Kaplan FS. Bone formation and inflammation in cardiac valves. *Circulation*. 2001;103:1522-1528
14. Rajamannan NM, Subramaniam M, Rickard D, Stock SR, Donovan J, Springett M, Orszulak T, Fullerton DA, Tajik AJ, Bonow RO, Spelsberg T. Human aortic valve calcification is associated with an osteoblast phenotype. *Circulation*. 2003;107:2181-2184
15. Monzack EL, Masters KS. Can valvular interstitial cells become true osteoblasts? A side-by-side comparison. *J Heart Valve Dis*. 2011;20:449-463
16. New SE, Goettsch C, Aikawa M, Marchini JF, Shibasaki M, Yabusaki K, Libby P, Shanahan CM, Croce K, Aikawa E. Macrophage-derived matrix vesicles: An alternative novel mechanism for microcalcification in atherosclerotic plaques. *Circulation research*. 2013;113:72-77
17. Kapustin AN, Davies JD, Reynolds JL, McNair R, Jones GT, Sidibe A, Schurgers LJ, Skepper JN, Proudfoot D, Mayr M, Shanahan CM. Calcium regulates key components of vascular smooth muscle cell-derived matrix vesicles to enhance mineralization. *Circulation research*. 2011;109:e1-12
18. Nahrendorf M, Sosnovik D, Chen JW, Panizzi P, Figueiredo JL, Aikawa E, Libby P, Swirski FK, Weissleder R. Activatable magnetic resonance imaging agent reports myeloperoxidase activity in healing infarcts and noninvasively detects the antiinflammatory effects of atorvastatin on ischemia-reperfusion injury. *Circulation*. 2008;117:1153-1160
19. Aikawa E, Nahrendorf M, Sosnovik D, Lok VM, Jaffer FA, Aikawa M, Weissleder R. Multimodality molecular imaging identifies proteolytic and osteogenic activities in early aortic valve disease. *Circulation*. 2007;115:377-386

20. Jaffer FA, Kim DE, Quinti L, Tung CH, Aikawa E, Pande AN, Kohler RH, Shi GP, Libby P, Weissleder R. Optical visualization of cathepsin k activity in atherosclerosis with a novel, protease-activatable fluorescence sensor. *Circulation*. 2007;115:2292-2298
21. Hjortnaes J, Gottlieb D, Figueiredo JL, Melero-Martin J, Kohler RH, Bischoff J, Weissleder R, Mayer JE, Aikawa E. Intravital molecular imaging of small-diameter tissue-engineered vascular grafts in mice: A feasibility study. *Tissue Eng Part C Methods*. 2010;16:597-607
22. Aikawa E, Aikawa M, Libby P, Figueiredo JL, Rusanescu G, Iwamoto Y, Fukuda D, Kohler RH, Shi GP, Jaffer FA, Weissleder R. Arterial and aortic valve calcification abolished by elastolytic cathepsin s deficiency in chronic renal disease. *Circulation*. 2009;119:1785-1794
23. Aikawa E, Whittaker P, Farber M, Mendelson K, Padera RF, Aikawa M, Schoen FJ. Human semilunar cardiac valve remodeling by activated cells from fetus to adult: Implications for postnatal adaptation, pathology, and tissue engineering. *Circulation*. 2006;113:1344-1352
24. Deguchi JO, Aikawa M, Tung CH, Aikawa E, Kim DE, Ntziachristos V, Weissleder R, Libby P. Inflammation in atherosclerosis: Visualizing matrix metalloproteinase action in macrophages in vivo. *Circulation*. 2006;114:55-62
25. Hjortnaes J, Butcher J, Figueiredo JL, Riccio M, Kohler RH, Kozloff KM, Weissleder R, Aikawa E. Arterial and aortic valve calcification inversely correlates with osteoporotic bone remodelling: A role for inflammation. *Eur Heart J*. 2010;31:1975-1984
26. Dweck MR, Chow MW, Joshi NV, Williams MC, Jones C, Fletcher AM, Richardson H, White A, McKillop G, van Beek EJ, Boon NA, Rudd JH, Newby DE. Coronary arterial 18f-sodium fluoride uptake: A novel marker of plaque biology. *J Am Coll Cardiol*. 2012;59:1539-1548
27. Dweck MR, Jones C, Joshi NV, Fletcher AM, Richardson H, White A, Marsden M, Pessotto R, Clark JC, Wallace WA, Salter DM, McKillop G, van Beek EJ, Boon NA, Rudd JH, Newby DE. Assessment of valvular calcification and inflammation by positron emission tomography in patients with aortic stenosis. *Circulation*. 2012;125:76-86
28. Otto CM, Kuusisto J, Reichenbach DD, Gown AM, O'Brien KD. Characterization of the early lesion of 'degenerative' valvular aortic stenosis. Histological and immunohistochemical studies. *Circulation*. 1994;90:844-853
29. Miller JD, Weiss RM, Serrano KM, Brooks RM, 2nd, Berry CJ, Zimmerman K, Young SG, Heistad DD. Lowering plasma cholesterol levels halts progression of aortic valve disease in mice. *Circulation*. 2009;119:2693-2701
30. Demer LL, Tintut Y. Vascular calcification: Pathobiology of a multifaceted disease. *Circulation*. 2008;117:2938-2948
31. Ortlepp JR, Schmitz F, Bozoglu T, Hanrath P, Hoffmann R. Cardiovascular risk factors in patients with aortic stenosis predict prevalence of coronary artery disease but not of aortic stenosis: An angiographic pair matched case-control study. *Heart*. 2003;89:1019-1022
32. Adiguzel E, Ahmad PJ, Franco C, Bendeck MP. Collagens in the progression and complications of atherosclerosis. *Vascular medicine*. 2009;14:73-89
33. Libby P. Collagenases and cracks in the plaque. *The Journal of clinical investigation*. 2013;123:3201-3203
34. Libby P. The interface of atherosclerosis and thrombosis: Basic mechanisms. *Vascular medicine*. 1998;3:225-229
35. Newby AC, Zaltsman AB. Fibrous cap formation or destruction--the critical importance of vascular smooth muscle cell proliferation, migration and matrix formation. *Cardiovasc Res*. 1999;41:345-360
36. Libby P, Sasiela W. Plaque stabilization: Can we turn theory into evidence? *Am J Cardiol*. 2006;98:26P-33P
37. Lin TC, Tintut Y, Lyman A, Mack W, Demer LL, Hsiai TK. Mechanical response of a calcified plaque model to fluid shear force. *Annals of biomedical engineering*. 2006;34:1535-1541

38. Houslay ES, Cowell SJ, Prescott RJ, Reid J, Burton J, Northridge DB, Boon NA, Newby DE, Scottish Aortic S, Lipid Lowering Therapy loRtI. Progressive coronary calcification despite intensive lipid-lowering treatment: A randomised controlled trial. *Heart*. 2006;92:1207-1212
39. Aikawa E, Nahrendorf M, Figueiredo JL, Swirski FK, Shtatland T, Kohler RH, Jaffer FA, Aikawa M, Weissleder R. Osteogenesis associates with inflammation in early-stage atherosclerosis evaluated by molecular imaging in vivo. *Circulation*. 2007;116:2841-2850
40. Byon CH, Javed A, Dai Q, Kappes JC, Clemens TL, Darley-Usmar VM, McDonald JM, Chen Y. Oxidative stress induces vascular calcification through modulation of the osteogenic transcription factor runx2 by akt signaling. *The Journal of biological chemistry*. 2008;283:15319-15327
41. Ueland T, Aukrust P, Dahl CP, Husebye T, Solberg OG, Tonnessen T, Aakhus S, Gullestad L. Osteoprotegerin levels predict mortality in patients with symptomatic aortic stenosis. *Journal of internal medicine*. 2011;270:452-460
42. Carter S, Miard S, Roy-Bellavance C, Boivin L, Li Z, Pibarot P, Mathieu P, Picard F. Sirt1 inhibits resistin expression in aortic stenosis. *PloS one*. 2012;7:e35110
43. Mohty D, Pibarot P, Despres JP, Cartier A, Arsenault B, Picard F, Mathieu P. Age-related differences in the pathogenesis of calcific aortic stenosis: The potential role of resistin. *International journal of cardiology*. 2010;142:126-132
44. Everett BM, Pradhan AD, Solomon DH, Paynter N, Macfadyen J, Zaharris E, Gupta M, Clearfield M, Libby P, Hasan AA, Glynn RJ, Ridker PM. Rationale and design of the cardiovascular inflammation reduction trial: A test of the inflammatory hypothesis of atherothrombosis. *Am Heart J*. 2013;166:199-207 e115
45. Fordyce CB, Roe MT, Ahmad T, Libby P, Borer JS, Hiatt WR, Bristow MR, Packer M, Wasserman SM, Braunstein N, Pitt B, DeMets DL, Cooper-Arnold K, Armstrong PW, Berkowitz SD, Scott R, Prats J, Galis ZS, Stockbridge N, Peterson ED, Califf RM. Cardiovascular drug development: Is it dead or just hibernating? *J Am Coll Cardiol*. 2015;65:1567-1582
46. Rajamannan NM, Subramaniam M, Springett M, Sebo TC, Niekrasz M, McConnell JP, Singh RJ, Stone NJ, Bonow RO, Spelsberg TC. Atorvastatin inhibits hypercholesterolemia-induced cellular proliferation and bone matrix production in the rabbit aortic valve. *Circulation*. 2002;105:2660-2665
47. Drolet MC, Couet J, Arsenault M. Development of aortic valve sclerosis or stenosis in rabbits: Role of cholesterol and calcium. *J Heart Valve Dis*. 2008;17:381-387
48. Sider KL, Blaser MC, Simmons CA. Animal models of calcific aortic valve disease. *International journal of inflammation*. 2011;2011:364310
49. Bowler MA, Merryman WD. In vitro models of aortic valve calcification: Solidifying a system. *Cardiovasc Pathol*. 2015;24:1-10
50. Yip CY, Chen JH, Zhao R, Simmons CA. Calcification by valve interstitial cells is regulated by the stiffness of the extracellular matrix. *Arterioscler Thromb Vasc Biol*. 2009;29:936-942
51. Khademhosseini A, Peppas NA. Micro- and nanoengineering of biomaterials for healthcare applications. *Advanced healthcare materials*. 2013;2:10-12
52. Yip CY, Simmons CA. The aortic valve microenvironment and its role in calcific aortic valve disease. *Cardiovasc Pathol*. 2011;20:177-182
53. Sacks MS, Yoganathan AP. Heart valve function: A biomechanical perspective. *Philosophical transactions of the Royal Society of London*. 2007;362:1369-1391
54. Benton JA, Kern HB, Anseth KS. Substrate properties influence calcification in valvular interstitial cell culture. *J Heart Valve Dis*. 2008;17:689-699
55. Walker GA, Masters KS, Shah DN, Anseth KS, Leinwand LA. Valvular myofibroblast activation by transforming growth factor-beta: Implications for pathological extracellular matrix remodeling in heart valve disease. *Circulation research*. 2004;95:253-260

56. Wyss K, Yip CY, Mirzaei Z, Jin X, Chen JH, Simmons CA. The elastic properties of valve interstitial cells undergoing pathological differentiation. *J Biomech*. 2012;45:882-887
57. Merryman WD, Huang HY, Schoen FJ, Sacks MS. The effects of cellular contraction on aortic valve leaflet flexural stiffness. *J Biomech*. 2006;39:88-96
58. Balachandran K, Sucosky P, Jo H, Yoganathan AP. Elevated cyclic stretch induces aortic valve calcification in a bone morphogenic protein-dependent manner. *Am J Pathol*. 2010;177:49-57
59. Wang H, Tibbitt MW, Langer SJ, Leinwand LA, Anseth KS. Hydrogels preserve native phenotypes of valvular fibroblasts through an elasticity-regulated pi3k/akt pathway. *Proceedings of the National Academy of Sciences of the United States of America*. 2013;110:19336-19341
60. Gu X, Masters KS. Regulation of valvular interstitial cell calcification by adhesive peptide sequences. *Journal of biomedical materials research. Part A*. 2010;93:1620-1630
61. Seidl P, Huettinger R, Knuechel R, Kunz-Schughart LA. Three-dimensional fibroblast-tumor cell interaction causes downregulation of rack1 mrna expression in breast cancer cells in vitro. *International journal of cancer. Journal international du cancer*. 2002;102:129-136
62. Fisher CI, Chen J, Merryman WD. Calcific nodule morphogenesis by heart valve interstitial cells is strain dependent. *Biomechanics and modeling in mechanobiology*. 2013;12:5-17
63. Annabi N, Tamayol A, Shin SR, Ghaemmaghami AM, Peppas NA, Khademhosseini A. Surgical materials: Current challenges and nano-enabled solutions. *Nano today*. 2014;9:574-589
64. Annabi N, Mithieux SM, Boughton EA, Ruys AJ, Weiss AS, Dehghani F. Synthesis of highly porous crosslinked elastin hydrogels and their interaction with fibroblasts in vitro. *Biomaterials*. 2009;30:4550-4557
65. Sacks MS, David Merryman W, Schmidt DE. On the biomechanics of heart valve function. *J Biomech*. 2009;42:1804-1824
66. Merryman WD, Lukoff HD, Long RA, Engelmayr GC, Jr., Hopkins RA, Sacks MS. Synergistic effects of cyclic tension and transforming growth factor-beta1 on the aortic valve myofibroblast. *Cardiovasc Pathol*. 2007;16:268-276
67. Wipff PJ, Rifkin DB, Meister JJ, Hinz B. Myofibroblast contraction activates latent tgf-beta1 from the extracellular matrix. *The Journal of cell biology*. 2007;179:1311-1323
68. Butcher JT, Tressel S, Johnson T, Turner D, Sorescu G, Jo H, Nerem RM. Transcriptional profiles of valvular and vascular endothelial cells reveal phenotypic differences: Influence of shear stress. *Arterioscler Thromb Vasc Biol*. 2006;26:69-77
69. Butcher JT, Nerem RM. Valvular endothelial cells regulate the phenotype of interstitial cells in co-culture: Effects of steady shear stress. *Tissue Eng*. 2006;12:905-915
70. Richards J, El-Hamamsy I, Chen S, Sarang Z, Sarathchandra P, Yacoub MH, Chester AH, Butcher JT. Side-specific endothelial-dependent regulation of aortic valve calcification: Interplay of hemodynamics and nitric oxide signaling. *Am J Pathol*. 2013;182:1922-1931
71. Towler DA. Molecular and cellular aspects of calcific aortic valve disease. *Circulation research*. 2013;113:198-208
72. Gould ST, Srigunapalan S, Simmons CA, Anseth KS. Hemodynamic and cellular response feedback in calcific aortic valve disease. *Circulation research*. 2013;113:186-197
73. Bischoff J, Aikawa E. Progenitor cells confer plasticity to cardiac valve endothelium. *Journal of cardiovascular translational research*. 2011;4:710-719
74. Wylie-Sears J, Aikawa E, Levine RA, Yang JH, Bischoff J. Mitral valve endothelial cells with osteogenic differentiation potential. *Arterioscler Thromb Vasc Biol*. 2011;31:598-607

13

Samenvatting in het Nederlands

INLEIDING

Aortaklepverkalking is de meest voorkomende hartklepaandoening in de westerse wereld. Het is een progressieve ziekte die leidt tot vernauwing van de aortaklep, ook wel bekend als aortaklepstenose. Er bestaan tot nu toe geen therapeutische mogelijkheden om aortaklepverkalking te voorkomen of medicamenteus te behandelen. Tot op heden is chirurgische klepvervanging dan ook de enige effectieve behandeling van aortaklepstenose. Bij patiënten met een te hoog operatierisico kan de aortaklep minimaal invasieve worden vervangen middels kathetertechnieken. Wereldwijd worden per jaar meer dan 275.000 aortaklep vervangingen uitgevoerd. Met een steeds ouder wordende bevolking is de verwachting dat dit aantal in 2050 meer dan verdrievoudigd is. De omstandigheden die leiden tot verkalking van de aortaklep zijn tot op heden niet goed bekend. Het doel van dit proefschrift is tweeledig:

I Met behulp van moleculaire imaging de ontwikkeling van aortaklepverkalking te visualiseren om de kenmerken van het ziekteverloop te identificeren;

II Het ontwikkelen van een weefselmodel dat ons in staat stelt de mechanismen van aortaklepverkalking, zoals deze in de mens plaatsvindt, te onderzoeken.

VISUALISATIE VAN HET ONTSTAAN VAN AORTAKLEPVERKALKING

Symptomen zoals kortademigheid of pijn op de borst, ontstaan pas wanneer er sprake is van een significante aortaklepstenose. Dit wordt gezien als het eindstadium van de ziekte. Doordat de klepziekte pas in een late fase van het ziekteproces ontdekt wordt is het ontstaan van de aortaklepverkalking en de progressie in de mens moeilijk te bestuderen. Hierdoor baseren we onze kennis met name op diermodellen en celkweek studies. Alhoewel beide studiemethoden van onmiskenbaar belang zijn, zijn ze niet in staat gebleken om de ingewikkelde omstandigheden van aortaklepverkalking in de mens na te bootsen. Het is een aanzienlijke, maar klinisch zeer relevante uitdaging om alle fasen van het ziekte proces te visualiseren. Zo kan er mogelijk een ziektestadium worden bepaald waarin behandeling effect heeft. Daarnaast is meer onderzoek noodzakelijk om vast te stellen of er fasen bestaan in het ziekteproces waarin sprake kan zijn van reversibiliteit van de ziekte. Om dit te bereiken kan 'molecular imaging' een uitkomst bieden, doordat deze methode ons in staat stelt om cellulaire processen van het gehele ziekteverloop te visualiseren. Molecular imaging is een techniek die fluorescerende moleculen kan visualiseren. Zo wordt een fluorochroom geconjugeerd aan een molecuul. Enzymen die tot uiting komen bij een bepaald cellulair proces, kunnen met deze moleculen binden wat dan fluorescentie tot gevolg heeft. Dit betekent dat specifieke enzym activiteit zoals dat kan ontstaan bij ontsteking en botvorming gevisualiseerd kan worden.

Deel I van dit proefschrift beschrijft en gebruikt 'molecular imaging' om aortaklepverkalking te bestuderen. Thans worden zowel vasculaire als aortaklepverkalking in beeld gebracht met behulp imaging technieken zoals echocardiografie, computed tomography (CT) en magnetic resonance imaging (MRI). Zowel echocardiografie als CT zijn belangrijke diagnostische hulpmiddelen voor aortaklepverkalking. meestal worden ze verricht bij patiënten die reeds symptomen van verkalking vertonen. Deze technieken zijn mindergoed in staat om vroege pathologische veranderingen in de aortaklep te visualiseren. Nieuwe opsporingsmethoden zijn nodig om vroege pathologie in de klep te diagnosticeren.

Hoofdstuk 3 beschrijft hoe 'molecular imaging' kan worden gebruikt om mechanismen van cardiovasculaire verkalking te visualiseren en zo kan bijgedragen aan het in kaart brengen van de pathologie. In **Hoofdstuk 4** gebruiken we daadwerkelijk deze imaging methode in diermodellen van cardiovasculaire verkalking. Met behulp van deze techniek tonen we in muismodellen aan, dat er een omgekeerde relatie bestaat tussen cardiovasculaire verkalking en botdichtheid bij atherosclerose en nierfalen. Tevens suggereren onze resultaten dat er in deze modellen een relatie is tussen aortaklepverkalking en slagaderverkalking. Bovendien observeren we in deze modellen een toename in ontstekingsactiviteit van zowel slagaders, als aortakleppen, als in botten. Dit resultaat vormt mogelijk een aanwijzing voor systemische ontsteking als onderliggende verklaring voor de afname van botdichtheid en toename van ectopische verkalking in het cardiovasculair systeem. Deze studie toont aan hoe molecular imaging gebruikt kan worden om ingewikkelde cellulaire en moleculaire processen in ziekte minimaal-invasief te visualiseren.

Aortaklepstenose en coronarialijden hebben veel gemeenschappelijke risicofactoren, wat zou kunnen betekenen dat atherosclerose en aortaklepverkalking dezelfde etiologie delen. Studies in diermodellen laten zien dat aortaklepverkalking, net als atherosclerose, behandeld kan worden met cholesterolverlagende medicijnen zoals statines. Bovendien hebben in eerdere studies, histologische analyses atherosclerose-achtige plaques laten zien in verkalkte aortakleppen. Echter, gerandomiseerde klinische studies hebben bij mensen geen effect laten zien van behandeling met statines in de late fase van aortaklepverkalking. Het maar zeer de vraag of atherosclerose en aortaklepverkalking als dezelfde etiologische entiteit kunnen worden gezien. De tegenstrijdige resultaten van deze studies suggereren in ieder geval dat we het ziektemechanisme van aortaklepverkalking in de mens nog niet goed begrijpen.

MODELLEREN VAN AORTAKLEPVERKALKING

Om de ziekte zoals die in de mens bestaat te begrijpen, is een nieuwe aanpak nodig. Niet alleen vereist aortaklepverkalking in patiënten een verbetering van simulatie technieken, maar ook een hoger kennisniveau van de algemene klepbiologie,. Deze uitdaging werd aangegaan met behulp van tissue engineering en is beschreven in **Deel II** van dit proefschrift.

Tissue engineering streeft ernaar om organen of weefsel te maken met als doel aangedane biologische functies te vervangen of te verbeteren. In dit proefschrift gebruiken we hydrogel micro-engineering om een model van de aortaklep te maken, dat in staat is om de klepbiologie en pathologie te simuleren zoals deze in de mens optreedt. Hydrogels hebben namelijk een unieke eigenschap, ze kunnen gemaakt worden van natuurlijke extracellulaire matrixcomponenten. Dit stelt ons in staat om de natuurlijke omgeving van hartklepweefsel na te bootsen. **Hoofdstuk 5** beschrijft hoe hydrogels toegepast kunnen worden in tissue engineering. In **Hoofdstuk 6** wordt uitgeweid over de toepassing van hydrogel micro-engineering in hartkleponderzoek in zijn algemeenheid.

Hoofdstuk 7 beschrijft hoe we een aortaklepmodel hebben gemaakt met behulp van hydrogel micro-engineering door gebruik te maken van collageen en hyaluraanzuur: essentiële componenten van de extracellulaire matrix van de aortaklep. We tonen in dit hoofdstuk aan, dat ons hydrogel model de verandering in fenotype van klepcellen kan nabootsen. Door de collageen- en hyaluraanzuur concentratie te variëren en te testen zijn we in staat geweest om een hydrogel omgeving te creëren die overeenkomt met de weefselomgeving van de *zona fibrosa* van de aortaklep. Dit is tevens de laag waarin verkalking optreedt. Nadat we hebben vastgesteld dat we gezonde fibroblast-achtige "hartklep-interstitiele cellen" kunnen laten leven in ons hydrogel model, hebben we laten zien dat hartklepcellen gecontroleerd geactiveerd kunnen worden en zich differentieerden tot een myofibroblast-achtig fenotype. Dit proces wordt gezien als kenmerkend voor de fibrose die voorafgaat aan aortaklepverkalking. Uit de resultaten blijken ook dat aortaklepcellen in onze hydrogels dezelfde eigenschappen hebben als natuurlijke menselijke aortaklepcellen

Dit onderzoek heeft de basis gevormd voor de verdere ontwikkeling van een aortaklepverkalking model. In **hoofdstuk 8** gebruiken we de hydrogels om aortaklepverkalking daadwerkelijk te simuleren door de ze bloot te stellen aan osteogene oftewel botvormende stimuli die geassocieerd zijn met aortaklepverkalking;. We laten in dit hoofdstuk zien dat bij botvormende stimulatie eerst activatie van de aortaklepcellen, en uiteindelijk verkalking optreedt. Dit proces wordt bovendien versterkt wanneer we tumor necrose factor – alpha (TNFα) toevoegen aan ons model. TNFα is een cytokine dat verhoogd aanwezig is bij ziekten als diabetes, metabool syndroom en slagaderverkalking. We hebben met deze benaderingswijze in één model de verschillende stadia waarin cellen zich kunnen bevinden in de hartklepbiologie en -pathologie weten te stimuleren. Dit betekent dat ons hartklepmodel gebruikt kan worden om het beginstadium van aortaklepverkalking te simuleren, wat tot op heden nog niet mogelijk is geweest. Ook associaties met een andere etiologie van klepziekten kunnen hiermee bestudeerd worden.

Hoofdstuk 9 beschrijft een pilot experiment waarin we de relatie tussen bestraling en aortaklepverkalking hebben onderzocht. Bestraling die wordt toegepast in de behandeling van borstkanker of lymfomen en kan leiden tot versnelde ontwikkeling van klepverkalking. Door onze hartklepmodellen bloot te stellen aan bestraling, hebben we aangetoond dat de aortaklepcellen inderdaad een versnelde activatie van het verkalkingsproces doorgaan.

Een belangrijk aspect van de aortaklepbiologie en -pathologie is de rol van endotheelcellen die de buitenkant van de hartklep bekleden. Er zijn steeds meer aanwijzingen dat de klep-

endotheelcellen een nauwe relatie onderhouden met de hartklepcellen met betrekking tot de handhaving van de structurele integriteit van een hartklep. **Hoofdstuk 10** onderzoekt de relatie tussen hartklep-endotheelcellen en hartklep-interstitiële cellen in een osteogene omgeving. We tonen aan dat endotheelcellen ook de potentie hebben om zich te differentiëren in botvormende cellen en kalkafzetting teweeg brengen. Deze transitie lijkt zich te voltrekken doordat endotheel cellen zich eerst differentiëren in myofibroblasten. We laten bovendien zien dat hartklepcellen deze transitie lijken te inhiberen. Dezelfde relatie tonen we aan in zowel muismodellen als in humane verkalkte kleppen. Gebaseerd op deze studie kunnen we concluderen dat hartklep endotheelcellen kunnen differentiëren in hartklepcellen en zelfs botvormende cellen om zo bij te dragen aan het ontstaan van aortaklepverkalking.

Dit proefschrift heeft als doel gehad om belangrijke uitdagingen in bestaand onderzoek naar aortaklepverkalking te overwinnen. Allereerst hebben we 'molecular imaging' gebruikt om ziekteprogressie *in vivo* te visualiseren en belangrijke componenten voor deze progressie te identificeren. Daarna hebben we een driedimensionaal hartklepmodel ontwikkeld, wat ons in staat heeft gesteld om het begin en de progressie van aortaklepverkalking te simuleren. Dit model kan tevens gebruikt worden om nieuwe aanknopingspunten voor medicamenteuze behandeling van aortaklepverkalking te onderzoeken. Tot slot biedt dit model ons de kans om kennis te vergaren over de ontwikkeling van de hartklep, wat van wezenlijk belang is voor nader onderzoek naar de ontwikkeling van tissue-engineered hartkleppen.

Appendix

APPENDIX I LIST OF ABBREVIATIONS

18-FDG	18 Fludeoxyglucose
18-NaF	18- SodiumFluoride
ACE	Angiotensin Converting Enzyme
Ao	Aorta
AoV	Aortic Valve
AoS	Aortic valve stenosis
ATII	Angiotensin II
αSMA	alpha- Smooth Muscle Actin
Apo E	Apolipoprotein E
BMP	Bone Morphogenetic Protein
BK	Bradykinin
CAVD	Calcific Aortic Valve Disease
CD31	Cluster of Differentiation-31
CRD	Chronic Renal Disease
CT	Computed Tomography
ECM	Extracellular Matrix
EndMT	Endothelial to Mesenchymal Transition
eNOS	endothelial Nitric Oxide Synthase
FGF	Fibroblast Growth Factor
GAG	Glycosaminoglycan
GelMA	Methacrylated Gelatin
HA	Hyaluronic Acid
HAMA	Methacrylated Hyaluronic Acid
HPF	High Power Field
HMG-CoA	3-hydroxy-3-methyl-glutaryl-CoA reductase
IL	Interleukin
KKS	Kalikrein-kinin system
LDL	Low Density Lipoprotein
LRP-5	LDL receptor related protein 5
MAPK	Mitogen Activated Protein Kinase
MMP	Matrixmetalloproteinase
MRI	Magnetic Resonance Imaging
NFκB	Nuclear Factor kappa beta
OCT	Optical coherence tomography
PBS	Phosphate Buffered Saline
PEGDA	Polyethylene Glycol Diacrylate
PET	Positron Emission Tomography

PI	Photo-Initiator
RAAS	Renin-Angiotensin-Aldosterone System
RANK	Receptor activator of nuclear factor kappa-B
RANK-L	Receptor activator of nuclear factor kappa-B ligand
ROS	Reactive Oxygen Species
Runx2	Runt-related transcription factor 2
TGFβ	Transforming Growth Factor beta
TIMP	Tissue Inhibitor of MetalloProteinases
TNFα	Tumor Necrosis Factor- alpha
VCAM-1	Vascular Cell Adhesion Molecule-1
VEC	Valvular Endothelial Cell
VIC	Valvular Interstitial Cell
aVIC	activated VIC
eVIC	endothelial derived VIC
qVIC	quiescent VIC
oVIC	osteoblast VIC
pVIC	progenitor VIC
WT	Wildtype

APPENDIX II LIST OF PUBLICATIONS

J. Hjortnaes, C. Goettsch, G. Camci-Unal J.D. Hutcheson, L. Lax, K. Scherer, F. J. Schoen, J. Kluin, A. Khademhosseini, E. Aikawa 'A key role for myofibroblast actiativation in 3D model for early calcific aortic valve disease' *(under revision for Journal of Molecular and Cellular Cardiology)*.

J. Hjortnaes, K. Shapero, C. Goettsch, J. Kluin, J.E. Mayer, R.A. Levine, J. Bisschoff, E. Aikawa 'Valvular interstitical cells suppress calcification by valvular endothelial cells' (*Atherosclerosis 2015)*.

N. Masoumi,, N. Annabi,, A. Assman, B. Larsson, **J. Hjortnaes** A. Cubberly, A. Khademhosseini, J.E. Mayer 'Tri-layered MSC-seeded elastomeric scaffolds mimic architectural and mechanical properties of native heart valve leaflets' *(Advanced Materials 2014)*

-L.E.Bertassoni, Martina Cecconi, Vijayan Manoharan**, J. Hjortnaes**, A.L.Christino, M. Nikkah, P.H. Molin, G. Barabaschi, D. Demarchi, M. Dokmeci, Y. Yang, A. Khademhosseini 'Engineering microchannel networks via bioprinting for prevascularization of hydrogels for tissue engineering' (*Lab on a Chip 2014)*.

-N. Alemdar G. Camci-Unal, **J. Hjortnaes**, A. Paul P. Mostafalu, A. K. Gaharwar Y. Qiu, Sameer Sonkusale R. Liao, A. Khademhosseini 'Oxygen-generating photo-crosslinkable hydrogel for improved survival of cardiac progenitor cells under hypoxic conditions: preparation and in vitro analysis' *(submitted)*

-**J. Hjortnaes**, J. Keegan, E. Schwartz, P. Bruneval, F.J. Schoen, A. Carpentier, R.Levine, A. Hagège, E. Aikawa 'Histopathological differentiation of Barlow's Disease and fibroelastic deficiency in patients with degenerative mitral valve disease' *(submitted)*

- **J. Hjortnaes**, G. Camci-Unal, S. Jung, F.J. Schoen, J. Kluin, E. Aikawa, A. Khademhosseini 'Hydrogel composition directs valvular interstitical cell fate' *(Advanced HealthCare Materials 2015)*.

J. Hjortnaes, S.N. New, E. Alkawa 'Visualizing new concepts of cardiovascular calcification' *Trends Cardiovascular Medicine*. 2013

J. Hjortnaes, F. J. Ten Cate, P.J. Leemans, L.A. Van Herwerden 'Surgical treatment of SAM after successful PTSMA: a case report' *J Thorac Cardiovasc Surg*. 2012 Aug; 144(2):506-8*y*.

J. Hjortnaes, J. Butcher, J. Figueiredo, M. Riccio, R.H. Kohler, Kozloff K, R. Weissleder, E. Aikawa 'Inverse correlation of arterial and aortic valve calcification with low bone mineral density evaluated by molecular imaging' *Eur Heart J* 2010 Aug;31(16):1975-84.

A

-**J. Hjortnaes**, D. Gottlieb, J. Figueiredo, J. Melero-martin, R.H. Kohler, J. Bischoff, R. Weissleder, J. E. Mayer Jr., E. Aikawa 'Intravital molecular imaging of small-diameter tissue-engineered vascular grafts: A feasibility study' *Tissue Eng Part C Methods*. 2010 Aug;16(4):597-607.

J. Hjortnaes, C.V.C. Bouten, L.A. Van Herwerden, P.F. Gründeman, J. Kluin 'Translating autologous heart valve tissue engineering from bench to bed' *Tissue Eng Part B Reviews*. 2009 Sep; 15(3):307-17.

J. Hjortnaes, A. Algra, J. Olijhoek, M. Huisman, J. Jacobs, Y. van der Graaf, F. Visseren 'Serum uric acid levels and risk for vascular diseases in patients with metabolic syndrome' *J Rheumatol*. 2007 Sep; 34(9):1882-7.

Book Chapters

-**J. Hjortnaes**, F.J.Schoen 'The role of microengineering in Tissue Engineered Heart Valves ((Gels Handbook, World Scientific Publishing Co, 2015)

G. Gamci-Unal, **J. Hjortnaes**, H. Bae, M. Dokmeci, A. Khademhosseini 'Microfabricated gels for tissue engineering' (2012) *Biomaterials and Regenerative Medicine, Cambridge: Cambridge University Press.*

J. Hjortnaes, E. Aikawa 'Calcific aortic valve disease' (2011) InTech OpenSource.

APPENDIX III ACKNOWLEDGEMENTS

Throughout the course of this thesis a great deal of people have crossed my path. Their contribution to this work varies from substantial laboratory work to unwavering support to lasting inspiration. Below you'll find names that may seem at random to the reader, but to me have been of invaluable importance not only in completing this doctorate but also instilling an un-erasable fun in doing scientific research. In addition, I would like to acknowledge a few people in particular.

Dear mentors, teachers, friends, colleagues, and family:

You have my sincere gratitude and deep respect.

Elena Aikawa
Masanori Aikawa
Neslihan Alemdar
Nasim Annabi
Alexander Assmann
Frank Baaijens
Luiz E. Bertassoni
Joyce Bischoff
Carlijn V.C. Bouten
Bart Brouwers
Marc Buijsrogge
Jonathan Butcher
Crema Cafe
Alex Cubberly
Esther van Eeuwijk
Janine Deddens
Gulden Gamci-Unal
Akhilesh Garharwar
Claudia Goettsch
Roel Goldschmeding
Darwin Ltd
Pieter J. Doevendans
Mehmet Dokmeci
Rob Driessen
Thibaut Gideault
Kjeld Hjortnaes
Anna-Grethe Hjortnaes
Thomas Hjortnaes
Linda de Heer
Lex A. van Herwerden
Josh D. Hutcheson
Josh Keegan
Ali Khademhosseini
Jolanda Kluin
David Kozono
Marloes Laaper-Ertmann
Lillian Lax
Robert Levine
Peter Libby
Marieke Liem
Anho Liem
Annelies Liem-Buirma
Ling Ling Lok
Eduardo Martinez-Martinez
John Mayer Jr.
Mellisa McCormack
Marina Moreira
Juan Melero-Martin
Nafiseh Masoumi
Sophie New
Mehdi Nikka
Alireza Pirouz
Paul Riem-Vis
Katrin Scherer
Su-Ryon Shin
Frederick J. Schoen
Els Schumacher
Kayle Shapiro
Joost Sluijter
Joke Steenis
Hanna Talacua
The Beehive
Mark Tibbit
Jorge Alfredo Uquillas
Marianne Verhaar
Frank Visseren
Josephine Walta
Chunyu Zheng

A

Prof. dr. L. A. Van Herwerden: Dear Professor, from the beginning of the 'onset' of this thesis, you have always supported the notion that basic transitional science and cardiothoracic surgery can go very well together. Yet as a surgeon, you've always maintained never to loose sight of what matters, which is to strive to become an excellent surgeon. You have been and will continue to be an inspiration. Thank you for your support and belief in me. I am proud for you to be a mentor and my *promotor*

Dr. J. Kluin: Dear Jolanda, your pursuit of translational scientific endeavors and your love for cardiothoracic surgery has always been an important inspiration for me to choose a similar path. It is a true privilege to know you, and even a greater one to have you as my *co-promotor*. Thank you for your belief in what started out as a crazy idea. Thank you for your support, advice and mentorship. I look forward to the years to come.

Dr. E. Aikawa: Dear Elena, we have known each other for many years now. What started out as a scientific internship as a medical student eventually culminated into a new home in Boston, an apprenticeship in your laboratory, and even a friendship. You said to me once: "I can open doors for you, but it's you who has to walk through them". Thank you not only for opening those doors, but also wisely advising me on which ones not to enter. Your unwavering support is a significant part of this thesis. It fills me with pride to have you as my *co-promotor.* I look forward to keep visiting our other home in Boston, a continuing apprenticeship, and hopefully a very long friendship.

Dr. H.B. Brouwers: Dear Bart, no question you were going to be my *paranymf.* If people didn't know any better, you could almost say that we planned our careers together. Meeting in Boston on our scientific internships, we decided after a few months that we were going to come back to Boston to do PhD work, because we were not ready to close the Boston-chapter yet. What a momentous fun time it has been and now we are done! I take great pride and joy from having shared this with you. But to be fair, we aren't done. It's just the beginning of a lifelong friendship, which I have come to cherish greatly. Thank you.

Kjeld Hjortnaes: Dear Dad, to be completely honest with you: mom has always wanted to see you in a white tie. So, of course I had to ask you to be my *paranymf.* I think you will look great. You see, it's not the clothes that dress the man. It's the man that dresses the clothes. And in my humble and completely unbiased opinion you are a great man indeed. Growing up on a farm and becoming a rocket-scientist is not the only thing that makes you great. Marrying my beautiful and smart mother, a civil engineer, with whom you have proudly created a wonderful life in the Netherlands, is also not really the thing that makes you great. Although marrying mom does help…

No, you are great, because you are my father. And nothing is bigger than the inspiration you and mom have had on me as a person, as a son, as a friend, as a husband and eventually as a father myself. My gratitude cannot be put into words. But I can say this. You really do look great in a white tie.

Kaere Marieke: Livet sammen med dig og vores familie er det mest vidunderlige i min verden, og bringer alt i perspektiv. Jeg glaeder mig til endu mere af vores eventyrlige liv sammen. Tak for din umiskendelig stytte , din kaerlighed, og tro paa mig. Du er mit et og ene.

APPENDIX IV CURRICULUM VITAE

Jesper Hjortnaes, son of Anna Grethe Indius Hjortnaes and Kjeld Hjortnaes, and brother to Thomas Hjortnaes, was born 28 juli 1983 in Leiden, the Netherlands. After graduating high school - the Stedelijk Gymnasium in Leiden – in 2001, he went to St. Anton am Arlberg in Austria to pursue his passion for skiing. In 2002, he started attending University College Utrecht, The Netherlands, from which he graduated with a Bachelor of Science in 2005. During his final year, he wrote and published his thesis on uric acid and cardiovascular disease under the supervision of Prof. dr. Frank Visseren at the University Medical Center Utrecht (UMCU). In that same year, he was admitted to SUMMA medical school of the UMCU. His scientific internship was conducted at the Massachusetts General Hospital/Harvard Medical School under the supervision of Dr. Elena Aikawa, which would serve as the foundation for his future scientific endeavors. In 2009 he graduated from medical school, after which he started as a house officer at the department of Cardiothoracic Surgery of the UMCU. During this time he was awarded the Dekker grant of the Dutch Heart Foundation, and the AGIKO grant of the Netherlands Organisation for Scientific Research (NWO) to pursue his PhD work under the supervision of Dr. Jolanda Kluin and Dr. Elena Aikawa in collaboration with Prof. dr. A. Khademhosseini and Prof dr. Frederick J. Schoen at the Brigham and Women's Hospital/ Harvard Medical School, in Boston. In December 2013, he started his residency at the department of Cardiothoracic Surgery, UMCU, the Netherlands under supervision of Prof. dr. L. A Van Herwerden and Prof dr. Willem Suyker. The initial training in general surgery is currently being conducted at the Diakonnessenhuis Utrecht, under supervision of Dr. T. van Dalen. His residency Cardiothoracic Surgery is expected to be completed in 2019. Jesper is married to Marieke Liem. Together they have a daughter, Saga.